

**THE BIOCHEMICAL ROLE OF THE SMALL G PROTEIN RAC1 IN CELL
SIGNALLING PATHWAYS – INTERACTION WITH RHOGDI AND THE
PHAGOCYTE NADPH OXIDASE COMPONENT, P67^{PHOX}**

Thesis submitted in accordance with the requirements of the
UNIVERSITY OF LONDON
for the degree of
DOCTOR OF PHILOSOPHY
by

Anthony R. Newcombe
Division of Physical Biochemistry
National Institute for Medical Research
Mill Hill
London NW7 1AA
(Registered at University College London)

ProQuest Number: 10042788

All rights reserved

INFORMATION TO ALL USERS

The quality of this reproduction is dependent upon the quality of the copy submitted.

In the unlikely event that the author did not send a complete manuscript and there are missing pages, these will be noted. Also, if material had to be removed, a note will indicate the deletion.



ProQuest 10042788

Published by ProQuest LLC(2016). Copyright of the Dissertation is held by the Author.

All rights reserved.

This work is protected against unauthorized copying under Title 17, United States Code.
Microform Edition © ProQuest LLC.

ProQuest LLC
789 East Eisenhower Parkway
P.O. Box 1346
Ann Arbor, MI 48106-1346

"You can tell whether a man is clever by his answers.
You can tell whether a man is wise by his questions."
-Naguib Mahfouz

CONTENTS

	Page
Title page	
Contents	(a)
Table of figures	(e)
Abbreviations	(h)
Abstract	(i)
 CHAPTER 1. INTRODUCTION	
1.1. G proteins	1
1.1.1. The Rho family of small G proteins	1
1.1.2. Rac proteins	3
1.2. Regulation of actin polymerisation by Rho family proteins	5
1.2.1. Other Rho targets involved in cytoskeletal control	8
1.3. Rac and the NADPH oxidase system	9
1.3.1. The electron transporter of the NADPH oxidase	11
1.3.2. Activation of the NADPH oxidase	11
1.3.3. Role of the cytoskeleton in the NADPH oxidase	13
1.3.4. The cell-free, in vitro NADPH oxidase	14
1.4. Role of Rho proteins in smooth muscle contraction	15
1.5. Role of Rho proteins in cytokinesis	16
1.6. Rac proteins and gene transcription	17
1.7. The activation of p21 activated kinases (PAKs) by Rac1	17
1.8. Interaction of Rac with other proteins	19
1.9. Conserved sequence motifs of the Ras superfamily	20
1.9.1. The G1 motif	20
1.9.2. G2 – the ‘effector loop’	21
1.9.3. G3, G4 and G5 motifs	21
1.9.4. The C terminal region	22
1.10. Mechanism of GTP hydrolysis by Ras family proteins	22
1.11. DH proteins – exchange factors for Rho family proteins	24
1.12. GTPase-Activating Proteins (GAPs)	25
1.12.1. p50 RhoGAP	28
1.12.2. Additional regulatory mechanisms	29
1.13. Structure and sequence motifs of Human Rac1	30
1.13.1. Post-translational modifications of Rac	33
1.13.2. Carboxyl terminal methylation of Rac	35
1.14. Rho guanine nucleotide dissociation inhibitors (GDIs)	36
1.14.1. Structure of RhoGDI	37
1.14.2. Dissociation of the Rac1·GDI complex	39
1.14.3. In vivo studies into the role of RhoGDI	41

1.14.4. Regulation of membrane translocation by GDI	41
---	----

CHAPTER 2. MATERIALS AND METHODS

2.1. Materials used for protein studies	43
2.2. Protein purification from <i>E.coli</i>	43
2.2.1. Expression and purification of recombinant Rac1 from <i>E.coli</i>	44
2.2.2. Purification of full length recombinant Rac1 from <i>E.coli</i>	49
2.2.3. Purification of p67 ¹⁻¹⁹⁹ from <i>E.coli</i>	52
2.2.4. Purification of p47 ^{phox} and p67 ^{phox} from <i>E.coli</i>	52
2.3. Baculovirus methods	54
2.3.1. Quantification of viral titre by serial dilution plaque assay	54
2.3.2. Baculovirus amplification	55
2.3.3. Infection of <i>Spodoptera frugiperda</i> 9 insect cells with p67 ^{phox} baculovirus	56
2.3.4. Purification of recombinant p67 ^{phox} from baculovirus infected sf9 insect cells	56
2.4. Methods used to determine protein purity and concentration	59
2.4.1. Electrospray mass spectrometry of purified proteins and peptides	59
2.4.2. SDS polyacrylamide gel electrophoresis (SDS-PAGE)	59
2.4.3. Determination of recombinant protein concentration	60
2.5. Peptide methods	60
2.5.1. Modifying a Rac C-terminal peptide (12mer) with farnesyl bromide	62
2.5.2. Methylating a Rac C-terminal (9mer and 11mer) peptides	65
2.5.3. Farnesylating methylated Rac C-terminal peptides (9mer and 11mer)	65
2.5.4. Determination of peptide concentration by reverse phase HPLC	67
2.5.5. Determination of peptide concentration using TNBSA	67
2.6. Molecular biology methods	67
2.6.1. Isolation of plasmid DNA	71
2.6.2. DNA manipulation - bacterial transformation	72
2.6.3. Site directed mutagenesis of Rac1	72
2.6.4. Preparation of a Rac1-Ras chimaera construct	74
2.6.5. 'Freeze squeeze' purification of plasmid from an agarose gel	77
2.6.6. Ligation of primers	78
2.6.7. DNA sequencing - the dideoxy-chain termination method	83
2.6.8. Synthesis of mantGMPPNP	84
2.6.9. Formation of Rac1 nucleotide and nucleotide analogue complexes	86
2.6.10. Formation of Rac1 complexes with non-hydrolysable nucleotide analogues	86
2.6.11. Reaction of p67 ¹⁻¹⁹⁹ with 5,5'-Dithiobis-(2-nitrobenzoic acid) (DTNB)	87

2.7.	Fluorescence measurements	87
------	---------------------------	----

CHAPTER 3. BIOCHEMICAL CHARACTERISATION OF RAC1

3.0.	Introduction	91
3.1.	Analysis of the Rac1 GTPase cycle	91
3.2.	Properties of Rac1 with fluorescent nucleotide analogues	91
3.2.1.	Dissociation of mantGDP from Rac1 (k_{+1})	94
3.2.2.	Dissociation of GDP from Rac1	96
3.3.	Hydrolysis of GTP by Rac1 (k_{+2})	98
3.4.	Novel fluorescent nucleotide analogues – cou-edaGTP and but-edaGTP	100
3.4.1.	Fluorescent properties of Rac1 with coumarin derivatised GTP analogues	102
3.4.2.	The dissociation of cou-edaGTP and but-edaGTP from Rac1 (k_{+1})	102
3.4.3.	Hydrolysis of cou-edaGTP and but-edaGTP by Rac1 (k_{+2})	105

CHAPTER 4. DESIGN & CHARACTERISATION OF RAC1 MUTANTS

4.1.	Rac1 mutations to study the interaction with p67 ^{phox}	108
4.2.	Rac1 mutations to study the interaction with GDI	110
4.3.	Rac1/H-Ras chimaera	112
4.4.	Analysis of mutant Rac1 nucleotide complexes	113
4.5.	Nucleotide binding properties of Rac1 mutants	113
4.5.1.	Nucleotide exchange by F37E Rac1	116
4.6.	Hydrolysis of GTP by a Rac1/H-Ras chimaera	116
4.7.	Hydrolysis of GTP by D63E Rac1	116
4.8.	Q61L – a GTPase deficient Rac1 point mutant	119
4.9.	Summary of results	120

CHAPTER 5. INTERACTION OF RAC1 WITH P67^{PHOX}

5.0.	Introduction	122
5.1.	Aim of experiments	122
5.2.	Purification of p67 ^{phox} proteins	123
5.3.	Characterisation of p67 ¹⁻¹⁹⁹	124
5.4.	Effect of p67 ^{phox} and p67 ¹⁻¹⁹⁹ on Rac1·mantGMPPNP fluorescence	127
5.4.1.	Effect of arachidonate on the Rac1·mantGMPPNP·p67 ^{phox} Interaction	131
5.5.	Interaction of p67 ^{phox} with Rac1·but-edaGMPPNP	131
5.6.	Using labelled p67 ¹⁻¹⁹⁹ to measure the interaction with Rac1	133

5.7.	Effect of p67 ¹⁻¹⁹⁹ on hydrolysis of GTP by Rac1	134
5.8.	Summary of results	137

CHAPTER 6. INTERACTION OF RAC1 WITH GDI

6.1.	Introduction	140
6.2.	Farnesylated peptides	143
6.3.	Effect of Rac1 and farnesyl 12-mer on MDCC-GDI fluorescence	143
6.4.	Effect of BSA on MDCC-GDI fluorescence	146
6.5.	Displacement of MDCC-GDI from a Rac1·MDCC-GDI complex	146
6.6.	Effect of NaCl on the Rac1·MDCC-GDI interaction	149
6.7.	Affinity of the Rac1·MDCC-GDI interaction	149
6.7.1.	Affinity of the farnesyl 12-mer·MDCC-GDI interaction	151
6.8.	Interaction of Rac1·GTP with MDCC-GDI	154
6.9.	Interaction of full length Rac1 with MDCC-GDI	156
6.10.	Inhibition of nucleotide dissociation by GDI	156
6.11.	The interaction of cdc42·GDP and cdc42·GMPPNP with MDCC-GDI	158
6.12.	The interaction of N-Ras with MDCC-GDI	160
6.13.	Effect of GDI on Rac1·mantGDP fluorescence	163
6.14.	Interaction of Rac1 mutants with GDI	163
6.14.1.	Effect of GDI on the rate of nucleotide exchange from I33D Rac1	165
6.15.	Binding studies with a farnesylated C-terminal 9-mer	169
6.15.1.	Affinity of the farnesyl 9-mer·MDCC-GDI interaction	169
6.15.2.	Affinity of the Rac1·MDCC-GDI interaction in the presence of modified 9-mer	171
6.16.	Analysis of the Rac1·GDI interaction by stopped-flow spectrophotometry	171
6.16.1.	Kinetic mechanism of Rac1 binding to MDCC-GDI	172
6.16.2.	Dissociation of the Rac1·MDCC-GDI complex	177

CHAPTER 7. CONCLUSION

7.1.	Interaction of Rac1 with p67 ^{phox}	180
7.2.	Interaction of Rac1 with p67 ¹⁻¹⁹⁹	181
7.3.	Interaction of Rac1 with GDI	181
7.3.1.	Interaction of Rac1·GTP with GDI	184
7.3.2.	Interaction of Rac1 mutants with GDI	185
7.3.3.	Interaction of the Rac1/H-Ras chimera with GDI	186
7.4.	The role of the effector loop in GDI interaction	187
	Acknowledgments	191
	References	192

TABLE OF FIGURES

Figure	page
1.1. The GTPase cycle of Rac1 and its regulators	2
1.2. Sequence alignment of some of the Rho and Ras family proteins	4
1.3. A number of mammalian effectors of Rac and cdc42	6
1.4. Activation of the NADPH oxidase	10
1.5. Mechanism of GTP hydrolysis by Ras	23
Table 1.1. In vitro specificities of DH proteins for activating Rho GTPases	26
Table 1.2. In vitro specificities of proteins containing a RhoGAP domain	27
1.6. Comparison of the Rac1 and H-Ras structures	31
1.7. Crystal structure of human Rac1-GDP	32
1.8. Post-translational modification of Rac1	34
2.1. Analysis of a Rac1 preparation by SDS-PAGE	45
2.2. Analysis of an E131K Rac1 preparation by SDS-PAGE	47
2.3. Absorbance spectrum of purified Rac1	48
2.4. & 2.5. Electrospray mass spectrometry of Rac1	50
2.6. SDS polyacrylamide gel electrophoresis (SDS-PAGE) of purified proteins	53
2.7. Purification of p67 ^{phox} by anion exchange chromatography	58
Table 2.1. Calculated extinction coefficients for purified recombinant proteins	61
2.8. HPLC chromatograms showing the farnesylation of a Rac1 C-terminal 12mer peptide	63
2.9. Electrospray mass spectrometry of a farnesylated rac1 C-terminal 12mer	64
2.10. HPLC chromatograms showing the methylation of a Rac C-terminal 11mer peptide	66
2.11. HPLC chromatograms showing the farnesylation of a methylated 9mer	68
2.12. Electrospray mass spectrometry of a methylated, farnesylated 9mer	69
2.13. Reaction of TNBSA with glycine	70
Table 2.2. Oligonucleotide primers used for site-directed mutagenesis of Rac1	73
2.14. Quick change site-directed mutagenesis	75

2.15.	Method used to create a Rac1/H-Ras chimaera	76
2.16.	H-Ras 'insertion loop' oligonucleotides	79
2.17.	SDS-PAGE analysis of Rac1/H-Ras expression	80
2.18.	DNA sequence of a Rac1/H-Ras chimaera	81
2.19.	Mass spectrometry of a Rac1/H-Ras chimaera	82
2.20.	HPLC analysis of mantGMPPNP	85
2.21.	HPLC analysis of the nucleotide bound to Rac1 following exchange with the non-hydrolysable nucleotide analogue, GMPPNP	88
2.22.	Absorbance spectrum of purified Rac1·mantGMPPNP	89
Scheme 3.1.	The GTPase cycle of Rac1	92
3.1.	Structure of 2'(3')-O-(N-methyl)anthraniloyl (mant) GTP	93
3.2.	Dissociation of mantGDP from Rac1 (k_{+4})	95
3.3.	Rac1 nucleotide exchange under accelerated exchange conditions	97
3.4.	Time course for the hydrolysis of GTP by Rac1	99
3.5.	The structures of cou-edaGTP and but-edaGTP	101
3.6.	Fluorescent properties of Rac1 with coumarin derivatised nucleotides	103
3.7.	Dissociation of but-edaGTP and cou-edaGTP from Rac1	104
3.8.	Hydrolysis of cou-edaGTP and but-edaGTP by Rac1	106
4.1.	Rac1 point mutations	109
4.2.	A comparison of the effector loop of Rac1 with Ras	111
4.3.	Analysis of nucleotide bound to Rac1 and Rac1 mutants	114
Table 4.1.	Nucleotide binding properties of Rac1 mutants	115
4.4.	F37E Rac1 nucleotide exchange under accelerated exchange conditions	117
4.5.	Hydrolysis of GTP by a Rac1/H-Ras 'insertion loop' chimaera	118
5.1.	N- and C- terminal residues of p67 ¹⁻¹⁹⁹	125
5.2.	Electrospray mass spectrometry of p67 ¹⁻¹⁹⁹	126
5.3.	Secondary structure prediction of p67 ¹⁻⁹⁹	128
5.4.	Effect of p67 ^{phox} on Rac1·mantGMPPNP fluorescence using similar conditions as described by Nisimoto <i>et al.</i> , 1997	130
5.5.	The effect of p67 ^{phox} on Rac1·mantGMPPNP	130
5.6.	Effect of arachidonate on the interaction of Rac1 with p67 ^{phox}	132

5.7.	Reaction of p67 ¹⁻¹⁹⁹ with 5,5'-dithiobis-(2-nitrobenzoic acid) (DTNB)	135
5.8.	Absorbance spectra of MDCC-p67 ¹⁻¹⁹⁹	135
5.9.	Interaction of Rac1·GTP with MDCC-p67 ¹⁻¹⁹⁹	136
5.10.	Effect of p67 ¹⁻¹⁹⁹ on the rate of GTP hydrolysis by Rac1	138
6.1	Proposed mechanism for the interaction of unmodified Rac1 and a farnesylated peptide with MDCC-GDI	142
6.2.	C-terminal regions of Rac1 proteins and Rac1 peptide sequences	144
6.3.	Emission spectra of MDCC-GDI	145
6.4.	Effect of BSA on MDCC-GDI fluorescence	147
6.5.	Displacement of MDCC-GDI from a Rac1·MDCC-GDI complex	148
6.6.	The effect of NaCl concentration on the Rac1·MDCC-GDI interaction	150
6.7.	Interaction of Rac1 with farnesyl 12-mer and MDCC-GDI	152
6.8.	Interaction of farnesylated peptides with Rac1 and MDCC-GDI	153
6.9.	Interaction of Rac1·GMPPNP and Q61L Rac1·GTP with MDCC-GDI and farnesyl 12-mer	155
6.10.	Interaction of full length rac1 with MDCC-GDI and farnesyl 12-mer	157
6.11.	Inhibition of nucleotide exchange by GDI and farnesyl 12-mer	159
Table 6.1.	The effect of GDI and 12-mer peptides on the rate of Rac1 nucleotide exchange	159
6.12.	Interaction of cdc42 with farnesyl 12-mer and MDCC-GDI	161
6.13.	The interaction of N-Ras with MDCC-GDI and farnesyl 12-mer	162
6.14.	Effect of GDI on Rac1·mantGDP fluorescence	164
Table 6.2.	Dissociation constants for Rac1 mutants from MDCC-GDI	166
6.15.	Interaction of I33D and F37E Rac1 mutants with MDCC-GDI	167
6.16.	Effect of GDI and farnesyl 12-mer on the rate of GDP dissociation from I33D Rac1	168
6.17.	Binding studies using a farnesylated Rac1 C terminal 9-mer	170
6.18.	Diagram of the stopped flow apparatus	173
6.19.	Kinetics of the Rac1·MDCC-GDI interaction	174
Scheme 6.1.	Kinetic mechanism of Rac1 binding to MDCC-GDI	176
6.20.	Displacement kinetics (k_{+2}) of MDCC-GDI from a complex with Rac1	178

ABBREVIATIONS

BSA	= Bovine serum albumin
DMF	= dimethylformamide
DTNB	= 5,5'-dithiobis(2-nitrobenzoic acid)
DTT	= dithiothreitol
EDTA	= ethylenediaminetetraacetic acid
FAD	= flavin adenine dinucleotide
FCS	= Foetal calf serum
FPLC	= fast performance liquid chromatography
GAP	= GTPase activating protein
GMPPNP	= guanosine-5'-($\beta\gamma$ -imino) triphosphate
GST	= Glutathione-S-transferase
HPLC	= high performance liquid chromatography
IPTG	= isopropylthio- β -D-galactoside
JNK	= c-Jun N-terminal kinase
Mant	= 2'(3')O-(N-methylanthraniloyl)
MAPK	= mitogen activated protein kinase
MDCC	= N-2-I-(maleimidyl)ethyl-7-(diethylamino)coumarin-3-carboxamide
NADPH	= Reduced nicotinamide dinucleotide phosphate
PBP	= <i>E.coli</i> phosphate binding protein
PIP-2	= Phosphatidyl inositol 4,5-bisphosphate
PIP-5 kinase	= PtdIns-4-P 5-kinase
PFUs	= plaque forming units
PMSF	= phenylmethanesulphonyl fluoride
TAE	= 40mM Tris-acetate pH 7.4, 1mM EDTA
TCEP	= tris(2-carboxyethyl) phosphine hydrochloride
TE	= 10mM Tris-HCl pH 7.6, 1mM EDTA
TEAB	= tetraethylammonium bromide
TEMED	= <i>N, N, N', N'</i> -Tetramethylethylenediamine
TFA	= Trifluoroacetic acid
TNBSA	= 2,4,6 – Trinitrobenzene sulphonic acid
TPR	= tetracoipeptide repeat
DDIW	= Distilled deionised water.

ABSTRACT

Rac is a small G protein with a number of signalling roles. Along with other members of the Rho family of small GTPases, it is involved in the control of the actin cytoskeleton (Hall, 1992) and an apparently separate role in the activation of the NADPH oxidase, an enzymatic mechanism in phagocytes which forms superoxide in response to bacterial infection. In an inactive state, Rho family proteins exist in a complex with a second cytosolic protein, Rho guanine nucleotide dissociation inhibitor, RhoGDI. Activation causes dissociation of the Rac·GDI complex and movement of Rac to the membrane.

Spectroscopic studies have been used to investigate the interaction of Rac1 with other molecules, such as p67^{phox}, a component of the NADPH oxidase complex. Complexes of rac1 with 2'(3')O-(*N*-methylanthraniloyl) (mant) fluorescent nucleotide analogues (eg. mantGDP) have been used to try to develop methods to study the interaction of Rac1 and p67^{phox}. Although a previous report indicates a fluorescent change when Rac1 (complexed to a fluorescent nucleotide analogue) is incubated with p67^{phox}, these experiments could not be repeated. A number of other approaches have been taken to develop a system to monitor the interaction of Rac and p67^{phox}.

Fluorescent approaches have also been developed to study the interaction of Rac and RhoGDI. GDI has previously been labelled with the fluorophore *N*-[2-1-(maleimidyl)ethyl]-7-(diethylamino)coumarin-3-carboxamide (MDCC) on a single cysteine in our laboratory and shows a large fluorescence decrease on Rac binding. Rac requires a lipid modification at the C-terminus to interact with RhoGDI, which presents a number of experimental difficulties. A system has been developed using C-terminally truncated (*E.coli* expressed) Rac and a farnesylated C-terminal peptide that mimics full length Rac1 that has been lipid modified *in vivo* (Newcombe *et al.*, 1999). We are currently using this system to study the interaction of Rac1 with GDI and a number Rac1 point mutants have been made in the major regions of divergence between Ras superfamily proteins, based on the crystal structure of Rac1 (Hirshberg *et al.*, 1997). In addition, a Rac1/H-Ras chimaeric protein has been made and expressed in this laboratory. Results indicate that a region of the Rac1 effector loop is important for the Rac1·GDI interaction, with mutations in the insertion loop of Rac1 having little or no effect on the affinity of the Rac1·GDI interaction (Newcombe, Hunter & Webb, unpublished results).

In addition, the interaction of Rac1 with a number of novel fluorescent nucleotide analogues including 3'-O - [N - [2 - (7 - diethylaminocoumarin - 3 - carboxamido) ethyl] carbamoyl] GTP (cou-edaGTP) and coumarin343-edaGTP (but-edaGTP) have been tested, and Rac1 complexes have shown that the rate of nucleotide hydrolysis and exchange by Rac1 shows them to be good analogues of GTP. It is hoped that these analogues will be useful to study the interaction of Rac1 with other proteins, such as GDI and p67^{phox}.

1. INTRODUCTION

1.1. G proteins

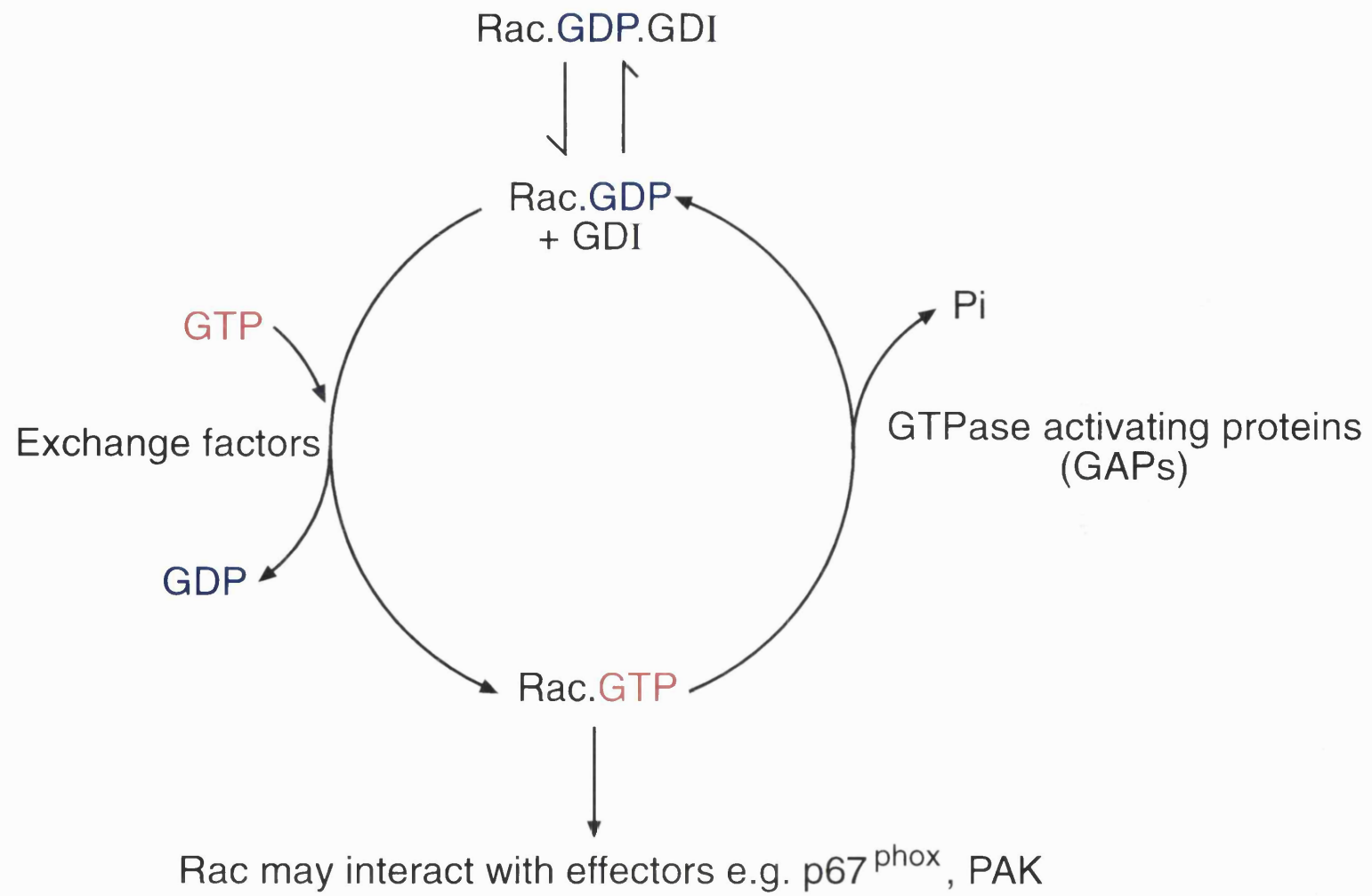
In mammalian tissues, two classes of GTP-binding proteins involved in cell signalling have been identified. One class is the heterotrimeric G proteins, consisting of α , β and γ subunits. The α subunits (39,000-52,000 Da) bind and hydrolyse GTP. The second class is the small G proteins with Mr values of 20,000-30,000. G-proteins act as molecular switches, cycling between GDP and GTP bound conformations. In the GDP bound state, these proteins are usually inactive, whilst in the GTP bound conformation are able to bind to effectors and transmit a signal, such as the initiation of a protein kinase cascade, that transmits a signal from transmembrane receptors to the nucleus to influence gene transcription. The switching function of G proteins in the cell is determined by the differing abilities of its conformational states to interact with specific effector molecules. The biological activity is time-limited by the intrinsic GTPase activity of G proteins. Nucleotide exchange and GTP hydrolysis are catalysed by guanine nucleotide exchange factors and GTPase activating proteins (GAPs) respectively (figure 1.1.).

1.1.1. The Rho family of small G proteins

H-Ras was the first small G protein to be characterised at the molecular level (Shih *et al.*, 1979, Chang *et al.*, 1984). Ras proteins (H, K and N Ras) are ubiquitous in eukaryotes, and have become proteins of special interest as mutations in mammalian Ras genes cause cellular transformation. Ras mutations are found in ~30% of human tumours (Barbacid, 1987). The Ras superfamily of small G proteins is composed of a number of families that includes Ras, Rho, Rab and Arf. The Ras superfamily regulates gene expression directly through MAP kinase cascades (Burgering *et al.*, 1995), the Rho family is mainly involved in re-organisation of the actin cytoskeleton (Hall, 1998), Rab (Martinez & Goud, 1998) and Arf (Moss & Vaughan, 1995) families regulate intracellular vesicle trafficking and the Ran family regulates nuclear transport (Moore, 1998). Members of the Rho family were first discovered during the search for proteins homologous to the Ras proto-oncogene, but were shown to have quite

Figure 1.1. The GTPase cycle of Rac1 and its regulators

The conformational change accompanying GTP hydrolysis allows GTPases such as Rac1 to function as molecular switches in a variety of cellular processes. Interaction with effectors usually occurs when the protein is in the GTP bound conformation. GTP hydrolysis and nucleotide exchange occur in vitro at a very low rate but are catalysed in vivo by GTPase activating proteins (GAPs) and guanine nucleotide exchange factors, respectively. In the case of Rho and Rab families, GDP dissociation inhibitors (GDIs) stabilise the GDP bound conformation.



distinct roles from Ras. At least 12 members of the Rho family have been identified (Aspenström, 1999), and mammalian isoforms include RhoA (A, B and C isoforms), Rac (1, 2 and 3 isoforms), cdc42 (cdc42Hs and G25K isoforms), RhoG and TC10, with Rac1, RhoA and cdc42Hs the most studied family members (Symons, 1996). The two mammalian cdc42 isoforms differ by 9 amino acids (Shinjo *et al.*, 1990) and are splice variants with different C terminal sequences. Rho proteins are primarily involved in the organisation of the cytoskeleton. Polymerised actin (associated with myosin filaments and other proteins) is assembled into a variety of distinct structures such as lamellipodia, filipodia and stress fibres (Hall, 1992) which are controlled by members of the Rho family in all eukaryotic cells. Recent evidence has also suggested a role for these proteins in the control of cell proliferation. Rac and Rho are essential for transformation by Ras, and reports indicate that active Rac mutants are sufficient to cause malignant transformation of rodent fibroblasts (Qui *et al.*, 1995). Rac and cdc42 also bind and activate an increasing number of protein kinase cascades, such as JNK and p38 MAP kinase pathways. Rac also activates the NADPH oxidase in phagocytes; an enzyme complex used to produce O_2^- to destroy engulfed pathogens. Through interactions with multiple targets, Rho family proteins are able to co-ordinate a variety of diverse cellular functions, and these will be discussed in the following sections. Rho proteins are found in a variety of locations in the cell and it has been proposed that these proteins cycle on and off the plasma membrane. A second cytosolic protein, called a guanine nucleotide dissociation inhibitor (GDI) is an excellent candidate for regulating such cycling (Nomanbhoy *et al.*, 1996).

1.1.2. Rac Proteins

The Rac family of proteins comprises of Rac1, Rac2 (Didsbury *et al.*, 1989) and a recently discovered Rac3 (Haataja *et al.*, 1997). All three proteins have ~ 90% sequence similarity with one another, with the greatest divergence between the C-terminal residues 180-192 (figure 1.2.). They have ~58% sequence similarity with Rho proteins and 26-30% similarity with Ras. Most G proteins hydrolyse GTP to GDP very slowly. Rac is the notable exception

Figure 1.2. Sequence alignment of some of the Rho and Ras sub-family proteins

Protein sequences were aligned using the Clustal method with the PC program DNASTar (v3.12). Residue numbering for individual proteins is shown on the far right and residues in the majority of aligned sequences are shown above the solid line. The effector loop (residues 30-40 of Rac1) is shown in green, the insertion loop of Rho sub-family proteins (residues 120-137 of Rac1) is shown in red.

	MQA-----	IKLVVVVGDAVGKTCLLISYTTNAPPEEYVPTV	
	10	20	30
H-RAS	MTE-----	YKLVVVVGAGGVGKSALT	QLIQNHFVDSYDPTI 36
K-RAS	MTE-----	YKLVVVVGAGGVGKSALT	QLIQNHFVDEYDPTI 36
N-RAS	MTE-----	YKLVVVVGAGGVGKSALT	QLIQNHFVDEYDPTI 36
RAC1	MQA-----	IKCVVVVGDAVGKTCLLISYTTNAP	PEEYIPTV 36
RAC2	MQA-----	IKCVVVVGDAVGKTCLLISYTTNAP	PEEYIPTV 36
RAC3	MQA-----	IKCVVVVGDAVGKTCLLISYTTNAP	PEEYIPTV 36
RHOA	M-----	AAIRKKLVIVGDGACGKTCLLIVFSKDQFP	PEYVPTV 38
RHOB	M-----	AAIRKKLVVVGDGACGKTCLLIVFSKDQFP	PEYVPTV 38
RHOC	M-----	AAIRKKLVIVGDGACGKTCLLIVFSKDQFP	PEYVPTV 38
RHOG	MQS-----	IKCVVVVGDAVGKTCLLICYTTNAP	PEEYIPTV 36
TC10	MPGAGRSSMAHGPGALMLKCVVVVGDAVGKTCLLMSYANDAFP	PEYVPTV 50	
CDC42HS	MQT-----	IKCVVVVGDAVGKTCLLISYTTNKFP	PEYVPTV 36

	FDNYSAQVMVDGKTVLLGLWD	TAGQEDYDRLRPLSY	PQTDVFLICFSIVS	
	60	70	80	90
H-RAS	EDSYRKQVV	IDGETCLLD	ILDTAGQEEYSAMRDQYMR	TGEGFLCVFAINN 86
K-RAS	EDSYRKQVV	IDGETCLLD	ILDTAGQEEYSAMRDQYMR	TGEGFLCVFAINN 86
N-RAS	EDSYRKQVV	IDGETCLLD	ILDTAGQEEYSAMRDQYMR	TGEGFLCVFAINN 86
RAC1	FDNYSANVMVDGKPVNLGLWD	TAGQEDYDRLRPLSY	PQTDVFLICFSIVS 86	
RAC2	FDNYSANVMVDGKPVNLGLWD	TAGQEDYDRLRPLSY	PQTDVFLICFSIVS 86	
RAC3	FDNYSANVMVDGKPVNLGLWD	TAGQEDYDRLRPLSY	PQTDVFLICFSIVS 86	
RHOA	FENYVADIEVDGKQVELALWD	TAGQEDYDRLRPLSY	PDVILMCF9IDS 88	
RHOB	FENYVADIEVDGKQVELALWD	TAGQEDYDRLRPLSY	PDVILMCF9IDS 88	
RHOC	FENYVADIEVDGKQVELALWD	TAGQEDYDRLRPLSY	PDVILMCF9IDS 88	
RHOG	FDNYSAQSAVDGRTVNLNLWD	TAGQEEYDRLRPLSY	PQTNVFCFSIAS 86	
TC10	FDKYAVSVTVGGKQYLLGLYD	TAGQEDYDRLRPLSY	PMTDVFICFSVNN 100	
CDC42HS	FDNYAVTVMIGGEPYTLGLFD	TAGQEDYDRLRPLSY	PQTDVFLVCF9SVS 86	

	PASFENVREKVVPEVKHH--	CPNVPIILVGT	KKDLRDDTDTIEELAEMKQ	
	110	120	130	140
H-RAS	TKSFEDIHQ-YREQIKRVKDSDDVPMVLVGNKCDLAART-----			125
K-RAS	TKSFEDIHQ-YREQIKRVKDSDDVPMVLVGNKCDLPST-----			125
N-RAS	TKSFADINL-YREQIKRVKDSDDVPMVLVGNKCDLPST-----			125
RAC1	PASFENVRAKWPPEVRHH--	CPNTPIILVGT	KKDLRDDKDTIEKLKEKKL 134	
RAC2	PASYENVRAKWPPEVRHH--	CPSTPIILVGT	KKDLRDDKDTIEKLKEKKL 134	
RAC3	PASFENVRAKWPPEVRHH--	CPHTPIILVGT	KKDLRDDKDTIEKLKEKKL 134	
RHOA	PDSLENIPEKWTPEVKHF--	CPNVPIILVGNKCDLRNDEHTRRELAKMKQ 136		
RHOB	PDSLENIPEKWTPEVKHF--	CPNVPIILVANKCDLRNDEHVRTELAKMKQ 136		
RHOC	PDSLENIPEKWTPEVKHF--	CPNVPIILVGNKCDLRNDEHTRRELAKMKQ 136		
RHOG	PPSYENVVRHKKWPEVCHH--	CPDVPIILVGT	KKDLRAQPDTLRLKKEQGO 134	
TC10	PASFNQVKEEWPELKEY--	APNVPFLLIGTQIDLRDDPKTLARLNOMKE 148		
CDC42HS	PSSFENVKEKWPPEITHH--	CPKTPFLLVGT	QIDLRDDPKSTIEKLAKKNKO 134	

	APVTTEQGQALAKEIGAVKYLECSALTQGGVKTVPDEAIRAV---	LCP-	
	160	170	180
H-RAS	--VESRQAQDLARSYG-IPYIETSAKTRQGVEDAFYTLVREIRQHKLRLK 171		
K-RAS	--VDTKQAQDLARSYG-IPFIETSAKTRQGVEDAFYTLVREIRQYRLKKI 171		
N-RAS	--VDTKQAHLAKSYG-IPFIETSAKTRQGVEDAFYTLVREIRQYRMKKL 171		
RAC1	TPITYPQGLAMAKEIGAVKYLECSALTQGLKTVFDEAIRAV---	LCPP 180	
RAC2	APITYPQGLALAKEIDSVKYLECSALTQGLKTVFDEAIRAV---	LCPP 180	
RAC3	APITYPQGLAMAREIGSVKYLECSALTQGLKTVFDEAIRAV---	LCPP 180	
RHOA	EPVKPEEGRDMANRIGAPGYMBCSAKTKDGVREVPEMATRAA---	L--- 180	
RHOB	EPVRTDDGRAMAVRIQAYDYLECSAKTKEGVREVPEMATRAA---	L--- 180	
RHOC	EPVRSEEGRDMANRISAFGYLECSAKTKEGVREVPEMATRAG---	L--- 180	
RHOG	APITPQGGQALAKQIHAVRYLECSALQQDGVKEVFAEAVRAV---	LNPT 180	
TC10	KPICVEQGQKLAKAIGACCYVECSALTQKGLKTVFDEAIIAI---	LTPK 194	
CDC42HS	KPIPTETAEXKLARDLKAVKYVECSALTQKGLKNVFDEAILAA---	LEP- 180	

	PVKKGKRK-----	CVLL-	
	210	220	
H-RAS	NPPDESGPGCMSCK-CVLSF		190
K-RAS	-SKEEKTPGCVKIKKCIIMF		190
N-RAS	NSSDDGTQGCMLP-CVVMF		190
RAC1	PVKKRKRK-----	CLLL	192
RAC2	PTQQKRA-----	CSLL	192
RAC3	PVKKPGKK-----	CTVF	192
RHOA	QARRGKKK-----	SGCLVL	193
RHOB	QKRYGSQNG-----	CINCKVL	196
RHOC	QVRKNKRR-----	RGCPIL	193
RHOG	PIKR-GRS-----	CILLY	192
TC10	KHTVKKRIGSRCINCLITV		214
CDC42HS	PEPKKSRR-----	CVLL	191

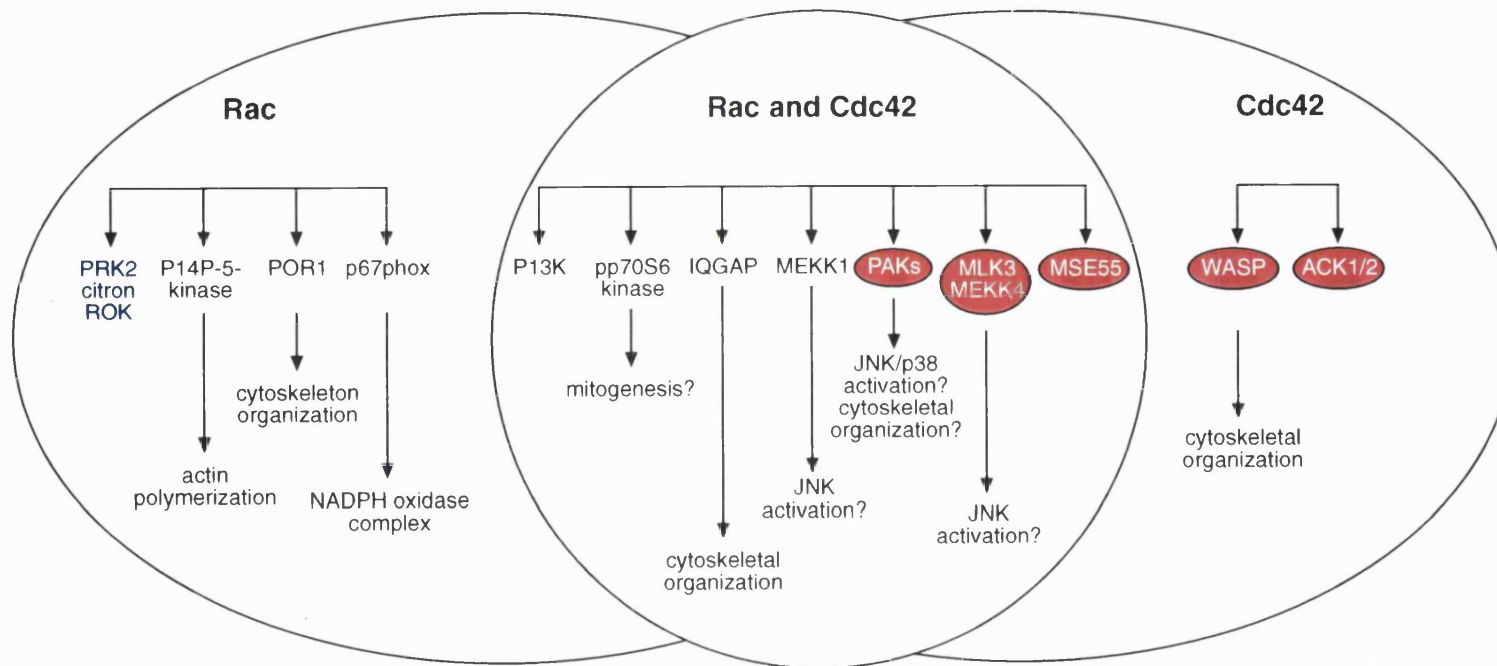
having hydrolysis rates of at least 50-fold those of Ras and Rho (Chuang *et al.*, 1993). One difference between the Rac1 and Rac2 isoforms appears to be in their tissue distribution; Rac2 is found predominantly in haematopoietic cells, whereas Rac1 seems to be more ubiquitously expressed (Dorseuil *et al.*, 1996). A number of human Rac-interacting effectors and regulators have been identified (figure 1.3.). Regulatory proteins include α -chiamerin, that shows GAP activity specific for Rac, Bcr, Abr and IQ-GAP that show GAP activity towards Rac and cdc42, (Kuroda *et al.*, 1996) and RhoGAP that has GAP activity towards most Rho family proteins (Ridley *et al.*, 1993). Rac participates in signal transduction from the membrane to the nucleus by at least two distinct mitogen-activating protein kinases. These include the JNK/stress activated protein kinase pathway (Teramoto *et al.*, 1996).

1.2. Regulation of actin polymerisation by Rho family proteins

The first indication of the role of Rho family proteins in cytoskeletal re-organisation was obtained from microinjection of bacterial toxins into cultured cells (that inactivate RhoGTPases) that resulted in rounding and dissolution of actin fibres in the cells (Rubin *et al.*, 1988, Chardin *et al.*, 1988). Microinjection of a constitutively active Rho mutant into Swiss 3T3 cells resulted in finger-like processes extending at the periphery of the cells, with the actin fibres originating from processes known as focal adhesions or focal contacts and extend across the cell (Ridley *et al.*, 1992). Microinjection of constitutively active Rac and cdc42 also cause distinct phenotypic changes. Both proteins induce the formation of different types of cytoskeletal organisation – Rac induces ‘lamellipodia’ with membrane ruffles, and cdc42 induces ‘filipodia’ with actin microspikes (Tapon & Hall, 1997). It has been shown that such morphological changes occur in a defined sequence in the cell – cdc42 induced filipodia, followed by Rac dependent membrane ruffles, the Rho dependent stress fibre formation. It is likely that sequential activation of Rho GTPases occurs – cdc42 \rightarrow Rac \rightarrow Rho (Tapon & Hall, 1997). Microinjection studies have also shown that Ras can also induce Rac dependent membrane ruffles, then Rho dependent stress fibre formation, indicating an additional GTPase cascade from Ras \rightarrow Rac \rightarrow Rho (Bar-Sagi & Feramisco, 1986).

Figure 1.3. A number of mammalian effectors of Rac and cdc42

Rac and cdc42 share a variety of effector molecules and play a role in multiple biological processes. The PAKs, MLK3, MEKK4, MSE55, WASP and ACKs share a common cdc42/Rac interacting domain (CRIB), shown in red. PRK2, citron and ROK also interact with Rho (Jeanteur, 1999).



The signalling pathways utilised by Rho GTPases to mediate cytoskeletal re-organisation remain unclear. Reports by Mullins *et al.* (1998) have shown that a seven protein complex is essential for the organisation of actin structures. This complex contains two actin-related binding proteins, Arp2 and Arp3, and it has been suggested that this complex may initiate and play a regulatory role in the formation of actin structures, such as lamellipodia (sheets) and filipodia (spikes). The Arp2/3 complex was first identified in *Acanthamoeba*, and is conserved from yeast to mammals (Machesky *et al.*, 1994). In human fibroblasts, the complex is located at the leading edge of the cell membrane – an ideal position to control actin polymerisation required for motility. The Arp2/3 complex has been shown to ‘seed’ or nucleate filaments to polymerise from their barbed ends. Mullins *et al.* (1998) have proposed a model for the regulation of actin polymerisation. It is thought that the Arp2/3 complex ‘caps’ the pointed end of the actin filament, allowing elongation of the barbed (fast growing) ends. In vitro data also suggests that the Arp2/3 complex also initiates actin filaments to elongate from the sides of pre-existing filaments to form a branched network of actin.

Among the best candidates for mediating the effects of Rho proteins on the actin cytoskeleton are the Wiscott-Aldrich Syndrome proteins (WASPs) which were originally identified as proteins mutated in patients with this syndrome (Derry *et al.*, 1994). The WASP family is composed of two homologous proteins – WASP and N-WASP. WASP is expressed in haematopoietic cells, whereas N-WASP is more ubiquitously expressed. Both isoforms contain several protein binding domains, including a GBD domain. WASP family proteins interact with cdc42, but only weakly interact with Rac and not at all with Rho isoforms (Ramesh *et al.*, 1999). A recent report has shown that the C-terminus of N-WASP binds to the Arp2/3 complex, stimulating its ability to nucleate actin polymerisation (Rohatagi *et al.*, 1999). This provides a direct connection between signalling pathways mediated by cdc42 and cytoskeletal re-organisation. Research by Takenawa’s group has recently identified a novel member of the WASP family. WASP family verprolin – homologous protein (WAVE) induces the formation of actin clusters, and expression of a dominant active Rac mutant

induced the translocation of WAVE from the cytosol to membrane ruffling areas (Miki *et al.*, 1998). WAVE may play a critical role downstream of Rac in the regulation of the cytoskeleton. Whether WAVE interacts with components of the Arp2/3 complex has yet to be determined.

It has been suggested that the Rac-interacting protein, IQGAP may also play a role in cytoskeletal re-organisation. IQGAPs 1 and 2 share the same domain structure and ~62% sequence identity (Brill *et al.*, 1996 & McCallum *et al.*, 1996). IQGAP1 is liver specific, whereas IQGAP2 is more ubiquitously expressed. Both isoforms interact with Rac and cdc42 in the GTP bound forms, and although they contain a region at the C terminus homologous to RasGAP, IQGAPs do not interact with Ras or catalyse GTP hydrolysis of Rac or cdc42. Contrary their name, IQGAPs inhibit GTP hydrolysis of Rac and cdc42, maintaining these proteins in an active (GTP) bound state. Both IQGAP isoforms also fail to bind to Rho (Brill *et al.*, 1996, Hart *et al.*, 1996). IQGAPs bind to Rac and cdc42 through their C terminal domain, and also contain regions that interact with calmodulin (Joyal *et al.*, 1997) and actin (Bashour *et al.*, 1997). Recently it has been shown that calmodulin is able to modulate the interaction between IQGAP and cdc42.

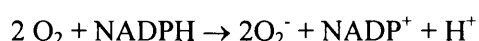
1.2.1. Other Rho targets involved in cytoskeletal control

GTP γ S-loaded Rho added to lysates of C3H fibroblasts has shown to increase the activation of PIP-5 kinase and Rac has been shown to interact with PIP-5 kinase in vitro and in vivo (Tolias *et al.*, 1995). This interaction is of particular importance as the product formed from PIP-5 kinase activation, PIP-2, binds to a variety of actin binding proteins and is thought to regulate actin filament assembly by uncapping barbed ends of actin filaments and releasing actin monomers (DiNubile & Huang, 1997, Schafer *et al.*, 1996). Rac has recently been shown to mediate thrombin-induced phosphoinositide formation in permeabilised platelets, which in turn triggered actin filament elongation (Hartwig *et al.*, 1995). However, the role of PIP-2 in

controlling cytoskeletal reorganisation via the action of Rho family proteins in intact cells remains controversial.

1.3. Rac and the NADPH oxidase system

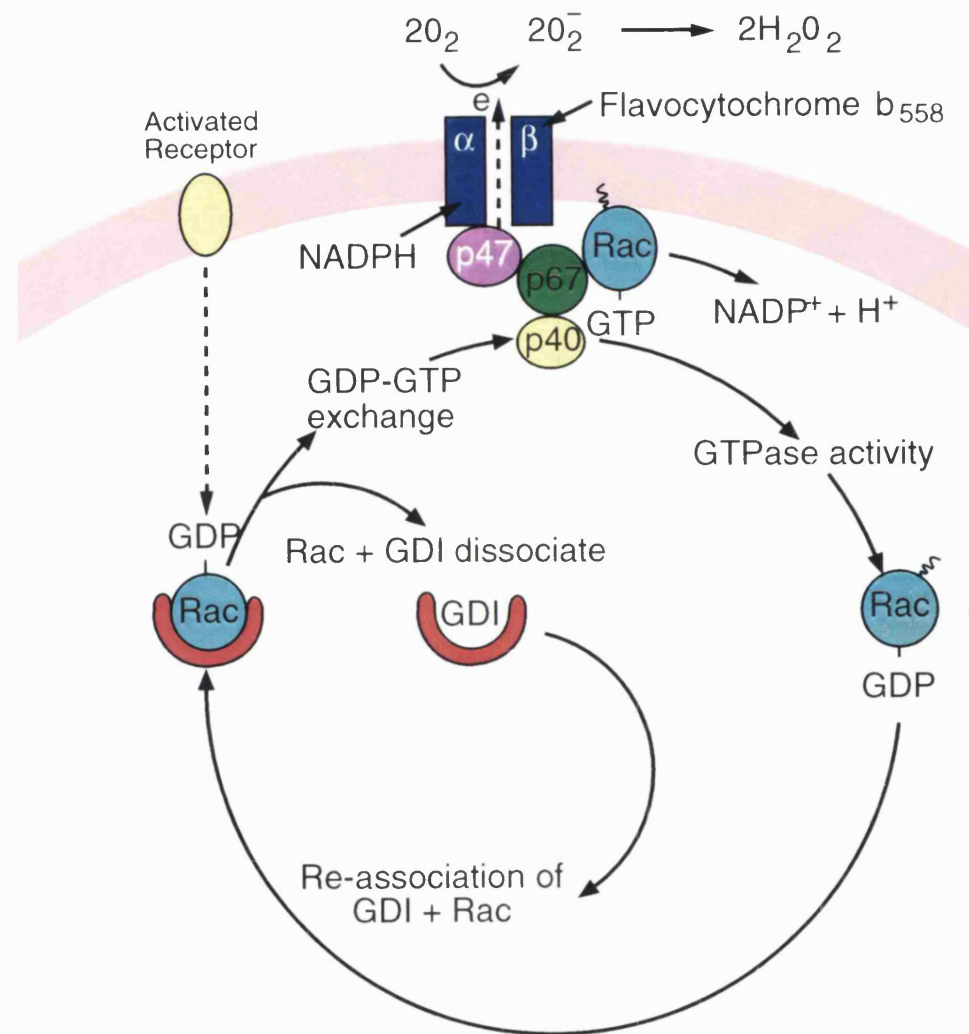
Rac proteins have an apparently independent role from other Rho family proteins in the activation of a multi component enzyme known as the NADPH oxidase. This is a mechanism used by phagocytic cells such as macrophages to destroy engulfed pathogens. Invading micro-organisms (coated in immunoglobulins and complement) (Segal, 1996) bind to receptors on macrophages and are engulfed to form a phagocytic vacuole. Stimuli such as this typically act in through trimeric G protein coupled receptors that result in secondary events such as a rise in Ca^{2+} , activation of serine/threonine and tyrosine kinases. The signal transduction pathways leading to the activation of the NADPH oxidase are not fully understood. Phagocytic cells have a number of responses to a variety of physiological stimuli and it is very difficult to identify individual pathways involved in the activation of the NADPH oxidase. The NADPH oxidase is used to form superoxide (O_2^-) which is subsequently converted to other reactive oxygen species such as H_2O_2 in phagocytic vacuoles that may be used to destroy engulfed pathogens (Segal & Shatwell, 1997).



The most likely reason for the complexity of the NADPH oxidase is due to the potentially harmful effects of reactive oxygen metabolites. It is essential that products of the NADPH oxidase be confined to the phagocytic vacuole to prevent normal cellular damage. Following activation of the cell, Rac and GDI dissociate, and Rac translocates to the membrane to form a cytosolic complex with three other phagocyte oxidase (phox) components called p67^{phox} , p47^{phox} and p40^{phox} . Assembly of this complex activates a membrane bound flavocytochrome b to produce O_2^- . (figure 1.4.).

Figure 1.4. Activation of the NADPH oxidase

A diagram showing the assembly of the NADPH oxidase components at the membrane of an activated macrophage. Following activation of the cell, Rac dissociates from its guanine nucleotide dissociation inhibitor (GDI) and translocates to the membrane to form a complex with other phagocyte oxidase components. Rac interacts with p67^{phox}, but the precise interactions between the oxidase components are not fully understood. The complex stimulates the flavocytochrome to produce superoxide until the response is terminated. The precise mechanisms for termination are poorly understood, but may be mediated by GTPase activity of Rac and dissociation from the complex. p40, p47 and p67 shown here represent phagocyte oxidase (phox) components.



1.3.1. The electron transporter of the NADPH oxidase

The electron transport chain that generates superoxide is a membrane bound flavocytochrome b (known as b₅₅₈ or b₂₄₅) incorporated into the wall of the phagocytic vacuole. The flavocytochrome is composed of two subunits; p21^{phox} (or the α subunit) containing 195 amino acids and gp91^{phox} (β subunit) containing 570 amino acids. The β subunit (gp indicates that this sub-unit is glycosylated, 91 is the approximate molecular weight) contains the main structural components of the NADPH oxidase. This makes this cytochrome unusual as most mammalian cytochromes are composed of a single polypeptide chain, about the size of the α subunit. The β subunit is comprised of two domains, a hydrophobic N-terminus that is likely to form 4-5 transmembrane helices, and a hydrophilic C-terminus that is probably cytosolic (Imajoh-Ohmi *et al.*, 1992). This hydrophilic region is believed to be a soluble, globular domain that has binding sites for NADPH and FAD to which electrons are passed. Electrons are transferred to two hemes (attached to one or both sub-units) located in the transmembrane domain (Quinn *et al.*, 1992, Yu *et al.*, 1998) then to molecular oxygen to produce superoxide (O₂⁻). Whether the two electrons pass independently or sequentially to the two hemes remains to be determined. The α subunit of the flavocytochrome is thought to be attached to the membrane via two transmembrane helices, with a hydrophilic, proline rich C-terminal region. This region is thought to bind cytosolic factors, but the precise role of this subunit has yet to be established. Binding of cytosolic factors to the α subunit suggests that p21^{phox} may induce a conformational change in the flavocytochrome favourable for NADPH binding and electron transport.

1.3.2. Activation of the NADPH oxidase

Due to the complexity of the NADPH oxidase, the precise mechanism of activation is not fully understood. The genes encoding the cytosolic components p67^{phox}, p47^{phox} and p40^{phox} have been cloned and sequenced, but the primary sequences show no indication for a structural role in the NADPH oxidase, or structural similarities to any other known protein. All of the phox components contain Src homology 3 (SH3) domains. This is a well-defined

domain first characterised in the oncoprotein Src. This domain binds to proline rich domains on other proteins and has been shown to have a role in directing signalling proteins to intracellular receptors. In addition, p47^{phox} contains a number of recognition sites for protein kinases. (Johnson *et al.*, 1998). The phosphorylation target of p47^{phox} is known to be a group of serine residues (aa's 303-379) in the C-terminal half of the protein (Park, 1999). Upon activation of the cell, p47^{phox} becomes phosphorylated on up to 9 serine residues, with only the most acidic isoforms associated with the membrane. In vitro binding studies suggest that the three phox proteins bind to one another by SH3-proline rich regions (McPhail, 1994, DeMendez *et al.*, 1994). p67^{phox} and p40^{phox} are in a tight association in the cytosol, with p47^{phox} more loosely associated with the p67-p40^{phox} complex. It is thought that upon activation, p67^{phox} (El Benna *et al.*, 1997), p47^{phox} (Johnson *et al.*, 1998, Park & Baboir, 1997) and p40^{phox} (Fuchs *et al.*, 1997) become phosphorylated. p47^{phox} is then thought to bind to the flavocytochrome b (Nakanishi *et al.*, 1992), with p67^{phox} interacting with the p47^{phox}-flavocytochrome complex. p67^{phox} is also thought to interact with a small region of α helix that covers the nucleotide binding site of the flavocytochrome and this interaction has also been implicated in the mechanism of activation (Leusen *et al.*, 1994). Although the precise role of phosphorylation in the activation of the NADPH oxidase is not clear, this indicates that at least one kinase may have a regulatory role in this system.

In addition to the three cytosolic factors p67^{phox}, p47^{phox} and p40^{phox}, the GTP binding protein Rac in an activated (GTP) state (predominantly Rac2 in haematopoietic cells) is essential for activation of the NADPH oxidase. Rac has been shown to interact with a region within the N-terminal 199 amino acids of p67^{phox} (Ahmed *et al.*, 1998, Diekmann *et al.*, 1994). Experiments using peptides spanning the amino acid sequence of Rac1 have shown that several groups of peptides inhibit the NADPH oxidase in a cell free system, but showed no inhibitory effect when added 1 minute after activation of the oxidase (Joseph & Pick, 1995). This suggests that Rac1 forms contacts with a number of components during assembly of the NADPH oxidase. A recent report has shown that both Rac2 and cdc42 bind to an additional site at the C-

terminus of p67^{phox} (Faris *et al.*, 1998). This suggests that cdc42 may interact with p67^{phox} under certain conditions, but is unable to activate the oxidase. Rac is likely to act as a switch, with the hydrolysis of bound GTP to GDP further regulating the activity of the NADPH oxidase.

The small G protein Rap1A has also been reported to co-purify and cross-immunoprecipitate with the flavocytochrome b and has also been shown to increase NADPH oxidase activity 4 fold when overexpressed in HL-60 cells (Gabig *et al.*, 1995). In Neutrophils, Rap1A has shown to be phosphorylated on Ser¹⁸⁰. This phosphorylation prevents the interaction with the cytochrome b (Bokoch *et al.*, 1991). The precise role of this additional small G protein in the regulation of the NADPH oxidase has yet to be established. Research by Fujii *et al.* (1997) has shown that nitric oxide (NO) has also been shown to dose-dependently inhibit superoxide generation of the NADPH oxidase, but showed no inhibition after activation. The precise role of NO in the assembly of the NADPH oxidase has yet to be established, although the actions of NO may be mediated at least in part by peroxynitrite. This may be generated by the reaction of nitric oxide with superoxide, both produced in inflammatory tissues. Peroxynitrite has been shown to inhibit the binding of the fluorescent nucleotide analogue, mantGDP to Rac2 in a dose dependent manner (Rohn *et al.*, 1999), and this is thought to occur by peroxynitrite-mediated tyrosine modification of Rac2 (Rohn *et al.*, 1999, Ischiropoulos & al-Mehdi, 1995).

1.3.3. Role of the cytoskeleton in the NADPH oxidase

The control of the cytoskeleton may also play an important role in the regulation of the NADPH oxidase. The NADPH oxidase is activated at specific regions of the plasma membrane surrounding the phagocytic vacuole. It is not clear what regulates the localisation of the NADPH oxidase, but it is possible that cytoskeletal changes that result in the formation of the phagocytic vacuole are also involved in localising the activation. p67^{phox} is also thought to interact with the cytoskeleton, as it remains in the insoluble pellet after the cell has

been permeabilised with detergents (Woodman *et al.*, 1991). Binding studies have also shown that coronin, an actin binding protein, interacts with the C terminal half of p47^{phox} (Grogan *et al.*, 1997). The role of Rho family proteins in the control of the actin cytoskeleton also suggests that cytoskeletal changes may be important.

1.3.4. The cell-free, in vitro NADPH oxidase system

Many of the recent advances in the understanding of the activation of the NADPH oxidase comes from studies using a cell free NADPH oxidase system (Abo *et al.*, 1992). This in vitro system uses neutrophil membranes (containing the flavocytochrome) and three cytosolic factors p67^{phox}, p47^{phox} and Rac. The oxidase component p40^{phox} is not required in the cell free assay and the in vivo role of this protein is currently unknown. However, it is thought to play a role in stabilising p67^{phox} in intact cells as it forms a 1:1 complex with p67^{phox} and translocates to the membrane in a flavocytochrome dependent manner (Wientjes *et al.*, 1993). It is possible that p40^{phox} forms a bridge between the oxidase components and the cytoskeleton, or it may act as a regulatory molecule, preventing p67^{phox} and other cytosolic components from interacting. This system is activated by Rac in the GTP bound conformation (using Rac complexed to non-hydrolysable nucleotide analogues GTPγS or GMPPNP) and an amphiphilic reagent such as SDS or arachidonic acid. A number of important differences have been observed between the in vivo and in vitro NADPH oxidase activation. In the cell, continuous activation of the oxidase is probably required, such as phosphorylation of p47^{phox} and GTP loading of Rac. Such a dynamic mechanism is not required in vitro. Once the NADPH oxidase complex is assembled, the system remains active. Also, synthetic peptides that reduce NADPH oxidase activity in a cell free system show no affect in vivo (Park *et al.*, 1997b, Leusen *et al.*, 1996). In a cell free system, neither p40^{phox} or Rap1A are required for activation (Abo *et al.*, 1992), and a complex between p67^{phox} and p47^{phox} is also thought not to be essential, as truncated forms of p47^{phox} retain the ability to activate the oxidase in a cell free system (Leusen *et al.*, 1995). The in vitro oxidase system also requires the addition of amphiphiles such as arachidonate or SDS. Research by Swain *et al.* has shown that

amphiphilic reagents induce a conformational change in the structure of p47^{phox} (Swain *et al.*, 1997) similar to the changes induced by phosphorylation in vivo. These results suggest that the dynamic nature of NADPH oxidase activation is lost in a cell free system, and such results may not always be extrapolated to intact cells.

1.4. Role of Rho family proteins in smooth muscle contraction

Rho family proteins have also been shown to play a role in smooth muscle contraction. A rise and fall in intracellular Ca^{2+} levels is the principal stimulus that activates muscle contraction. In striated muscle, Ca^{2+} binds to troponin, a component of the thin filament and induces a conformational change permitting the interaction of the myosin head with actin. In contrast, in vertebrate smooth muscle is activated by a less direct mechanism. Ca^{2+} binds to calmodulin, which binds and activates a myosin light chain kinase (MLCK), which in turn phosphorylates serine 19 of the regulatory light chain (MLC) of smooth muscle myosin. This activates the ATPase mechanism, inducing contraction (reviewed by Somlyo & Somlyo; 1994). Relaxation of smooth muscle is usually initiated by a fall in Ca^{2+} levels and de-phosphorylation of MLC by a protein phosphatase.

Increase Ca^{2+} → MLCK activation → phosphorylation of MLC → smooth muscle contraction

This indirect coupling of contraction to Ca^{2+} allows contraction to be regulated by other mechanisms and the extent of smooth muscle contraction differs depending on the agonist that initially stimulates the contraction. This phenomenon is known as ‘calcium sensitivity’ (Somlyo & Somlyo, 1994). Research by Takai’s laboratory has shown that GTP is involved in calcium sensitivity. When GTP was added to pre-incubated smooth muscle cells, additional contraction was induced at a fixed Ca^{2+} concentration (Hirata *et al.*; 1992). Treatment of cells with bacterial enzymes (that inactivate Rho family G proteins) (Rubin *et al.*; 1988) abolished the GTP induced sensitivity. This could be reversed by the addition of constitutively active, Rho-GTPγS, but not Rho in the GDP bound form (Hirata *et al.*; 1992). Rho has shown to

increase phosphorylated MLC levels by decreasing the rate of dephosphorylation of the light chain (Noda *et al*; 1995) and report has shown that phosphorylation of a regulatory subunit of MLCK phosphatase causes a 5 fold decrease in the activity of this enzyme, and a large increase in calcium sensitivity (Trinkle-Mulcahy *et al*; 1995). However, the precise role of Rho family proteins in smooth muscle contraction remains controversial.

A report has also indicated that a Rho associated kinase (ROK or P160^{ROCK}) can directly phosphorylate MLC on ser 19 (Eyk *et al.*, 1998). Recently it has been shown that a p21 activated kinase (PAK) that is activated by Rac and cdc42 can cause Ca²⁺ independent contraction of smooth muscle fibres by a different molecular mechanism to ROK (Eyk *et al.*, 1998). PAK1 has also been shown to phosphorylate MLCK, resulting in decreased MLCK activity and decreased MLC phosphorylation in some cell types (Sanders *et al.*, 1999). It is possible that MLCK is a target for PAKs, and PAKs may regulate cytoskeletal dynamics (via Rac and cdc42) by decreasing MLCK activity and MLC phosphorylation.

1.5. Role of Rho proteins in cytokinesis

When a cell undergoes cell division, cytokinesis is mediated by a contractile ring of actin formed at a cleavage furrow in the centre of the cell body. Research has shown that microinjection of C3 exoenzyme or RhoGDI into fertilised eggs of *Xenopus laevis* and sea urchin inhibited the formation of the contractile ring. (Kishi *et al*; 1993, Narumiya, 1996). Cytokinesis was aborted, and the contractile ring disappeared. However, nuclear division continued in these cells, resulting in multinucleate eggs. The inhibitory action of RhoGDI in fertilised *Xenopus* eggs was prevented by co-microinjection of RhoGDI with the GTPγS form of RhoA. This suggests that Rho proteins play a role in the formation of the contractile ring during cytokinesis and may induce the formation of different actin structures at specific stages of the cell cycle.

1.6. Rac proteins and gene transcription

Both Rac and cdc42 have been shown to activate at least two distinct sub-groups of mammalian protein kinases called the c-Jun amino (JNK)/stress activated protein kinase (SAPK), and the p38 MAP kinase cascades and influence gene transcription in response to cellular stresses (Mackay & Hall, 1998). Although numerous reports have shown that Rac and cdc42 can activate these pathways, the exact role of these proteins in MAP kinase activation remains unclear. Activated Rac and cdc42 have been shown to modestly activate the JNK pathway, which may be mediated by the activation of PAKs (1.7.) (Zhang *et al.*, 1995), but the exact roles of Rac and cdc42 in this response is poorly understood. Rho, Rac and cdc42 have also been reported to activate serum response factor (SRF)-dependent transcription and activate NF κ B (Sulciner *et al.*, 1996). A Rac target protein called plenty of SH3's (POSH) has been identified by Professor Hall's laboratory. Activation of POSH activates the JNK pathway and nuclear translocation of NF κ B, providing a link between Rac and activation of protein kinase cascades (Tapon *et al.*, 1998). Other possible mediators of the JNK pathway are members of the mixed lineage kinase (MLK) family. These have been shown to directly interact with cdc42 and Rac (Nagata *et al.*, 1998). Lfc, a Rac1 binding protein has also been shown to stimulate JNK activity in COS-7 cells (Glaven *et al.*, 1999) and it has also been suggested that activation of NF κ B may be triggered by reactive oxygen species generated by Rac (Sulciner *et al.*, 1996). Rac, Rho and cdc42 have also been shown to be involved in G₁ cell cycle progression (Lamarche *et al.*, 1996). However, it is possible that this is due to cytoskeletal changes influenced by Rho proteins rather than direct effects on gene transcription. Rac and Rho have also been shown to be essential for transformation by Ras, and reports also indicate that Rac mutants are sufficient to cause malignant transformation of rodent fibroblasts (Qui *et al.*, 1995).

1.7. The activation of p21 Activated Kinases (PAKs) by Rac1

In their GTP bound forms, both Rac1 and cdc42 bind to and stimulate the activation of a group of Ser/Thr kinases in mammalian cells called p21-activated kinases (PAKs) (Daniels &

Bokoch, 1999). The PAK family of proteins was first identified for their ability to interact with the activated (GTP) bound forms of Rac1 and cdc42 and no other Ras superfamily small G protein (Manser *et al.*, 1994). Mammalian tissues contain at least four PAK isoforms: a 68kDa PAK 1 (or PAK α) (Manser *et al.*, 1994) expressed in brain, muscle and spleen, a 62kDa PAK 2 (also known as PAK γ , PAK-I and hPAK65), which is ubiquitously expressed (Knaus *et al.*, 1995, Teo *et al.*, 1995, Jakobi *et al.*, 1996), and PAK 3 (or PAK β), a 65kDa protein that is highly expressed in brain and shows different tissue distribution to PAK 1 (Manser *et al.*, 1995, Bagrodia *et al.*, 1995). A recently discovered PAK isoform, PAK4 has been identified and interacts with activated cdc42 (Abo *et al.*, 1998).

Upon binding to Rac1 or cdc42, PAKs autophosphorylate at several serine or threonine residues (Gatti *et al.*, 1999), possibly due to a conformational change induced by the small G protein. PAKs contain a C-terminal serine/threonine kinase domain, and a highly conserved domain at the N-terminus of ~60 residues. This N-terminal domain contains a cdc42/Rac interactive binding (CRIB) domain (also known as the GBD – GTPase binding domain or PBD – p21-binding domain). PAKs 1, 2 and 3 show 78% overall sequence similarity, with 92% sequence identity in the kinase domain. The kinase domain of PAK4 shares 53% sequence identity with other PAKs, but has a unique N-terminal domain (Abo *et al.*, 1998). PAK mutants lacking the N-terminal domain show increased activity. Interaction between the catalytic and regulatory domains of PAK1 has been detected using a yeast two-hybrid system (Tu & Wigler, 1999) and it has been suggested that Rac1 and cdc42 disrupt intramolecular interactions between these two PAK domains, releasing autoinhibition of the kinase. Other notable features of these PAKs are the presence of a proline rich region at the N-terminus, and a stretch of acidic residues C-terminal to the CRIB. The N-terminal proline rich domain of PAK has also been shown to mediate interactions with the SH3 domain of an adaptor protein Nck (Galisteo *et al.*, 1996). The functions of PAKs are not entirely known. Mammalian PAKs have been shown to activate JNK and p38 mitogen activated protein kinases, but not mitogen activated protein kinase cascades activated by Ras (Bagrodia *et al.*, 1995b, Zhang *et al.*, 1995,

Polverino *et al.*, 1995), and activated Rac1 and cdc42 have also shown to activate SAPKs. It is possible that Rac1 activates SAPKs via interactions with PAKs.

Research also indicates a role for PAKs in actin organisation. The fission yeast PAK homologue, shk1 has shown to play a role in cell morphogenesis (Marcus *et al.*, 1995, Otilie *et al.*, 1995), PAKs from *Drosophila* (Harden *et al.*, 1996) and mammalian fibroblasts (Manser *et al.*, 1997, Sells *et al.*, 1997) localise to focal complexes and membrane ruffles, and in mammalian cells, expression of activated PAK alleles induces actin re-organisation. The budding yeast PAK homologue Ste20p has also been shown to bind to Bem1p, a protein shown to bind actin (Leeuw *et al.*, 1995). However, in some instances (Teramoto *et al.*, 1996) expression of PAKs has been shown to inhibit rather than enhance Rac1 induced SAPK activation, and growth factors that activate PAKs have shown to have little effect on SAPKs. Research has also shown that activated Y40C Rac1 and cdc42 mutants that inhibit the interaction with PAKs still induce normal cytoskeletal reorganisation in fibroblasts (Lamarche *et al.*, 1996, Joneson *et al.*, 1996), indicating that the role of PAKs in Rac1 induced activation of SAPKs and actin organisation are not fully understood. A recent report has indicated interaction of an activated cdc42 Y40C mutant with PAK4, indicating that this isoform may play a role in cytoskeletal organisation (Abo *et al.*, 1998). PAK isoforms have also been shown to phosphorylate both p47^{phox} (Knaus *et al.*, 1995) and p67^{phox} (Ahmed *et al.*, 1998), providing a further role for Rac in the activation of the NADPH oxidase, and results have also shown that PAK3 has the ability to phosphorylate serine residues of Raf1 in vitro and in vivo (King *et al.*, 1998). Phosphorylation of the catalytic domain of Raf regulates its activation on response to Ras. These results suggest the involvement of PAK3 and Rho proteins in Ras activation.

1.8. Interaction of Rac with other proteins

Rac proteins have also been shown to interact with a number of other molecules. Rac1 has been shown to bind directly to tubulin in a GTP dependent manner (Best *et al.*, 1996). The

physiological significance of this interaction is unknown, but is possible that Rac-tubulin interactions are important for the localisation of Rac1. Bovine brain G $\beta\gamma$ heterodimers of heterotrimeric G proteins have also been shown to interact directly with the GDP bound forms of RhoA and Rac1 and inhibit GTP γ S binding, but not to cdc42 (Harhammer *et al.*, 1996). It is possible that G $\beta\gamma$ heterotrimers function as guanine nucleotide dissociation inhibitors for Rac and Rho at the membrane, or are involved in membrane localisation of these small G proteins. G $\beta\gamma$ heterodimers have also been shown to directly interact with the small G protein ARF (Colombo *et al.*, 1995) suggesting a possible role for the G $\beta\gamma$ subunit in a variety of small G protein mediated responses. Although the biological activities and molecular interactions of Rho family proteins are significantly different from those of Ras proteins, both families share a number of conserved sequencing motifs. These motifs and the biochemistry of Rac1 will be discussed in the following chapters.

1.9. Conserved structural motifs of the Ras superfamily

1.9.1. The G1 motif

The Ras superfamily of small GTPases share a number of conserved sequencing elements, all involved in binding of guanine nucleotides and hydrolysis of GTP (Kjeldgaard *et al.*, 1996, Valencia *et al.*, 1991). The first sequence motif GxxxxGK(S/T) (x corresponds to any amino acid) is often called the phosphate binding loop or the P-loop. This loop refers to residues 10-17 of Rac and Ras. The loop containing this motif wraps around the β phosphate group, with main chain N atoms of residues 13-15, along with the side chain of lysine 16 pointing towards the phosphate group, creating a positive environment for these charges. The conserved threonine of Rac at position 17 following lysine 16 co-ordinates to a Mg²⁺ ion. The importance of this residue in the catalytic mechanism of Rac is shown as point mutation to alanine or Asn causes a dominant negative mutant that remains in the GDP bound conformation. This sequence motif is found in a number of proteins that bind purine nucleotide triphosphates, including ATP synthetases and myosin.

1.9.2. G2 - The 'effector loop'

The effector loop is extremely variable in different G protein structures. The effector loop comprises residues 32-40 of Rac. This region shows a significant conformational change in Rac (and all of the known structures of members of the Rho family) between the two nucleotide bound states. A conserved threonine at position 35 is involved in binding the γ phosphate of GTP and is a key residue involved in conformational change following GTP hydrolysis. Threonine 35 is also a direct ligand for the Mg^{2+} ion. This ion is essential for GTP hydrolysis, and is also co-ordinated to the β and γ phosphates of GTP. Amino acid changes in this region that are not involved in nucleotide binding and hydrolysis have been shown to inhibit the transforming ability of Ras and prevent the interaction of Rho family proteins with a number of effectors; hence this region has been termed the 'effector' loop.

1.9.3. G3, G4 and G5 motifs

The third motif, DxxG (residues 57-60 of Rac) is situated close to the phosphate binding loop, and is typically a region involved in conformational change of small GTPases between the two nucleotide bound states. This motif is highly conserved in Ras superfamily G proteins. Aspartate 57 in this region is thought to bind the catalytic Mg^{2+} via a water molecule (John *et al.*, 1993) with the amide proton of the conserved glycine forming a H-bond with the γ phosphate of GTP. The G4 motif, NKxD is known as the guanine recognition motif and is thought to determine specificity for the guanine. Carboxyl oxygens of aspartate 118 of Rac form a double H-bond with the guanine ring that is thought to play a role in nucleotide specificity, and the amide proton of lysine 116 stabilises the nucleotide binding site through H bonds to residues 13 and 14 in the G1 region. The G5 motif consists of residues 156-160 of Rac and has the conserved sequence ExSAx. Alanine 146 has shown to have a direct contact with the GTP in Ras, but other residues in this region of Ras have shown to stabilise side chains of Asn 116 and aspartate 119 through H-bonds.

1.9.4. The C terminal region

The C terminal residues of small GTPases, extending from residue ~165 to the C terminus is highly variable, even amongst closely related family proteins. The number of residues following amino acid ~164 of Ras superfamily GTPases also varies greatly in length, but typically have the same length in each family. When sequences are aligned at the conserved cysteine residue motifs at the C terminus, the shortest C terminal extensions are seen in the Rho family (14-17 residues) (figure 1.2.), with C terminal residues of Ras family proteins extending by 18-30 residues. The last four C terminal residues always include a cysteine motif that is required for in vivo modification (Adamson *et al.*, 1992). Rac1 (but not Rac2) contains a polybasic region at the C terminus (sequence KKRRKR). As well as being an important site for post-translational geranylgeranylation, Research by Chuang *et al.* (1994) has shown that smgGDS, a guanine nucleotide dissociation inhibitor, specific for Rac interacts with full length (un-modified) Rac, but not with Rac truncated at the C terminus. It is possible that the polybasic region at the C terminus of Rac1 may be important for interaction with GDI.

1.10. Mechanism of GTP hydrolysis by Ras superfamily proteins

Despite the biological importance of signal transduction by Ras superfamily GTPases, the mechanism of Ras catalysed GTP hydrolysis remains poorly understood. Using chirally labelled $[\gamma\text{-}^{17}\text{O}, ^{18}\text{O}]$ guanosine 5'-O-(γ -thio) triphosphate, Feuerstein *et al.* (1989) demonstrated that hydrolysis of Ras occurs with an inversion of the γ -phosphorous, indicating that the most likely mechanism for hydrolysis is a single step, in line transfer of the terminal phosphate from GTP to water without a phosphoenzyme intermediate.

The crystal structure of H-Ras at 1.35Å resolution (Pai *et al.*, 1990) indicates that 211 water molecules are incorporated into the structure, with the water molecules, Wat175 close enough to the γ phosphorous atom to be involved in GTP hydrolysis and perform in-line nucleophilic attack (figure 1.5A). Thr35 and Gln61 are likely to be close enough to Wat175 to form hydrogen bonds, making it more nucleophilic. The carboxylate group of Glu63 is close

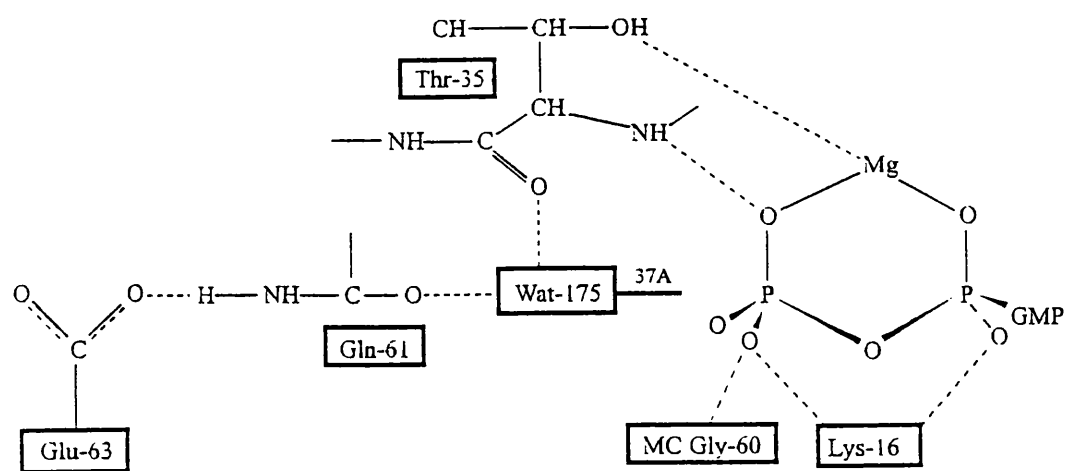
Figure 1.5. Mechanism of GTP hydrolysis by Ras

A. Proposed mechanism of GTP hydrolysis by nucleophilic activation of the γ phosphate of Ras·GTP by water, activated by Gln61 (diagram from Pai *et al.*, 1990).

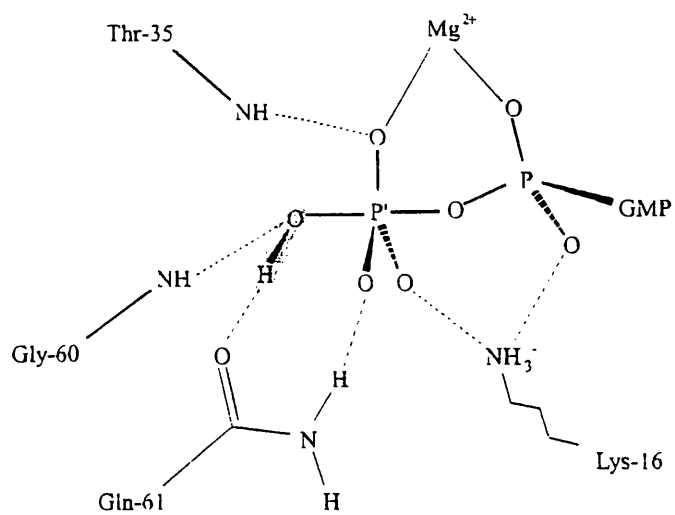
B. Transition state stabilisation mechanism of GTP hydrolysis as proposed by Privé *et al.* Gln61 stabilises a transition state formed between the pentavalent γ phosphate and the side chain of Gln61 (diagram from Privé *et al.*, 1992).

GMP = guanosine monophosphate.

A



B



enough to the amido group of Gln61 to form a hydrogen bond, and may maintain correct orientation of Gln61.

An alternative mechanism for GTP hydrolysis has been proposed by Privé *et al.* (1992). Based on the crystal structures of Ras mutants, a transition state stabilisation mechanism for GTP hydrolysis has been proposed. This provides a rationale for the effects of oncogenic mutations at positions 12 and 59 of Ras. Crystal structures of mutant Ras proteins indicate that Gln61 is not required to 'fix' Wat175 to an attacking position. Instead, the water molecule is tightly bound and probably activated by the main chain carbonyl group of Thr35 and strong interactions with the γ phosphate. In this mechanism, Gln61 is involved in stabilising a transition complex formed between the side chain of Gln61 and the pentavalent γ phosphate of the GTP transition state once a water molecule has bound to the γ phosphate and lost a proton (figure 1.5B.). The involvement of Glu63 in the GTPase mechanism as proposed by Pai *et al.* is suspect as Glu63 is not conserved among Ras related proteins. Gln61 is therefore an important residue involved in GTP hydrolysis, but it is still not clear whether it has a role as a general base or has a more structural role.

1.11. DH proteins – exchange factors for Rho family GTPases

A number of Rho family nucleotide exchange factors have been identified that catalyse the release of bound GDP (and subsequent binding of GTP) to Rho family proteins. Genetic evidence for a Rho family exchange factor came from studies with CDC (cell division cycle) mutants of *S. cerevisiae*. The Cdc24 protein and the small GTPase cdc42 regulate the development of cell morphology in yeast (Adams *et al.*, 1990), and defects in Cdc24 could be complemented by over expression of cdc42, indicating that Cdc24 is an upregulator of cdc42 (Bender & Pringle, 1989). Biochemical evidence for exchange factors came from studies with the proto-oncogene Dbl. Dbl and Cdc24 contain a homologous region of ~180 amino acids known as the DH (Dbl homology) domain (Ron *et al.*, 1991). This region has been shown to

be responsible for the nucleotide exchange activity of Dbl and Cdc24 (Hart *et al.*, 1991 & Zheng *et al.*, 1994).

DH containing proteins activate Rho family GTPases, and a large number of DH proteins have been identified (table 1.1). The DH domain is usually flanked at its C-terminus by a pleckstrin homology (PH) domain of ~100 amino acids (Gibson *et al.*, 1994). This domain has been identified in a large number of signalling proteins (Musacchio *et al.*, 1993) and it has been reported that PH domains show distinct binding affinities for phosphatidyl inositol (PI) phosphoinositides, indicating that proteins with a PH domain may respond to lipid signalling (Lemmon *et al.*, 1996). As PI lipids are membrane bound, this indicates that PH domains may mediate signal-dependent membrane localisation (Shaw *et al.*, 1996).

1.12. GTPase-Activating Proteins (GAPs)

Following biochemical identification and cloning of p50 RhoGAP, the first GAP for Rho proteins, over 25 Rac GAPs have been identified from yeast to human. The mammalian Rho GAP family of proteins include p50 RhoGAP, Bcr, Abr, α -chimaerin, β -chimaerin, p190, p85, 3BP-1, Myr5, p122-Arp, p155 and cdGAP (table 1.2). All share a homologous catalytic domain, which mediates binding and catalytic activity with Rho family proteins, but in addition, many Rho GAPs contain additional domains involved in signalling. Although the rate of GTP hydrolysis of Rac1 is ~50 fold faster than Ras or Rho (Chuang *et al.*, 1993) the GTPase rate of Rac1 may be increased by several orders of magnitude by interaction with GAPs (Lancaster *et al.*, 1994). All RhoGAPs contain a homologous catalytic domain; within this domain is a single conserved arginine residue (Lancaster *et al.*, 1994). In contrast to heterotrimeric G proteins, Ras superfamily small G proteins typically have a slow rate of intrinsic GTP hydrolysis in vitro, and their in vivo conversion of the GDP bound form depends largely on GAP activity in vivo. This suggests that the biochemical function of GAPs is to down-regulate Rho family proteins. However, Rho GAPs contain a variety of additional

Table 1.1. In vitro specificities of DH proteins for activating Rho family GTPases

A table showing in vitro specificities (that have been tested) and schematic representations of a number of DH containing proteins. Many of these proteins show nucleotide exchange activity on Rac (shown in green) and other Rho family proteins. Schematic representations of Tiam1, Trio and Vav are not shown due to the complexity of the domain structures. *Ect2 shows no exchange factor activity on Rac1 or H-Ras in vitro (Jeanteur, 1999).

Sc. = *Saccharomyces cerevisiae*, M = mouse, R = Rat, H = Human, DH = Dbl homology, PH = pleckstrin homology, RhoGAP = GTPase activating domain for Rho GTPases, S/T kinase = serine/threonine kinase, C2 = domain involved in calcium binding, vimetin rod like = coiled-coil region, SH3 = Src homology 3, binds proline rich motifs, CR = cysteine rich, EF = EF hand, calcium binding.












Name	Organism	Specificity <i>in vitro</i>	Schematic Representation
Abr	H	Cdc42, Rac1, 2, RhoA	
Bcr	H	Cdc42, Rac1, 2, RhoA	
Cdc24	Sc	Cdc42Sc	
Dbl	H	Cdc42Hs, RhoA, Rac1 lipid modified	
Dbp	H	Cdc42, RhoA	
Ect2*	H		
Fgd1	H	Cdc42Hs	
Lbc	H	RhoA	
Lfc	M	RhoA	
Lsc	M	RhoA	
Ost	R	Cdc42, RhoA	
Tiam1	M	Cdc42Hs, Rac1, RhoA	
Trio	H	D1: Rac1 D2: RhoA	
Vav	M	Cdc42, Rac, Rho	

Table 1.2. In vitro specificities of proteins containing a RhoGAP domain

A table showing in vitro specificity of a number of mammalian proteins containing a RhoGAP domain. ? = not determined, + and - = tested positive and negative respectively (Jeanteur, 1999).

Rho-GAP proteins	M.W. (predicted, in kDa)	<i>In vitro</i> GAP specificity for			Tissue distribution
		Rho	Rac	Cdc42	
p50-RhoGAP	50	+	+	++	Ubiquitous
Bcr	142	-	+	+	Brain, hematopoietic cells
Abr	92/97	-	+	+	mainly brain
n-Chimaerin (α 1)	38	-	++	+	Brain
α 2-Chimaerin	50	-	++	+	Brain, testes
β 1-Chimaerin	34	-	+	-	Testes
β 2-Chimaerin	54	-	+	-	Brain
p85a, p85b	83 and 81	-	-	-	Ubiquitous
p190	171	++	+	+	Ubiquitous
3BP-1	65	-	+	+	mainly spleen and brain
RLIP76	76	-	+	+	Ubiquitous
Myr5	225	++	+	++	Ubiquitous
Myosin-IXb	229	?	?	?	mainly myeloid cells
p122-Arp	122	+	-	-	?
p190b	172	++	++	+	Ubiquitous
p115	115	?	?	?	Hematopoietic cells
p58-Mgc	58	+	++	++	mainly testes

structural domains that may allow them to interact with other signalling molecules. It is therefore possible that Rho GAPs also act as downstream effectors of Rho family proteins.

1.12.1. p50 RhoGAP

The first Rho GAP identified was p50 RhoGAP, a 29kDa protein extracted from cytoplasmic cell extracts (Garrett *et al.*, 1991). Partial sequencing and cDNA cloning revealed that this fragment was the catalytic domain of p50 RhoGAP, resulting from proteolytic cleavage of the full length (50kDa), ubiquitously expressed, p50 RhoGAP protein (Lancaster *et al.*, 1994). The crystal structure of p50 RhoGAP has been recently described (Barrett *et al.*, 1997) and crystal structures of cdc42·GMPPNP and RhoA·AlF₄⁻ in complex with the GAP domain of p50 RhoGAP have been solved to high resolution at N.I.M.R. (Rittinger *et al.*, 1997 & Rittinger *et al.*, 1997b). The structure of the GAP domain is an unusual arrangement of nine helices, the core of which consists of a four helix bundle. Conserved residues of the RhoGAP domain are mostly located on one side of this bundle, which may constitute a binding site for Rho family GTPases. Cdc42 interacts with this catalytic domain through switch I and switch II contacts with a shallow pocket on the RhoGAP catalytic domain. Structural and biochemical data suggests that RhoGAP acts on intrinsic GTPase activity by stabilising the GTPase structure, and directly by supplying a catalytic residue to the GTPase reaction. In the complex of RhoA·AlF₄⁻ with RhoGAP (catalytic domain), there is a rotation of ~20° between RhoA and RhoGAP when compared to the ground state complex cdc42·GMPPNP/RhoGAP, in which cdc42 is bound to the non-hydrolysable GTP analogue, GMPPNP. Consequently, in the transition state, Arg85 (identical to Arg282 of the full length RhoGAP protein) is placed directly into the active site of the protein suggesting a role for Arg282 in the hydrolysis of GTP by RhoGAP.

Biochemical data also suggests a role for Arg282 of RhoGAP in the activation of GTP hydrolysis. Changes in fluorescence anisotropy have shown that RhoGAP binds tightly to RhoA·mantGDP in the presence, but not in the absence of AlF₄⁻. Furthermore, mutation of

Arg282 to lysine abolishes the formation of the RhoGAP/RhoA·GDP·AlF₄⁻ complex and reduces the RhoGAP activation of GTP hydrolysis by a factor of ~10⁴ (Graham *et al.*, 1999). Biochemical studies of GAP specificity towards Ras superfamily GTPases have shown that only cdc42, Rac and Rho are targets of p50 RhoGAP, and although p50 RhoGAP binds Rac, Rho and cdc42 bind equally well, cdc42 is the best substrate and RhoGAP is equally active on Rac and Rho (Lancaster *et al.*, 1994) *in vitro*.

1.12.2. Additional regulatory mechanisms

Research by Zhang & Zheng has shown that cdc42, Rac2 and RhoA form homodimers in both the GDP and GTP bound states *in vitro*. The dimerisation appeared to be mediated by the C-terminal polybasic regions. This interaction was shown to cause a significant increase in the GTPase activity of Rac and cdc42 (Zhang & Zheng 1998). Rho family members containing an arginine at position 186 in the C-terminal polybasic region have been shown to possess self stimulatory GTPase activation through homophilic interactions (Zhang *et al.*, 1999). It is possible that Rho family proteins utilise a built in arginine finger for negative regulation in addition to GTPase activating proteins (GAPs).

Recent reports have indicated toxic induced activation of RhoA *in vivo* by deamination of glutamine 63. Cytotoxic necrotizing factors (CNF 1 and 2) are produced by a number of *Escherichia coli* strains. These toxins have been shown to cause tissue damage and often death in animal hosts. CNFs have shown to activate polymerisation, inhibit cytokinesis and induce membrane ruffling, and reports have identified Rho proteins as targets for these *E. Coli* toxins (Oswald *et al.*, 1994, Fiorentini *et al.*, 1995). Two recent reports show that ^{CNF}~~NCF~~1 deaminates glutamine 63 of RhoA (equivalent to position 61 in Ras and Rac) to glutamate, resulting in a constitutively active form of the protein, blocking intrinsic and RhoGAP stimulated GTP hydrolysis (Schmidt *et al.*, 1997, Flatau *et al.*, 1997).

1.13. Structure and sequence motifs of Human Rac1

Rac1 is a protein of 192 amino acids with a molecular weight of 21.5kDa. The crystal structure of Rac complexed to a non-hydrolysable GTP analogue (GMPPNP) has been solved to 1.35Å resolution at NIMR (Hirshberg *et al.*, 1997) (figure 1.6.). This clearly illustrates structural difference between Rac and other small G proteins, such as Ras. Although Rac and Ras appear to be very similar, they differ in conformation and mobility of the effector loop when complexed to GMPPNP, and in the precise interactions of the protein and the nucleotide. The overall fold of Rac1 is similar to that of Ras, but Rac has an additional 13 amino acid 'insertion loop' (residues 123-135) with the corresponding structure in Ras being a short loop. This additional α helical domain is mobile, exposed to the solvent and presents a highly charged surface, suggesting it is involved with the interaction of effectors. This loop is unique to Rho family GTPases and shows considerable sequence divergence between individual members. The Rac insert region has been implicated in the activation of the NADPH oxidase (Freeman *et al.*, 1996), and recent experiments suggest an essential role for the insertion loop in cell proliferation and transformation (Joneson & Bar-Sagi, 1998, Wu *et al.*, 1998). Residues Thr 125, Ile 126, Leu 129, Pro 136 and Val 85 of the insertion loop form a loosely packed hydrophobic core that are all (with the exception of Ile 126) completely conserved or conservatively substituted in this helix in all known Rho family proteins. Available structures of RhoA and cdc42 suggest that other Rho family proteins adopt a structure similar to Rac rather than Ras.

The structure of Rac·GDP has recently been solved by collaboration with this laboratory and the Division of Protein Structure (unpublished results) (figure 1.7.). The GMPPNP and GDP bound forms of Rac are similar in structure but show differences in the effector loop (residues 30-40). With GDP bound, the effector loop is rigid and adopts a single conformation. In the GMPPNP bound form, this loop is mobile and may adopt several sub-structures. The switch 2 region of Rac1 shows significant conformational change between the two nucleotide bound states (figure 1.7.). This loop does not adopt a similar conformation in the crystal structures of

Figure 1.6. Comparison of the Rac1 and H-Ras structures

Ribbon diagrams of the overall fold of Rac1 (a) and H-Ras (b), bound to non-hydrolysable GTP analogues (Hirshberg *et al.*, 1997). Colour scheme: α -helices are shown in green, β -strands in red and 3_{10} helices in blue. A ball and stick representation of the non-hydrolysable nucleotide analogue is shown in yellow.

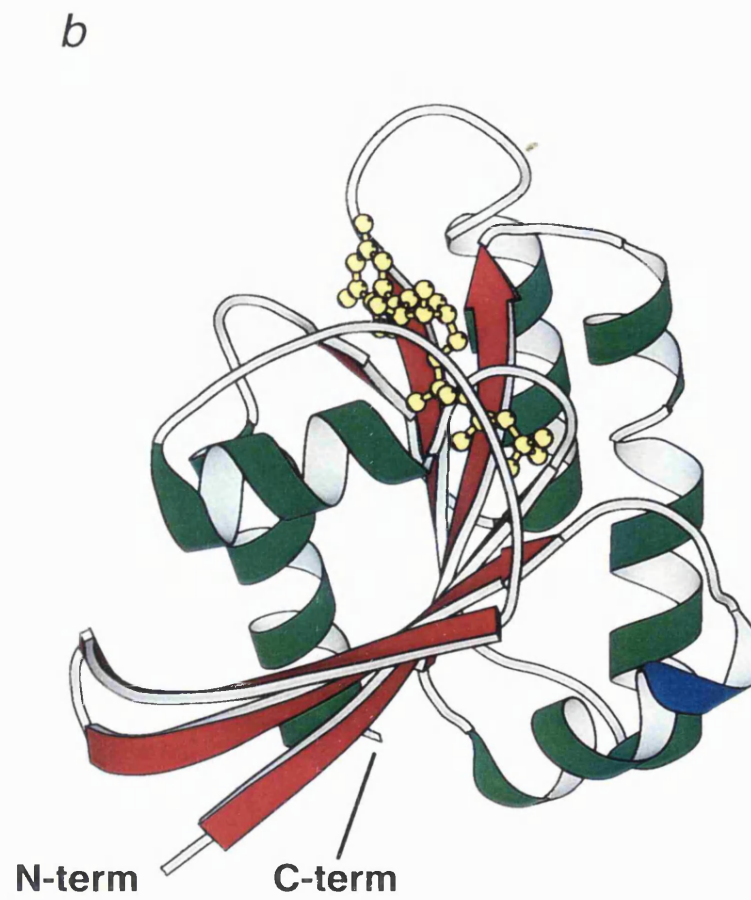
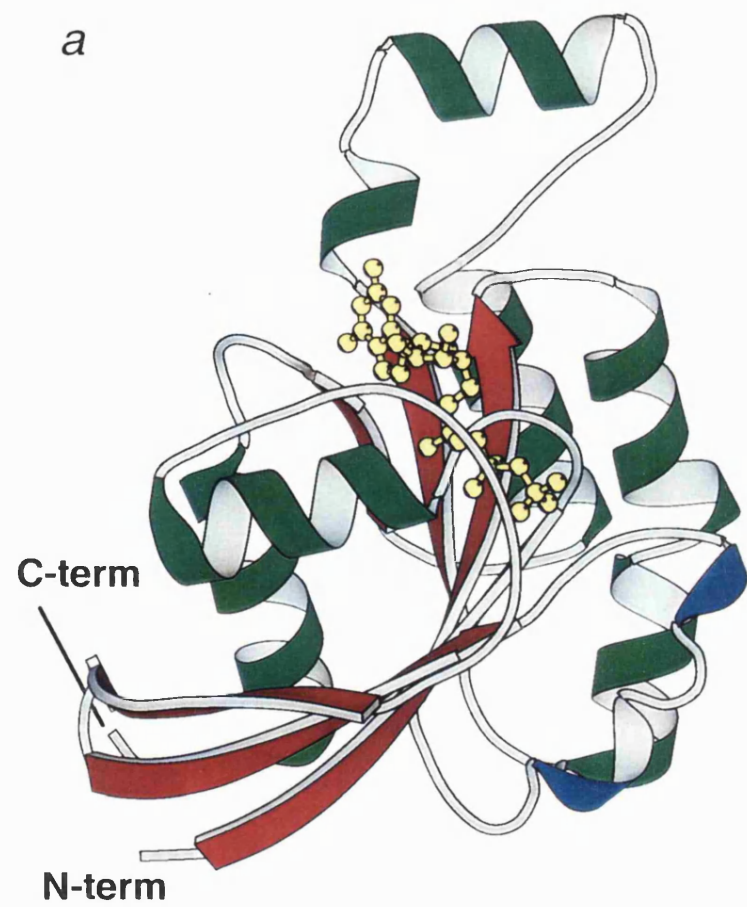
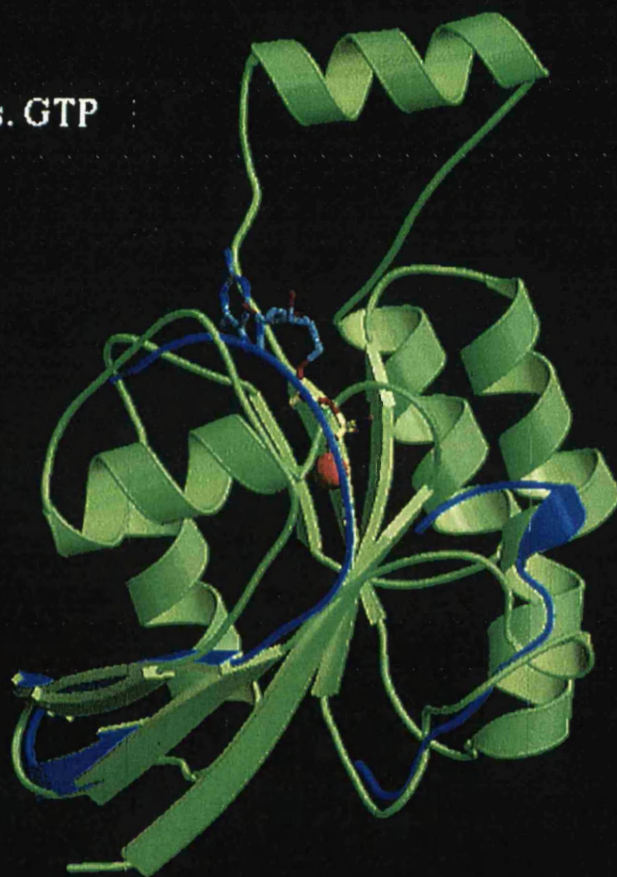


Figure 1.7. Crystal structure of human Rac1.GDP

A ribbon diagram showing the overall fold of human Rac1 bound to GDP (Hirshberg *et al.*, unpublished results). The Rac1·GDP structure is shown in green, with regions of the Rac1·GMPPNP structure that show significant conformational change between the two nucleotide states shown in blue. These two regions represent the effector loop (shown closest to the nucleotide) and the switch II region. The nucleotide is represented as a ball and stick model, with the red sphere representing a water molecule.

RAC1
GDP vs. GTP



Rho·GDP or cdc42·GDP (Wei *et al.*, 1997, Rudolph *et al.*, 1999) and may be important for Rac-specific interactions with effectors such as p67^{phox}.

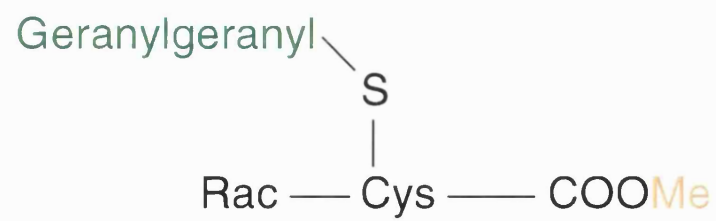
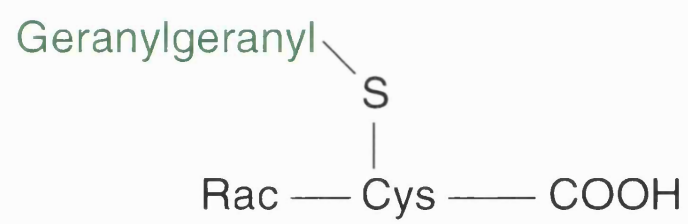
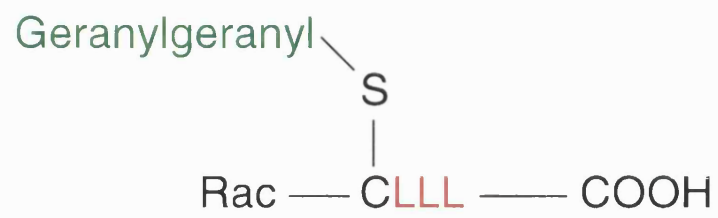
1.13.1. Post-translational modifications of Rac

In order to associate with membranes and interact with regulatory targets, most members of the Ras superfamily are post-translationally modified by covalent attachment of an isoprenoid to a C-terminal cysteine residue. The C-terminal sequence specifies the type of modification – the CAAX motif of Ras (C=cysteine, A= any aliphatic residue, X= usually methionine or serine) undergoes farnesylation (C-15 isoprenoid). Most Rho proteins have a CAAX motif (where X= a leucine) that is modified by the addition of a geranylgeranyl (C-20 isoprenoid) (Didsbury *et al.*, 1990). The importance of this terminal amino acid in prenylation specificity is supported by the observation that mutagenesis of the terminal residue of Ras to leucine results in geranylgeranylation of the protein (Kinsella *et al.*, 1991). Isoprenylation is catalysed by the enzymes farnesyltransferase and geranylgeranyltransferase. Following isoprenylation, the C-terminal –AAX motif is proteolytically removed, and the C-terminal cysteine is carboxyl methylated (figure 1.8.). Ras proteins (with the exception of K-Ras) are further modified by palmitoylation of additional C-terminal cysteines (upstream from the CAAX motif) (Dudler & Gelb, 1996). Rho proteins are not palmitoylated, but some do have a stretch of polybasic amino acids near their C-terminus thought to be essential for correct localisation of the proteins.

All members of the Rho family have a CAAX motif ending in leucine or phenylalanine and are geranylgeranylated, with three notable exceptions. RhoB has been found in both farnesylated and geranylgeranylated forms (Adamson *et al.*, 1992) and it has been shown that this modification can be catalysed by geranylgeranyl transferase (Armstrong *et al.*, 1995), RhoE (Foster *et al.*, 1996) and the recently identified Rnd group of Rho family proteins (Nobes *et al.*, 1998). RhoE shows ~54% sequence identity with RhoA, B and C yet exhibits structural difference both in the catalytic domain of the protein and at the C terminus.

Figure 1.8. Post-translational modification of Rac1

Following isoprenylation of Rac1 by geranylgeranyltransferase, the C-terminal leucines (-LLL) are proteolytically removed and the resulting C-terminal cysteine is carboxyl methylated.



Sequence alignment of RhoE with H-Ras indicates that this protein has serine residues at positions 17, 64 and 66, which correspond to positions 12, 59 and 61 in H-Ras. Mutations at these positions in Ras have been shown to produce constitutively active, oncogenic forms of Ras by interfering with the mechanism of nucleotide hydrolysis. RhoE is consequently unable to hydrolyse its bound GTP and appears to be maintained in a GTP bound state, suggesting its activity may not be controlled by the conventional cycling mechanism involving exchange factors and GAPs (Foster *et al.*, 1996). RhoE has a C-terminal methionine, which is also seen in K- and N- Ras and has been shown to be modified by farnesylation. Evidence for a constitutively active form of RhoE has been shown by microinjection of fibroblasts, which induced the formation of ruffles and filipodia-like membrane protrusions (Guasch *et al.*, 1998). The precise biochemical role of RhoE in cellular processes remains to be established, but like other Rho family proteins, it is probably involved in cytoskeletal organisation, with its activity controlled by an unknown mechanism.

The Rnd proteins form a distinct branch of the Rho family of small G proteins. They have higher molecular weights (25-28 kDa) than other Rho family proteins and share 45-49% sequence identity with Rho, slightly less with Rac and cdc42. Rnd proteins exchange GTP rapidly, have a low affinity for GDP and lack significant intrinsic GTP activity (Nobes *et al.*, 1998), suggesting that these proteins are in a constitutively GTP bound conformation. Sequence alignment has revealed that RhoE is identical to Rnd3 (Foster *et al.*, 1996) except that the published RhoE sequence lacks 15 N-terminal residues. The sequence motif MKERRA in this additional N-terminal region is essential for intracellular location of Rnd3. Rnd proteins have polybasic motifs at their C termini, but these are separated from the protein core by ~ 30 amino acids.

1.13.2. Carboxyl terminal methylation of Rac

~~In eukaryotic cells, proteins are commonly methylated on carboxyl groups on side chain nitrogens of amino acids lysine, arginine or histidine.~~ Protein methylation has shown to be

involved in a number of cellular processes such as stress responses and ageing and repair of proteins (Desrosiers & Tonguay, 1988). Many G proteins are methylated on the C terminal carboxyl group of the protein (figure 1.8.) and a role for methylation in G protein signalling has been indicated by the relationship between prenylcysteine carboxy methylation and G protein activation in neutrophils (Philips *et al.*, 1993). Research suggests that protein methylation is catalysed by membrane bound, prenyl cysteine methyl transferases that act on Ras and other signalling molecules that contain either a carboxyl-terminal farnesyl or geranylgeranyl cysteine (Clarke *et al.*, 1988). Unmethylated cdc42 from brain (also known as G25K) purifies as a soluble complex with RhoGDI, and RhoGDI blocks methylation until cdc42 is in the active (GTP γ S) conformation. In the active conformation, cdc42 can translocate to the membrane where methylation can occur (Backlund, 1993). The role of methylation in Rho protein function has not been clearly defined. In vitro studies with K-Ras indicates that C terminal carboxyl methylation may play a role in membrane association of the protein by neutralising the negative charge at the C terminus (Silvus & l'Heureux, 1994), and research by ~~Backlund~~ *et al.* (1997) suggest that carboxyl methylation protects Rho and related proteins from degradation. Unlike isoprenylation and proteolysis, methylation has been shown to be reversible under physiological conditions (Venkatasubramanian *et al.*, 1980). This reversibility suggests that methylation may play an important regulatory role in signal transduction.

1.14. Rho Guanine nucleotide Dissociation Inhibitors (GDIs)

Under non-activating conditions in the cell, Rho family proteins exist mainly in a complex with a second cytosolic protein, Guanine nucleotide Dissociation Inhibitor, (GDI). In order to bind tightly to GDI, Rho subfamily proteins require post-translational geranylgeranylation at their C terminus. Research in this laboratory has shown that a region of the effector loop of Rac1 (aa's 30-40) is important for the interaction with GDI (see results), indicating that regions other than the C-terminal domain of Rac1 are important for this interaction. GDIs are capable of three biochemical activities – they preferentially bind to the GDP bound form of

Rho proteins and inhibit the release of GDP (and subsequent binding of GTP) (Mizuno *et al.*, 1992), stimulate the release Rho family proteins from membranes (Isomura *et al.*, 1991, Leonard *et al.*, 1992, Sesaki *et al.*, 1993), and inhibit GTP hydrolysis (Hart *et al.*, 1992, Sasaki *et al.*, 1993, Hancock & Hall, 1993).

Three human GDIs specific for Rho family proteins have been identified – RhoGDI (Fukimoto *et al.*, 1990, Ueda *et al.*, 1990), and two closely related homologues, GDI/D4 (Lelias *et al.*, 1993) or Ly-GDI (Scherle *et al.*, 1993) (sequence alignment shows D4 and Ly-GDI encode the same protein) and RhoGDI γ (Adra *et al.*, 1997). RhoGDI was the first Rho family GDI discovered. It is a protein of 204 amino acids, 23.4 kDa and was first purified from brain cytosol on the basis of its ability to inhibit GDP dissociation from RhoA. Tissue specificity of RhoGDI mRNA expression has shown that RhoGDI is ubiquitously expressed (although with weak expression in heart and liver) (Fukimoto *et al.*, 1990, Shimizu *et al.*, 1991). Western blot analysis shows a similar tissue distribution of RhoGDI (Shimizu *et al.*, 1991) suggesting that RhoGDI plays a role in most cell types. GDI/D4 is expressed almost exclusively in haematopoietic cells, and RhoGDI γ is expressed preferentially in the brain and pancreas (Adra *et al.*, 1997). Both RhoGDI and GDI/D4 function as GDIs for Rho Rac and Cdc42 proteins, whereas RhoGDI γ has been shown to act as a GDI against cdc42 and RhoB, but unable to bind to Rac1 or Rac2 (Adra *et al.* 1997). The ability of RhoGDI γ to bind other Rho family proteins has yet to be established. GDI/D4 and RhoGDI γ show ~67% and ~50% sequence similarity to RhoGDI respectively, and are 10 and 20 fold less efficient than RhoGDI at binding and regulating Rho family GTPases, respectively (Nomanbhoy & Cerione, 1996, Gorvel *et al.*, 1998).

1.14.1. Structure of RhoGDI

The structure of RhoGDI has been solved by X-ray crystallography (Keep *et al.*, 1997). RhoGDI has two domains – the first ~60 N-terminal residues form a highly flexible domain that is disordered in the absence of bound G protein, and an ordered folded domain. This

ordered region has an immunoglobulin-like fold comprising the remaining ~140 residues and contains a hydrophobic cavity of the dimensions $\sim 12 \times 8 \times 10$ Å. This suggests that the binding and inhibitory functions of RhoGDI are due to two structurally distinct domains. The base of the hydrophobic cavity contains a region of negative electrostatic potential. It is possible that this region interacts with the basic C terminal region of Rho family proteins. There is no structural similarity between RhoGDI and RabGDI (Schalk *et al.*, 1996), which is likely to perform the same cellular function for the Rab family of small GTPases.

The solution structure of the RhoGDI has also been solved using NMR spectroscopy (Gosser *et al.*, 1997). The addition of a farnesylated peptide, acetyl-KKSRC(S-farnesyl) to GDI caused large changes to the GDI structure. No changes were observed when non-isoprenylated peptide was added. This suggests that the farnesyl group interacts with RhoGDI in solution, probably by interacting with the hydrophobic cavity of RhoGDI and may induce a conformational change in the RhoGDI structure. RhoGDI mutants that are truncated at the N-terminus show decreasing affinity for cdc42 as increasing amounts of the N-terminus are removed. However, a RhoGDI mutant truncated at the N-terminus by 59 residues still binds to isoprenylated cdc42 in the high nanomolar range. Truncated RhoGDI constructs have also been tested for their ability to inhibit nucleotide exchange from isoprenylated cdc42. Full length RhoGDI and a truncated GDI lacking the N-terminal 22 amino acids reduced GDP dissociation, but not truncated RhoGDI lacking the N-terminal 42 amino acids. This suggests that the region of GDI involved in inhibiting nucleotide dissociation resides between the N-terminal residues 23-42. Experiments using an N-terminal GDI peptide (residues 23-58) shows a low affinity ($K_d > 5\text{mM}$) for cdc42 (Gosser *et al.*, 1997). However, It is possible that the flexible N-terminal domain of GDI forms a structured loop in the complex with cdc42, which may be positioned in the correct orientation to make contacts with more than one region of the cdc42 structure. This may account for the weak affinity of this peptide for cdc42. The crystal structure of a recombinant RhoGDI·RhoA·GDP complex expressed in yeast has been solved to 5Å resolution (Longenecker *et al.*, 1999). These results show that the N-

terminal region of GDI is likely to form a loop in the complex with RhoA and may make contacts with the effector loop and switch II of RhoA.

RhoGDI contains a single cysteine at position 79. This residue is close to the hydrophobic cavity of RhoGDI and has been previously labelled with an environmentally sensitive fluorophore *N*-[2-(1-maleimidyl)ethyl]-7-(diethylamino)coumarin-3-carboxamide (MDCC) by R.W. Stockley in this laboratory. The labelled protein shows ~75% decrease in fluorescence upon Rac1 binding, providing a direct spectroscopic approach to monitor the binding of Rac1 to GDI. The labelled protein has been used to monitor the interaction of GDI with Rac1 (see results). Titration profiles of modified Rac1 induced quenching of MDCC-GDI fluorescence and individual rate constants for this interaction have been fitted to a binding model for the Rac1:GDI interaction with a K_d of 0.4nM (Newcombe *et al.*, 1999).

1.14.2. Dissociation of the Rac1·GDI complex

Activation causes Rac and GDI to dissociate by an unknown mechanism, although it has been reported that this interaction may be disrupted by the presence of a number of biologically active lipids. These include arachidonic acid, phosphatidic acid and phosphatidylinositols (Chuang *et al.* 1993b). These are second messengers generated upon membrane receptor activation and are involved in a variety of cell functions. Arachidonic acid and phosphatidic acid have also been shown to stimulate NADPH oxidase activity both in intact cells and in a cell free system (Sawai *et al.*, 1993), with stimulation of the NADPH oxidase occurring at concentrations of arachidonic acid similar to those shown to disrupt the Rac·GDI interaction. It is possible that the presence of these lipids maintain Rho proteins in a dissociated state by competing for the lipid binding pocket of GDI. However, amphiphiles such as arachidonic acid are usually required in a cell free NADPH oxidase system where Rac, but not GDI, is present; hence these lipids may also have potential effects on the cell membrane or other phagocyte oxidase components.

A recent report has also shown that GDI/D4 is a substrate of the apoptosis protease GPP32 and is truncated at its C terminus, suggesting that regulation of Rho family GTPases by GDI/D4 may be disrupted during apoptosis by GPP32 cleavage (Na *et al.*, 1996). GDI/D4 differs primarily from RhoGDI at the N-terminal 25 amino acids. The consensus sequence required for cleavage (between Asp¹⁹ and Ser²⁰ of the cleavage sequence DELD¹⁹S) is not seen in RhoGDI or RhoGDIγ. This may illustrate an important role for Rho family GTPases in the differentiation of haematopoietic cells and the cytoskeletal re-arrangements that occur during programmed cell death. Research by Vignais's group has shown that RhoGDI is phosphorylated in neutrophils, indicating that in the RhoA-RhoGDI complex the GDI may be present in a phosphorylated form, with the affinity of the interaction between the two proteins dependent on the phosphorylation state of the RhoGDI (Bourmeyster & Vignais, 1996). The phosphorylation of GDI/D4 and RabGDI (a nucleotide dissociation inhibitor for the Rab family of small GTPases) has also been reported (Steele-Mortimer *et al.*, 1993), suggesting that the action of specific phosphatase(s) and kinase(s) may at least in part, control the dissociation of the Rac·RhoGDI complex. A recent report by Takai and colleagues suggests that C terminal regions of the ezrin/radixin/moesin (ERM) family of proteins interact with RhoGDI and reduce the inhibitory effect of GDI on Rac1 nucleotide exchange (Takahashi *et al.*, 1997). ERMs are intracellular proteins that function as linkers between the plasma membrane and actin based cytoskeletons. ERMs contain at least two functionally distinct domains – a highly conserved N terminal domain that interacts with a number of integral membrane proteins, and a C terminal domain that interacts with actin filaments (Tsukita *et al.*, 1994). ERM proteins may provide a link between dissociation of Rac1 from RhoGDI and cytoskeletal organisation.

A recent report by ^{Fauré}~~Faur~~ *et al.* (1999) has shown that phosphoinositides partially open, but not fully dissociate a RhoA·GDP·GDI complex. These results are consistent with experiments using truncated (unmodified) Rac1·GDP in this laboratory. A combination of C-terminally truncated (*E.coli* expressed) rac1 and a farnesyl modified C-terminal peptide mimics

geranylgeranylated rac1 and binds to RhoGDI (see results). Because the C-terminal peptide and the 'rest' of Rac are not attached in this system, Rac is likely to interact with GDI through an additional site other than the via the isoprenyl tail of Rac and the hydrophobic pocket of GDI.

1.14.3. In vivo studies into the role of RhoGDI

The function of RhoGDI has been investigated by microinjecting Swiss 3T3 cells with RhoGDI. Microinjection has shown to induce morphological change in these cells accompanied by the disappearance of stress fibres (Miura *et al.*, 1993), and has also shown to inhibit Swiss 3T3 cell motility (Takaishi *et al.*, 1993). RhoGDI-induced morphological changes and inhibition of cell motility were prevented by microinjection of RhoA in the GTP γ S (active) form. These results suggest that RhoGDI binds preferentially to the GDP-bound form of RhoA in vivo, inhibiting further nucleotide exchange and maintaining RhoA in the inactive state. It is also possible that RhoGDI down-regulates Rho subfamily activity by releasing proteins from membranes, interfering with the correct intracellular localisation of the protein.

1.14.4. Regulation of membrane translocation by GDI

The mechanisms which trigger the dissociation of rac1 from membranes remains poorly understood, despite the likely physiological importance of this dissociation. A recent report by Isomura *et al.* (1991) has shown that RhoGDI inhibits the binding of the GDP bound form of RhoB interacting with synaptic plasma membranes, but not RhoB in the GTP bound form. This data also indicates that RhoGDI is able to stimulate the dissociation of only the GDP bound form of membrane bound RhoB. Results have also shown that an N terminally truncated GDI can still bind to membrane bound, isoprenylated cdc42, but is unable to stimulate its release from membranes (Nomanbhoy *et al.*, 1999). It is likely that RhoGDI makes at least two contacts with Rho family proteins. One is likely to occur between the carboxyl terminal domain and the geranylgeranyl group of Rac with the hydrophobic pocket

of RhoGDI. A second contact probably occurs at the amino terminal domain of GDI and appears to be necessary for GDI-induced release of cdc42 from membranes and inhibition of GDP dissociation from cdc42. Recent experiments using a chimaeric cdc42/Ras protein (with the insertion loop of cdc42 removed and replaced by corresponding residues of Ras) suggests that the insertion loop (residues 120-132) of cdc42 is important for the inhibition of nucleotide dissociation by RhoGDI, but not essential for interaction with GDI (Wu *et al.*, 1997). A Ras protein with the insertion loop and the C terminal 8 amino acids (including the CVLL~~Y~~ modification sequence) of cdc42 did not render GDI sensitivity to Ras (Wu *et al.*, 1997), suggesting that other regions of cdc42 are essential for the interaction with RhoGDI. Experiments in this laboratory indicate that residues of the effector loop (aa's 30-40) may be critical for the interaction with GDI; this may account for the lack of effect on affinity of the cdc42/Ras chimaera with GDI.

CHAPTER 2. MATERIALS & METHODS

2.1. Materials used for protein studies

Standard biochemical reagents were from Sigma or BDH unless otherwise stated. IPTG, alkaline phosphatase, farnesyl bromide, guanine nucleotides and the nucleotide analogue GMPPNP were also purchased from Sigma. Fluorescent probes and TCEP were from Molecular Probes Inc., agarose solutions (for agarose gel electrophoresis and plaque assays) were from FMC Bioproducts and polyacrylamide solutions for SDS-PAGE were from Severn Biotech Ltd. Supercompetent *E.coli* cells were from Stratagene, and *sf9* insect cells were from Invitrogen and cultured in media laboratories, N.I.M.R. Cells were sonicated on ice using a VibraCell sonicator (Sonics & Materials Inc.) using a 0.5 inch diameter probe. RhoGDI was purified from *E.coli* and subsequently labelled with MDCC as described (Newcombe *et al.*, 1999) in DR. M. Webb's laboratory by J. Hunter. GDI was first labelled with MDCC by R. Stockley (UCL) at the N.I.M.R. DR K. Rittinger (Division of Protein Structure, N.I.M.R.) kindly provided truncated cdc42Hs (residues 1-184, with Gly-Ser-His and the native Met at the N-terminus) and full length N-Ras and RhoA were kind gifts from DR J. Eccleston's laboratory (N.I.M.R.).

2.2. Protein purification from *E.coli*

Escherichia coli containing vectors of Q61L Rac, p47^{phox}, p67^{phox} and the domain of p67^{phox} that interacts with Rac (N-terminal residues 1-199) were provided by Professor A. Hall (University College London). The wild type Rac clone was available in our laboratory. All *E.coli* expressed Rac proteins were purified from pGEX-2T vectors expressed in DH5 α , BL21 or XL-1 blue strains of *E.coli*. p67¹⁻¹⁹⁹ was purified from a modified pGEX-2T plasmid vector, pGEX-GK. Professor D. Lambeth (Emory University Medical School, Atlanta, Georgia) kindly provided baculoviruses containing the p67^{phox} and p47^{phox} baculovirus vectors.

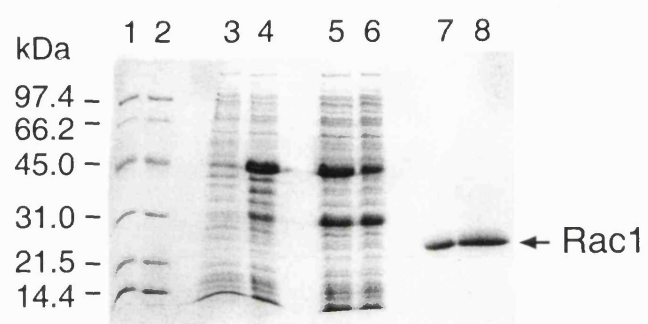
2.2.1. Expression and purification of recombinant Rac1 from *E.coli*

Wild type and mutant Rac1 was expressed in a pGEX-2T vector (Pharmacia) under the control of a *tac* promoter as glutathione-S-transferase (GST) fusion proteins. A 100ml starter culture containing 50 μ g ml⁻¹ ampicillin was inoculated with a small loop of the *E.coli* strain DH5 α or XL1-blue containing the pGEX2T-Rac1 vector from a frozen glycerol stock and incubated overnight. The following day 10ml of starter culture was added to each of eight 500ml aliquots of L-broth in 2 litre shaker flasks (total volume 4 litres) containing 50 μ g ml⁻¹ ampicillin and the cells grown at 37°C with vigorous shaking until an absorbance at 600nm of 0.8cm⁻¹ was obtained. The cells were induced by the addition of 1mM IPTG (Sigma) and grown at 37°C for a further 4 hours. A sample of the cells was removed before and after induction and analysed by SDS-PAGE (figure 2.1.). The cells were harvested by centrifugation (4500 x g Beckman J6-HC centrifuge, JS 4.2 rotor) for 15 minutes and the cell pellet re-suspended in 20mM Tris-HCl pH 7.6, 1mM MgCl₂, (buffer A) containing 1mM PMSF. The cells were frozen on dry ice and stored at -80°C.

The pellet was freeze-thawed and sonicated (half inch probe, Vibra Cell, Sonics & Materials Inc.) for 3x120s bursts to break the cells (power setting 6 or until surface vibrates; 1x2min then 2x2min at 50% pulsing). The cell lysate was spun (185,000 x g, 45Ti rotor) for 1 hour in a Beckman L-70 ultracentrifuge and the soluble fraction was loaded onto a 7ml glutathione-sepharose column (Pharmacia) at 0.5ml min⁻¹ equilibrated in buffer A. 20 minute fractions were collected and the absorbance at 280nm of the eluate was measured. Once the soluble fraction was loaded, the column was washed to baseline with buffer A, then with a salt wash (buffer A containing 200mM NaCl) until an additional peak was eluted and washed to baseline. Samples of the eluate were analysed by SDS-PAGE to check that the GST-Rac1 fusion protein had bound to the glutathione-sepharose column (figure 2.1.). The column was washed overnight with buffer A containing 2.5mM CaCl₂ at 1ml min⁻¹. The GST-Rac1 fusion protein was cleaved with

Figure 2.1. Analysis of a Rac1 preparation by SDS-PAGE

Analysis of samples taken during a Rac1 preparation (2.4.2.). Lanes 1+2 = Mw markers, lane 3. = Pre-induction cell extract, lane 4. = post-induction cell extract, lane 5. = extract loaded onto the glutathione-sepharose column, lane 6. = flow through from the glutathione-sepharose column. Lanes 7. + 8. = 2µg and 4µg of purified Rac1 respectively (post-concentration). Rac1 was greater than 95% pure as estimated by SDS-PAGE.



thrombin whilst bound to the glutathione-sepharose column. A 5ml Antithrombin III agarose column (Sigma), equilibrated in buffer A containing 2.5mM CaCl_2 was connected in series to the glutathione-sepharose column in order to remove thrombin after cleavage. A solution of 50ml buffer A containing 2.5mM CaCl_2 and 500 units of human thrombin (Calbiochem) was loaded at $100\mu\text{l min}^{-1}$ collecting 1 hour fractions. Once 25mls had been loaded, 50mM NaCl was added to the remaining buffer to aid the elution of the protein from the column. The fractions containing Rac1 were pooled and dialysed overnight against 2 litres of buffer A to remove the CaCl_2 and NaCl. Some Rac1 mutants bind non-specifically to the glutathione-sepharose column after cleavage. For these proteins, the same protocol was applied except that 150mM NaCl was added to all buffers (figure 2.2.). Purified Rac was concentrated using an amicon pressure concentrator to 15-25mg/ml, centrifuged for 2 minutes ($12,000 \times g$) in an eppendorf centrifuge to remove any precipitated protein, aliquoted and stored at -80°C . Yields of 2.5-8mg/litre were consistently obtained. Rac preparations were greater than 95% pure as judged by Coomassie-blue stained polyacrylamide gels and have an apparent molecular mass of 23kDa (figure 2.1.). The concentration of Rac proteins was calculated from the absorbance spectrum (figure 2.3.) and a calculated extinction co-efficient of $29828 \text{ M}^{-1}\text{cm}^{-1}$ (Gill & von Hippel, 1989). Rac proteins purified from *E.coli* had the additional amino acids glycine and serine at the N-terminus remaining from the thrombin cleavage site and methionine replaced for proline at position 1 to aid the stability of the protein. Electrospray mass spectrometry also revealed the presence of dimers in the purified protein solution. These dimers were lost after the addition of DTT to the buffer, and are probably due to C-terminal Cys176 disulphide interactions.

Expression of Rac1 from the *E.coli* strains XL-1 Blue and DH5 α yields 'truncated' Rac with a number of C-terminal residues (usually 8) missing (figure 2.4.). This is thought to be mainly due to bacterial proteases. Unless otherwise stated, 'Rac' in this report refers to the truncated (residues 1-184) form of the protein used routinely in this laboratory. Many

Figure 2.2. Analysis of an E131K Rac1 preparation by SDS-PAGE

Analysis of samples taken during an E131K Rac1 preparation. Lanes 1.+2. = Mw markers, lane 3.= post-induction cell extract prior to loading onto a glutathione-sepharose column, lane 4. = flow through from the glutathione-sepharose column.

After the cell extract had been loaded onto the column, no protein eluted when the column was washed with 20mM Tris·HCl pH7.6, 1mM MgCl₂, 2.5mM CaCl₂ containing 500 units of thrombin. To examine the protein bound to the column, protein was eluted with 20mM Tris·HCl pH7.6, 1mM MgCl₂ containing 5mM glutathione, and fractions collected. Lanes 5.+6. = eluted protein following glutathione wash. Two proteins eluted from the column corresponding to Rac1 and GST. Only a small amount of the GST-Rac1 fusion protein was detected. This indicates that the fusion protein is cleaved by the thrombin, but the Rac1 binds non-specifically to the column. The addition of >50mM NaCl to the thrombin cleavage buffer in subsequent preparations eluted the E131K Rac1 from the column following cleavage. NaCl was added to the thrombin cleavage buffer when purifying K130A, E127A and E131K Rac1 mutants.

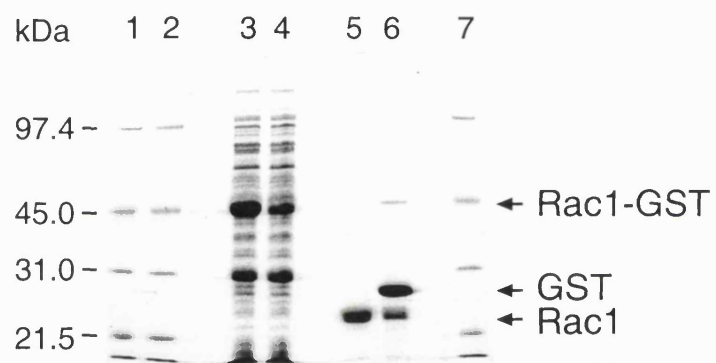
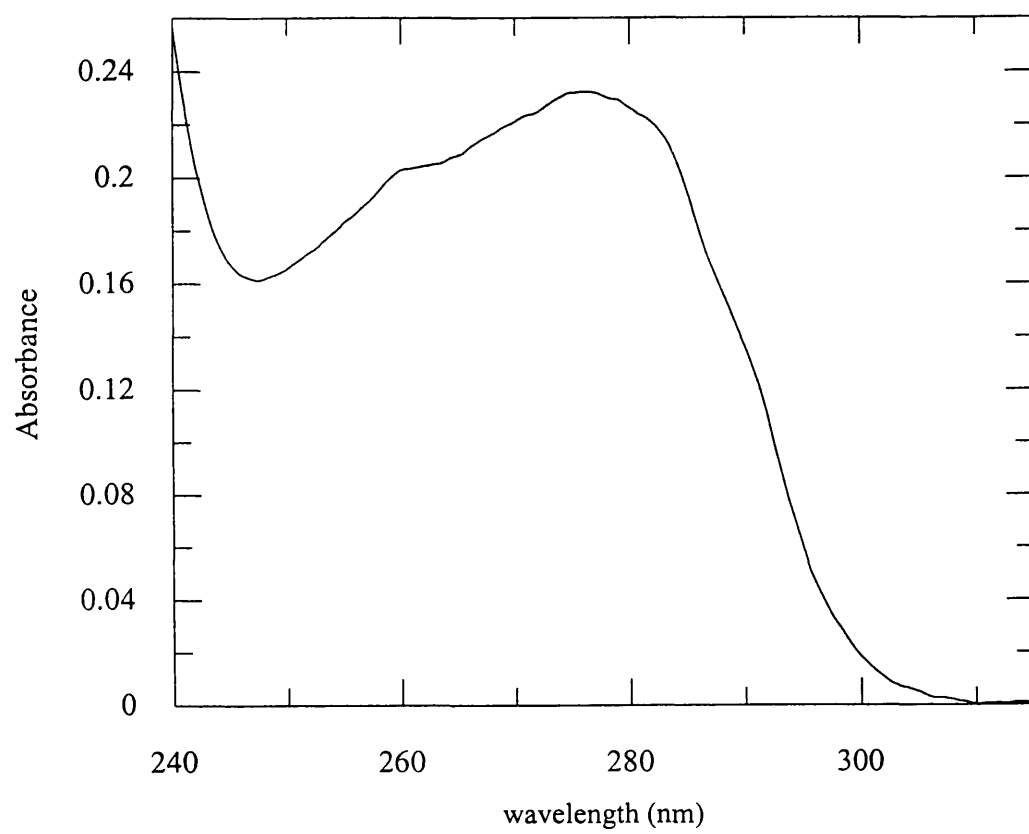


Figure 2.3. Absorbance spectrum of purified Rac1

Absorbance spectrum of 8 μ M purified Rac1 in 20mM Tris·HCl pH 7.6, 1mM MgCl₂.

Rac1 shows a λ_{max} at 276nm. The peak at ~260nm is due to absorbance of the guanine nucleotide bound to the protein.



Rho family G-proteins are substantially clipped at their C-terminus during this purification procedure. A similar observation is seen with Ras expression plasmids, with Ki-Ras in particular susceptible to proteolysis at its C-terminus in *E. coli*. By optimising the purification conditions, pure full length recombinant Rac1 has been obtained.

2.2.2. Purification of full length recombinant Rac1 from *E. coli*

Expression of full length, wild type Rac1 was purified as described above but with the following modifications: the *E.coli* strain BL21 was used to express the protein, and 250 units of thrombin (Calbiochem) was used to cleave the protein from the GST when bound to the column. Due to decreased solubility of the protein and increased viscosity of the bacterial extract, 150mM NaCl was added to all buffers. After loading the cell extract, a high salt wash of 100mls buffer A containing 500mM NaCl followed by an overnight wash of buffer A containing 100mM NaCl + 2.5mM CaCl₂ was required to aid the elution of nucleic acids from the column prior to cleavage of the fusion protein.

Bacterial polysaccharides and other partly solubilised cell wall materials probably account for the increased viscosity of the BL21 bacterial extract. This causes gradual elution of nucleic acid material from the glutathione-sepharose column, resulting in contamination of the purified protein solution by nucleic acids. This results in high absorbance at 260nm in the purified protein solution, masking the absorbance of the protein. This problem was not encountered when truncated Rac was purified from XL-1 blue or DH5 α strains of *E.coli* using this procedure, and this has shown be a problem inherent when using this bacterial strain. The addition of DNase to reduce DNA viscosity or protamine sulphate to precipitate nucleic acid material prior to loading the extract onto the glutathione-sepharose column (Scopes, 1982) did not reduce DNA contamination significantly. The predicted mass of full length Rac1 was confirmed by electrospray mass spectrometry (figure 2.5.) which also indicated that dimerisation of the protein does not occur. Full length Rac1 purified from BL21 *E. coli* was dialysed overnight against 20mM

Figures 2.4. & 2.5. Electrospray mass spectrometry of Rac1

The various peaks correspond to protein molecules with varying net positive charges, z . The mass-to -charge ratio m/z of each of the major peaks is given by the larger number above each corresponding peak.

Figure 2.4. Rac1 purified from DH5 α strain of *E. coli* was analysed by mass spectrometry and two species were observed of 20548.03 (\pm 1.00) Da and 41094.97 (\pm 1.29) Da that represent monomer and dimer of Rac1 truncated by 8 residues at the C-terminus, with Gly-Ser-Pro residues at the N-terminus remaining from the thrombin cleavage site.

Figure 2.5. Rac1 purified from the BL21 strain of *E.coli* was analysed by mass spectrometry. A single species of 21558.35 (\pm 1.21) Da was observed corresponding to full length Rac1 (+ Gly-Ser-Pro at the N-terminus).

Rac 1

10-Feb-1998

97357 195 (3.610) Sm (Mn, 2x3.00); Sb (0,10.00); Cm (181:235)

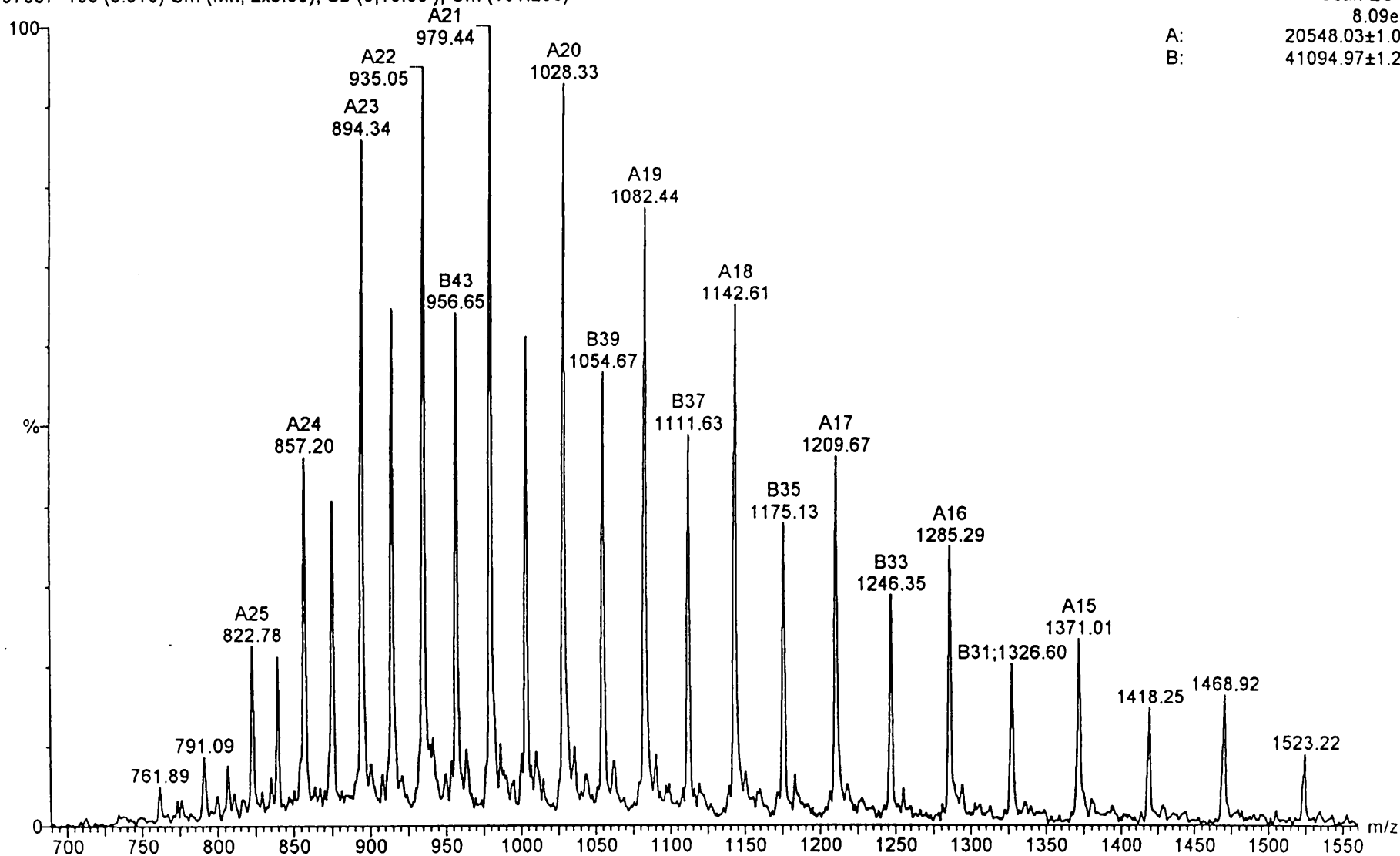
Scan ES+

8.09e6

A: 20548.03±1.00

B: 41094.97±1.29

Figure 2.4.



BL21 Rac1

97206 181 (5.632) Sm (Mn, 2x3.00); Sb (0,10.00); Cm (171:210)

06-Aug-1997

Scan ES+

3.89e6

A: 21558.35±1.21

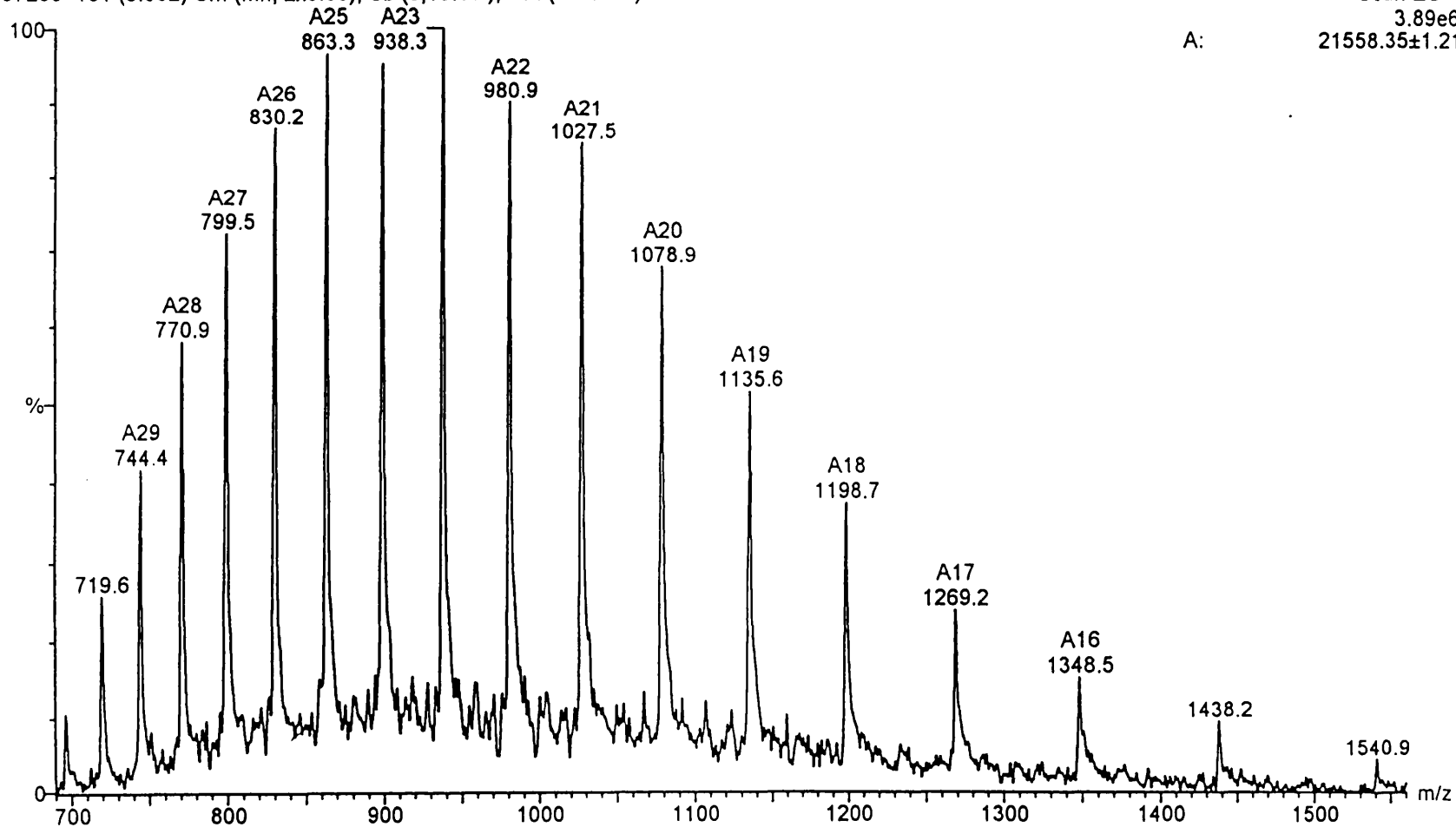


Figure 2.5.

Tris·HCl, 1mM MgCl₂ + 150mM NaCl and was concentrated using an amicon concentrator to 6.5-13mg/ml.

2.2.3. Purification of p67¹⁻¹⁹⁹ from *E.coli*

An N-terminal fragment of p67^{phox} (p67¹⁻¹⁹⁹) that includes the Rac1 binding region (1.3.) was purified from the BL21 strain of *E.coli* using the method described for Rac proteins, except that after loading the cell extract onto the glutathione-sepharose column, 200mM NaCl was added to all buffers. This was required to prevent non-specific binding of the protein to the column following cleavage from the glutathione-S-transferase. The final protein was dialysed and concentrated in 20mM Tris·HCl pH 7.6, 150mM NaCl. SDS-PAGE analysis of the protein indicated greater than 95% purity (figure 2.6.). This protein fragment shows solubility problems dependent on temperature and ionic strength; a temperature greater than 4°C, or buffer containing less than 100mM NaCl causes gradual precipitation of a dilute (5μM) p67¹⁻¹⁹⁹ solution (in 20mM Tris·HCl pH 7.6). The molecular weight of this purified protein did not initially correspond to that predicted by the sequence. Dideoxy sequencing of the N- and C-termini has revealed the presence of 20 additional residues that are not part of the p67^{phox} cDNA.

2.2.4. Purification of p67^{phox} and p47^{phox} from *E.coli*

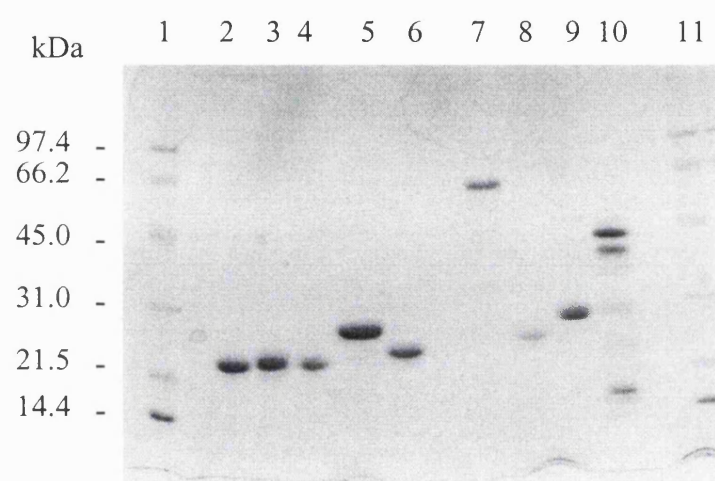
Purification of full length p67^{phox} from *E.coli* as yet has been unsuccessful. This seems to be due to solubility problems encountered during the purification procedure, and may be due to loss of protein into bacterial inclusion granules. Several other bacterial strains and growth conditions (various incubation temperatures, shorter growth time after induction) were tested in order to alter the expression pattern, but the GST-p67^{phox} fusion protein remained in the insoluble fraction in all cases. Although p47^{phox} protein has been obtained (using the purification procedure described for Rac proteins), SDS-PAGE analysis of the protein has revealed 4-6 bands (figure 2.6.), suggesting that this protein when expressed

Figure 2.6. SDS polyacrylamide gel electrophoresis (SDS-PAGE) of purified proteins

Purified proteins (~5µg) were analysed by SDS-PAGE using a 15% polyacrylamide gel (2.4.2.) and de-stained in 50% methanol, 10% glacial acetic acid overnight to assess protein purity. Lanes 1. and 11. show molecular weight markers, Lane 2. = Rac1 (aa's 1-184), Lane 3. = Rac1 (full length), Lane 4. = cdc42 (aa's 1-184), Lane 5. = RhoA (full length), Lane 6. = N-Ras (full length), Lane 7. = p67^{phox}, Lane 8. = p67¹⁻¹⁹⁹, Lane 9. = GDI, Lane 10 = p47^{phox}. Even in the presence of bacterial protease inhibitors, p47^{phox} is susceptible to major proteolytic degradation. All other proteins are >95% pure as analysed by SDS-PAGE.

Although ~5µg of each protein was added to each well, the intensity of each protein band following an overnight de-stain is variable. This may be because Coomassie brilliant blue R250 does not react chemically with proteins, but forms non-covalent complexes. This interaction is thought to be primarily ionic, involving basic groups on proteins. Due to this, the dye may not bind equally to all proteins when examined by Coomassie stained polyacrylamide gels (Crichton, 1993).

It can be seen from figure 2.6. that full length RhoA migrates slower than full length Rac1, despite both proteins having similar molecular weights (Rac1 = 21450 Da, RhoA = 21768 Da). This may be because the binding of SDS to polypeptides seems to depend on ionic interactions. Proteins that are intrinsically very basic or acidic may produce complexes with SDS that have atypical charge densities that may affect the migration of protein through a polyacrylamide gel (Creighton, 1993).



in *E.coli* is susceptible to major proteolytic degradation, probably due to bacterial proteases.

2.3. Baculovirus methods

Due to the insolubility of the p67^{phox} fusion protein in *E.coli*, p67^{phox} was expressed using a baculovirus expression system. This eukaryotic expression system has a number of advantages over bacterial expression systems. Many bacterially expressed, recombinant proteins are insoluble, aggregated or incorrectly folded. In contrast, proteins expressed in a baculovirus expression system are in most cases, soluble and functionally active. In addition, several post-translational modifications have been reported to occur in insect cells, including isoprenylation (Kloc *et al.*, 1991). Protein expression and purification using a baculovirus expression system is performed in three stages - 1) Baculovirus quantification and amplification, 2) Infection of insect cells, and 3) Purification of recombinant p67^{phox} protein. To maintain healthy cultures, *sf9* insect cells were subcultured 1:3 with serum free media (TC100) when they reached a spinner bottle density of $>1 \times 10^6$ cells/ml. Stocks of active virus were frozen in small aliquots at -80°C .

2.3.1. Quantification of viral titre by serial dilution plaque assay

The baculovirus plaque assay was used to calculate the virus titre of an unknown viral stock solution so that known amounts of virus can be used to infect cells during subsequent experimental procedures. Viral titre is expressed as plaque forming units per ml (PFUs/ml). 3×10^6 log phase *sf9* cells were pipetted into 3cm wells of a 6 well tissue culture dish and allowed to adhere for 30 minutes. The cells were examined using a microscope to ensure a confluent monolayer was formed. When 90-95% confluence was achieved, the media was aspirated off. Whilst the cells were adhering, the viral dilutions were prepared. The virus solution was serially diluted in TC100 + 10% FCS by a factor of 10^{-5} to 10^{-9} . 1ml of each viral dilution was added to a single well, with a negative control of media only. This was carried out in duplicate. The tissue culture dishes were gently

rocked for 90 minutes at room temperature to allow infection of the monolayer. Whilst the cells were infecting, a solution of 3% agarose (Sea Plaque, low melting temperature, FMC Bioproducts) was melted in a microwave and left to cool in a 40°C water bath. Once cooled, a solution of 1.5% agarose, 10% FCS was made, and placed at 40°C to prevent the agar setting. Once the cells were infected, the virus was removed. The agarose solution was left to cool for a few minutes at room temperature, then 2mls of the agarose mix was gently added to each well, overlaying the *sf9*s, and left for fifteen minutes at room temperature to set. Once set, the dishes were placed in a humidity box, and incubated at 27°C. The following day, 1ml of TC100 + 10% FCS was added to each well to feed the cells, and incubated at 27°C for a further 3 days. The media was removed, and 1ml of PBS + 50µl of 0.5% (w/v) neutral red (Sigma) was added to the agar of each well, and the cells left to stain at 27°C for at least 4 hours. The plaques were visualised and the PFUs/ml calculated by pouring off the stain and examining the cells over a light box. Areas of missing cells were often seen in virally infected wells. These ‘crescents’ appear to be due to the addition of the virus to the monolayer as they were not seen in control wells where buffer alone was added. When crescents were seen, the number of PFUs/ml was estimated from the remaining cells.

2.3.2. *Baculovirus amplification*

Baculovirus amplification was carried out under aseptic conditions. 3.6×10^8 *sf9* cells in *sf900II* serum free media with a density of 1.25×10^6 cells.ml⁻¹ were plated into 6x sterile 175cm² tissue culture flasks (6×10^7 cells/flask) and left at room temperature to attach to the surface. After 90 minutes, media was removed to leave a final volume of 20mls per flask. 1.5mls of low titre baculovirus (2×10^7 PFUs/ml) was added to each flask to provide a multiplicity of infection of 0.5 PFUs/cell, and the flasks were incubated at room temperature for 1 hour. It was essential to keep the multiplicity of infection low; passaging the virus at high PFUs/cell increases the number of virus with extensive mutations in the genome (Crossen & Gruenwald, 1997). Flasks were incubated at 27°C

for 12 days, or until 60-70% of the cells were detached when examined under a light microscope. The remaining cells were detached from the surface of the flask using a scraper, poured into sterile centrifuge tubes and spun (410 x g, Beckman J6-HC centrifuge, JS 4.2 rotor) for 10 minutes to remove remaining cells and cell debris. The supernatant was poured into a sterile 85cm² tissue culture flask and stored in the dark at 4°C. The viral titre of the amplification solution was determined using the plaque assay procedure (2.3.1.).

2.3.3. Infection of *Spodoptera frugiperda* 9 insect cells with p67^{phox} baculovirus

2.4x10⁸ *sf9* cells in serum free media with a density of 1.3x10⁶ cells.ml⁻¹ were plated into 6 x 175cm² tissue culture flasks (4x10⁷ cells/flask) and left at room temperature to attach to the surface. After 1 hour, 2mls of recombinant baculovirus with a titre of 1x10⁸ plaque forming units per ml (PFU.ml⁻¹) was added to each flask to provide a multiplicity of infection of 5 PFUs/cell, and the flasks were then incubated at 27°C. A flask containing non-infected cells was used as a negative control. After 89 hours of viral infection, 40-50% of cells in virally infected flasks were detached from the surface of the plate. A cell scraper was used to detach cells the remaining cells from the sides of the flasks into the existing media, and poured into 4 x 50ml centrifuge tubes, and a sample was taken for analysis by SDS-PAGE. The infected cells were harvested by centrifugation (410 x g, J6-HC centrifuge in a JS 4.2 rotor) for 15 minutes at room temperature, the supernatant discarded, and the pelleted cells frozen on dry ice and stored at -80°C.

2.3.4. Purification of recombinant p67^{phox} from baculovirus infected *sf9* insect cells

The cell pellet was thawed rapidly in a 22°C water bath, and the pellets gently re-suspended in lysis buffer (5mM PIPES, pH 7.6, 50mM KCl, 3mM NaCl, 4mM MgCl₂, 2mM PMSF) containing 2x protease inhibitor cocktail (Sigma P-2714) (4mM AEBSF, 2mM EDTA, 260µM Bestatin, 2.8µM E64, 2µM Leupeptin, 0.6µM Aprotinin) to a final volume of 20mls. The pH was adjusted to 7.5 by carefully adding 6M NaOH, and the

cells were disrupted by sonication on ice using a 0.5 inch probe for 3x30s bursts (power setting 3 or until surface vibrates). To check for complete lysis, a sample was examined under a microscope. The cell extract was centrifuged (11,000 x g, 70.1Ti rotor) in a Beckman L-70 ultracentrifuge for 15 minutes at 4°C to pellet cell debris, and a sample taken for SDS-PAGE. The resulting supernatant was topped up to 25mls with lysis buffer, and re-centrifuged (112,000 x g, 70Ti rotor) in a Beckman L-70 ultracentrifuge for 1 hour at 4°C. The supernatant was removed, and this crude recombinant p67^{phox} preparation was filtered then through a 0.2µm acrodisc, and the pH carefully adjusted to pH 7.5 with 6M NaOH. A sample of the post-filtered extract was taken for SDS-PAGE.

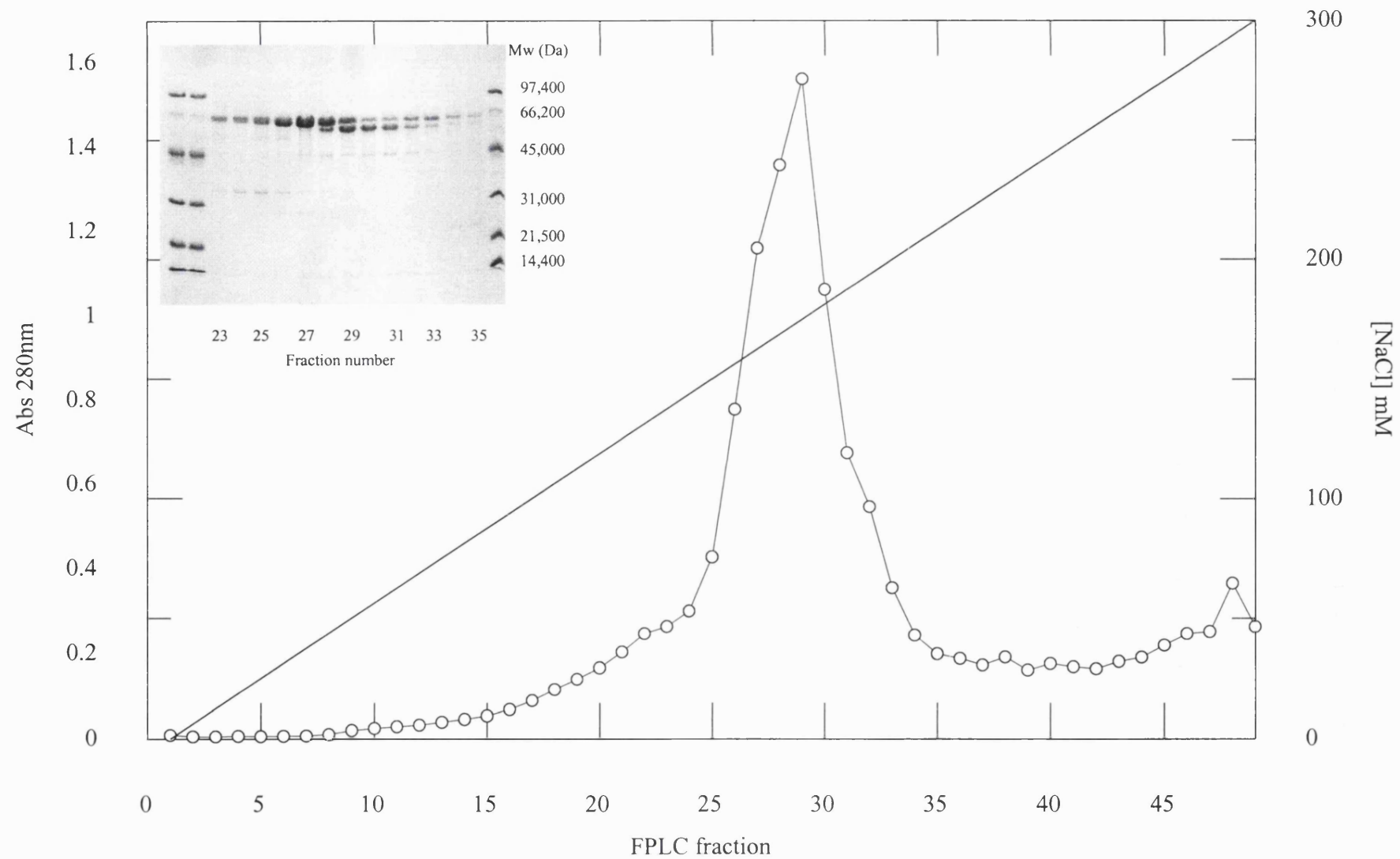
The cell extract was loaded at 1ml.min⁻¹ using a 50ml superloop (Pharmacia) onto a 1ml FPLC mono-Q anion exchange column (Pharmacia) equilibrated in buffer A (50mM Tris-HCl, pH 7.5, 0.1mM DTT) and the flow through collected. After the sample was loaded, the column was washed with 45mls of buffer A (until baseline near zero at 280nm). Protein was eluted with a 0-0.3M NaCl gradient (50mls, flow rate 1ml.min⁻¹) and 1ml fractions collected. Samples were taken for analysis by SDS-PAGE, and the fractions frozen at -80°C. The fractions containing p67^{phox} were pooled and concentrated in a centrprep 10 (Amicon) to a final volume of 0.6mls. The concentration of p67^{phox} was determined using a calculated extinction coefficient (2.4.3.) of 65580 M⁻¹ cm⁻¹. Samples were taken for analysis by SDS-PAGE and electrospray mass spectrometry, and the p67^{phox} frozen and stored in aliquots at -80°C. A slightly smaller protein was observed in the trailing half of the major peak eluted from the mono-Q column (figure 2.7.), suggesting that p67^{phox} is susceptible to minor proteolytic degradation, consistent with previous reports (Leto *et al.*, 1991). The heavier protein band had an apparent molecular mass of 60kDa.

Figure 2.7. Purification of p67^{phox} by anion exchange chromatography

The lysate from 2.4×10^8 baculovirus infected insect cells was loaded onto a 1ml mono-Q anion exchange FPLC column equilibrated in 50mM Tris.HCl pH 7.5, 0.1mM DTT. The protein was eluted with a 0-0.3M NaCl gradient with a flow rate of $1\text{ml}\cdot\text{min}^{-1}$, and the absorbance of the fractions at 280nm measured.

Gel inlay - Analysis of eluted protein by SDS-PAGE

Samples of fractions collected were analysed using SDS-PAGE. A smaller protein was observed in the trailing half of the major peak eluted from the mono-Q column, suggesting p67^{phox} is susceptible to minor proteolytic degradation.



2.4. Methods used to determine protein purity and concentration

2.4.1. Electrospray mass spectrometry of purified proteins and peptides

The molecular weight of purified proteins and peptides was analysed by pneumatically assisted, electrospray ionization mass spectrometry. In this technique, protein molecules in a volatile solvent are sprayed into the mass spectrometer. The solvent evaporates, leaving the protein suspended. The initial solution is at acidic pH, in which the protein molecules have a positive charge. The various intact protein molecules with varying net positive charges allow them to be separated by mass spectrometry.

Mass spectrometry of proteins and peptides was carried out by DR. S. Howell (N.I.M.R.) using a modified 130A HPLC (Perkin Elmer, USA) coupled on-line to a platform electrospray mass spectrometer (Micromass, UK). Reverse phase chromatography was performed using a Poros RII (Perseptive Biosystems, USA) 0.25mm x 100mm PEEK column, slurry packed in-house, at a flow rate of 10 μ l/min over a 0-100% B linear gradient in 10 mins (buffer A = 0.12% formic acid, 90% water 10% acetonitrile; buffer B = 0.10% formic acid, 15% water, 85% acetonitrile) with UV monitoring at 214nm. The low flow rate was achieved by incorporating a valco tee, coupled to a microbore dummy column, just prior to the rheodyne injection valve. The mass spectrometer was calibrated using myoglobin. Small peptides were flow injected and analysed using the same system.

2.4.2. SDS polyacrylamide gel electrophoresis (SDS-PAGE).

SDS-PAGE was routinely used to determine protein purity throughout purification procedures (figure 2.6.). A 'mighty small' electrophoresis unit was used (Hoefer Scientific Instruments) with gels of 73mm x 83mm x 0.5mm. The stacking gel consisted of 5% polyacrylamide, 200mM Tris·HCl pH 6.8, 0.1% SDS and the resolving gel contained 15% polyacrylamide, 375mM Tris·HCl pH 8.8, 0.1% SDS. Samples of protein were boiled at 95°C for 5 minutes with sample buffer (100 μ M DTT, 2% (w/v) SDS, 10%

glycerol (v/v), 25mM Tris pH 6.6, 0.0025% (w/v) bromophenol blue) with a typical volume of 15µl per lane and ran at 16mA/gel in running buffer (25mM Tris-HCl pH 8.6, 250mM glycine, 0.02% SDS) until the bromophenol blue reached the bottom of the resolving gel. Gels were stained with 2.5g.l⁻¹ Coomassie brilliant blue R250 (Biorad) in 45% methanol, 10% glacial acetic acid for 15-20 minutes, de-stained in 50% methanol, 10% glacial acetic acid and a permanent record of the gel was made using a UVItec gel scanner.

2.4.3. Determination of recombinant protein concentration

The concentrations of purified recombinant proteins from *E.coli* and baculovirus infected insect cells were determined using UV absorbance spectroscopy using a Beckman DU640 spectrophotometer based on molar extinction co-efficients calculated from the primary sequence (table 2.1.). Values of 5540 M⁻¹cm⁻¹, 1480 M⁻¹cm⁻¹ and 60 M⁻¹cm⁻¹ at 280nm were used for the extinction co-efficients of tryptophan, tyrosine and cysteine respectively (Gill & von Hippel, 1989, Mach *et al.*, 1992). All Rho family proteins were purified with stoichiometric bound guanine nucleotide and an additional extinction coefficient of 7953 M⁻¹cm⁻¹ (calculated from the GDP absorbance spectra and the molar extinction co-efficient at 260nm of 11800 M⁻¹cm⁻¹) was added to the calculated extinction co-efficients for these proteins (Dawson *et al.*, 1984).

2.5. Peptide methods

Peptides corresponding to the C-terminus of Rac1 were synthesised by P. Fletcher (Division of Protein Structure, N.I.M.R.) using fluorenylmethoxycarbonyl ('fast-moc') chemistry on an Applied Biosystems 430A peptide synthesiser. After removal from the resin and deprotection, peptides were purified by HPLC on a C18 reverse phase silica column with a water/acetonitrile gradient containing 0.1% trifluoroacetic acid and characterised by electrospray mass spectrometry (2.4.1.). Lyophilised peptides were stored at 4°C, and all peptide solutions were stored at -20°C. *Trans, trans* farnesyl

Table 2.1. Calculated extinction co-efficients for purified recombinant proteins

Calculated extinction co-efficients

Protein	M ⁻¹ cm ⁻¹ (280nm)
Rac1 (1-184)	29828
Cdc42Hs (1-184)	24213
RhoA (full length)	26793
N-Ras (full length)	21573
p67 ^{phox}	65580
p67 ¹⁻¹⁹⁹	37200
p47 ^{phox}	56780
RhoGDI	27370

bromide was purchased from Sigma and re-distilled under low pressure by Drs M.R. Webb and J.E.T. Corrie (N.I.M.R.) then stored under nitrogen at -80°C. To minimise impurities, high purity H₂O (Romil) was used for all HPLC buffers, and solutions containing acetonitrile were de-gassed to remove dissolved gasses and minimise bubbles prior to use. Rac1 C-terminal 7-mer peptide was farnesylated by J. Hunter (Newcombe *et al.*, 1999).

2.5.1. Modifying a Rac C-terminal peptide (12-mer) with farnesyl bromide

The Rac C-terminal 12-mer (sequence PVKKRK RKCLLL) corresponds to the native C-terminal Rac1 sequence prior to *in vivo* geranylgeranylation and proteolytic cleavage of the 3 terminal leucines. 2.7mmol of 12-mer was incubated in a multi-phase reaction mixture containing 0.8% (v/v) *trans, trans* farnesyl bromide (Sigma), 20% (v/v) DMF, 4mM EDTA, (volume 500μl) and the pH titrated to 7.8-8.0 with 1M Tris base. The mixture was incubated at room temperature typically for 8 hours under continuous nitrogen flow and maintained at pH 8.0 by occasional addition of 1M Tris base. To monitor the labelling reaction, 2 hourly samples were taken and analysed by HPLC on a reverse phase silica column (Whatman Partisil-10 ODS, C18, 250 x 46mm) using a 40 minute 10% to 75% acetonitrile (v/v) gradient containing 0.1% trifluoroacetic acid at a flow rate of 1ml.min⁻¹. After ~8 hours, the reaction mix was frozen on dry ice and stored overnight at -20°C. An 8 hour sample was analysed the following day and the modified peptide was purified by HPLC using the same column (figure 2.8.). The buffer was evaporated from the fractions containing the labelled peptide using a speedvac evaporator, the TFA was removed by 3 evaporation cycles and the labelled peptide finally re-suspended in 50% (v/v) acetonitrile/water. Mass spectrometry confirmed that the peptide had a single farnesyl group attached (figure 2.9.).

Modifying quantitative yields of a Rac1 C-terminal 9mer (with the 3 terminal leucines omitted) using the same conditions was unsuccessful. It is possible that the hydrophilicity

Figure 2.8. HPLC chromatograms showing the farnesylation of a Rac1 C-terminal 12mer peptide

Analysis of the 12mer peptide modification reaction by HPLC. A) 20 μ g unlabelled Rac1 C-terminal peptide. B) A sample (~20 μ g) of the 8 hour reaction mixture. The 2 major peaks eluting at 20 and 33 minutes correspond to unmodified and modified 12mer. These peaks were collected, and the peak containing Farnesyl bromide-modified peptide confirmed by mass spectrometry (figure 2.9.). C) A sample (~5 μ g) of the concentrated farnesyl-12mer. The concentration of modified product was determined by comparison of peak areas after injection of a known amount of un-modified 12mer. Absorbance shown is in arbitrary units.

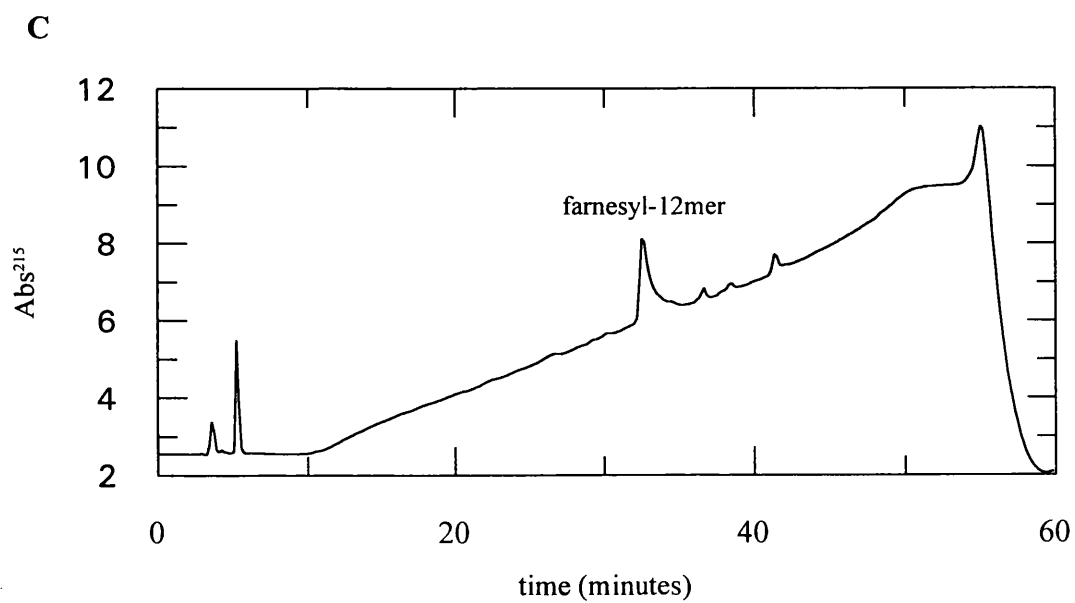
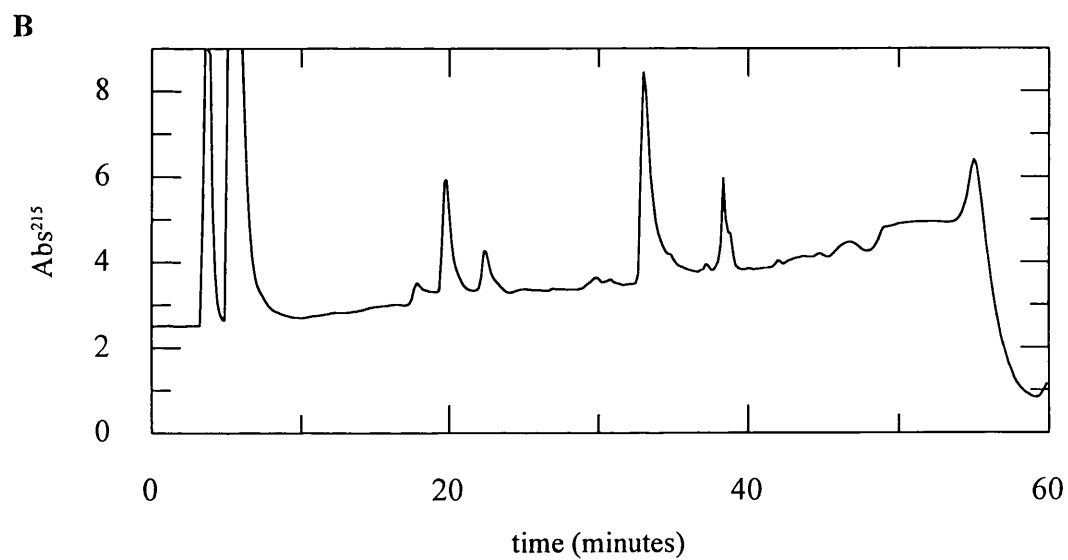
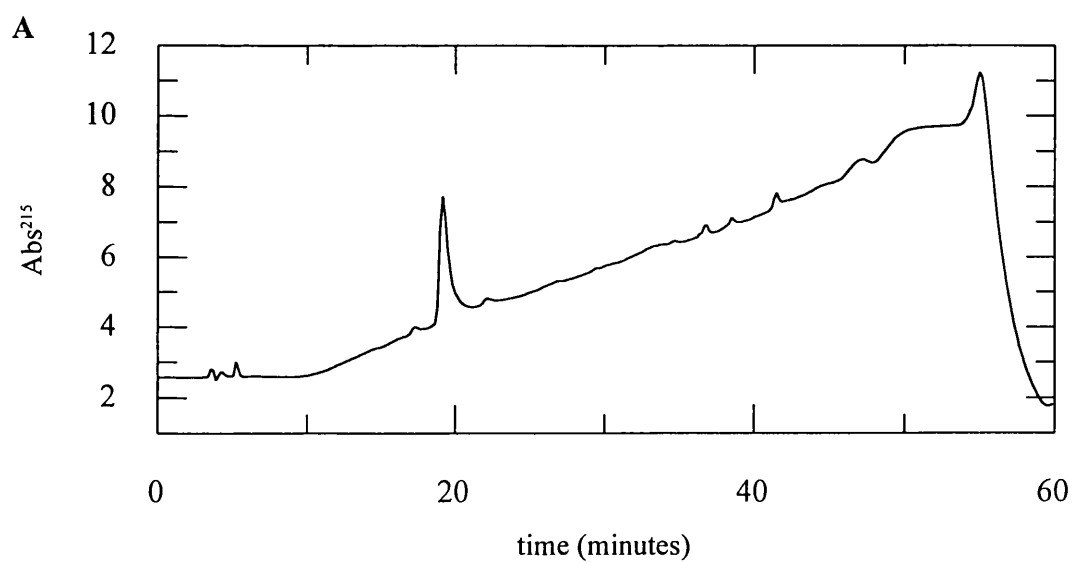


Figure 2.9. Electrospray mass spectrometry of a farnesylated Rac1 C-terminal 12mer

Peaks A2, A3 and A4 correspond to farnesylated 12mer peptide differing by one unit of charge and by a proton in mass. A species of 1684.98 (\pm 0.19) was detected corresponding to a Rac1 C-terminal 12mer with a single farnesyl group attached.

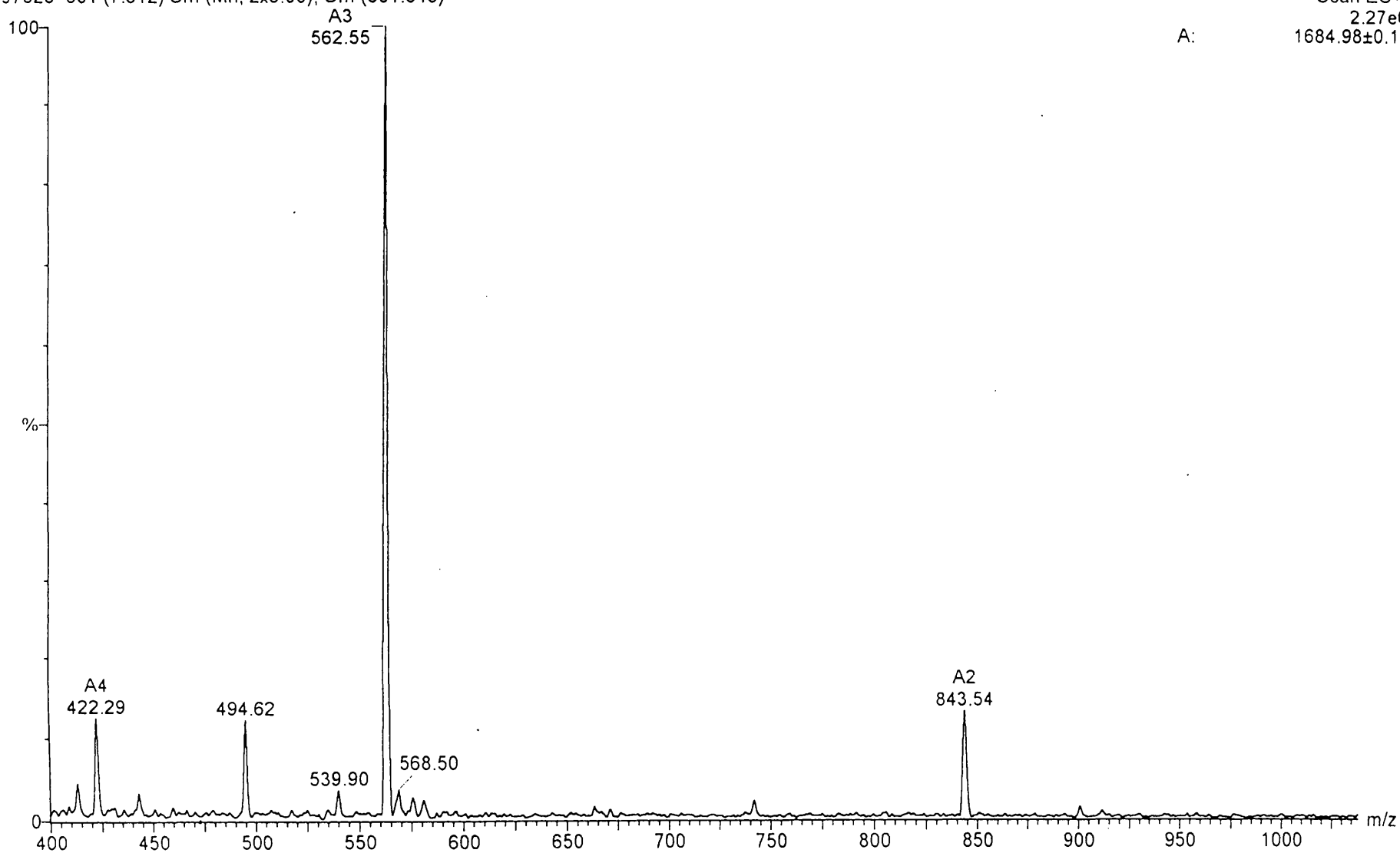
97323 301 (7.612) Sm (Mn, 2x3.00); Cm (301:345)

Scan ES+

2.27e6

A:

1684.98±0.19



of this peptide reduces the solubility under these conditions and prevents efficient modification with the hydrophobic farnesyl group. It was hoped that carboxyl methylating the C-terminal cysteine prior to farnesyl modification would improve yields of modified peptide.

2.5.2. Methylating Rac C-terminal (9mer and 11mer) peptides

A Rac C-terminal 9mer (sequence PVKKRKRC) corresponding to the C-terminal sequence of the native protein following cleavage of the 3 terminal leucines (1.13.1.) and a C-terminal 11mer containing two additional proline residues at the N-terminus (sequence PPPVKKRKRC) were carboxyl methylated on the C-terminal cysteine. 20mgs of peptide was dissolved in 0.5ml dried methanol containing 4% concentrated HCl, pH 2.7. The reaction was left at room temperature for 8-9 hours with continuous stirring. To monitor the extent of the reaction, 2 hourly samples were analysed by HPLC a reverse phase silica column (Whatman Partisil-10 ODS, C18, 250 x 46mm) using a 45 minute 0.1% TFA in water to 40% acetonitrile (v/v), 0.1% TFA (Merck) gradient with a flow rate of 1ml.min⁻¹. After 6 hours >80% of the peptide was methylated (figure 2.10.). The column was washed for 3 minutes in 75% acetonitrile (v/v), 0.1% TFA then 10 minutes 0.1% TFA prior to subsequent injections. The reaction mix was stored at 20°C overnight, then concentrated and washed with 3 volumes of dry methanol using a speedvac evaporator until dry, and the peptide re-suspended in 60% DMF in water and stored at 20°C. For further modification, it was assumed that ~100% of the peptide had been carboxyl methylated.

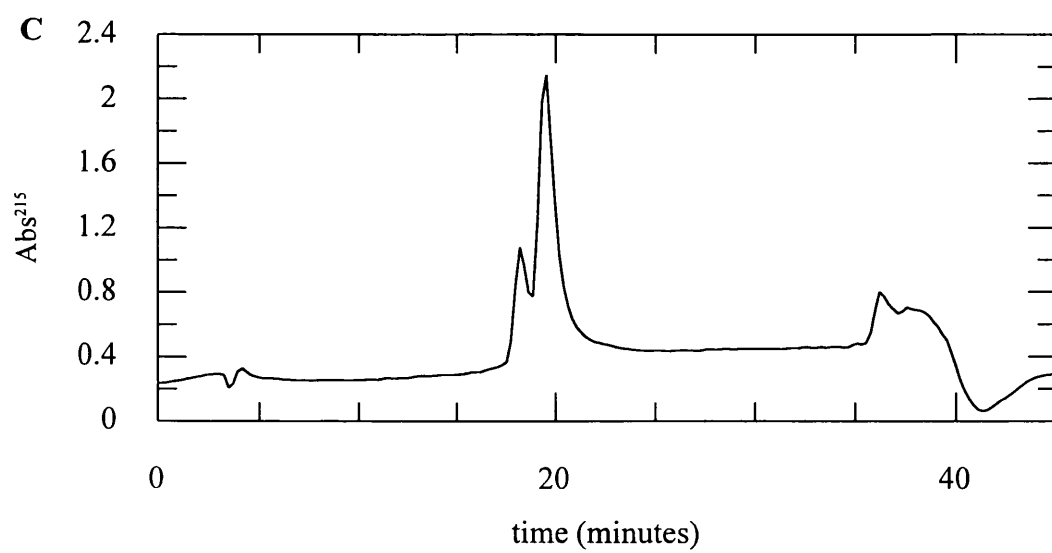
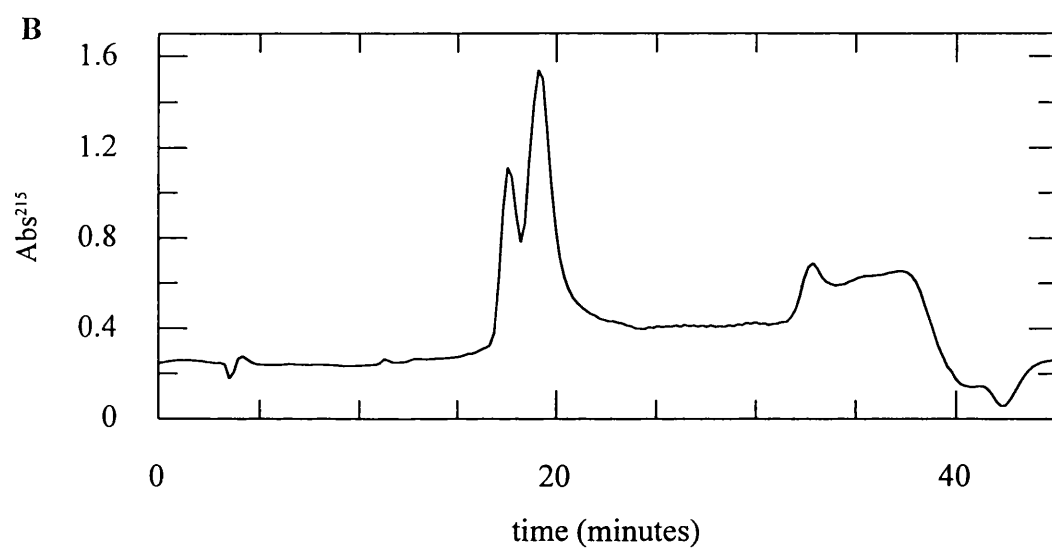
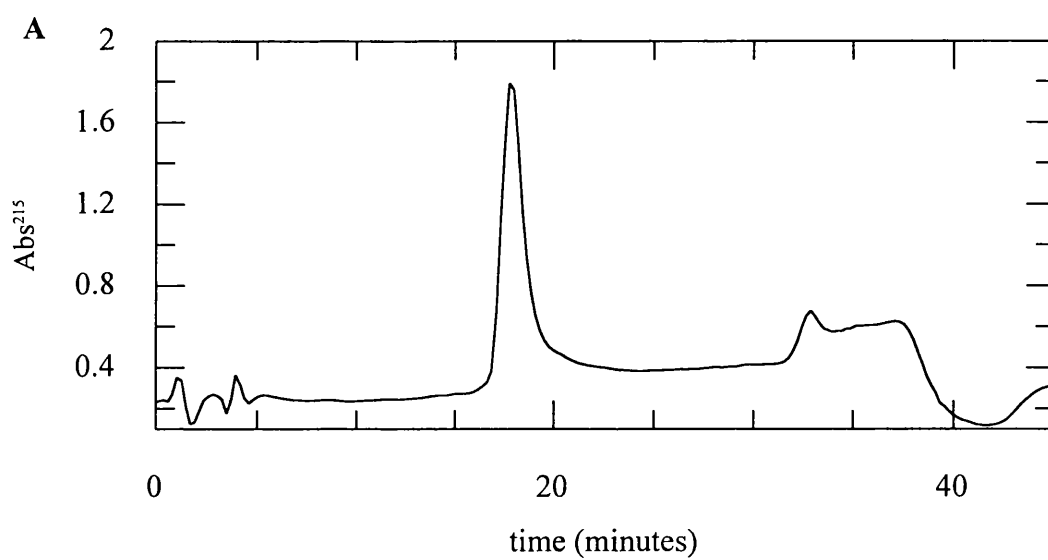
2.5.3. Farnesylating methylated Rac C-terminal peptides (9mer & 11mer)

Farnesylation of a methylated Rac C-terminal 9mer was carried out under the same conditions used to modify a Rac C-terminal 12-mer with the following modifications – 8mgs of methylated 9mer was incubated in a mixture containing 0.8% (v/v) *trans trans* farnesyl bromide (Sigma), 60% (v/v) DMF, 4mM TCEP (vol. 1ml) titrated to pH 7.8-8.0

Figure 2.10. HPLC chromatograms showing the methylation of a Rac C-terminal 11mer peptide

Analysis of the methylation reaction by HPLC. A) A sample of the reaction mix at time 0. B) A sample of the reaction mix after 4 hours. C) A sample of the reaction mix after 6 hours.

Methylation of a Rac C-terminal 9mer showed a similar elution profile after 6 hours. Mass spectrometry of the 8 hour reaction mix confirmed the presence of methylated 9mer or 11mer (data not shown). Analysis of an 8 hour sample following incubation with DTT did not alter the elution time of the peaks, indicating that this peak shift is not due to dimerisation of the peptide. Absorbance shown is in arbitrary units.



with 1M Tris base. Two hourly samples were analysed using a 0-75% acetonitrile gradient containing 0.1% trifluoroacetic acid at 1ml.min⁻¹ (figure 2.11.). The farnesylated 9mer was analysed by mass spectrometry (figure 2.12.), concentrated and stored as described for a C-terminal 12-mer (2.5.1).

2.5.4. Determination of peptide concentration using reverse phase HPLC

Due to the absence of aromatic residues in all of the Rac C-terminal peptides used, peptide concentrations were determined by comparison of peak areas of a known concentration of unmodified peptide, with a known volume of modified peptide under conditions used to monitor the farnesylation reaction.

2.5.5. Determination of peptide concentration using TNBSA

2,4,6-Trinitrobenzene sulphonic acid (TNBSA) forms a highly chromogenic derivative upon reaction with primary amines, hydrazine or sulfhydryl groups and may be used to assay the amine content of compounds by measuring the increase absorbance at 335nm or 450nm (figure 2.13.). 0.5ml TNBSA (0.01% v/v) in 0.1M sodium bicarbonate, pH 8.5 was added to 3-5µl of modified peptide in 0.1M sodium bicarbonate pH 8.5 (vol. 1ml) and incubated at 37°C for 2 hours. 0.5ml of 10% SDS and 0.25ml of 1M HCl were added to each sample and the absorbance at 335nm measured. Determination of the number of amines present was calculated by comparison with a standard curve generated with glycine dissolved at a series of known concentrations and used to calculate peptide concentration. However, due to the instability of TNBSA, consistent results with using this method could not be obtained. The use of TNBSA to accurately measure peptide concentration is currently under investigation in this laboratory.

2.6. Molecular biology methods

Thermal cycling techniques used for oligonucleotide-mediated mutagenesis were carried out using a Techne PHC-3 or Hybaid OmniGene thermal cycler unless otherwise stated.

Figure 2.11. HPLC chromatograms showing the farnesylation of a methylated 9mer

A) A sample of the reaction at time 0. B) A 6 hour sample of the farnesylation reaction, showing additional peaks eluting between 44 and 48 minutes. These fractions were collected and concentrated as described. C) A sample of the final concentrated 9mer. Mass spectrometry confirmed the presence of methylated, farnesylated 9mer peptide.

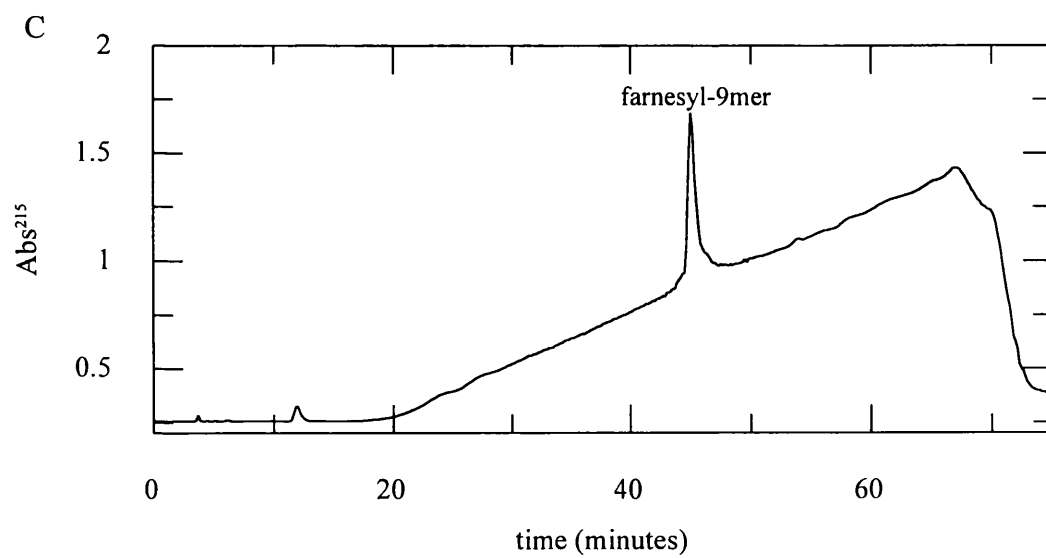
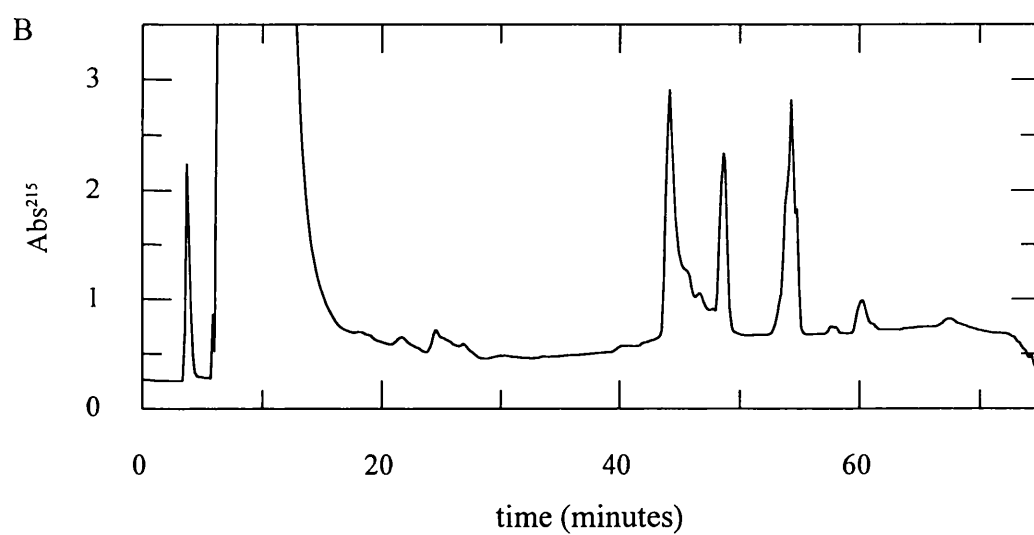
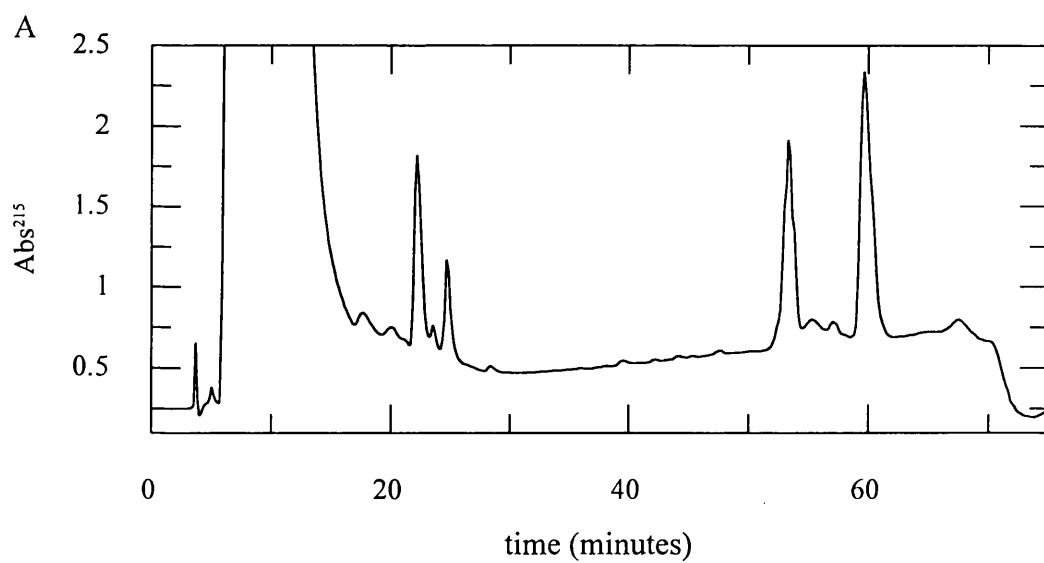


Figure 2.12. Electrospray mass spectrometry of a methylated, farnesylated 9mer

Peaks A2 and A3 correspond to a methylated, farnesylated 9mer peptide differing by one unit of charge and by a proton in mass. A species of 1359.34 (\pm 0.29) was detected corresponding to a methylated Rac1 C-terminal 9mer with a single farnesyl group attached. Additional peaks may represent impurities or fragmentation of the modified peptide.

97792 369 (8.837) Sm (Mn, 2x3.00); Cm (365:390-42:114x1.500)

Scan ES+
1.80e6
A: 1359.34±0.29

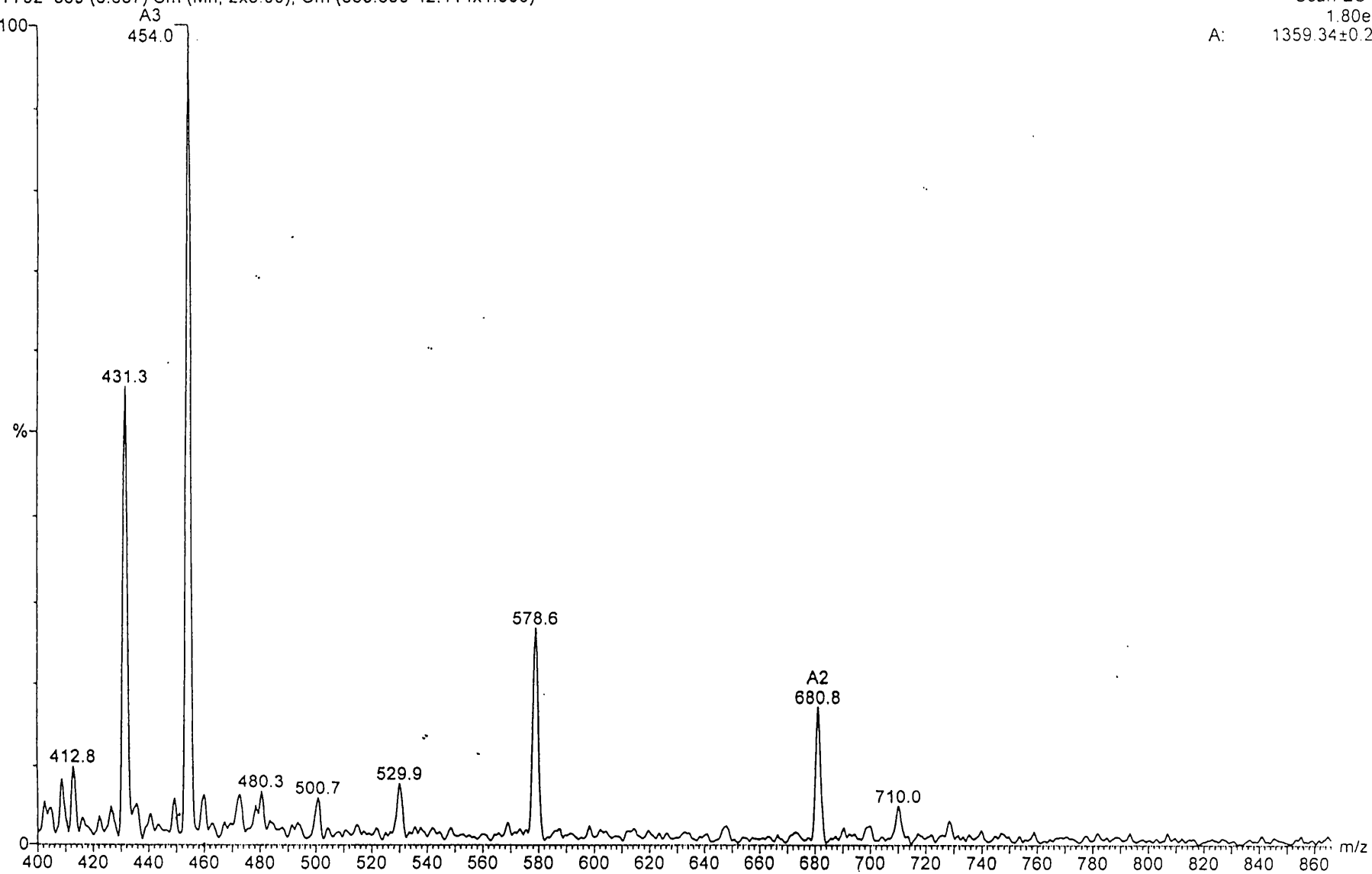
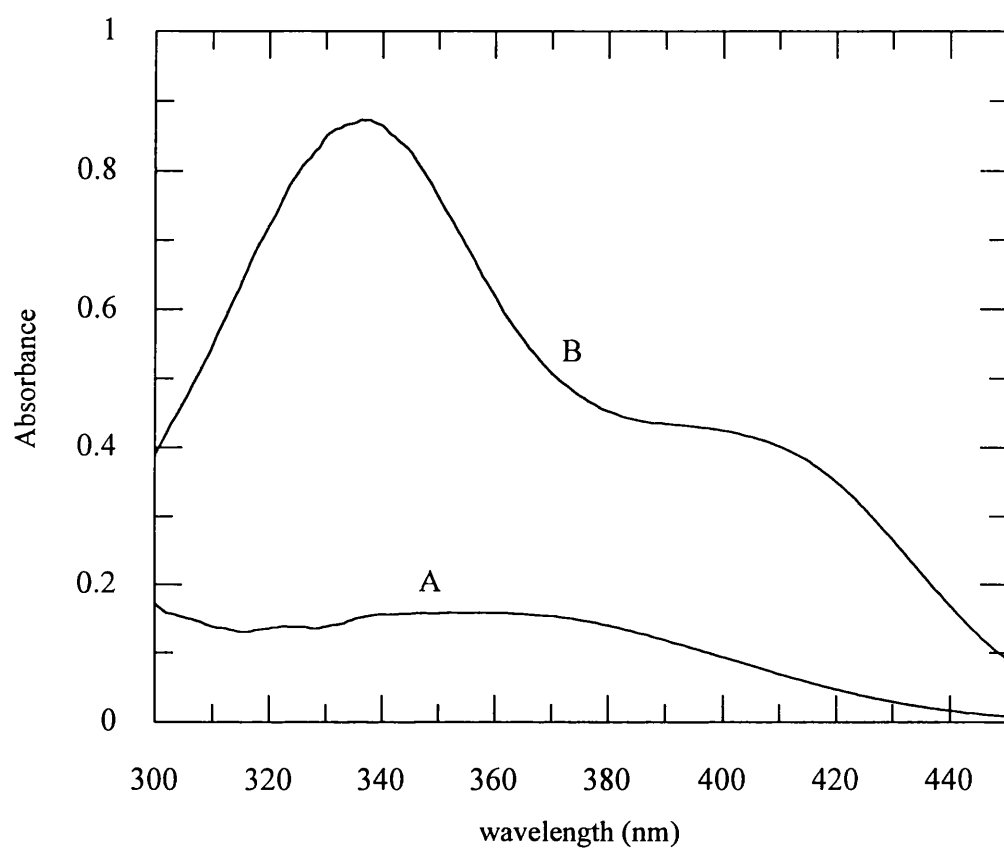


Figure 2.13. Reaction of TNBSA with glycine

The primary amine of glycine reacts with TNBSA to form a highly chromogenic derivative. This reaction may be used to assay the amine content of peptides by measuring the absorbance of the orange coloured product at the λ_{max} of 335nm. A) TNBSA reaction containing no glycine. B) Reaction containing 20 μ g glycine.



All restriction enzymes were purchased commercially from Boehringer Mannheim or Stratagene, and oligonucleotides were from Genosys (desalted, 0.2 μ mol scale). Confirmatory DNA sequencing of Rac1 mutants by dideoxy-mediated sequencing (Sanger *et al.*, 1977) was achieved using Stratagene baseAce Jr electrophoresis apparatus. Agarose gel electrophoresis was routinely used to assess plasmid purity and to examine restriction digest products. 60mls of 1% agarose (SeaKem GTG, FMC Bioproducts) in TAE buffer was boiled in a microwave, and ethidium bromide (Bio-rad) was added to a final concentration of 0.8 μ g/ml. The solution was mixed, and poured into a gel mould to form a gel of 88mm x 98mm x 6mm. A comb was inserted at one end to form loading wells, and the gel was left for 1 hour at room temperature to set. Once set, the gel was transferred to an electrophoresis tank, and submerged in TAE buffer. Samples were mixed with the desired amount of 6x sample buffer (0.25% bromophenol blue (w/v), 0.25% xylene cyanol FF (w/v), 30% glycerol (v/v) in H₂O) and applied to the gel in a typical volume of 15 μ l. A voltage of 100V, 400mA was applied for 1 hour and the samples were visualised using transmitted UV light at 312nm using a UVItec gel scanner. A photograph of the gel was obtained using a Fujifilm FTI-500 thermal imaging system.

2.6.1. Isolation of plasmid DNA

Plasmid DNA was amplified in *Escherichia coli* host bacteria. A 100ml sterile flask with 50mls of L-broth containing 50 μ g ml⁻¹ was inoculated with a small loop from a frozen glycerol stock of *E.coli* and incubated overnight at 37°C with vigorous shaking. 1ml of the culture was centrifuged (12,000 x g, 2 mins, eppendorf centrifuge). The cell pellet was re-suspended in 100 μ l of solution I (25mM Tris·HCl pH 8.0, 10mM EDTA, 50mM glucose) by vigorous vortexing. 200 μ l of solution II (200mM NaOH, 1% SDS) was then added to lyse the cells, and the solution inverted gently 4-5 times. Then 150 μ l of solution III (3M potassium acetate, 10% glacial acetic acid (v/v) was added and gently inverted 4-5 times and incubated on ice for 5 minutes. The bacterial lysate was centrifuged (12,000 x

g, 15 minutes in eppendorf centrifuge) at 4°C. The supernatant was added to 1ml of ice cold ethanol to precipitate the plasmid and centrifuged (12,000 x g. 5 mins, eppendorf centrifuge). The pellet was dried and re-suspended in 30µl of sterile H₂O or TE buffer and stored at -20°C. To obtain consistent yields of plasmid DNA for sequencing, plasmid was isolated using the Wizard Plus miniprep DNA purification system (Promega) according to the manufacturer's instructions. Large scale purification of plasmid DNA was achieved using the ~~Quiaagen~~ ^{Qiagen} Plasmid Midi Kit according to the supplied methods.

2.6.2. DNA manipulation - Bacterial transformation

1µl of mini-prep plasmid DNA was added to 25-50µl of competent cells that had been thawed slowly on ice. This was left for 20 minutes on ice, followed by a 45 second heat shock at 42°C. The mixture was then transferred back on ice for a further 2 minutes. The mixture was added to 400µl of L-broth and incubated for 40 minutes at 37°C with vigorous shaking. 100µl was plated onto agar plates (1.5% (w/v) agar in L-broth containing 100µg ml⁻¹ ampicillin) to select for recombinant transformants. Plates were incubated overnight at 37°C and single colonies were picked for further analysis.

2.6.3. Site directed mutagenesis of Rac1

Rac1 point mutants have been produced as one approach to study the interaction of Rac with RhoGDI and p67^{phox}. These mutations have been confirmed using dideoxy DNA or automated sequencing techniques, and the proteins purified as described. Site directed mutants of the wild type Rac1 construct were generated using the Quick Change Site-Directed Mutagenesis Kit (Stratagene). This method utilises two synthetic oligonucleotide primers containing the desired point mutation (table 2.2.). These primers, complementary to opposite strands of the vector are extended during thermal cycling by means of *Pfu* polymerase. Following temperature cycling, the reaction is treated with DpnI, which is specific for methylated and hemimethylated DNA (Nelson & McClelland, 1992). This

Table 2.2. Oligonucleotide primers used for the site-directed mutagenesis of Rac1

Green nucleotides indicate a silent base change to create or remove a restriction enzyme cleavage site. Nucleotides coloured red indicate a base change and subsequent point mutation in the Rac1 primary sequence. All oligonucleotides were purchased from Genosys.

Mutation	Primer Name	Sequence	Restriction Site
A27K	ARN062015 ARN062016	5' T TGC CTA CTG ATC AGT TAC ACA ACC AAT AAG TTT CCT GGA G 3' 3' A ACG GAT GAC TAG TCA ATG TGT TGG TTA TTC AAA GGA CCT C 5'	
I33D	ARN062023 ARN062024	5' CCT GGA GAG TAC GAC CCT ACT GTC TTT GAC AAT TAT TCT GCC 3' 3' GGA CCT CTC ATG CTG GGA TGA CAG AAA CTG TTA ATA AGA CGG 5'	RsaI created
T35A	T35A T35AC	5' GGA GAA TAT ATC CCT GCA GTC TTT GAC AAT TAT TCT GCC 3' 3' CCT CTT ATA TAG GGA CGT CAG AAA CTG TTA ATA AGA CGG 5'	PstI created
F37E	ARN062027 ARN062028	5' CCT GGA GAG TAC ATC CCT ACT GTC GAA GAC AAT TAT TCT GCC 3' 3' GGA CCT CTC ATG TAG GGA TGA CAG CTT CTG TTA ATA AGA CGG 5'	RsaI created
D63E	D63E D63EC	5' GG GAT ACA GCC GGA CAA GAA GAG TAT GAC AG 3' 3' CC CTA TGT CGG CCT GTT CTT CTC ATA CTG TC 5'	PvuII removed
D124S	ARN062007 ARN062008	5' GG GAT GAT AAA AGC ACG ATA GAG AAA CTG AAG GAG AAG AAG CTG 3' 3' CC CTA CTA TTT TCG TGC TAT CTC TTT GAC TTC CTC TTC TTC GAC 5'	PvuI removed
E127A	ARN062045 ARN062046	5' GAC ACG ATC GCG AAA CTG AAG G 3' 3' CTG TGC TAG CGC TTT GAC TTC C 5'	
K130A	ARN062010 ARN062011	5' GG GAT GAT AAA GAC ACG ATC GAG AAA CTG GCC GAG AAG AAG CTG 3' 3' CC CTA CTA TTT CTG TGC TAG CTC TTT GAC CGG CTC TTC TTC GAC 5'	
E131K	ARN06202 ARN06203	5' GAT AAA GAC ACA ATT GAG AAA CTG AAG AAG AAG AAG CTG ACT CCC 3' 3' CTA TTT CTG TGT TAA CTC TTT GAC TTC TTC TTC TTC GAC TGA GGG 5'	
K133E	ARN062031 ARN062032	5' CTG AAG GAG AAG GAG TTA ACT CCC ATC ACC 3' 3' GAC TTC CTC TTC CTC AAT TGA GGG TAG TGG 5'	HpaI created

digests parental DNA and selects for mutant plasmid. DNA isolated from almost all *E.coli* strains is *Dam* methylated and susceptible to DpnI digestion. The mutant plasmid DNA is then transformed into XL1-Blue supercompetent cells and the mutation confirmed by restriction digestion of the plasmid and DNA sequencing (figure 2.14.). Mutants were generated using the instructions provided with the following modifications: where possible, a natural restriction site was removed, or a translationally silent site created to identify mutant plasmids. The PC programs DNASTar (v3.12, DNASTAR Inc.) and GMAP (v2.0, Institute of Microbial Technology, India) were used to search for natural and translationally silent restriction sites in the pGEX-2T plasmid and oligonucleotide primers. If the melting temperature of mutant oligonucleotide primers was near to the *Pfu* extension temperature of 68°C, the extension temperature was reduced to 5°C below the T_m of the primers and the extension time increased to ensure binding of primers and complete synthesis of the mutant plasmid. Mutagenesis was typically >80%. As with wild type Rac, mutant proteins was analysed by mass spectrometry (2.4.1.) to confirm C-terminal truncation and that the mass was consistent with that predicted by the primary sequence.

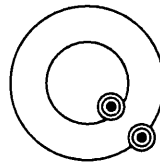
2.6.4. Preparation of a Rac1-Ras chimaera construct

The Rac1-Ras chimaera, which contained amino acids 122-128 from H-Ras in place of residues 120-139 from Rac1 (the insertion loop), was prepared by removal of this region from Rac1 using restriction enzymes, and ligating primers to replace this region corresponding to amino acids 122-128 of Ras. The construct was made in 3 stages – 1) creation of a Bgl II restriction site by a single point mutation 2) restriction digest to remove the insertion loop of Rac1, and 3) ligation of primers corresponding to residues 122-128 of H-Ras (figure 2.15.). Attempts to create a chimaeric Rac1/H-Ras construct using an overlapping PCR method as described by Wu *et al.* (1997) was unsuccessful.

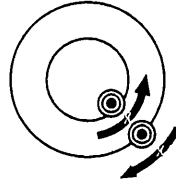
Figure 2.14. Quick change site-directed mutagenesis

Site specific mutations in the Rac1 gene were produced using the Stratagene site directed mutagenesis kit (V2) using the standard protocol shown. Mutagenesis efficiency was typically >80%.

Rac1 gene in plasmid with target site ◎ for mutation

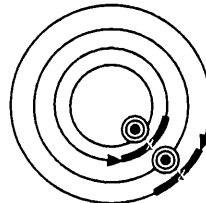


Denature plasmid and anneal primers containing the desired mutation X

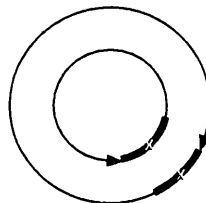


Mutagenic primers

Temperature cycle to extend and incorporate mutation primers resulting in nicked circular strands



Digest methylated nonmutated parental DNA template

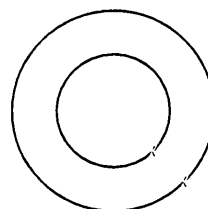


Mutated plasmid

Transform the resulting annealed double-stranded nicked DNA molecules



After transformation the XL2-Blue *E. coli* cell repairs the nicks in the plasmid

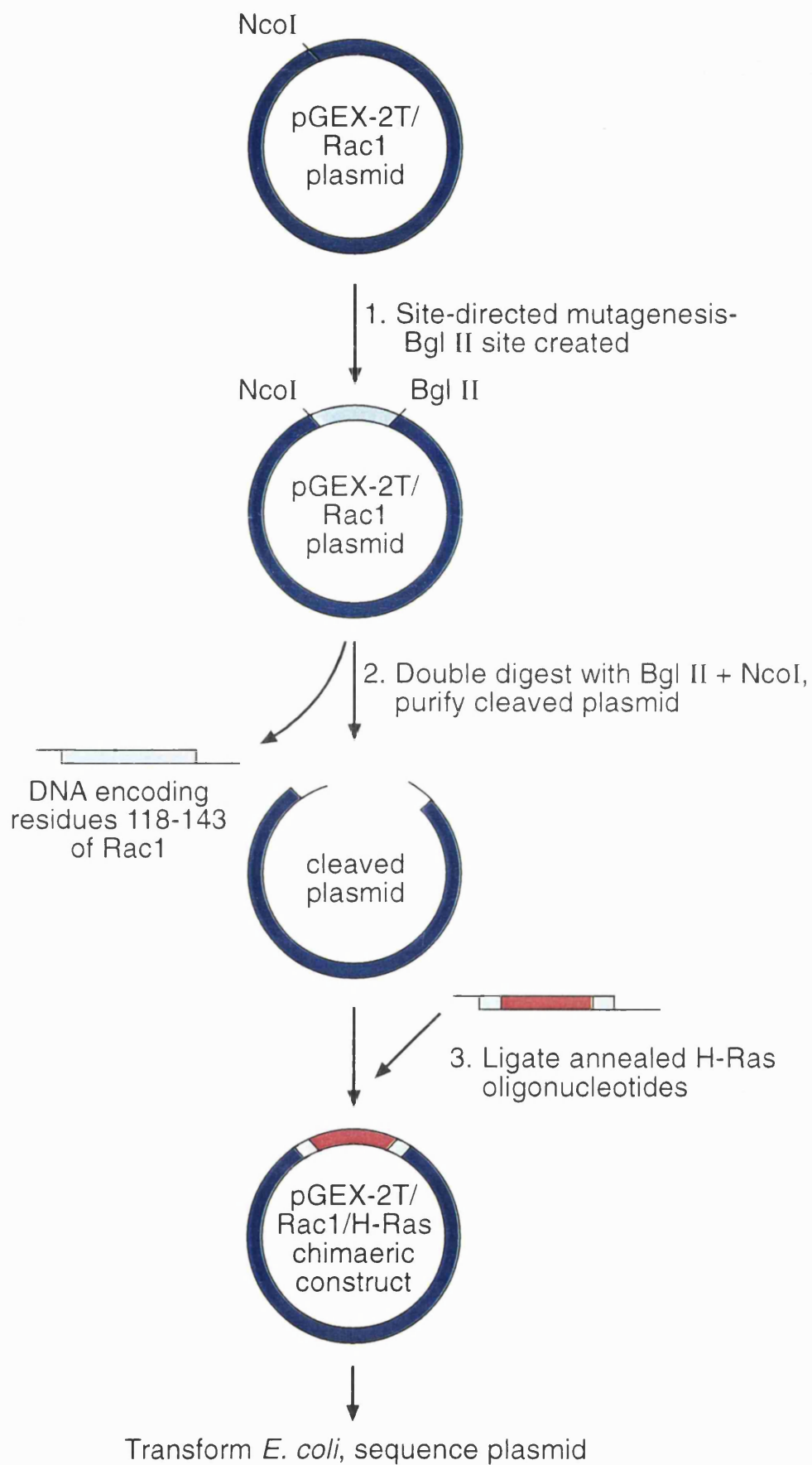


Confirm mutation by restriction digest + DNA sequencing



Figure 2.15. Method used to create a Rac1/H-Ras chimaera

A Rac1/H-Ras chimaeric plasmid was created in three stages – 1. Creation of a Bgl II restriction site by site directed mutagenesis, 2. Digestion with Bgl II and Nco I, and 3. Ligation of annealed primers containing the DNA sequence coding for residues 122-128 of H-Ras.



A silent point mutation was created using the Stratagene site directed mutagenesis kit as described previously (2.6.3.) to create a single Bgl II restriction site using the following oligonucleotide primers. Underlined residues indicate a silent base change.

5' CCC ATC ATC CTA GTG GGA ACT AAA CTA GAT CTT AGG G 3'

3' GGG TAG TAG GAT CAC CCT TGA TTT GAT CTA GAA TCC C 5'

The mutant plasmid was transformed into XL1-blue strain of *E.coli* to amplify the mutant DNA, and then purified using the Quiagen midi prep purification kit. The insertion loop of Rac1 (residues 120-139) was removed by cleavage of the plasmid with the restriction enzymes Bgl II and Nco I (figure 2.15.). Both of these enzymes produce single, cohesive ended cuts in the Rac1 cDNA. 10µg of the pGEX-2T/Rac plasmid containing the Bgl II restriction site (purified using the Quiagen Midi prep kit) was incubated with 10 units of Bgl II and 10 units of Nco I in Boehringer buffer H (50mM Tris·HCl pH 7.5, 10mM MgCl₂, 100mM NaCl, 1mM dithioerythritol). The reaction was incubated at 37°C for 2 hours to remove the DNA encoding the Rac1 insertion loop. The linear pGEX-2T plasmid was isolated from the cleaved fragment by agarose gel electrophoresis, and the plasmid (lacking the DNA encoding the insertion loop) was purified using the 'freeze squeeze' method.

2.6.5. 'Freeze squeeze' purification of plasmid from an agarose gel

The section of agarose containing the plasmid was excised from the gel following visualisation under UV light and placed in an eppendorf tube. 1ml of 0.3M sodium acetate, 1mM EDTA, pH 7.0 was added, and the gel sample left in the dark for 15 minutes to equilibrate with the buffer. The gel slice was transferred to a small (200µl capacity) eppendorf with a small hole in the bottom, plugged with glass wool. The small

ependorf containing the gel slice was placed in liquid nitrogen for 3 minutes, placed into a large (1.5ml capacity) eppendorf and spun in an eppendorf centrifuge at 12,000 x g for 10 minutes. 0.1% acetic acid, 10mM MgCl₂ was added to the liquid collected (~200µl), then 2.5 volumes (500µl) of ethanol to precipitate the purified DNA. The solution was placed back into liquid nitrogen, then spun again for 10 minutes at (12,000 x g) in an eppendorf centrifuge. The solution was poured off to leave a white precipitate. This pellet was washed with 2x150µl of ethanol and left at room temperature overnight to dry. The following day, the dried pellet containing the DNA was re-suspended in 10µl TE buffer and stored at -20°C.

2.6.6. Ligation of primers

Primers containing the coding region for residues 122-128 of H-Ras (figure 2.16.) were ligated to the pGEX-2T Rac1 plasmid using T4 DNA ligase. 1pmol of each of the H-Ras insert oligonucleotides was incubated in 10µl sterile H₂O and heated to 95°C for 2 minutes, then cooled slowly to 37°C to ensure annealing of the complementary oligos. The annealed oligos were incubated with 0.3pmol of pGEX-2T plasmid, 3 units of T4 DNA ligase, 1mM ATP, 30mM Tris-HCl pH 7.8, 10mM MgCl₂, 10mM DTT in a final volume of 20µl. The ligation reaction was incubated overnight at 19°C. 3µl of the ligation mixture was used to transform competent *E.coli* (2.6.2.), plated out and incubated at 37°C overnight. The following day, colonies were picked, and tested for expression (figure 2.17.). DNA sequencing confirmed the chimaeric sequence (figure 2.18.) The chimaeric protein was purified as described for wild type Rac1 (2.2.1.). A yield of 1.5mg/litre was obtained. The mass of the chimaeric protein was confirmed by mass spectrometry (figure 2.19.).

Figure 2.16. H-Ras 'insertion loop' oligonucleotides

Oligonucleotides containing the coding sequence for residues 122-128 of H-Ras were used to create a Rac1/H-Ras chimaera. Nucleotides coloured yellow indicate H-Ras sequence, and bold bases indicate silent mutations to create a Csp I site. This restriction site was initially created to identify the mutant construct, but DNA sequencing of the plasmid confirmed the chimaeric sequence. Residues are labelled according to the single letter amino acid code.

	Rac1					H-Ras				Rac1				
Residue	D	L	A	A	R	T	V	E	S	P	Q	G	L	
Codon #	118	119	122	123	124	125	126	127	128	140	141	142	143	
Coding seq.	5' <u>GAT</u> <u>CTT</u> <u>GCT</u> <u>GCA</u> <u>CGG</u> <u>ACC</u> <u>GTG</u> <u>GAA</u> <u>TCT</u> <u>CCG</u> <u>CAG</u> <u>GGT</u> <u>CTA</u> <u>GC</u> 3'													
	3' <u>AA</u> <u>GGA</u> <u>CGT</u> <u>GCCC</u> <u>TGG</u> <u>CAC</u> <u>CTT</u> <u>AGA</u> <u>GGC</u> <u>GTC</u> <u>CCA</u> <u>GAT</u> <u>CGG</u> <u>TAC</u> 5'													

Figure 2.17. SDS-PAGE analysis of Rac1/H-Ras expression

E. coli (XL-1-blue strain) were transformed with the pGEX-2T plasmid containing the chimaeric Rac1/H-Ras construct and were tested for their ability to express the GST-fusion protein (~47kDa). Pre and post induction samples were separated by SDS-PAGE as described (2.4.2.) to assess protein expression. Lanes 1-6: Pre and post induction samples of 6 freshly transformed colonies. Clone 2. was used for subsequent expression and purification of the protein. Lane 7. = 5µg purified Q61L Rac1; Lane 8. = 5µg purified Rac1/H-Ras chimaera.

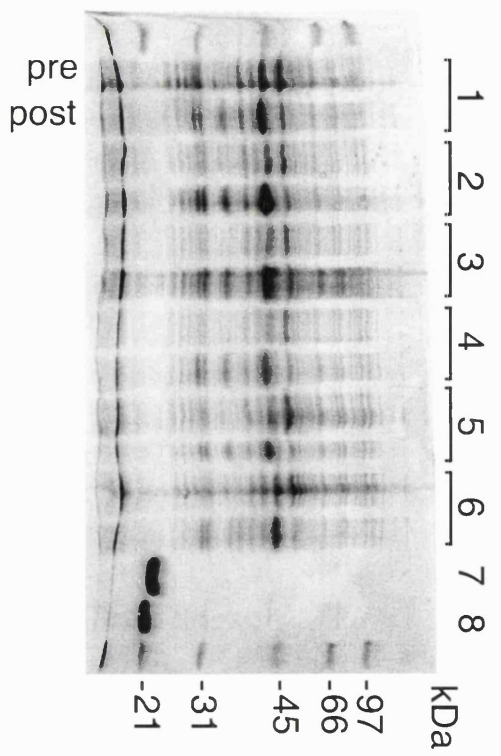


Figure 2.18. DNA sequence of a Rac1/H-Ras chimaera

DNA sequencing of the chimaeric Rac1/H-Ras construct was performed by Oswel DNA sequencing using an ABI PRISM 377 DNA sequencer and the 5' pGEX sequencing primer, (sequence 5'GGGCTGGCAAGCCACGTTTGGTG3') purchased from Pharmacia. DNA coding for H-Ras residues 122-128 is highlighted in yellow, and the silent base change to create a Bgl II restriction site is shown in pink.

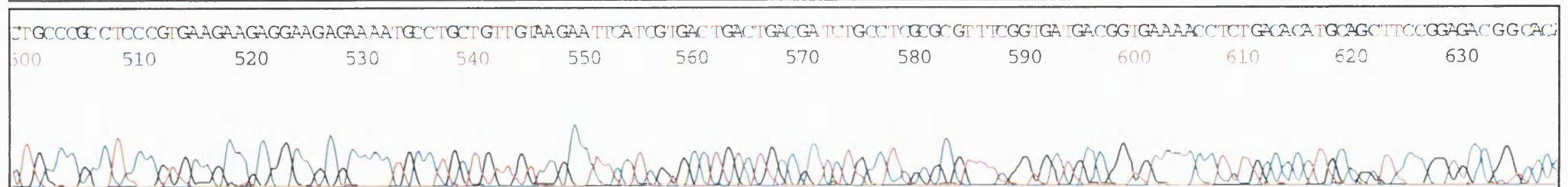
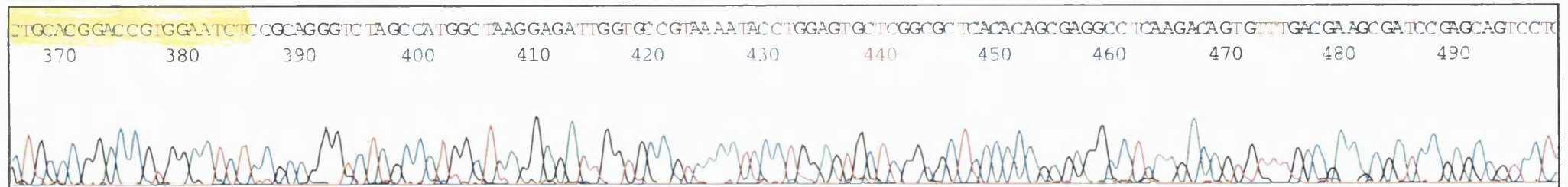
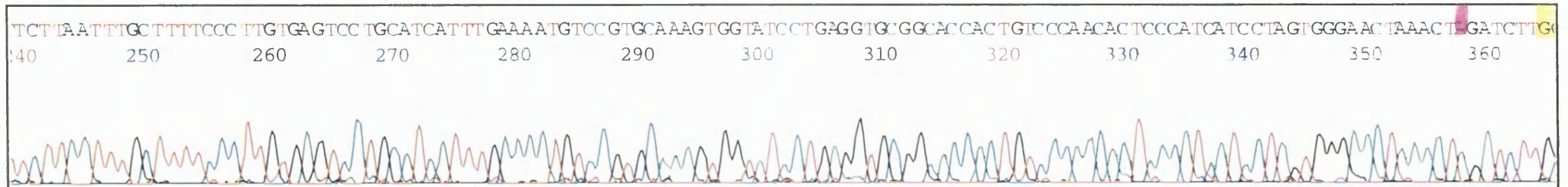
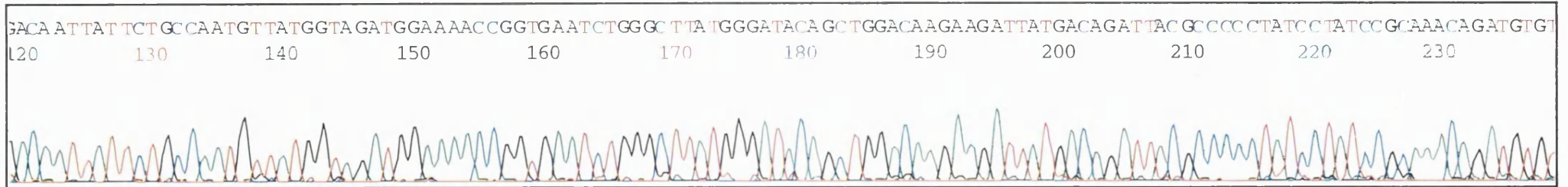
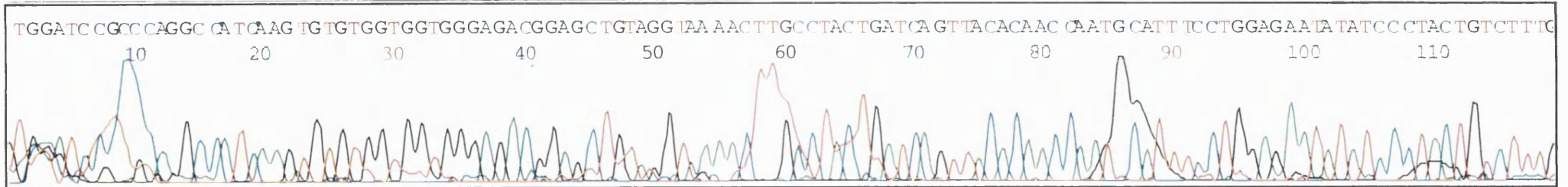


Figure 2.19. Mass spectrometry of a Rac1/H-Ras ‘insertion loop’ chimaera

Purified Rac1/H-Ras chimaera was analysed by mass spectrometry and a major species of 18846.64 (\pm 3.61) Da was observed. The mass of the chimaeric protein calculated from the primary sequence (truncated by 8 residues at the C-terminus) is 18848 Da.

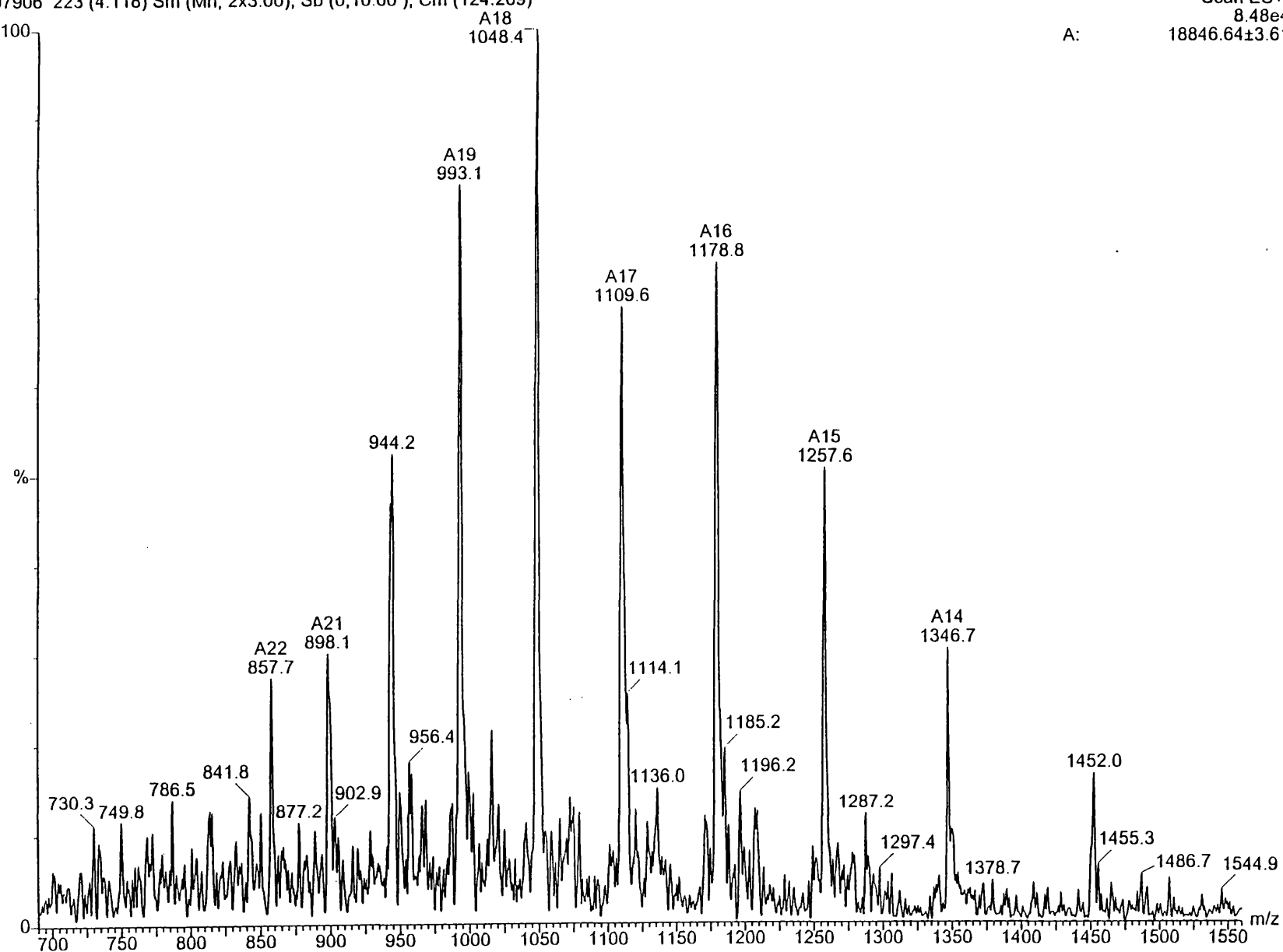
97906 223 (4.118) Sm (Mn, 2x3.00); Sb (0,10.00); Cm (124:269)

Scan ES+

8.48e4

A:

18846.64±3.61



2.6.7. DNA sequencing - The dideoxy-chain termination method

Nucleotide sequences were determined by the direct double stranded chain termination sequencing method using the USB Sequenase version 2.0 sequencing kit (Amersham). Approximately 5-10µg of wizard miniprep purified plasmid was denatured in 0.2M NaOH, 0.2mM EDTA at 37°C for 25 minutes. The denaturation step was neutralised by adding 0.1 volumes (v/v) of 3M NaAcetate pH 5.2 the DNA was precipitated by adding 200µl of absolute alcohol and incubating at -20°C for 20 minutes. The DNA was pelleted by centrifugation (12,000 x g, eppendorf centrifuge) at 4°C, the ethanol removed and the precipitated DNA left to dry at room temperature for 1-2 hours, then at 37°C for >1 hour. Once dry, the DNA was re-suspended in 7µl sterile H₂O plus 2µl 5x Sequenase reaction buffer. Approximately 30ng of oligonucleotide primer was added, the mixture heated rapidly to 65°C and then cooled slowly to 35°C to allow annealing between the primer and the template, and then placed on ice. The labelling reaction was performed by adding 1µl of 100mM DTT, 2µl of labelling mix, 0.5µl ³⁵S-dATP (Amersham) and 2µl of freshly diluted Sequenase T7 DNA polymerase version 2.0 to the annealed template and primer. The reactions were incubated at ambient temperature for 5 minutes before transferring 3.5 µl to each of 4 tubes pre-warmed to 37°C each containing 2.5µl of either ddG/ddA/ddT or ddC termination mix. After 5 minutes at 37°C, 4µl of stop solution was added to each termination tube and samples were stored at -20°C. Prior to running the samples on a gel, the samples were heated to 75°C for 2 minutes to denature oligonucleotides from the plasmid DNA and the transferred to ice before loading on a pre-heated acrylamide/urea gel.

Sequencing plates were washed with detergent, then rinsed with ethanol and H₂O then left to air-dry for 1-2 hours or overnight. Once dry, the back plate was coated with acrylease non-stick plate coating (Stratagene) and the gel mould constructed of the dimensions 200mm x 380mm x 0.4mm. 6% polyacrylamide gels were prepared by mixing 15mls of 40% acrylamide solution, 35mls gel diluent (Sequagel, national diagnostics), and 10mls

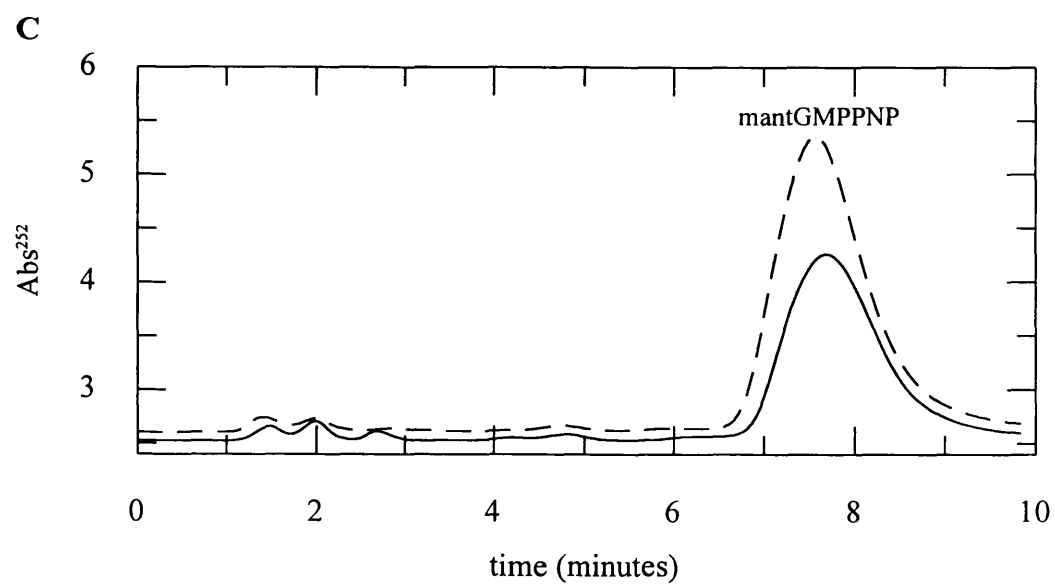
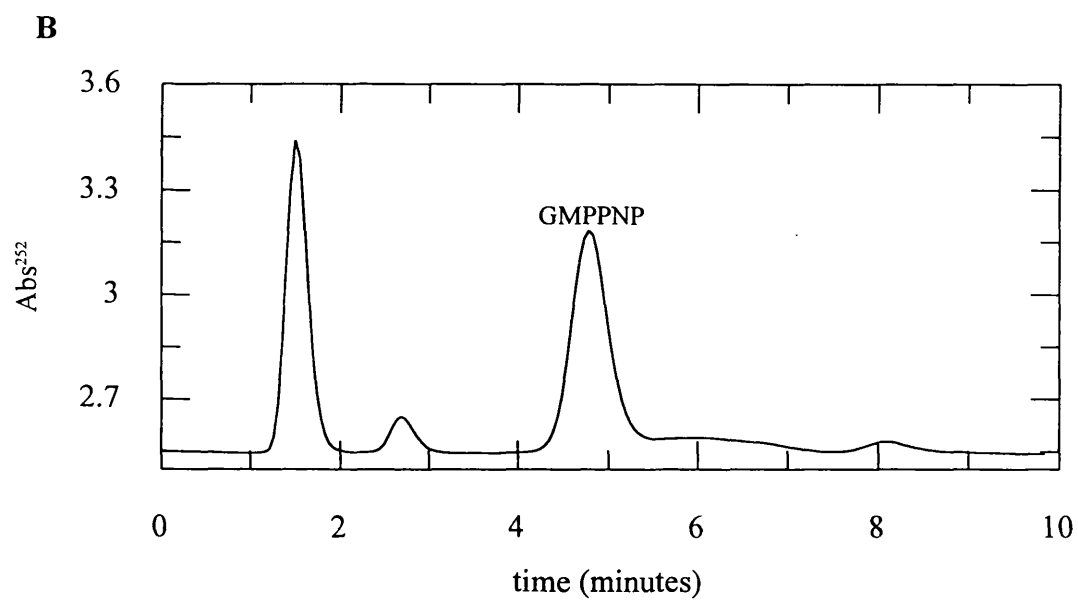
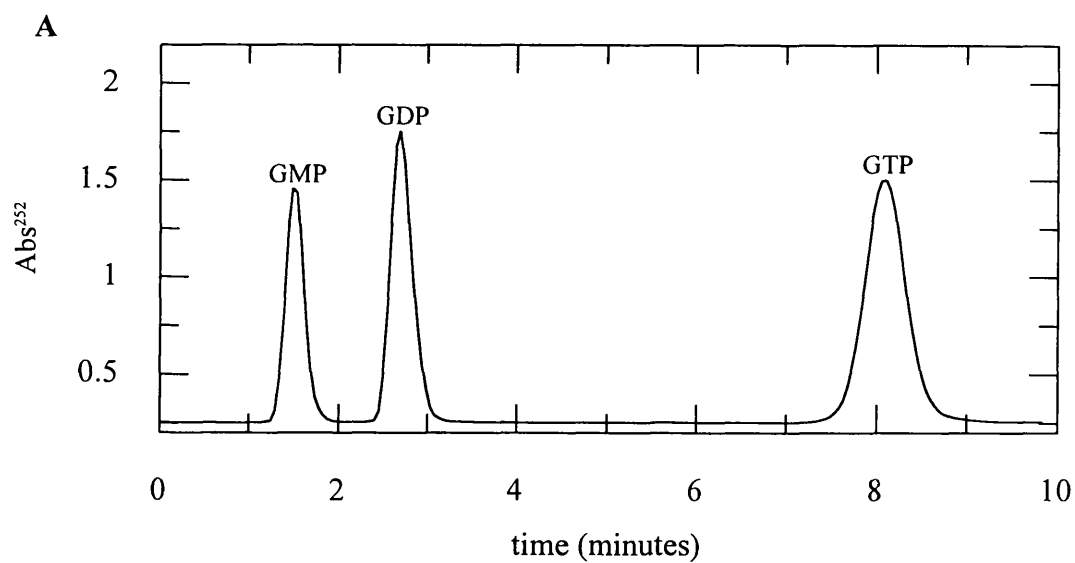
10x TBE. The gel mix was transferred to ice and once chilled, 400 μ l of 10% (w/v) ammonium persulphate (Pharmacia) and 20 μ l of TEMED were added to start polymerisation. The mould was held vertically and poured using a 50ml syringe. The gel was left to set for 90 minutes or overnight. The gel was pre-run to >55°C and 3.5 μ l samples were electrophoresed for 2-4 hours at a constant voltage of 1500V with TBE as the running buffer. The gel was transferred to a sheet of Whatman nitrocellulose paper, covered with Saran wrap and dried for 90 minutes at 80°C under vacuum using a Bio-Rad 583 gel drier. The labelled DNA fragments were visualised by autoradiography using Kodak X-OMAT AR film.

2.6.8. Synthesis of mantGMPPNP

GMPPNP was reacted with *N*-methyloisatoic anhydride to produce the *N*-methylantraniloyl derivative (mantGMPPNP) as described (Hiratsuka, 1983). 75mg of GMPPNP was dissolved in 2mls of DDIW in a jacketed water bath at 37°C. To this solution, 46mgs of *N*-methyl isatoic anhydride (mant) was added with continuous stirring and the pH maintained at 9.6 by the addition of 5M KOH. After completion of the reaction, the reaction mix was poured into a conical flask and filled to 150mls with DDIW. The pH was adjusted to 7.6 with 1M HCl and the conductivity checked against 10mM triethylamine (TEAB). The reaction mix was loaded onto a 1.5 x 40cm DEAE cellulose anion exchange column that had been equilibrated in 10mM TEAB, pH 7.6, and the nucleotide analogues were eluted overnight with a 10-600mM TEAB gradient, and fractions of 14mls were collected. A wavelength scan and HPLC analysis (SAX-10 column, eluting with 0.4M (NH₄)₂HPO₄ + 12% methanol) of the major peak fractions indicated the fractions containing the mantGMPPNP. These were pooled and evaporated using a Rotavapor-R and the resulting mantGMPPNP was resuspended in 800 μ l methanol (Aristar) and the purity of the final mantGMPPNP determined by HPLC (figure 2.20.). The concentration of mantGMPPNP was determined from an absorbance scan and the

Figure 2.20. HPLC analysis of mantGMPPNP

GMPPNP was reacted with *N*-methylisatoic anhydride to produce the *N*-methylantraniloyl derivative (mantGMPPNP) and purified as described. (2.6.8.). A) GMP, GDP and GTP nucleotide standards. B) GMPPNP standard. C) *Solid line*: The DEAE cellulose eluted fraction containing mantGMPPNP. *Dotted line*: mantGMPPNP standard from a previous preparation. Absorbance in arbitrary units.



calculated mant molar extinction co-efficient of $5700\text{M}^{-1}\cdot\text{cm}^{-1}$. The mantGMPPNP was aliquoted, frozen on dry ice and stored at -80°C .

2.6.9. Formation of Rac1 nucleotide and nucleotide analogue complexes

Complexes of Rac with GTP, mantGDP, cou-edaGTP and but-edaGTP were formed under conditions that facilitate rapid nucleotide exchange. This was done by lowering the magnesium concentration by the addition of excess EDTA over Mg^{2+} and increasing the nucleotide exchange rate by the addition of ammonium sulphate. This method has been well established from work on Ras and other small G proteins (Brownbridge *et al.*, 1993). 50nmol of Rac was incubated with 50-60 fold excess nucleotide in fast exchange buffer (20mM Tris·HCl pH 7.6, 40mM EDTA, 20mM $(\text{NH}_4)_2\text{SO}_4$). The reaction was incubated at 30°C for 5 minutes, and the exchange reaction stopped by the addition of MgCl_2 to a final concentration of 45mM. The protein was isolated and excess nucleotide removed using a PD-10 column (Pharmacia) equilibrated in 20mM Tris·HCl pH 7.6, 1mM MgCl_2 . 0.5ml fractions were collected and the fractions containing protein were determined from the absorbance at 280nm. The concentration of the Rac1-nucleotide complex was determined using the Rac1 molar extinction co-efficient of $29828\text{M}^{-1}\text{cm}^{-1}$ (Gill & von Hippel, 1989) at 280nm, while the mantGDP concentration was determined using the molar extinction co-efficient of mant at 360nm of $5700\text{M}^{-1}\text{cm}^{-1}$ (Hiratsuka, 1983). Complexes were shown to be greater than 95% pure as determined by HPLC.

2.6.10. Formation of Rac1 complexes with non-hydrolysable nucleotide analogues

Complexes of Rac with non-hydrolysable nucleotide analogues mantGMPPNP and GMPPNP were formed by incubating 340nmol Rac1 with $1.2\mu\text{mol}$ of the nucleotide analogue in 20mM Tris·HCl pH 7.6, 200mM $(\text{NH}_4)_2\text{SO}_4$ with 15 units of alkaline phosphatase linked to agarose beads (Sigma) at 20°C with end-over-end stirring. Samples were analysed using an SAX-10 HPLC column (Whatman) in 0.5M $(\text{NH}_4)_2\text{HPO}_4$ pH 4.0 buffer for GMPPNP and 0.5M $(\text{NH}_4)_2\text{HPO}_4$ pH 4.0 + 25% methanol for mantGMPPNP,

eluting at $2\text{ml}\cdot\text{min}^{-1}$ to monitor the decrease in GDP (figure 2.21.). After 100 minutes or until the GDP was undetectable, MgCl_2 was added to the reaction mix to a final concentration of 1mM to ensure the Rac bound the nucleotide analogue. The mixture was centrifuged briefly to remove the phosphatase, and the excess nucleotide removed using a PD-10 desalting column. Protein concentration and nucleotide bound to the protein (figure 2.22.) were determined as described (2.4.3.).

Complexes of Rac1 with but-edaGMPPNP were formed by incubating 150nmol Rac1 with 450nmol but-edaGMPPNP in 20mM Tris-HCl pH 7.6, 200mM $(\text{NH}_4)_2\text{HPO}_4$ with 12 units of alkaline phosphatase linked to agarose beads at 20°C with end-over-end stirring. Samples were analysed using a partisphere SAX column (Whatman) in 0.5M $(\text{NH}_4)_2\text{HPO}_4$ pH 4.0 + 25% methanol eluting at $2\text{ml}\cdot\text{min}^{-1}$ to monitor the decrease in GDP. After 60 minutes, MgCl_2 was added to a final concentration of 1mM and the complex purified as described for Rac1-mantGMPPNP.

2.6.11. Reaction of p67¹⁻¹⁹⁹ with 5,5'-Dithiobis-(2-nitrobenzoic acid) (DTNB)

To determine the number of reactive thiols in this protein, p67¹⁻¹⁹⁹ was reacted with DTNB. This reacts with $-\text{SH}$ groups under mild alkaline conditions to form thionitrobenzoate-protein complex and stoichiometric amounts of thionitrobenzoate (NTB), which has an intense yellow colour. $5\mu\text{M}$ of p67¹⁻¹⁹⁹ was added to $100\mu\text{M}$ DTNB, 100mM Tris-HCl pH 8.0, 200mM NaCl (final vol. 1ml) and the absorbance at 412nm followed over time. The concentration of NTB produced due to reaction with thiols was calculated using the NTB extinction co-efficient of $13610\text{ M}^{-1}\text{ cm}^{-1}$ (Dawson *et al.*, 1984).

2.7. Fluorescence measurements

These were measured using a Perkin Elmer LS50B fluorimeter with a Xenon lamp using

Figure 2.21. HPLC analysis of the nucleotide bound to Rac1 following exchange with the non-hydrolysable nucleotide analogue, GMPPNP

Complexes of Rac1 with GMPPNP were formed by incubating Rac1 with excess nucleotide analogue and alkaline phosphatase under conditions of accelerated nucleotide exchange. A) GMP, GDP and GTP standards. B) Nucleotide bound to Rac1 prior to nucleotide exchange, indicating >98% GDP bound. C) *Solid line*: Nucleotide bound to Rac1 following exchange for GMPPNP. Although little GDP remained bound to the protein, ~8% of bound nucleotide is GDP-NH₂, the major contaminant of GMPPNP. *Dotted line*: GMPPNP standard. Absorbance in arbitrary units.

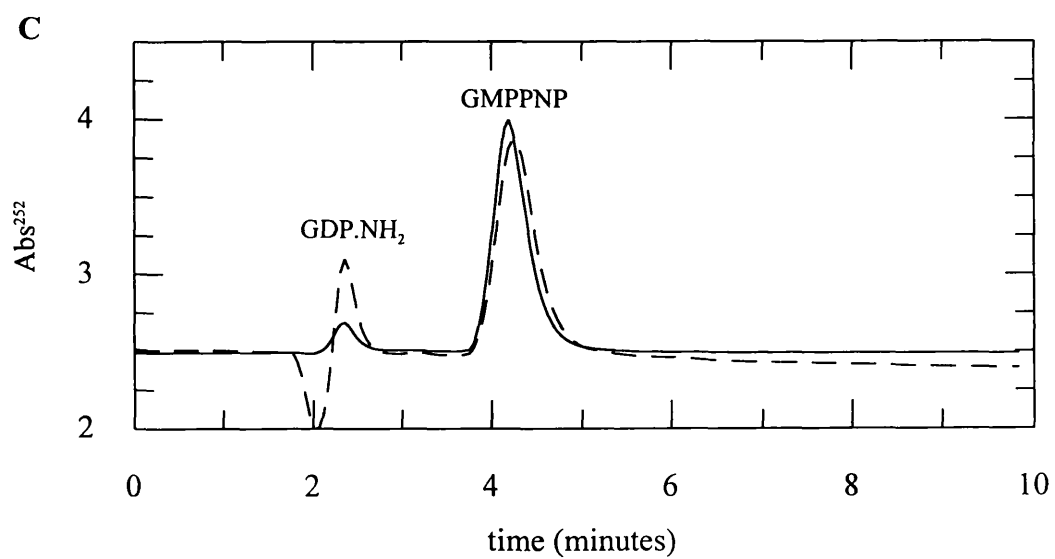
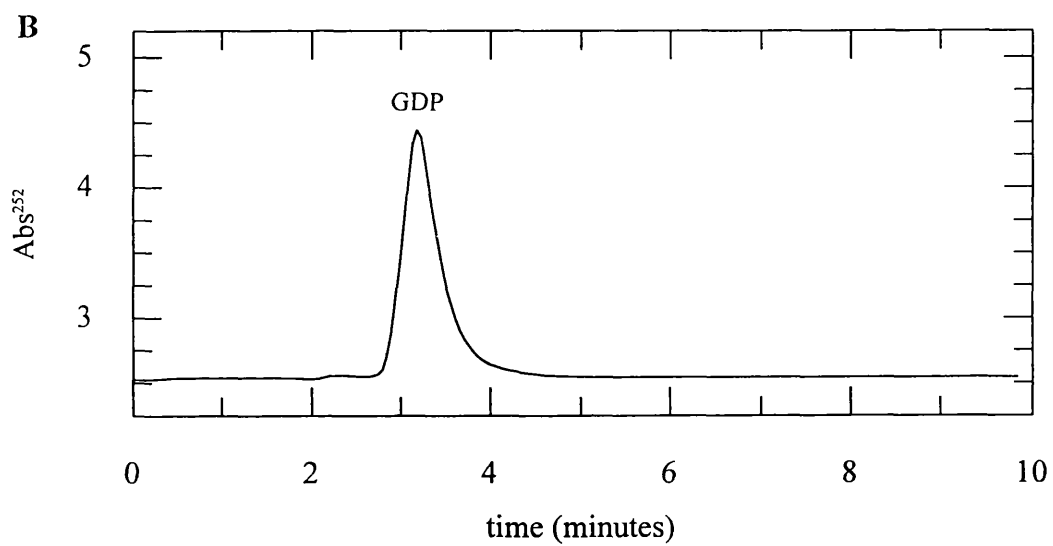
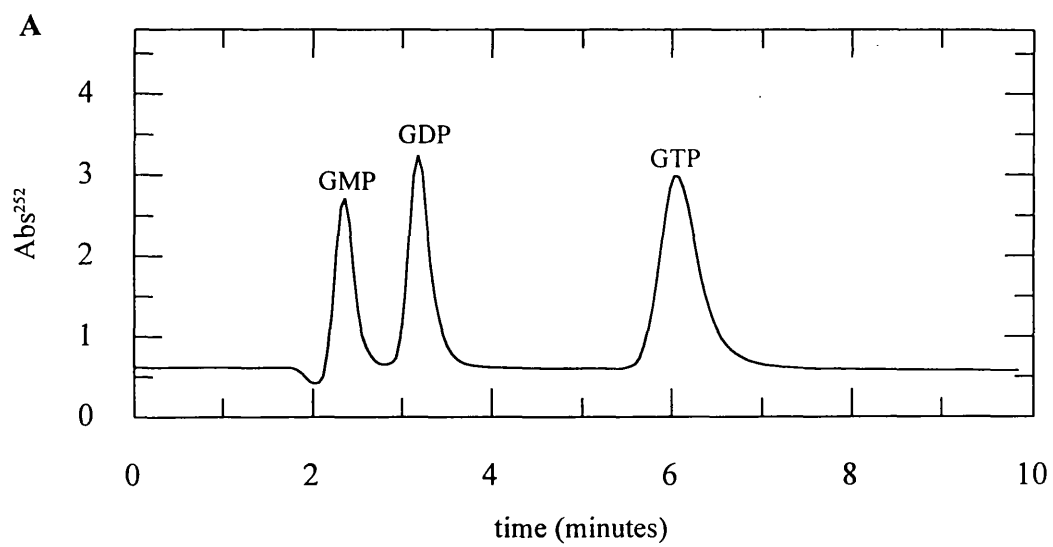
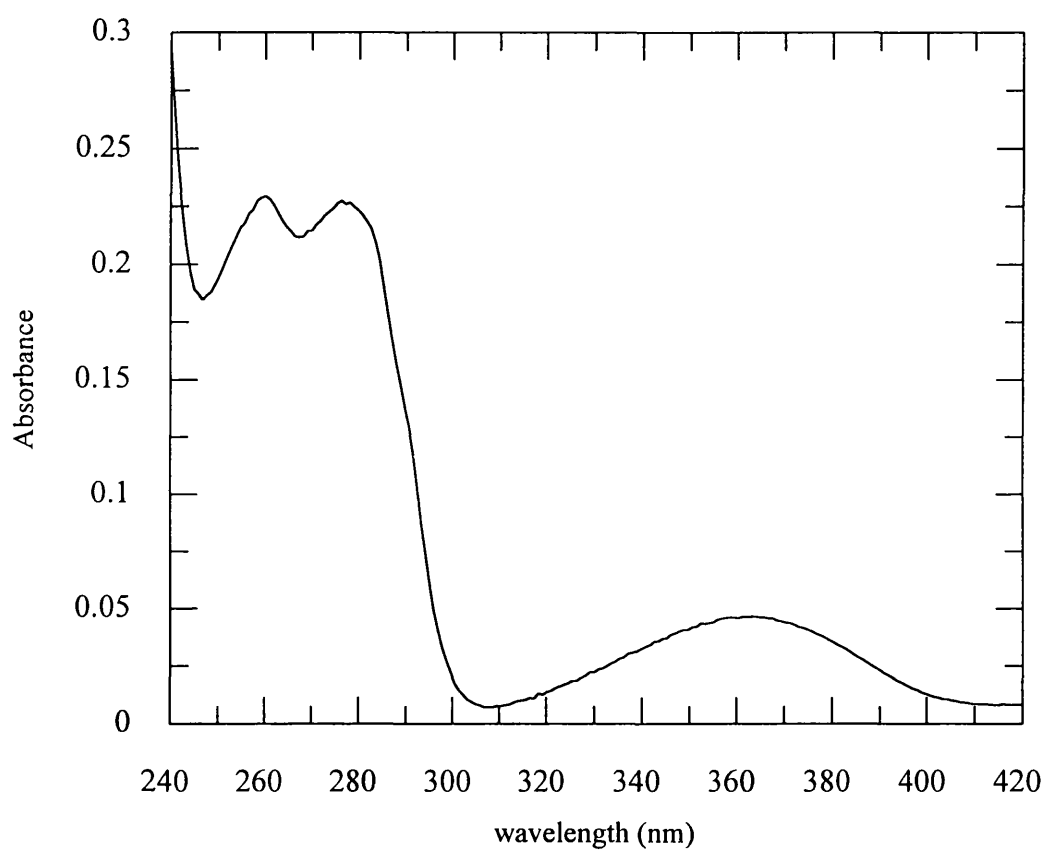


Figure 2.22. Absorbance spectrum of purified Rac1·mantGMPPNP

An absorbance spectrum of purified Rac1·mantGMPPNP complex. The complex was >92% pure as described in materials and methods. The concentration of Rac1 was calculated from the absorbance at 280nm (2.4.3.) and the purity of the complex determined by HPLC.



cuvettes with a 3mm path length in a reaction volume of 200 μ l. Experiments using mant nucleotide analogues and Rac1 mant nucleotide complexes were performed with excitation at either 290nm or 360nm, emission 440nm. Experiments using the cou-edaGTP nucleotide analogue were performed with excitation at 436nm, emission 480nm. Experiments to monitor hydrolysis with the Pi probe MDCC-PBP were performed with excitation at 425nm, emission 464nm, and experiments using MDCC-RhoGDI were performed with excitation at 430nm, emission at 460nm. Stopped flow experiments were performed using a HiTech SF61MX stopped flow apparatus with a Xenon lamp. There was a monochromator with 5nm slits on the exciting light at 436nm and a 435nm cut off filter on the emission. Exponential and hyperbolic fits to data were undertaken using the PC program Grafit v3.0 (Erithacus software).

3. BIOCHEMICAL CHARACTERISATION OF RAC1

3.0. Introduction

In an attempt to examine the regions of Rac1 involved in the interaction with p67^{phox} and GDI, a number of Rac1 mutants have been made. In order to characterise mutant Rac1 proteins, basic biochemical properties of Rac1 such as nucleotide dissociation and GTP hydrolysis have been examined and will be described as in the following sections. These techniques have been used to examine the activity of mutant Rac1 proteins as described in Chapter 4. In addition, initial tests with two novel coumarin derivatised nucleotides, cou-edaGTP and but-edaGTP have been undertaken. It was hoped that these nucleotide analogues would form complexes with Rac1 and may provide a signal to monitor the interaction with other proteins, such as p67^{phox} and GDI.

3.1. Analysis of the Rac1 GTPase cycle

The simplest model for the GTPase cycle is shown in scheme 3.1. Rate constants for individual steps in the reaction are numbered so that forward and reverse rate constants for step *a* are k_{+a} and k_{-a} respectively. By forming complexes with 2' (3') -*O*- (*N*-methyl) anthraniloyl (mant) fluorescent nucleotide analogues, rates of nucleotide dissociation (k_{+1}) and GTP hydrolysis (k_{+2}) ~~has~~ ^{have} been measured.

3.2. Properties of rac1 with fluorescent nucleotide analogues

Mant derivatives of guanine nucleotides (eg. mantGTP) (figure 3.1.) have been shown to behave as close analogues of the parent nucleotides and show a high sensitivity to small changes in fluorophore environment. Their use has been well established from work on Ras and have been used to demonstrate nucleotide binding to small G proteins, and the interaction of the guanine-nucleotide protein complex with other proteins such as GAPs (Eccleston *et al.*, 1993 & Moore *et al.*, 1993). Previous reports have also shown that mant

Scheme 3.1. The GTPase cycle of Rac1

The simplest model for the GTPase cycle of Rac1 (R represents Rac1). Individual steps are numbered so that forward and reverse rate constants for steps a are k_{+a} and k_{-a} respectively.

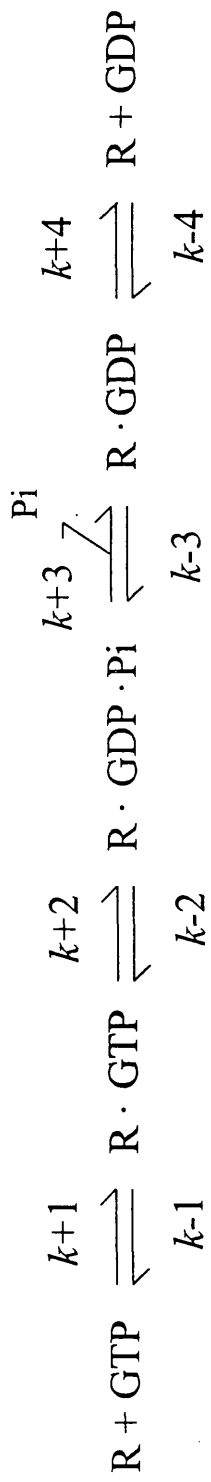
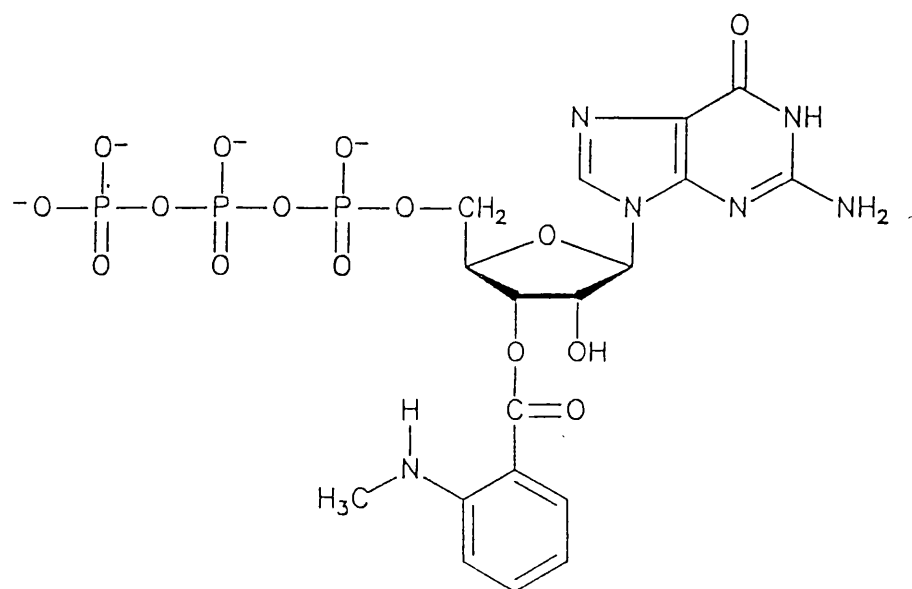


Figure 3.1. Structure of 2' (3')-O-(N-methyl) anthraniloyl (mant) GTP.



derivatised nucleotides undergo changes in fluorescent properties on binding to Rho family proteins, including Rac1 (Leonard *et al.*, 1997).

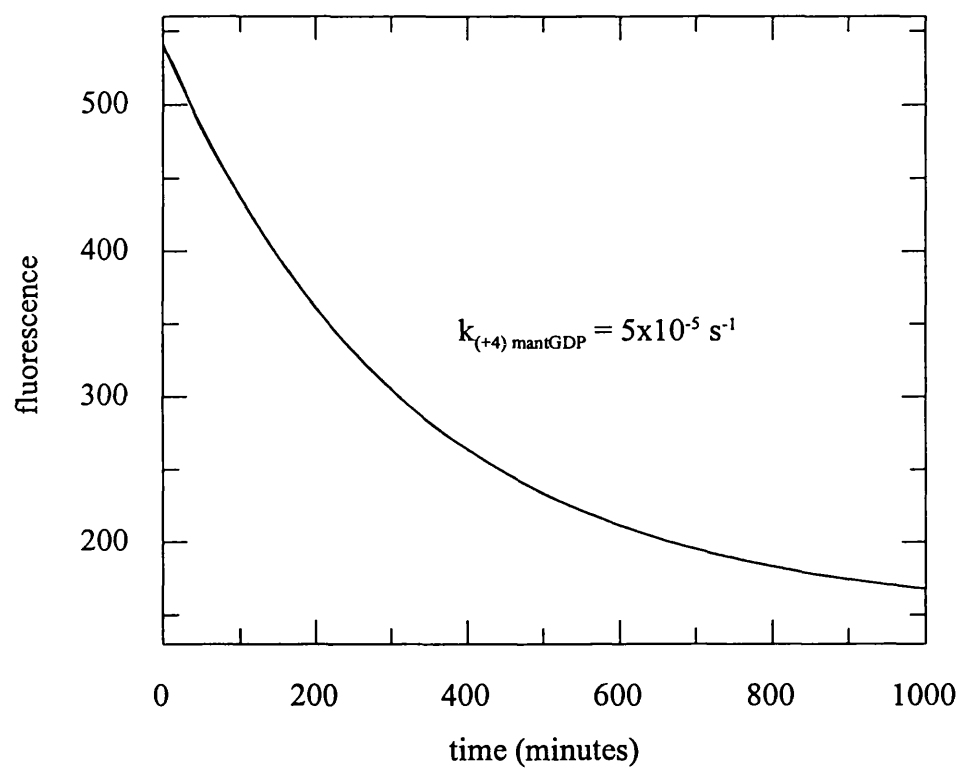
3.2.1. Dissociation of mantGDP from Rac1 (k_{-4})

By using the fluorescent properties of Rac1 complexed to mantGDP, the intrinsic dissociation rate of mantGDP was measured by monitoring the fluorescence decrease as mantGDP dissociates from a Rac1-mantGDP complex. As Rac1 contains two tryptophan residues, it was possible to excite the mantGDP using fluorescence resonance energy transfer by exciting at 290nm. This excited state interaction is dependent on distance and orientation in which the fluorescence emission of tryptophan(s) is coupled to the excitation of the mant fluorophore attached to the ribose moiety of the nucleotide. In this case, the mant fluorophore is close enough to a tryptophan in the tertiary structure and may be excited by the fluorescence emission of the tryptophan residue(s). Although mant absorbs at 290nm, this wavelength is well below the λ_{max} of 360nm for mant, and therefore this technique minimises the excitation of free mant nucleotide in the solution. As only the fluorophore bound to Rac1 is excited significantly, this results in a greater signal change.

When 1 μ M Rac1-mantGDP is incubated with 20 μ M GDP (in 20mM Tris-HCl pH7.6, 1mM MgCl₂, 1mM DTT) at 30°C and the dissociation of the nucleotide monitored over time (figure 3.2.), mantGDP dissociates with a first order rate constant of 5 $\times 10^{-5}$ s⁻¹, confirming that in the absence of exchange factors, Rac1 shows a slow rate of intrinsic mantGDP dissociation. The dissociation of mantGDP has also been determined for Rac1 in the presence of (NH₄)₂SO₄. This has been used to produce conditions of accelerated nucleotide exchange, making it practical to compare nucleotide dissociation rates under different conditions. 1 μ M Rac1 was incubated with 20 μ M mantGDP in 20mM Tris-HCl pH7.6, 1mM MgCl₂, 1mM DTT + 200mM (NH₄)₂SO₄ and the fluorescence emission

Figure 3.2. Dissociation of mantGDP from Rac1 (k_{+d})

Rac1·mantGDP (1 μ M) was incubated with excess GDP (20 μ M) in 20mM Tris·HCl pH7.6, 1mM MgCl₂, 1mM DTT, 30°C and the dissociation of the mantGDP monitored over time. Due to the slow rate of intrinsic nucleotide exchange by Rac1, time points were taken every 1.6 minutes (data interval = 10s). The lamp was turned off between time points (turned on 3s prior to each measurement) to minimise photobleaching of the fluorophore.



measured as the mantGDP dissociates from the Rac1·mantGDP complex. Data was fitted to a single exponential, showing that under these conditions, mantGDP dissociates from Rac1 with a first order rate constant of $3.5 \times 10^{-3} \text{ s}^{-1}$ (figure 3.3a.); the addition of 200mM $(\text{NH}_4)_2\text{SO}_4$ under these conditions increases the rate constant by almost 2 orders of magnitude.

Another method of creating a favourable environment for accelerated nucleotide exchange is to monitor the exchange reaction in the presence of excess EDTA. When $1 \mu\text{M}$ Rac·mantGDP was incubated with $20 \mu\text{M}$ GDP in 20mM Tris·HCl pH7.6, 1mM DTT containing 0.5mM EDTA at 30°C , mantGDP dissociated from the protein with a first order rate constant of $2.5 \times 10^{-2} \text{ s}^{-1}$ (figure 6.11.), 3 orders of magnitude faster than the intrinsic rate of mantGDP exchange. EDTA chelates Mg^{2+} ions required for tight binding of the nucleotide to the protein and this technique has been well established for accelerating conditions of nucleotide exchange (Sato *et al.*, 1988). The use of EDTA is particularly useful when examining the effect of other proteins such as GDI on the rate of nucleotide exchange, as EDTA does not increase the ionic strength of the solution.

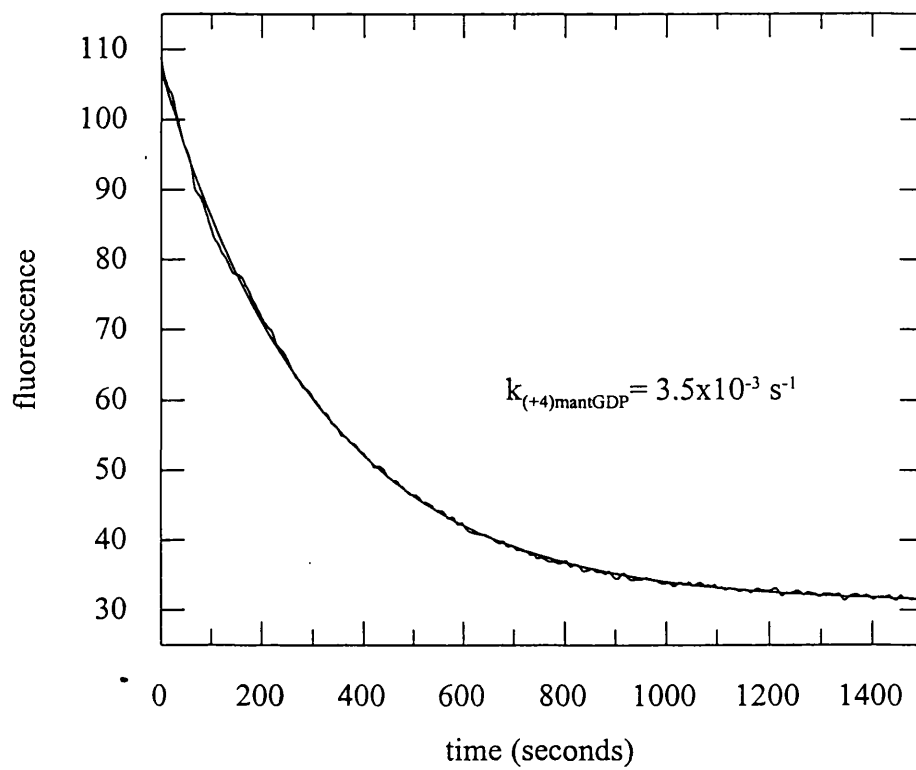
3.2.2. Dissociation of GDP from Rac1

The dissociation of GDP from Rac1 has been measured indirectly by monitoring the association of mantGDP with Rac1 in the presence of excess nucleotide to ensure the reaction was under pseudo-first order conditions. Incubation of $5 \mu\text{M}$ Rac1 was incubated with $50 \mu\text{M}$ mantGDP in 20mM Tris·HCl pH7.6, 1mM MgCl_2 containing 200mM $(\text{NH}_4)_2\text{SO}_4$ at 30°C created conditions of accelerated exchange, and the fluorescence change due to the association of mantGDP monitored. The data was fitted to a single exponential (figure 3.3b.). Under these conditions, the observed rate constant will be the dissociation of GDP (k_{-1}) + association of mantGDP (k_{+1}). The observed rate constant for GDP dissociation from Rac1 is $3.3 \times 10^{-3} \text{ s}^{-1}$.

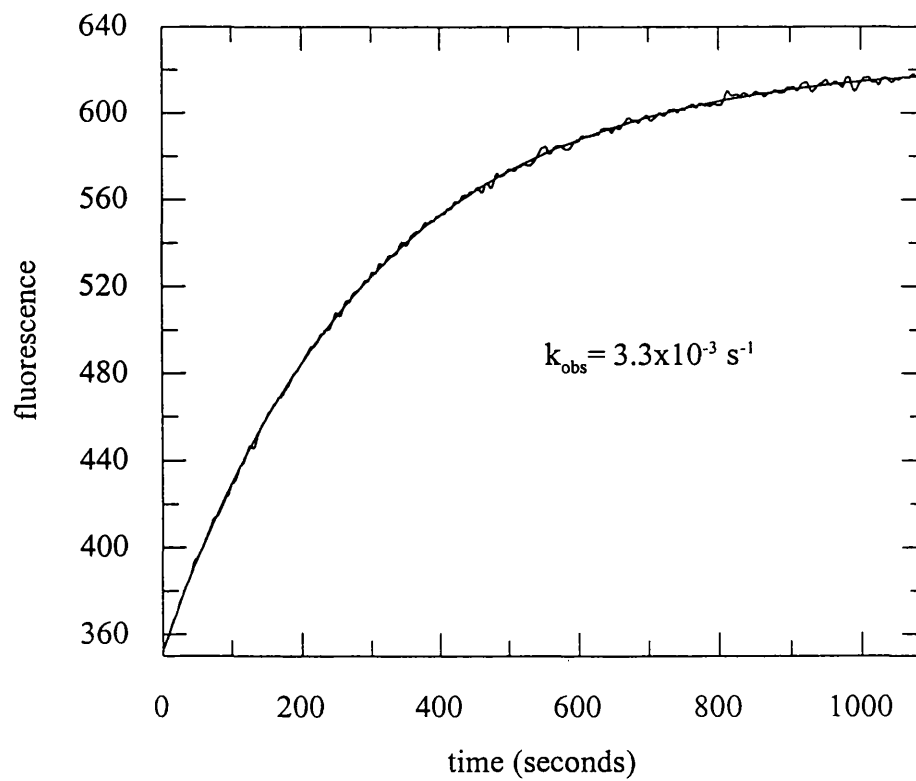
Figure 3.3. Rac1 nucleotide exchange under accelerated exchange conditions

a) Rac1·mantGDP (5 μ M) was incubated with GDP (100 μ M) in 20mM Tris·HCl pH7.6, 1mM MgCl₂, 200mM (NH₄)₂SO₄, 30°C. b) Rac1 (5 μ M) was incubated with mantGDP (50 μ M) in 20mM Tris·HCl pH7.6, 1mM MgCl₂, 200mM (NH₄)₂SO₄, 30°C. Lines shown are best fits to single exponentials and rate constants are the average of at least two independent determinations. Excitation 290nm.

a)



b)



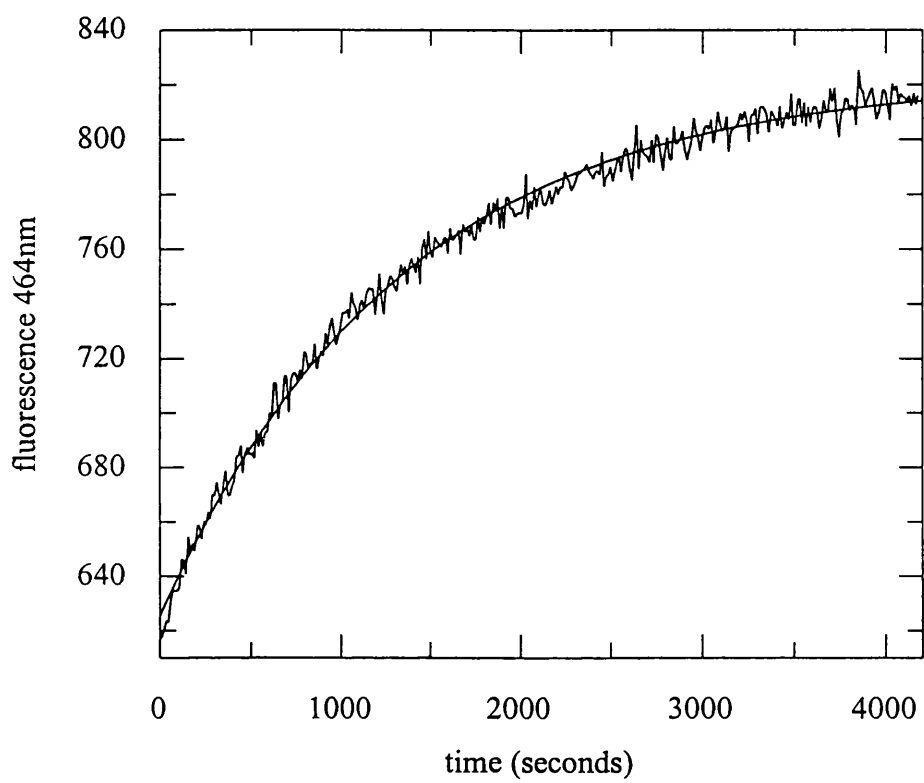
3.3. Hydrolysis of GTP by Rac1 (k_{+2})

By forming complexes of Rac1 with GTP, the rate of nucleotide triphosphate hydrolysis was measured using the Pi probe, MDCC-PBP. This probe consists of the fluorophore *N*-[2-(1-maleimidyl)ethyl]-7-(diethylamino)coumarin-3-carboxamide (MDCC) bound to the A197C mutant of the *E.coli* phosphate binding protein (MDCC-PBP) (Brune *et al.*, 1994). This labelled protein shows a ~5 fold increase in fluorescence emission at 464nm when complexed to Pi (pH 7.0, low ionic strength, 22°C). Pi binds rapidly and tightly ($K_d \sim 0.1 \mu\text{M}$) to the labelled protein. This coumarin labelled protein has been used to measure Pi release in a wide variety of biological processes, including Pi release during ATP hydrolysis by the actomyosin subfragment 1 from rabbit skeletal muscle (Brune *et al.*, 1994). To measure the rate of GTP hydrolysis by Rac1, $5 \mu\text{M}$ Rac1·GTP was incubated with $15 \mu\text{M}$ MDCC-PBP in 20mM Tris·HCl pH 7.6, 1mM MgCl_2 , 30°C, and the change in fluorescence monitored over time. The data were fitted to a single exponential (figure 3.4.). Under these conditions, the observed rate constant will be the rate limiting step determining Pi release (k_{+3}), probably GTP hydrolysis (k_{+2}) (scheme 1.) The observed first order rate constant of $2.8 \times 10^{-3} \text{s}^{-1}$, is ~40 fold faster than Ras.

The intensity of the fluorescence signal observed in this experiment will be dependent on the concentration of Rac1·GTP complex in the reaction. Due to the relatively fast rate of intrinsic hydrolysis by Rac1 ($t_{1/2} \sim 4$ minutes, 30°C) (figure 3.5.), a significant proportion of GTP will be hydrolysed during the purification of the complex (2.6.9.). Complexes of Rac1 with GTP were formed and analyzed by HPLC. Rac1·GTP complexes have been shown to contain ~25% GTP, with GDP the other nucleotide present. This is within reasonable agreement with previous data from this laboratory that indicates 47-60% GTP bound to Rac1 following purification of the complex (R.W. Stockley & M.R. Webb). As stoichiometric complexes to >95% purity have been obtained when forming Rac1 complexes with the non-hydrolysable GTP analogue, GMPPNP, the low triphosphate

Figure 3.4. Time course for the hydrolysis of GTP by Rac1

Rac1· GTP (5 μ M) was incubated with MDCC-PBP (15 μ M) in 20mM Tris· HCl pH 7.6, 1mM MgCl₂, 30°C and the fluorescence intensity measured over time (excitation λ = 425nm, emission λ = 464nm). The Solid line shows a best fit to a single exponential.



content is unlikely to be due to incomplete nucleotide exchange, but due to intrinsic hydrolysis of GTP during the formation and purification of the complex.

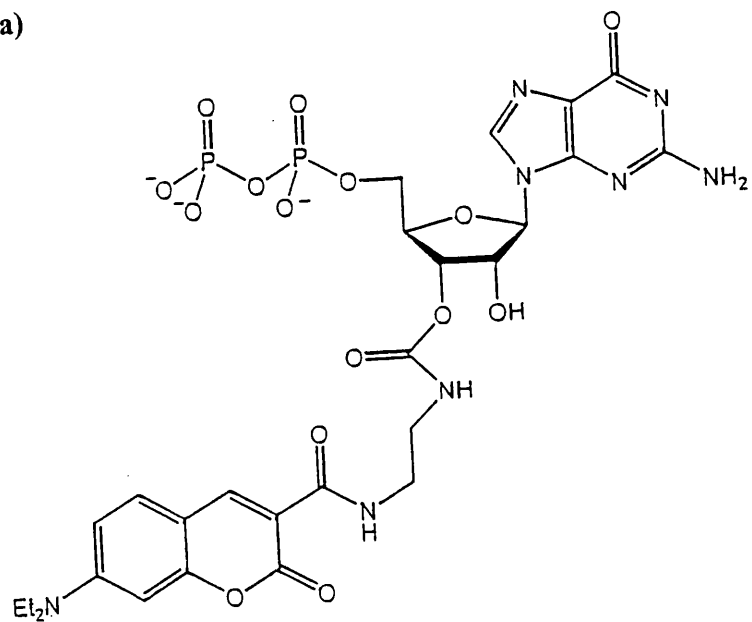
3.4. Novel fluorescent nucleotide analogues – cou-edaGTP & but-edaGTP

In addition to mant modified fluorescent nucleotide analogues, the interaction of two novel fluorescent nucleotide analogues with Rac1 has been examined. Both analogues have been synthesised in this laboratory by M.R. Webb (unpublished results). It was hoped that these coumarin-modified nucleotides would undergo a change in fluorescence emission upon Rac1 binding to other proteins and may be used to study the interaction with p67^{phox} and GDI. Similar experiments are currently underway at the N.I.M.R. using the nucleotide analogue cou-edaATP to study the actomyosin system; initial experiments have shown that this analogue has similar properties to ATP (unpublished results). Complexes of Rac1 have been produced with two novel fluorescent GTP analogues, 3'-O-{N-[2-(7-diethylaminocoumarin-3-carboxamido) ethyl] carbamoyl} GTP (cou-edaGTP) and coumarin343-edaGTP (but-edaGTP) (figure 3.5.). Both of these new fluorescent analogues have an ethylene linker between the coumarin group and the nucleotide. The advantage of this may be that the exposed nature of the coumarin group may be more susceptible to environment changes induced by Rac1-protein interactions.

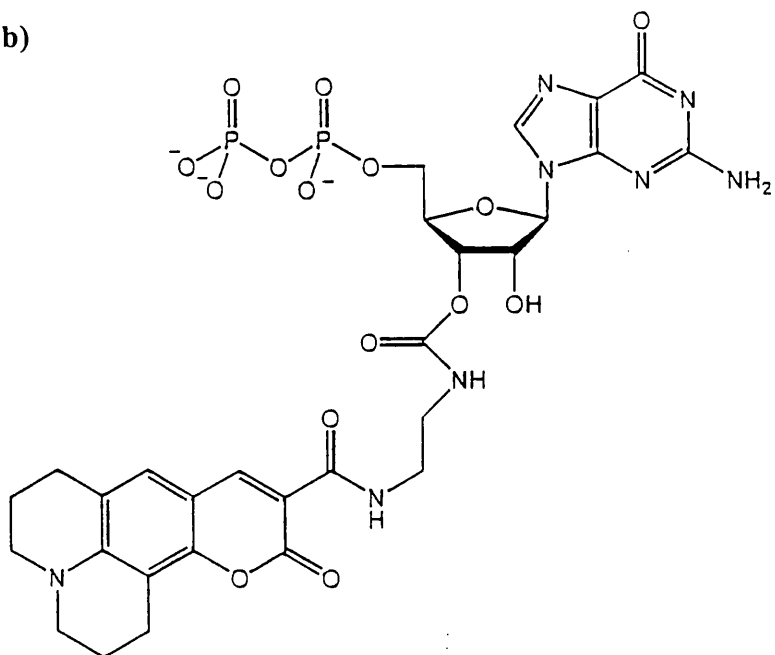
Another advantage of but-edaGTP is that the coumarin fluorophore of this nucleotide analogue has an additional pair of aliphatic rings containing a nitrogen atom (figure 3.6b.). The lone pair of electrons from the nitrogen are likely to interact with the ring system, and as a result, this fluorophore has a high fluorescence quantum yield (~0.5); the advantage being that very low concentrations of the fluorophore can be used and still retain a measurable signal. Possible disadvantages of these nucleotide analogues is that the ring structure is more hydrophobic, and may form non-specific interactions with proteins, and due to the high fluorescence quantum yield of but-edaGTP, this analogue will only be useful if a decrease in signal is observed.

Figure 3.5. The structures of cou-edaGDP (a) and but-edaGDP (b)

a)



b)



3.4.1. Fluorescent properties of Rac1 with coumarin-derivatised GTP analogues

It has been well documented that mant derivatised nucleotide analogues undergo change in their fluorescent properties upon binding to small G proteins such as Ras and Rac. It was hoped that a similar signal change would be observed when Rac1 interacts with cou-edaGTP and but-edaGTP, providing a detectable method to examine the interaction of these novel fluorescent nucleotides with Rac1. As an initial test, Rac1·GDP was incubated with equimolar concentrations of cou-edaGTP or but-edaGTP under accelerated exchange conditions (2.6.9.), and the fluorescence emission measured (figure 3.6.). When Rac1 was incubated with cou-edaGTP, a 16% increase in fluorescence was observed, when Rac1 was incubated with but-edaGTP, 23% quenching of fluorescence was observed. A quenching of but-edaGTP fluorescence is also observed when but-edaGTP binds to the S1 subunit of myosin (M.R. Webb *et al.*, unpublished results). Due to the hydrolysis of but-edaGTP and cou-edaGTP by Rac1 during the purification procedure, both analogues bound to Rac1 will be predominantly in the GDP state, although this has not been confirmed by HPLC.

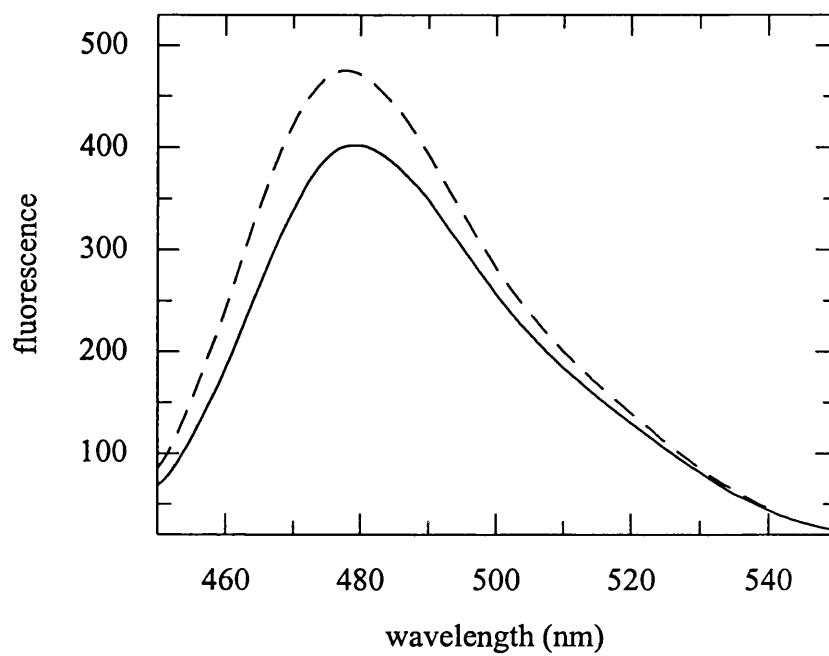
3.4.2. The dissociation of cou-edaGTP and but-edaGTP from Rac1 (k_{+4})

The dissociation of cou-edaGTP and but-edaGTP from Rac1 was measured essentially as described for the dissociation of mant nucleotides from Rac1 (3.2.1.). Complexes of Rac1 with cou-edaGTP or but-edaGTP were incubated under accelerated nucleotide exchange conditions with excess GDP to ensure the experiment was under pseudo-first order conditions. Nucleotide dissociation was measured by observing the fluorescence decrease when the fluorescent nucleotide dissociated from the protein and underwent exchange for GDP. The observed fluorescence changes were fitted to first order rate equations (figure 3.7.). These experiments reveal that cou-edaGTP and but-edaGTP dissociate from Rac1 with first order rate constants of $2.6 \times 10^{-3} \text{ s}^{-1}$ and $2.4 \times 10^{-3} \text{ s}^{-1}$ respectively.

Figure 3.6. Fluorescent properties of Rac1 with coumarin-derivatised nucleotides

a) 10 μ M cou-edaGTP (Solid line) was incubated with 10 μ M Rac1 under accelerated exchange conditions (20mM Tris·HCl pH 7.6, 1mM MgCl₂, 200mM (NH₄)₂SO₄ at 30°C and the fluorescence emission measured after 5 minutes (dotted line). Excitation λ = 436nm. b) 1 μ M but-edaGTP (solid line) was incubated with 1 μ M Rac1 under accelerated conditions (20mM Tris·HCl pH7.6, ^{1mM MgCl₂}~~50mM EDTA~~, 200mM (NH₄)₂SO₄ at 30°C and the fluorescence measured after 5 minutes (dotted line). Excitation λ = 450nm. Fluorescence did not change further with prolonged incubation.

a)



b)

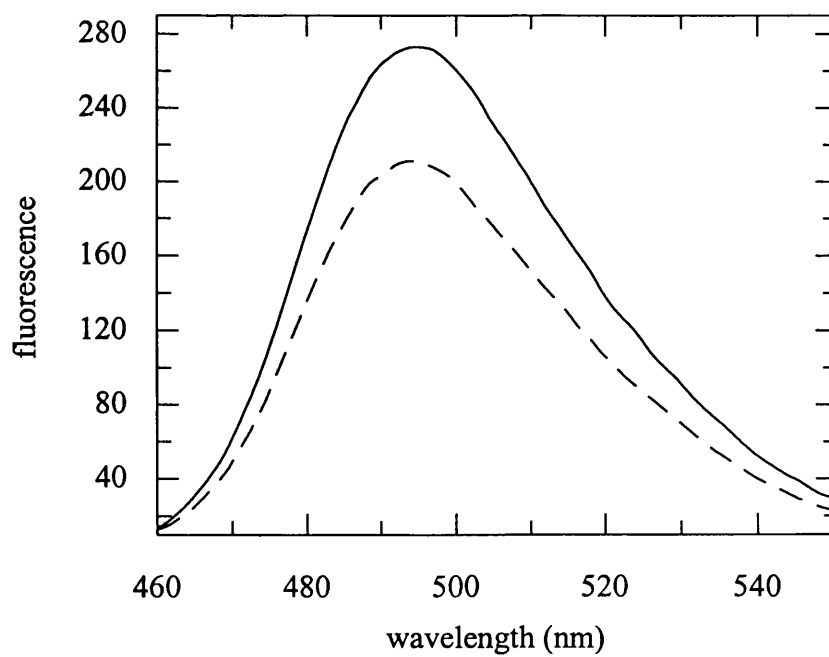
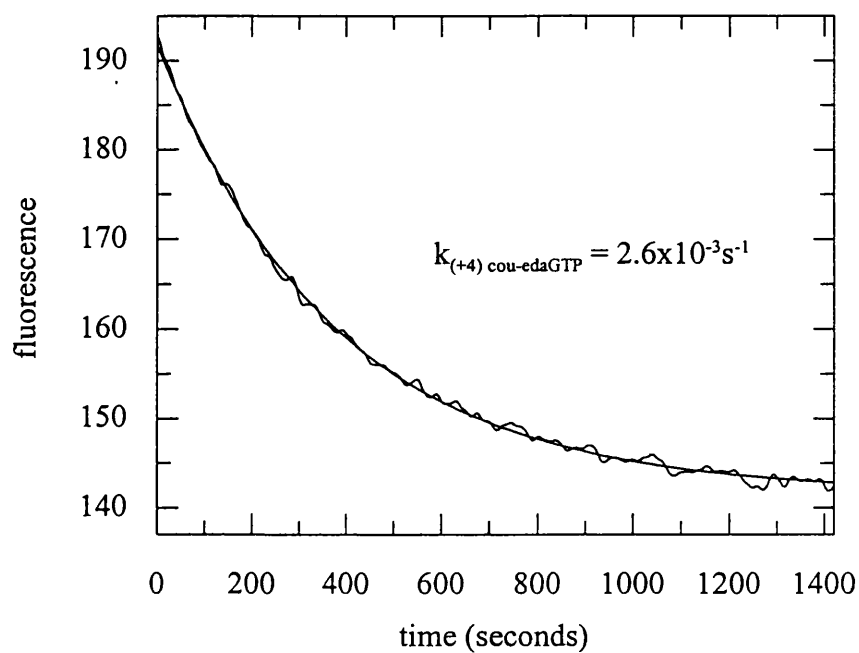


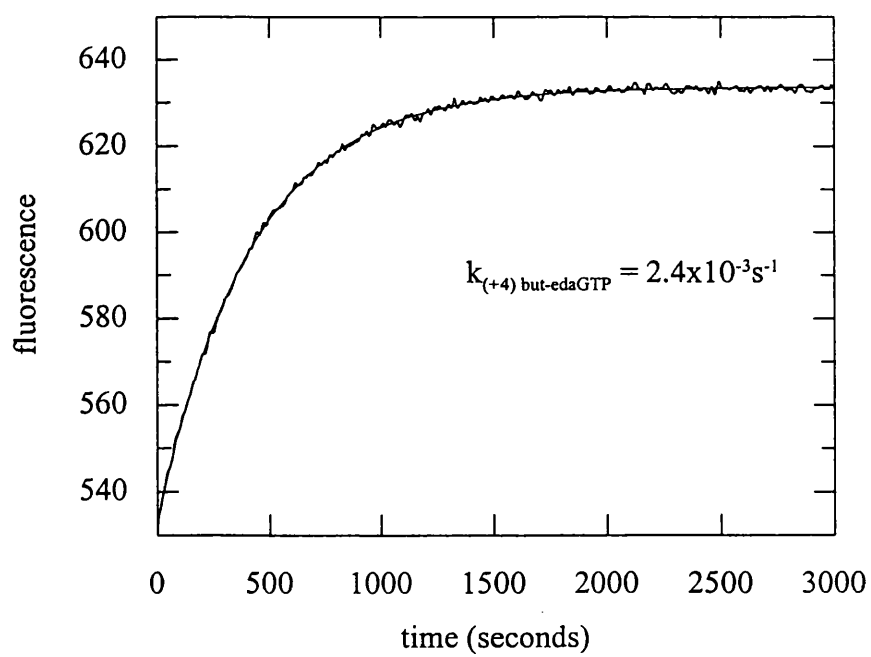
Figure 3.7. Dissociation of but-edaGTP and cou-edaGTP from Rac1

a) Rac1·cou-edaGTP (4μM) or b) Rac1·but-edaGTP (5μM) was incubated with GDP (100μM) in 20mM Tris·HCl pH7.6, 1mM MgCl₂, 200mM (NH₄)₂SO₄, 30°C and the dissociation of the nucleotide monitored over time. Solid lines show best fits to single exponentials.

a)



b)



3.4.3. Hydrolysis of cou-edaGTP and but-edaGTP by Rac1 (k_{+2})

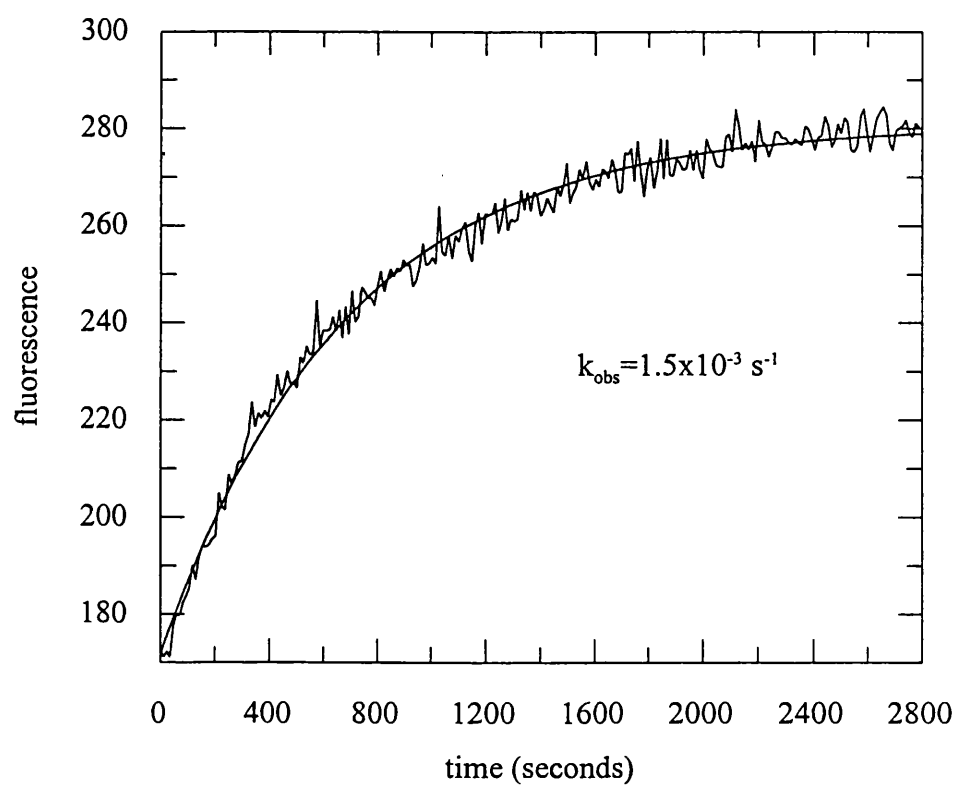
To examine the rate of cou-edaGTP and but-edaGTP hydrolysis by Rac1, complexes of Rac with both fluorescent nucleotides were formed and the complex purified as described (2.6.9.). The rate of nucleotide triphosphate hydrolysis was measured by the formation of Pi using the fluorescent Pi probe, MDCC-PBP as previously described for wild type Rac1 (3.2.). 5 μ M Rac1·cou-edaGTP or Rac1·but-edaGTP were incubated with 15 μ M MDCC-PBP in 20mM Tris·HCl pH7.6, 1mM MgCl₂, 30°C and the fluorescence monitored at 462nm over time. The data were fitted to a first order rate equation. The observed first order rate constant for cou-edaGTP hydrolysis was $1.5 \times 10^{-3} \text{ s}^{-1}$, and for but-edaGTP was $1.9 \times 10^{-3} \text{ s}^{-1}$ (figure 3.8.); both are within a factor of two for the first order rate constant of GTP hydrolysis by Rac1 under the same conditions ($2.8 \times 10^{-3} \text{ s}^{-1}$). These results indicate that the coumarin fluorophores do not significantly interfere with the mechanism of GTP hydrolysis of Rac1 and both coumarin derivatised nucleotides are good analogues of GTP. As described previously, the intensity of the signal change observed using this technique is dependent on the concentration of Rac1 complexed to the GTP form of the nucleotide analogue. As described earlier (3.3.), intrinsic hydrolysis of GTP by Rac1 is rapid compared to Ras, and due to this a significant amount of GTP will be hydrolysed during the purification of these complexes.

These results indicate that both cou-edaGTP and but-edaGTP bind to Rac1, and measured rate constants for the hydrolysis of GTP using the labelled phosphate binding protein, MDCC-PBP are within a factor of 2 of GTP for both coumarin-labelled nucleotides. Rate constants for the dissociation of cou-edaGTP and but-edaGTP (predominantly in the GDP state due to intrinsic hydrolysis by Rac1) are also similar to the dissociation of mantGDP. The small effect of these fluorophores attached to the ribose moiety of the nucleotide is consistent with crystal structures of Rac1 (Hirshberg *et al.*, 1997) that show the 2' and 3' hydroxyl groups of the nucleotide projecting away from the protein towards the solvent.

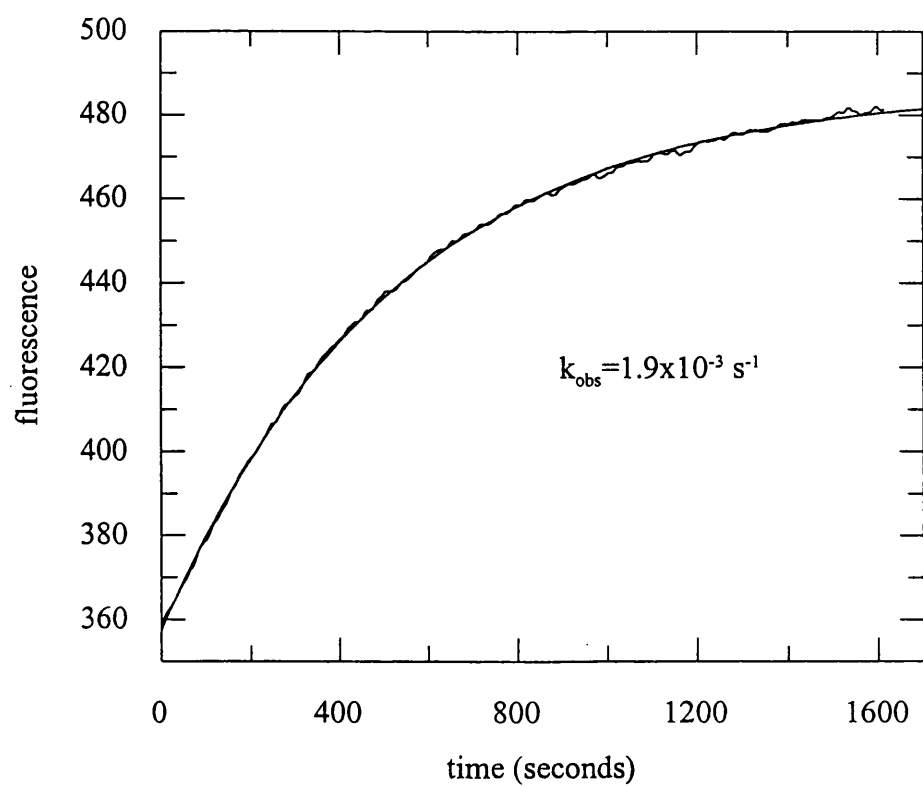
Figure 3.8. Hydrolysis of cou-edaGTP and but-edaGTP by Rac1

The rate of cou-edaGTP (a) and but-edaGTP (b) hydrolysis was measured using the Pi probe MDCC-PBP as described for GTP hydrolysis by Rac1 (3.3.). Rac1·cou-edaGTP (5 μ M) or Rac1·but-edaGTP (3 μ M) was incubated with MDCC-PBP (15 μ M and 10 μ M respectively) in 20mM Tris·HCl pH7.6, 1mM MgCl₂ at 30°C and the fluorescence measured over time (excitation λ = 425nm, emission λ = 464nm). Solid lines are best fits to single exponentials. Replacement of the Xenon lamp in the fluorimeter resulted in significantly lower signal to noise ratio when the hydrolysis of but-edaGTP was measured.

a)



b)



These results are also consistent with the small effect of mant modified nucleotides on the nucleotide exchange and hydrolysis of Rac1.

Both cou-edaGTP and but-edaGTP are environmentally sensitive, and on dissociation of the nucleotide from a complex with Rac1 there is ~20% change in fluorescence. With cou-edaGTP, an enhancement of fluorescence was observed, whereas when but-edaGTP was used a >20% quenching of fluorescence was monitored. This indicates that both coumarin modified nucleotides show differing environmentally sensitive properties. This is a significantly less fluorescence change than observed with mant derivatised nucleotides, and may reflect the greater distance of the coumarin fluorophores from the protein. It was hoped that due to the exposed nature of the fluorophore of cou-edaGTP and but-edaGTP, complexes of Rac1 with these novel fluorescent nucleotide analogues (predominantly in the GDP state due to intrinsic hydrolysis by Rac1) may be used to monitor the interaction of Rac1 with GDI. Recently the coumarin derivatised analogue but-edaGMPPNP has been synthesised in this laboratory (M.R. Webb, unpublished results). It was hoped that this non-hydrolysable analogue may provide a sensitive method to monitor the interaction with p67^{phox}. These experiments will be discussed in later chapters.

4. DESIGN & CHARACTERISATION OF RAC1 MUTANTS

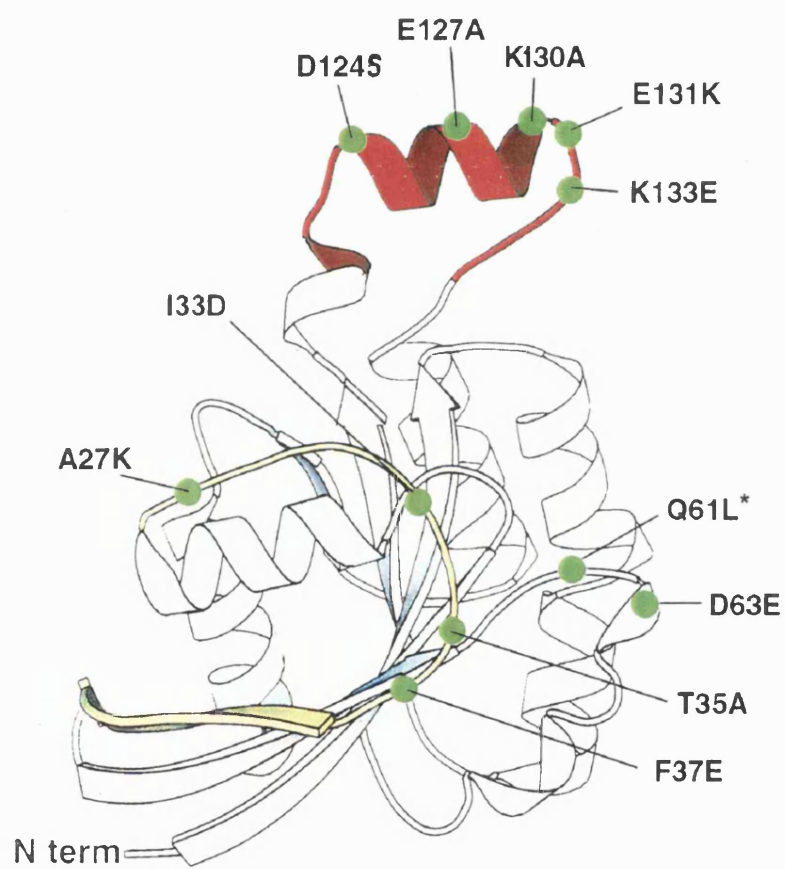
In order to study the interactions between Rac1 and other proteins, such as p67^{phox} and GDI, a number of Rac1 point mutants have been made (figure 4.1.). One of the major differences between Ras and Rho family proteins is the presence of an additional 12 amino acid 'insertion loop' (residues 124-125) in Rho proteins (figure 1.2.). This represents one of the several areas of divergence among Rho family members. Although recent reports indicate a role for this loop in mitogenesis (Joneson & Bar-Sagi, 1998), the precise role of this loop in the interaction with other proteins remains poorly defined; this loop represents one region currently under investigation in this laboratory.

4.1. Rac1 mutations to study the interaction with p67^{phox}

In order to examine the role of these regions, the Rac1·GMPPNP structure has been examined to design a number of point mutants that may have a role in the interaction with p67^{phox}. As Rac but not cdc42 proteins activate the NADPH oxidase system, residues in the insertion loop of Rac have been mutated to corresponding residues in cdc42 (figure 1.2.). These mutations include D124S, K130A and E131K and have been chosen as they are exposed residues of the insertion loop helix (based on the crystal structure of Rac1·GMPPNP) and are likely to be involved in the interaction with effectors such as p67^{phox}. Point mutations in the effector loop thought to be involved in this interaction (Nisimoto *et al.*, 1997), A27K and T35A mutations have also been made, and a mutation in a region that may be involved in nucleotide binding and hydrolysis, D63E, ~~has~~^{was} produced to examine the effect of these regions on the interaction with p67^{phox}. A comparison of the Rac1·GMPPNP and Rac1·GDP structures reveals conformational change between the two nucleotide bound states of Rac1 in the position and flexibility of the effector loop and switch II region (figure 1.7.). It is possible that Rac may bind through both the effector loop and insertion loop/switch II to different surfaces within the

Figure 4.1. Rac1 point mutations

A ribbon diagram of the Rac1·GMPPNP structure showing the positions of Rac1 point mutations that have been created. The overall fold of Rac1·GMPPNP is very similar to Ras·GMPPNP (figure 1.6.), except for two major regions of divergence. The insertion loop (shown in red), forms an exposed helical domain, and the effector loop (shown in yellow). Mutations in the effector loop have been chosen as they are not thought to directly interact with the nucleotide, are relatively exposed and are likely to accommodate the respective mutations without significant alteration to the Rac1 tertiary structure. The crystal structure of Rac1·GDP (Hirshberg *et al.*, unpublished results) has also revealed structural divergence between the switch II region of Rac1 and Ras in the GDP bound conformations (figure 1.7.). * The Q61L Rac1 mutant was a gift from Prof. A. Hall, UCL.



NADPH oxidase complex. This may convey the required specificity to permit Rac, but not cdc42 to function as an NADPH oxidase activator.

4.2. *Rac1* mutations to examine the interaction with GDI

Although GDI interacts with Rac1 in the GDP bound form and inhibits nucleotide exchange, the precise regions of Rac1 involved in this interaction have not been well defined. RhoGDI interacts with Rho family proteins, but no other Ras superfamily members. One of the major regions of structural divergence between Rac1 and Ras is the effector loop (aa's 30-40). Residues in the effector loop of Rac have been shown to be essential for the interaction with a number of other proteins, including PAK and ROCK (Lamarche *et al.*, 1996). To examine this region in the Rac1·GDI interaction, point mutations of Rac1 have been made between residues 31 and 40 of the effector loop. A comparison of this region of Rac1 and Ras (figure 4.2.) reveals a group of five hydrophobic residues in Rac (IPTVF), but only three in Ras (PTI), flanked either side by acidic residues (figure 4.2.). As other residues in this region are identical or conservatively substituted, two Rac1 point mutations have been made to corresponding residues of the Ras primary sequence – I33D and F37E. As it is well established that Ras proteins do not bind to RhoGDI, it is possible that this extended hydrophobic region in Rac1 is important for interaction with the flexible N-terminal region of GDI. This region is also of potential significance due to the differences in this loop between the Rac1·GMPPNP and Rac·GDP structures.

Residues in the insertion loop have been also chosen for site directed mutagenesis as they are largely exposed on the surface of the insert region; therefore mutations are unlikely to cause large structural perturbations outside this area. As isoprenylated Rho proteins bind to GDI, and the insertion loop of Rac1 lies at opposite ends from the C-terminus, it is unlikely that GDI interacts with both regions of Rac1 unless the flexible, N-terminus of GDI is in an extended conformation. A low resolution structure of the RhoA·RhoGDI

Figure 4.2. A comparison of the effector loop of Rac1 with Ras

A comparison of regions of the effector loop (aa's 31-40 of Rac1) with corresponding residues of Ras (see figure 1.2. for sequence alignment). Red circles indicate hydrophobic residues; those circled above in black are hydrophilic. Residues with charged functional groups (-) are also indicated.

Residue number	31							-		40
	●	●	●	●	●	●	●	●	●	●
Rac1	E	Y	I	P	T	V	F	D	N	Y
Ras	E	Y	D	P	T	I	E	D	S	Y
	●	●	●	●	●	●	●	●	●	●
	-		-				-	-		

complex suggests that this may not be the case. Although Rac and Rho proteins may bind to GDI via differing mechanisms, the crystal structure of this complex reveals that the N-terminal domain of GDI is likely to form a 'loop', with possible contacts with the effector loop and the switch II region (Longenecker *et al.*, 1999). This is consistent with mutations in the insertion loop having little effect on the interaction with GDI (Wu *et al.*, 1997). However, a report by Cerione's laboratory has revealed that the insertion loop is essential for the inhibition of nucleotide dissociation by GDI (Wu *et al.*, 1997). To further examine the role of this loop in the interaction with GDI, a number of additional *Rac1* point mutations have been made. As Ras proteins contain a short loop in place of the insertion loop of Rho family proteins (1.6.), point mutations in this region have been chosen to remove or reverse a charged functional group; mutations include E127A and K133E (figure 4.1.).

4.3. *Rac1/H-Ras chimaera*

The role of the insertion loop of *Rac1* has been further investigated by constructing a *Rac1/H-Ras* chimaeric protein. In this chimaeric construct, the 12 amino acid insertion loop (aa's 120-139) of *Rac1* has been replaced for the predicted region of 8 residues of H-Ras (aa's 122-128). Similar 'insertion loop' chimaeric constructs of a *cdc42/Ras* chimaera (baculovirus vector) (Wu *et al.*, 1997), a *Rac/Ras* chimaera (mammalian expression vector) (Joneson & Bar-Sagi, 1998) and a *Rho/Ras* chimaera (pGEX-2T vector) (Zong *et al.*, 1999) have been constructed using PCR based strategies, and functional protein has been obtained. Attempts to prepare a pGEX-2T *Rac1/H-Ras* construct using an overlapping PCR method as described by Wu *et al.* (1997) proved unsuccessful. Due to this, the construct has been created by restriction digest of the *Rac1* cDNA and ligation of primers corresponding to the H-Ras insert as described (2.6.4.).

4.4. Analysis of mutant Rac1 nucleotide complexes

Wild type recombinant Rac1, cdc42 and Rac1 mutants were all complexed exclusively to GDP (>98%) with the exception of Q61L Rac1, which was ~94% GTP bound when analysed by HPLC using a SAX-10 column (figure 4.3.). This is consistent with this mutant having a significantly reduced GTPase rate relative to wild type Rac1. These results suggest that purified mutant Rac proteins all retain the ability to bind guanine nucleotides, and the mutations introduced do not significantly disrupt the tertiary structure of Rac1.

4.5. Nucleotide binding properties of Rac1 mutants

To determine whether point mutations of Rac1 caused a major alteration to the basic biochemical properties of Rac1, they were tested for their ability to undergo nucleotide exchange using the fluorescent GDP analogue, mantGDP, in the presence of $(\text{NH}_4)_2\text{SO}_4$. The use of $(\text{NH}_4)_2\text{SO}_4$ has been well documented in studies with Ras (Eccleston *et al.*, 1993) and may be used as a tool to produce conditions of accelerated nucleotide exchange (3.2.2.). The presence of $(\text{NH}_4)_2\text{SO}_4$ increases the rate of exchange by ~30 fold making it practical to compare exchange rates.

The dissociation of GDP (and association of mantGDP) has been determined under accelerated conditions (3.2.2.), and the data fitted to a single exponential. The nucleotide binding properties of mutant Rac1 constructs have been compared to those of wild type Rac1 (table 4.1). Rac1 rapidly bound mantGDP under these conditions with an observed rate constant of $3.3 \times 10^{-3} \text{ s}^{-1}$, 30°C. These equilibrium binding results suggest that all of the Rac1 mutants have the ability to bind guanine nucleotides, (with the exception of F37E Rac1) with individual guanine nucleotide binding parameters differing little from those of wild type Rac1. These experiments reveal no significant difference in the kinetics of GDP release for the majority of mutants as compared to those of wild type Rac1.

Figure 4.3. Analysis of nucleotide bound to Rac1 and Rac1 mutants

Nucleotides bound to Rac1 were analysed using a partisil SAX-10 anion exchange HPLC column (Whatman) eluting at $2\text{ml}\cdot\text{min}^{-1}$ with 0.45M $(\text{NH}_4)_2\text{HPO}_4$ pH 4.0 buffer essentially as described (2.6.10.). **A)** Nucleotide standards GMP, GDP, GTP. **B)** Analysis of the nucleotide bound to wild type Rac1 indicates >98% GDP bound. Rac1 point mutants A27K, I33D, T35A, F37E, D63E, D124S, E127A, K130A, E131K and K133E, wild type Rac1, wild type cdc42 and the Rac1/H-Ras insert chimaera were all complexed almost exclusively with GDP (data not shown). **C)** Nucleotide bound to the Q61L Rac1 mutant was ~94% GTP bound. Absorbance at 252nm shown in arbitrary units.

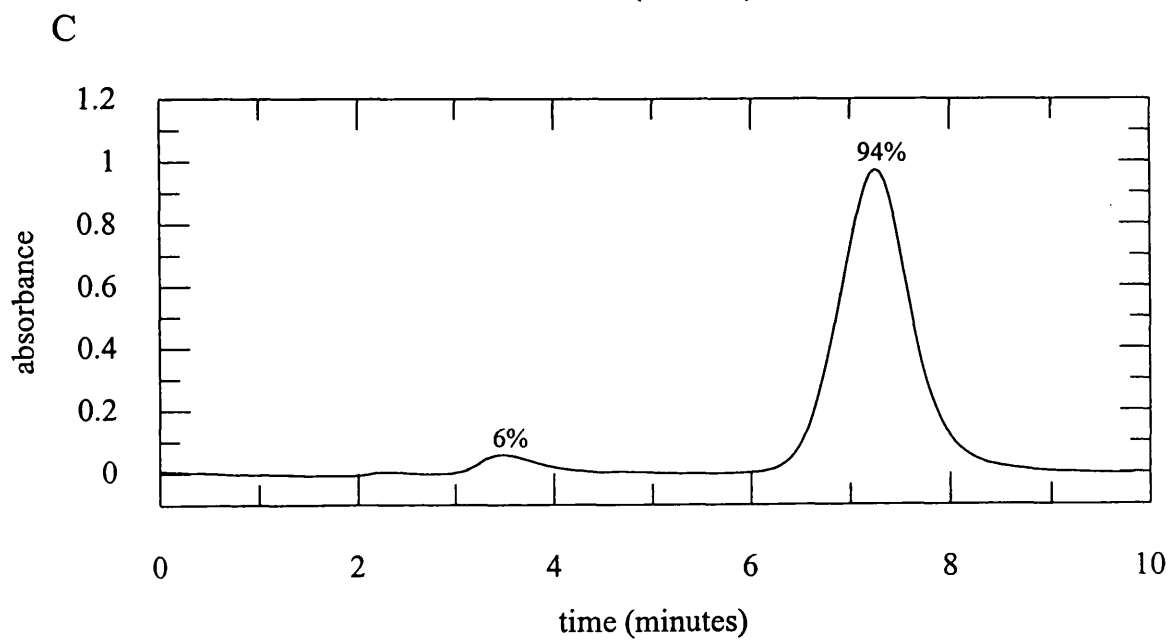
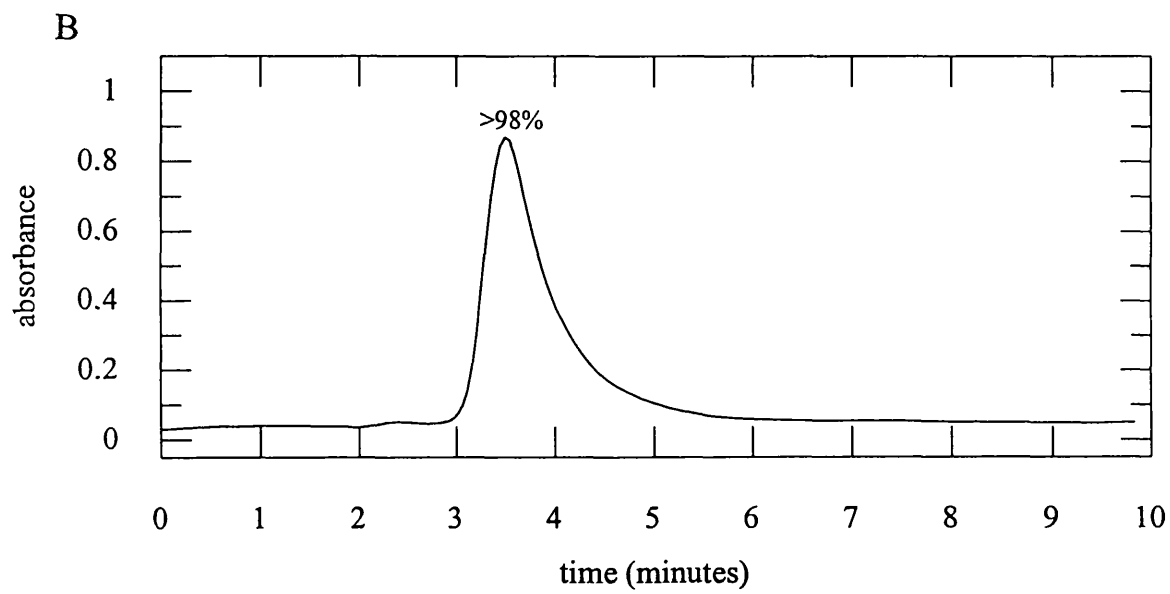
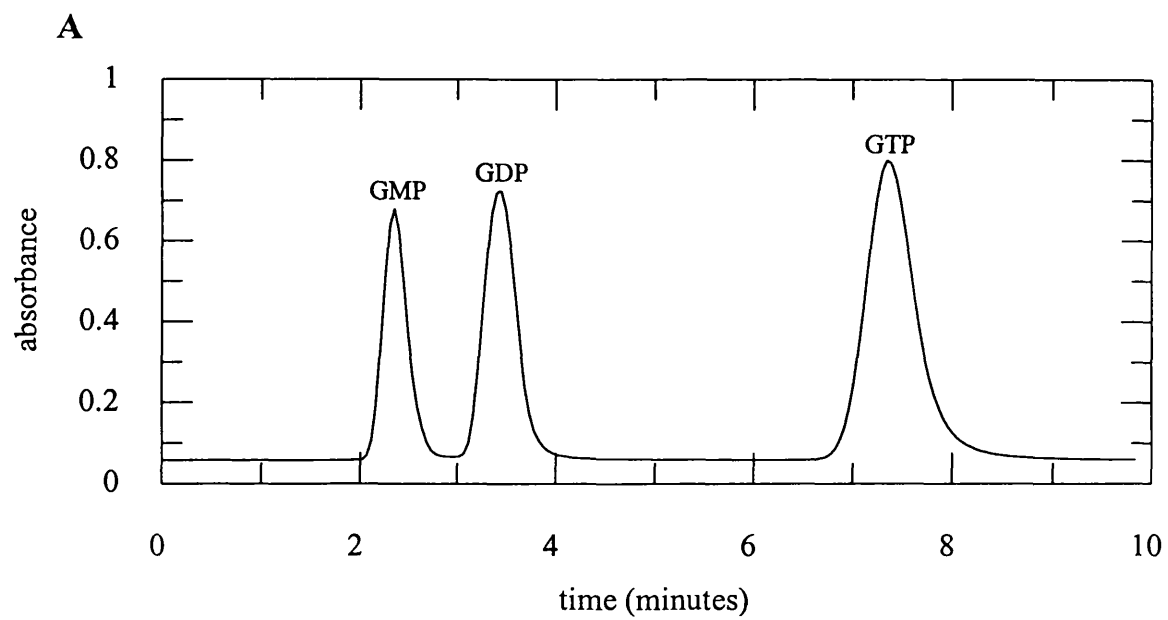


Table 4.1. Nucleotide binding properties of Rac mutants

The rate of nucleotide exchange for Rac1 mutants (figure 4.1.) was determined using fluorescence energy transfer (by exciting at 290nm) essentially as described for wild type Rac1 (figure 3.3b). Rac1 mutant (5 μ M) was incubated with mantGDP (50 μ M) in 20mM Tris·HCl pH7.6, 1mM MgCl₂, 200mM (NH₄)₂SO₄, 30⁰C and the fluorescence emission at 440nm monitored over time. Rate constants represent the average of at least two independent reactions.

^a F37E Rac1 showed no detectable binding of mantGDP under these conditions and this value represents a limit imposed by errors in the measurement. ^b The mass of K133E Rac1 determined by mass spectrometry (2.4.1.) does not correspond to the mass calculated from the primary sequence of the construct. It is possible that additional mutations are present in the sequence. A complete DNA sequence of this mutant has yet to be examined.

*First order rate constants for nucleotide exchange
of Rac1 and Rac1 mutants*

Protein	k_{obs} ($\times 10^{-3} \text{ s}^{-1}$)
Rac1	3.3
<i>Rac1 mutants</i>	
A27K	2.2
I33D	4.1
T35A	2.0
F37E ^a	>1000 NOT DETERMINED
D63E	3.9
D124S	5.3
E127A	4.8
K130A	3.3
E131K	6.1
K133E ^b	3.6
Rac1/H-Ras chimaera	2.9

4.5.1. Nucleotide exchange by F37E Rac1

The F37E Rac1 mutant showed no increase in mant fluorescence under conditions described (4.5.) (figure 4.4.). HPLC analysis indicates that F37E Rac1 is GDP bound, indicating that the protein retains the ability to bind GDP (4.4.). It is possible that the mantGDP does not bind to the F37E Rac1 mutant, or binding of the mant nucleotide does not result in a fluorescence signal under these conditions. As the F37E Rac1 mutant has only recently been obtained, examination of the nucleotide binding properties of the F37E Rac1 mutant using alternative methods (such as HPLC) is currently under investigation in this laboratory.

4.6. Hydrolysis of GTP by a Rac1/H-Ras chimaera

To examine whether removal of the insertion loop caused a major alteration to the mechanism of intrinsic GTP hydrolysis by Rac1, the rate of GTP hydrolysis was measured using the Pi probe, MDCC-PBP as described previously (3.3.). When 5µM Rac1/H-Ras chimaera (complexed to GTP) was incubated with 15µM MDCC-PBP in 20mM Tris-HCl pH7.6, 1mM MgCl₂ at 30°C, GTP was hydrolysed with an observed first order rate constant of $2.7 \times 10^{-3} \text{ s}^{-1}$ (figure 4.5.). These results indicate that the relatively rapid rate of intrinsic GTP hydrolysis by Rac1 is not dependent on a conformation induced by the insertion loop, as removal of this loop (and replacing it with a corresponding region from Ras) does not alter the rate of GTP hydrolysis by Rac1. As rates of nucleotide exchange and GTP hydrolysis by the Rac1/H-Ras chimaera were both within a factor of two of wild type Rac1, it is assumed for subsequent studies that this Rac1/H-Ras chimaera retains a biochemically active conformation.

4.7. Hydrolysis of GTP by D63E Rac1

Most small G proteins of the Ras superfamily hydrolyze GTP to GDP slowly (Ras $t_{1/2}$ = ~100 min, 20°C). Notable exceptions are the Rac proteins which have intrinsic hydrolysis

Figure 4.4. F37E Rac1 nucleotide exchange under accelerated exchange conditions

I33D or F37E (5 μ M) were incubated with mantGDP (50 μ M) in 20mM Tris·HCl pH 7.6, 1mM MgCl₂, 200mM (NH₄)₂SO₄, 30°C. Excitation 290nm. The F37E mutation completely abolished an observed change in mant fluorescence under these conditions (consistent results obtained with two independent experiments). As a control, nucleotide exchange by I33D Rac1 was examined using the same exchange buffer. As expected, this mutant underwent similar exchange as for wild type Rac1. I33D data fitted to a single exponential.

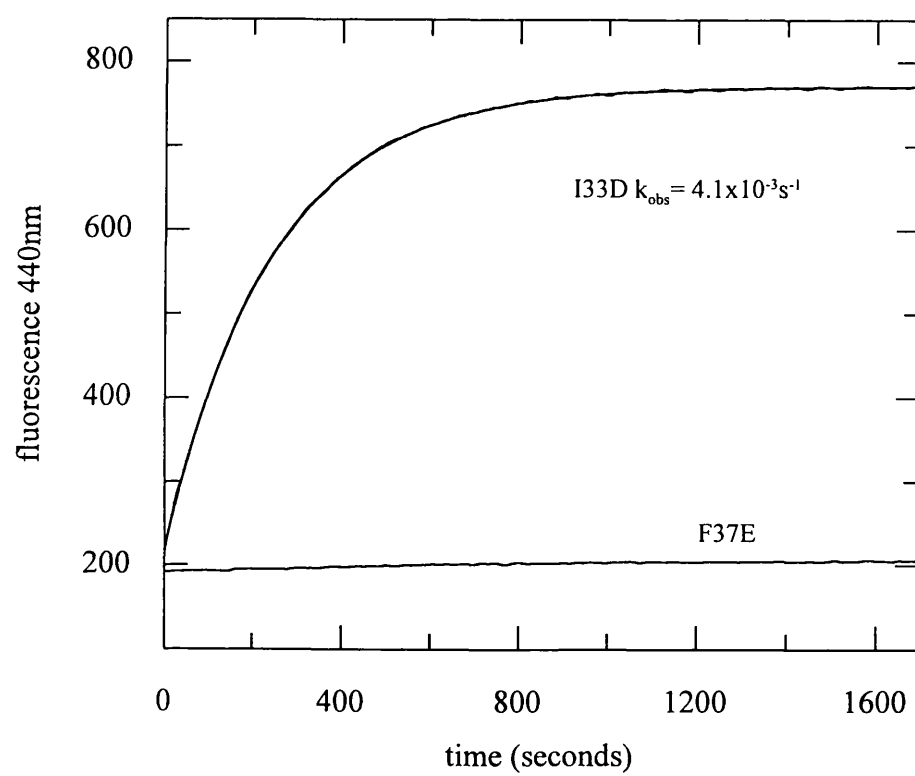
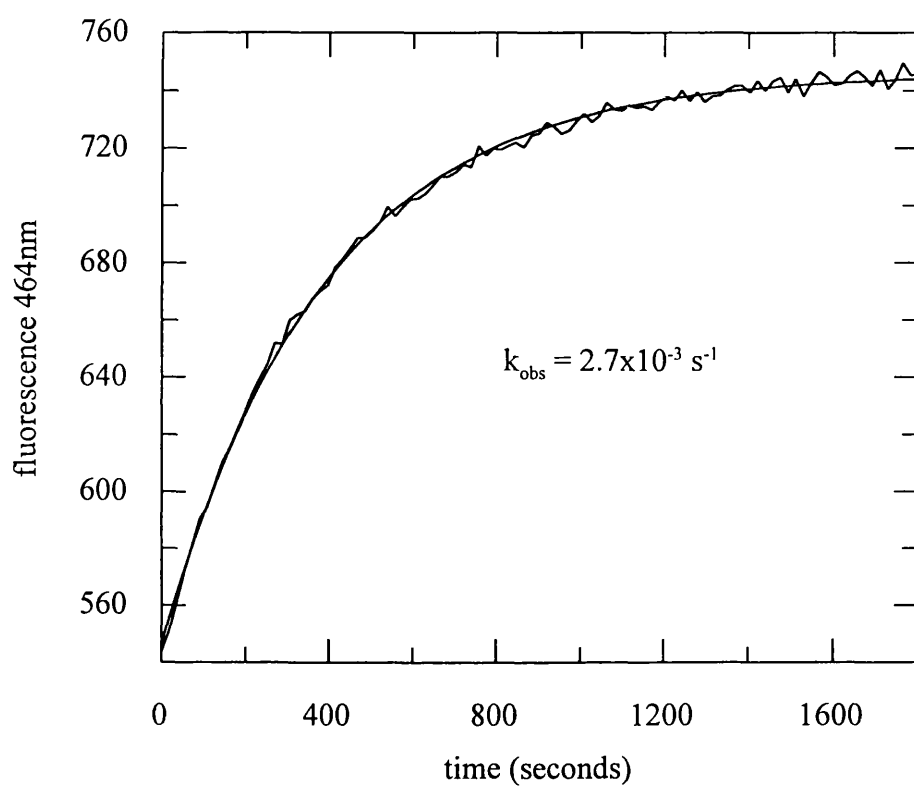


Figure 4.5. Hydrolysis of GTP by a Rac1/H-Ras 'insertion loop' chimaera

To examine if removal of the insertion loop of Rac1 had a significant effect on the biochemical properties of Rac1, the rate of GTP hydrolysis of the Rac1/H-Ras chimaera was examined using the Pi probe MDCC-PBP as described for wild type Rac1 (3.3.). Rac1/H-Ras chimaera (5 μ M) was incubated with MDCC-PBP (15 μ M) in 20mM Tris·HCl pH7.6, 1mM MgCl₂ at 30°C and the fluorescence monitored over time. The line shows a best fit to a single exponential and the observed rate constant is an average of two independent reactions. Excitation 425nm. Removal of the insertion loop of has no effect on the rate of intrinsic GTP hydrolysis by Rac1 (3.3.), indicating that this loop does not play a significant role in the mechanism of GTP hydrolysis.



rates of at least 40 fold higher than Ras and Rho ($\text{Rac } t_{1/2} = 2.5 \text{ min}$, 20°C) (Menard *et al.*, 1992). Such a high rate of GTP hydrolysis suggests that even in the absence of GTPase activating proteins, Rac would have its active state terminated by intrinsic GTP hydrolysis. A mechanism for hydrolysis of GTP by Ras has been proposed by Pai *et al.* (1990). This suggests that the carboxylate group of Glu63 is close enough to the amido group of Glu61 to form a H-bond, and maintain this residue in the correct orientation for GTP hydrolysis (1.10.). However, the residue at position 63 is not conserved between Ras and Rho family members. In Rac1, residue 63 is an Asp, which cannot stabilise Glu61 without substantial re-arrangement of the whole region, therefore a similar mechanism would not be possible. To examine the role of this residue in the mechanism of GTP hydrolysis by Rac, a D63E Rac1 mutant has been made which corresponds to a change to the residue found in this position in Ras. The rate of GTP hydrolysis by D63E Rac1 was measured using the Pi probe, MDCC-PBP as described for wild type Rac (3.3.). The rate constant for Pi production by this mutant was $3.3 \times 10^{-3} \text{ s}^{-1}$ (data not shown). This is within a factor of two of the rate of intrinsic GTP hydrolysis by Rac1 under the same conditions and indicates that mutation of Asp to Glu at position 63 of Rac1 does not significantly alter the rate of GTP hydrolysis by Rac1.

4.8. Q61L – a GTPase deficient Rac1 point mutant

When residue 61 is mutated in the Ras proto-oncogene, the resulting mutant Ras protein exhibits a greatly reduced rate of intrinsic GTP hydrolysis and a predominantly GTP bound phenotype (Krengel *et al.*, 1990). As shown by figure 4.3., the Q61L Rac1 mutant is predominantly GTP bound (~94%), maintaining significant levels of bound GTP even after an extensive period (3-4 days) of purification. This is consistent with this residue playing a key role in GTP hydrolysis (1.10.). The small amount of GDP detected by HPLC is probably due to the hydrolysis of GTP by this mutant throughout the purification procedure, resulting in ~7% Q61L Rac1·GDP. In an attempt to examine the rate of intrinsic GTP hydrolysis by Q61L Rac1 and obtain Q61L Rac1·GDP for biochemical

studies, 100 μ M Q61L Rac1·GTP was incubated in 20mM Tris·HCl pH7.6, 1mM MgCl₂ at room temperature (23°C). Aliquots were removed at regular intervals and the percentage of GDP bound to the protein analyzed by HPLC essentially as described (2.6.10.). Even after 20 hours at room temperature, the protein remained in a predominantly (>90%) GTP bound state.

4.9. Summary of results

In an attempt to examine the regions of Rac1 involved in the interaction with p67^{phox} and GDI, a number of Rac1 point mutants have been made and characterised. Point mutations have been created in the major regions of structural divergence between Rac1 and other Rho or Ras family proteins; these regions include the effector loop (aa's 30-40 of Rac1) and the insertion loop (aa's 120-137 of Rac1) (figure 1.2.). In addition, a Rac1/H-Ras 'insertion loop' chimaera has been produced. In this construct the cDNA encoding this loop of Rac1 has been removed and replaced with the corresponding sequence from H-Ras. Analysis of the nucleotide bound to Rac1 point mutants indicates they are all >98% GDP bound, with the exception of Q61L Rac1, which is ~94% GTP bound as analysed by HPLC. The small amount of GDP detected (~6%) when Q61L was examined is likely to be due to a small amount of GTP hydrolysed by Q61L Rac1 during the purification of the protein. This indicates that all mutant proteins produced retain the ability to bind guanine nucleotides.

To further examine if mutations alter the basic biochemical properties of Rac1, mutant Rac1 proteins have been characterised by their ability to bind mant derivatised guanine nucleotides. The rate of GDP release from Rac1 mutants has been examined under accelerated exchange conditions using mantGDP (3.2.2.). All Rac1 mutants (with the exception of F37E Rac1) show similar nucleotide binding properties to wild type Rac1. This indicates that the Rac1 mutations do not have an essential role in guanine nucleotide binding.

The F37E Rac1 showed no detectable binding of mantGDP under accelerated nucleotide exchange conditions (figure 4.4.). It is possible that the mantGDP does not bind to the F37E Rac1 mutant, or binding of the mant nucleotide does not result in a fluorescence signal under these conditions. As the F37E Rac1 mutant has only recently been obtained, alternative methods to examine the nucleotide binding properties of the F37E Rac1 are currently under investigation in this laboratory.

As removal of the insertion loop is a major change to the tertiary structure of Rac1, it was important to fully characterise the Rac1/H-Ras chimaera before using this protein for further biochemical studies. The rate of intrinsic GTP hydrolysis by the Rac1/H-Ras chimaera has been examined as described for wild type Rac1 (3.3.) using the Pi probe MDCC-PBP. The chimaeric protein has a rate of GTP hydrolysis similar to wild type Rac1. These results indicate that removal of this loop has little effect on the basic biochemical properties of Rac1.

5. INTERACTION OF RAC1 WITH p67^{phox}

5.0. Introduction

Activation of the NADPH oxidase requires the assembly of the membrane associated flavocytochrome b₅₅₈ with the cytosolic components p47^{phox}, p67^{phox} and Rac (1.3.2.). Activated (GTP bound) Rac1 interacts directly with p67^{phox}, but not with any other phagocyte oxidase component (Reviewed by Segal & Shatwell, 1997).

The N terminal 199 residues of p67^{phox} (p67¹⁻¹⁹⁹) are thought to contain ~~be~~ the domain that interacts with Rac (Diekmann *et al.*, 1994), and the region essential for the interaction with Rac1 and Rac2 has shown to be between residues 170-199 of p67^{phox} (Ahmed *et al.*, 1998). Deletion of p67^{phox} C-terminal sequences (aa's 193-526), the C-terminal SH3 domain (aa's 470-526) or the polyproline rich motif of p67^{phox} (aa's 226-236) stimulated Rac1 binding by ~ 8 fold as determined by dot-blot assays. It has been proposed that an intramolecular SH3-polyproline interaction within the p67^{phox} protein may inhibit Rac binding to residues 170-199 (Ahmed *et al.*, 1998). PAK phosphorylates p67^{phox}, with this phosphorylation stimulated by deletion of the C-terminal SH3 domain or polyproline motif (Ahmed *et al.*, 1998). This indicates a possible mechanism for the involvement of PAK in the regulation of the NADPH oxidase.

5.1. Aim of experiments

From the crystal structure of Rac1·GMPPNP (Hirshberg *et al.*, 1997) it has been possible to identify a number of positions where mutational studies may provide an insight into the mechanism by which Rac1 and p67^{phox} interact; the aim of these experiments was to elucidate this mechanism of interaction. One approach to monitor this interaction is to use Rac1 complexed to environmentally sensitive, non-hydrolysable fluorescent nucleotide analogues, such as mantGMPPNP. At least one laboratory has reported a fluorescence change when Rac1·mantGMPPNP is incubated with p67^{phox} (Nisimoto *et al.*, 1997). It

was hoped that this system might be used to examine the kinetics of this interaction and the effect of Rac mutants on the affinity for p67^{phox}. In addition, it was hoped that a novel binding assay could be developed to monitor this interaction using p67¹⁻¹⁹⁹ (the N terminal fragment of p67^{phox} thought to contain the Rac binding region) labelled with environmentally sensitive fluorophores. It was also hoped that a fluorescence change would be observed when p67^{phox} interacts with Rac1 complexed to a novel coumarin derivatised nucleotide – but-edaGMPPNP. Coumarin derivatised nucleotides have been shown to bind to Rac1 and have similar properties to parent nucleotides (3.4.1.). As but-edaGMPPNP has an exposed fluorophore, it was hoped that this may provide a sensitive method to directly monitor the interaction of Rac1 with p67^{phox}.

5.2. Purification of p67^{phox} proteins

To examine the interaction of Rac1 with p67^{phox}, full length p67^{phox} has been purified using a baculovirus expression system (2.3.). The N-terminal fragment (aa's 1-199) has also been purified using a pGEX-GK expression vector in *E.coli* (2.2.3.), and a synthetic peptide corresponding to residues 170-199 of p67^{phox} (the Rac1 binding region) has been obtained (synthesised as described for C terminal peptides (2.5.) at N.I.M.R.). Although the N-terminal fragment (residues 1-199) of p67^{phox} has been successfully purified, the protein shows stability and solubility problems dependent on temperature and ionic strength. Buffer with an ionic strength of >50mM is required to elute the protein from a glutathione-sepharose column following thrombin cleavage (2.2.3.) and a temperature of 15°C or above results in a gradual precipitation of a dilute (5µM) p67¹⁻¹⁹⁹ solution. This may reflect the instability of this domain in the absence of the remainder of the protein. Similar problems have also been reported when attempts have been made to purify N terminal fragments of p67^{phox} (Diekmann *et al.*, 1994 & Ahmed *et al.*, 1998). A small number of laboratories have reported successfully purifying the fusion protein GST-p67^{phox} and pure full length p67^{phox} from an *E.coli* expression system (Abo *et al.*, 1992 & Sumimoto *et al.*, 1996). Despite these reports, purification of p67^{phox} from *E.coli* is

typically problematic, and lower NADPH oxidase activities have been reported with *E.coli* derived recombinant p67^{phox} compared to the protein produced using baculovirus expression systems.

Because expression of full length p67^{phox} using an *E.coli* expression system has proved unsuccessful (2.2.4.), recombinant baculoviruses have been used to produce p67^{phox} in insect cells. As p67^{phox} purified from insect cells is susceptible to minor proteolytic degradation, p67^{phox} fractions with the greater apparent molecular weight (as analysed by SDS-PAGE) were used for subsequent studies (2.3.4.).

5.3. Characterisation of p67¹⁻¹⁹⁹

p67¹⁻¹⁹⁹ is the N-terminal domain of p67^{phox} containing the Rac interacting domain (Diekmann *et al.*, 1994) and has been successfully purified (2.2.3.). Mass spectrometry of the purified protein from *E.coli* revealed a molecular weight significantly greater than the value calculated from the primary sequence. To investigate the N- and C-terminal residues of the p67¹⁻¹⁹⁹ insert, dideoxy-sequencing of the N- and C- terminal regions of the p67¹⁻¹⁹⁹ cDNA was undertaken. This revealed 18 additional residues (excluding Gly-Ser-Pro residues remaining from the thrombin cleavage site) not part of the p67^{phox} gene, but probably inherent in the cloning procedure used (figure 5.1.). The mass determined by mass spectrometry of 24568Da agrees with that calculated from the sequence when these additional residues are included (figure 5.2.).

Although the structure of p67^{phox} has not been solved, sequence alignment with known protein structures suggests that p67¹⁻¹⁹⁹ shares greatest homology with the tetracoilpeptide repeat (TPR) region (Koga *et al.*, 1999). Although p67¹⁻¹⁹⁹ may adopt a tertiary structure with little homology with any other known protein, it is possible that the N-terminal domain of p67^{phox} forms a group of four TPRs. These motifs each comprise of a pair of antiparallel α helices (Das *et al.*, 1998) involved in a wide variety of protein-protein

Figure 5.1. N- and C- terminal residues of p67¹⁻¹⁹⁹

Results of the dideoxy-DNA sequencing of the amino and carboxyl terminal regions of p67¹⁻¹⁹⁹ cDNA in the pGEX-GK vector. The codons corresponding to the amino acid residues 2 to 16 and 194 to 199 of the p67¹⁻¹⁹⁹ cDNA were confirmed from the sequence to be correct. Blue underlined residues show the thrombin recognition sequence.

Although this construct has been termed p67¹⁻¹⁹⁹ by previous laboratories and throughout this report, DNA sequencing has revealed that the N-terminal methionine (residue 1) has been removed, probably during the cloning procedure. Hence this construct contains an insert encoding residues 2-199 of the p67^{phox} cDNA.

Additional N-terminal residues

Additional C-terminal residues

Leu Val Pro Arg Gly Ser Pro Gly Ile Ser Gly Gly Gly Gly Gly Gly Ile Leu Gly Ser
CTG GTT CCG CGT GGA TCC CCG GGA ATT TCC GGT GGT GGT GGT GGT GGA ATT CTA GGA TCC----P67¹⁻¹⁹⁹----CTA GAG CTT AAT TCA TCG TGA

↑
Thrombin cleavage site

↑
residue 2

↑
residue 199

Figure 5.2. Electrospray mass spectrometry of p67¹⁻¹⁹⁹

P67¹⁻¹⁹⁹ was purified from the BL21 strain of *E.coli* and analysed by mass spectrometry.

A single species of 24568 (\pm 1.05) Da was observed. This corresponds to the mass calculated from the primary sequence of residues 2-199 of p67^{phox} (22966.8 Da) plus the additional 21 residues at the N- and C- termini (24564.5 Da).

BL21 p67(1-199)

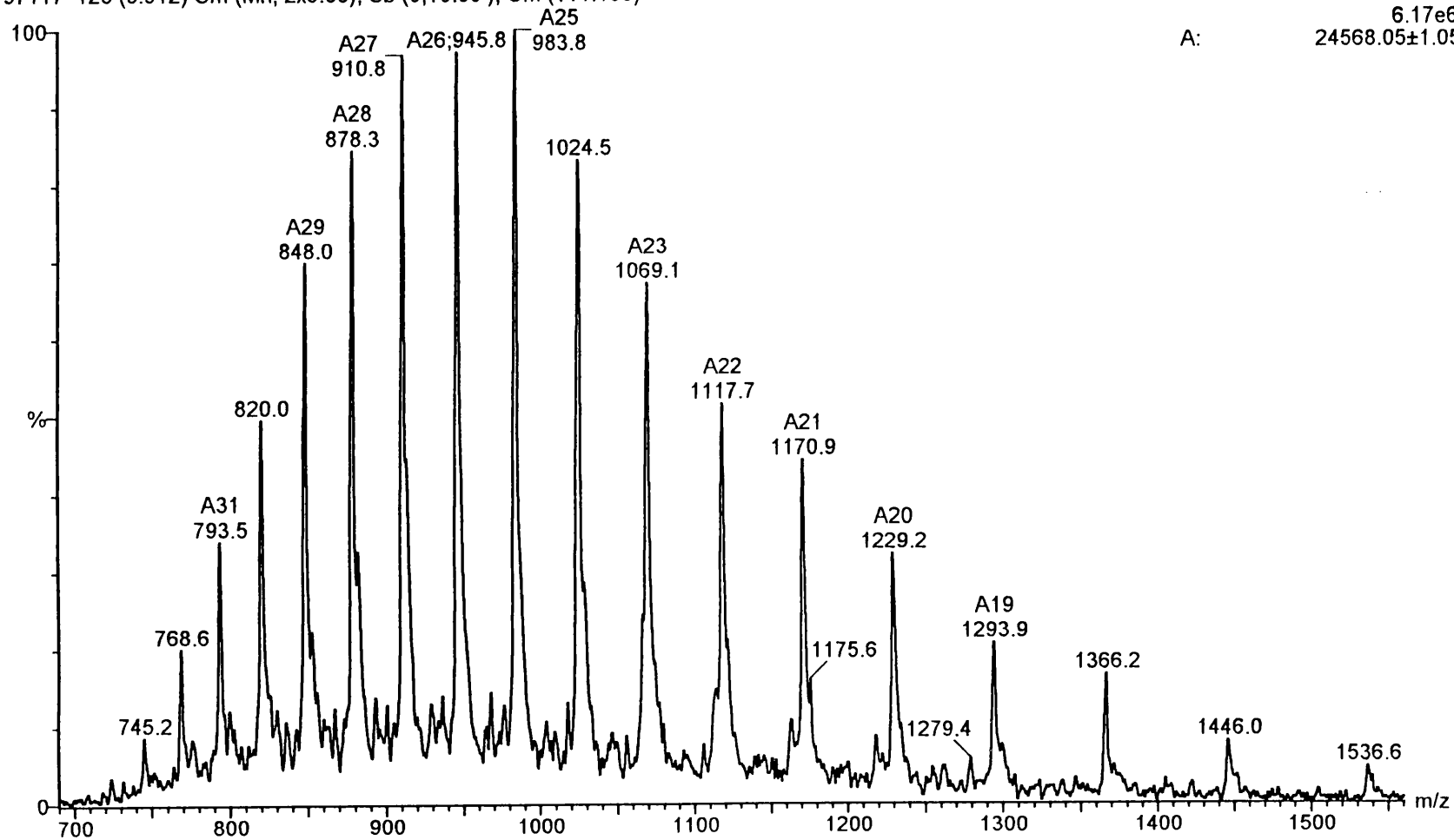
97117 123 (3.912) Sm (Mn, 2x3.00); Sb (0,10.00); Cm (111:135)

Scan ES+

6.17e6

A:

24568.05±1.05



interactions (Skinner *et al.*, 1997, Chen & Cohen, 1997). This motif has been identified in a large number of proteins, present in tandem arrays of 3-16 motifs. This would be consistent with secondary structure prediction of p67¹⁻¹⁹⁹, which indicates a predominantly α -helical conformation (figure 5.3.). However, little is known about the molecular nature of TPR mediated interactions and the Rac1 binding region of p67¹⁻¹⁹⁹ (aa's 170-199) does not align with any other Rac1 binding domain. Isolation of more Rac1 specific targets will need to be identified before a Rac1 specific binding motif in p67¹⁻¹⁹⁹ can be generated.

5.4. Effect of p67^{phox} and p67¹⁻¹⁹⁹ on Rac1·mantGMPPNP fluorescence

Direct binding of Rac1 and 2 to p67^{phox} and p67¹⁻¹⁹⁹ has previously been reported using Rac1 bound to the fluorescent nucleotide analogue, mantGMPPNP. A significant increase in mant fluorescence was observed when p67^{phox}, but not p47^{phox} was added. p67^{phox} bound tightly to Rac1 and Rac2, with K_d values of 120 and 60nM respectively (Nisimoto *et al.*, 1997). In the reported experiments, 0.25 μ M Rac1 was incubated with 0.12 μ M mantGMPPNP in 20mM Tris-HCl pH7.45, 0.1 μ M MgCl₂, 3mM NaCl, 50mM KCl for 20 minutes at 20°C. A stable fluorescence increase of 8% was reported (due to mantGMPPNP binding). Following nucleotide exchange, the addition of 0.3 μ M p67^{phox} resulted in a 30% increase in Rac1·mantGMPPNP fluorescence (Nisimoto *et al.*, 1997). As Rac1 added in this experiment contained bound GDP, and assuming that Rac1 at best, has a similar affinity for mantGMPPNP and GDP, as little as ~33% of the Rac1 may be complexed to mantGMPPNP at any one time. This suggests that the observed fluorescence change when Rac1·mantGMPPNP binds to p67^{phox} is under estimated in this system. Titration experiments have also been described by Nisimoto *et al.* (1997). p67^{phox} was titrated into a solution containing 0.25-0.6 μ M Rac1, mantGMPPNP (70% of the Rac concentration) in 20mM Tris-HCl pH7.6, 0.1 μ M MgCl₂, 3mM NaCl, 50mM KCl. This

Figure 5.3. Secondary structure prediction of p67¹⁻¹⁹⁹

The secondary structure of p67¹⁻¹⁹⁹ was predicted using two protein structure prediction servers available via the internet called PSIPred (A) (Altshul *et al.*, 1997) and Jpred (B) (Cuff *et al.*, 1998). H = α -helix, E = β strand. Gaps in the prediction represent random coil. Although there is a slight variation between the two methods, both predict that p67¹⁻¹⁹⁹ is most likely to exist as an almost completely α helical domain.

AA: MSLVEAISLWNEGVLAADKKDWKGALDAFSAVQDPHSRICFNIGCMYTILKNMTEAEKAF
 A: HHHHHHHHHHHHHHHHHHH HHHHHHHHHHHH HHHHHHHHHHHH HHHHHHHH
 B: HH EEEE HHHHHHHHHHHHHHHHH
 10 20 30 40 50 60

AA: TRSINRDKHLAVAYFQRGMLYYQTEKYDLAIKDLKEALIQLRGNQLIDYKILGLQFKLFA
 A: HHHHHH HHHHHHHHHHHHHHHHHHH HHHHHHHHHHHH HHHHHHHH
 B: HHHH HH HHHHHHHHHHHHHHHHHHH
 70 80 90 100 110 120

AA: CEVLYNIAFMYAKKEEWKKAEEQLALATSMKSEPRHSKIDKAMECVWKQKLYEPVVIPVG
 A: HHHHHHHHHHHHHHHHH HHHHHHHHHHHH HHHHHHHHHHHHHHHHH EEE
 B: HH HHHHHHHHHHHHHHHHH EEEE
 130 140 150 160 170 180

AA: KLFRPNERQVAQLAKKDYL
 A: HHHHHHHHHH
 B: HHHHHHHHHHHH
 190

report indicates a maximum fluorescence increase of >60% when saturating concentrations (>3 μ M) p67^{phox} is added.

In an attempt to use this system to directly monitor the interaction of Rac1 and Rac1 mutants with p67^{phox}, experiments were undertaken using similar conditions described by Nisimoto *et al.* (1997). Incubation of 1 μ M Rac1 with 0.5 μ M mantGMPPNP in 20mM Tris·HCl pH7.6, <5 μ M MgCl₂, 3mM NaCl, 50mM KCl, 1mM DTT, at 20°C resulted in a 70% increase in mantGMPPNP fluorescence (figure 5.4.). Following nucleotide exchange, 4 μ M p67^{phox} was added, and the fluorescence measured. Although a small fluorescence change was observed, this was variable and typically <10% (figure 5.4.). Additional experiments showed no significant change in fluorescence when full length Rac1 (2.2.2.) was used, or when p67¹⁻¹⁹⁹ or p67¹⁷⁰⁻¹⁹⁹ were added to the solution (data not shown).

Incubation of Rac1 with mantGMPPNP in this laboratory under conditions described above resulted in almost a 10 fold greater fluorescence change than described by Nisimoto *et al.* (1997). However, this change is consistent with previous reports in this laboratory of a ~2-fold increase in fluorescence when Rac1 binds mant derivatised nucleotides (R.W. Stockley & M.R. Webb). It is possible that a significant proportion of the Rac1 is not active in the experiments reported by Nisimoto *et al.* or nucleotide exchange was not complete, despite an extended (20 min, 20°C) incubation.

Similar experiments have also been undertaken using Rac1 complexed with mantGMPPNP (2.6.10.) {in which the complex is formed and excess nucleotide removed}. Formation and purification of the Rac1·mantGMPPNP is a more accurate method of determining the concentration of the complex, and purified Rac1·mantGMPPNP complexes were shown to be >90% pure as analysed by HPLC

Figure 5.4. Effect of $p67^{phox}$ on $Rac1 \cdot mantGMPPNP$ fluorescence using similar conditions as described by Nisimoto et al., 1997

Emission spectra of $mantGMPPNP$ ($0.5\mu M$) (A) in 20mM Tris-HCl pH7.6, 3mM NaCl, 50mM KCl, 1mM DTT at $20^{\circ}C$. The reaction mix contained $<5\mu M$ $MgCl_2$. (B) Addition of $1\mu M$ Rac and incubation for 15 minutes to allow nucleotide exchange, indicated by $\sim 70\%$ increase in fluorescence. (C) Emission scan following the addition of $4\mu M$ $p67^{phox}$. All scans are corrected for dilutions. $P67^{phox}$ shows no significant effect on truncated or full length $Rac1 \cdot mantGMPPNP$ fluorescence under these conditions. Although a small fluorescence increase was observed following the addition of $p67^{phox}$, this was variable and only seen once the scan had been corrected for the effect of dilutions. Excitation 355nm.

Figure 5.5. The effect of $p67^{phox}$ on $Rac1 \cdot mantGMPPNP$ fluorescence

$Rac1 \cdot mantGMPPNP$ ($1\mu M$) was incubated at $20^{\circ}C$ in 20mM Tris-HCl pH7.6, 1mM $MgCl_2$, 3mM NaCl, 50mM KCl and 1mM DTT (solid line) to which was added $3\mu M$ $p67^{phox}$ (dotted line-corrected for dilution). No significant change of $Rac \cdot mantGMPPNP$ fluorescence was observed under these conditions. Similar results were observed when Rac and $p67^{phox}$ were incubated in 20mM Tris-HCl, pH7.6, 1mM $MgCl_2 \pm$ 1mM DTT (data not shown). Excitation 360nm.

Figure 5.4.

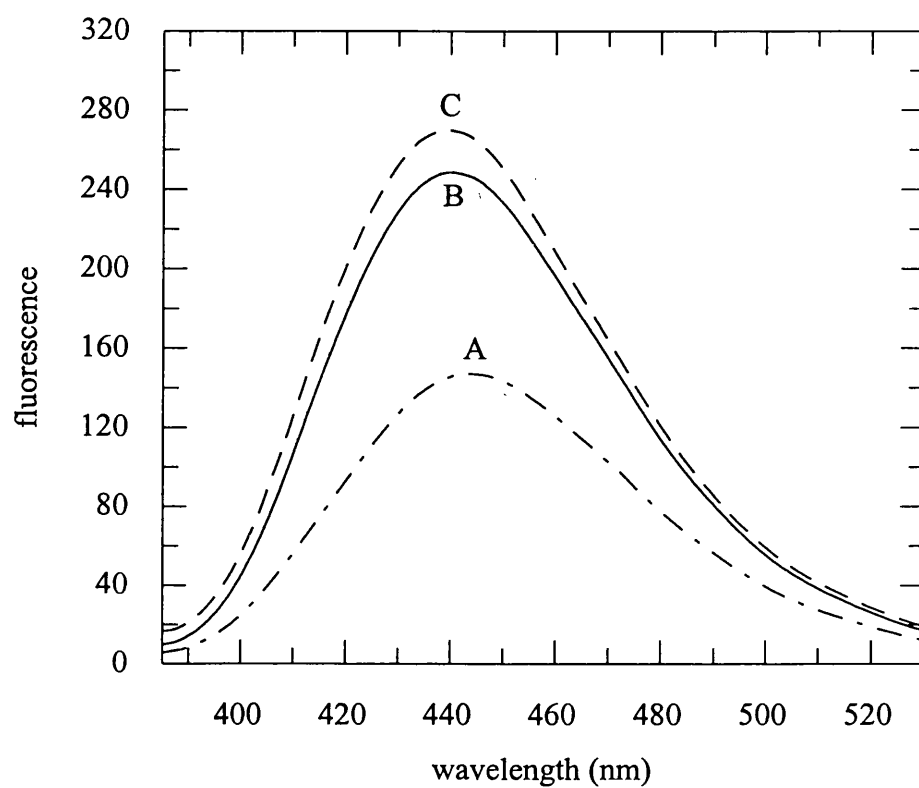
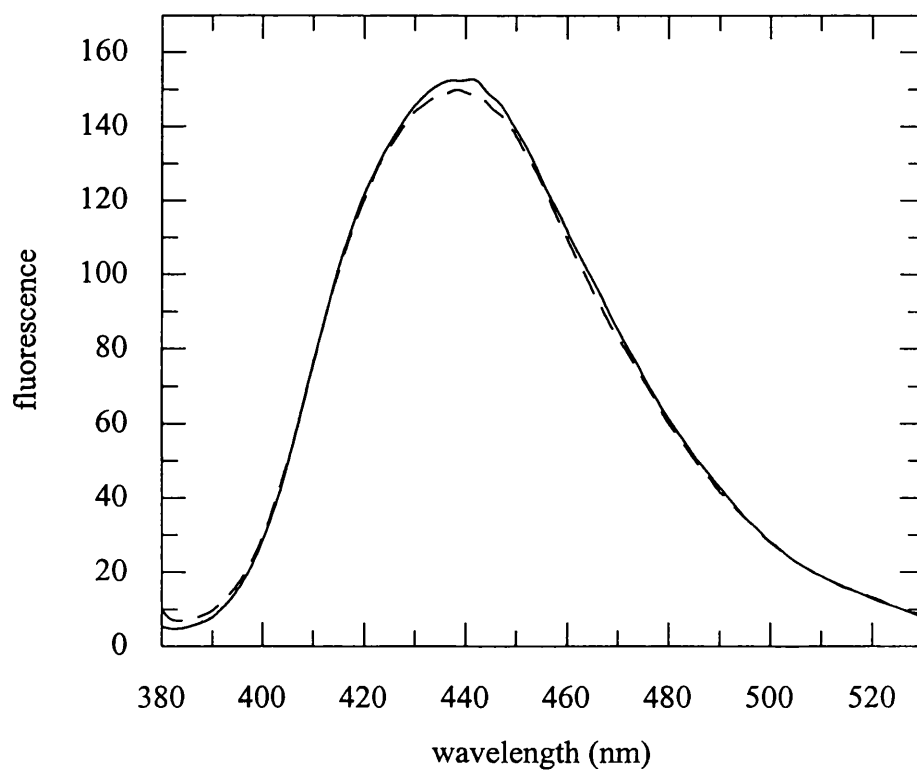


Figure 5.5.



(2.6.10.). It was hoped that this would improve experimental design by minimizing the concentration of Rac1·GDP in the solution. Excess baculovirus p67^{phox}, p67¹⁻¹⁹⁹ or p67¹⁷⁰⁻¹⁹⁹ had no significant effect on the fluorescence of a purified Rac1·mantGMPPNP complex (figure 5.5.).

5.4.1.. Effect of arachidonate on the Rac1·mantGMPPNP · p67^{phox} interaction

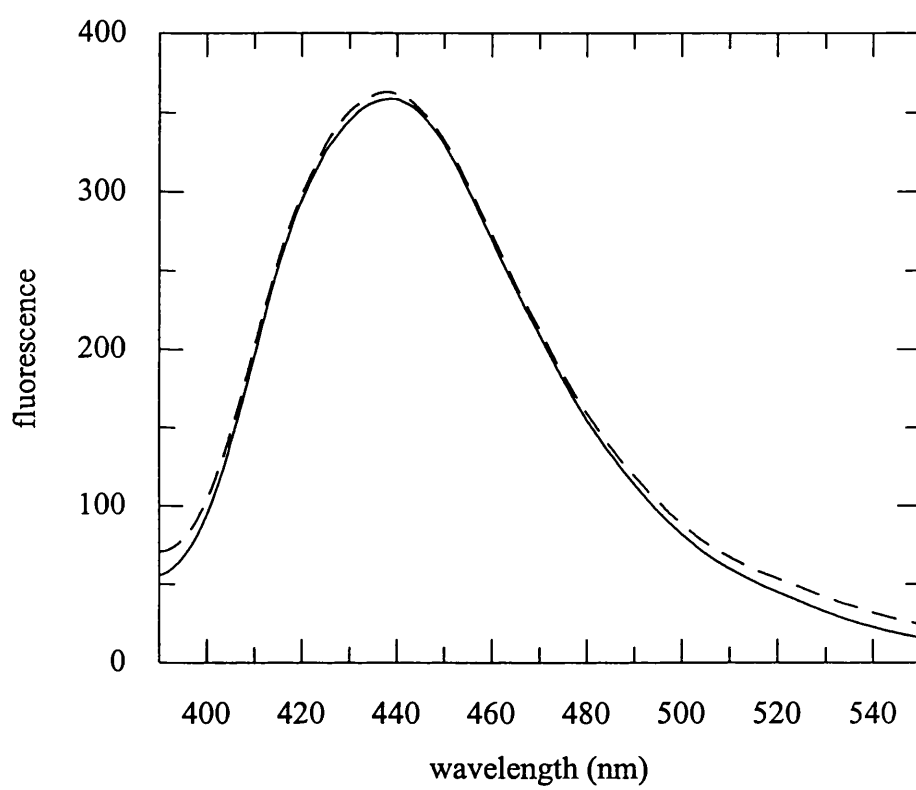
A recent report has suggested that intramolecular SH3 – polyproline interactions may occur with p67^{phox}, as C-terminally truncated p67^{phox} mutants bind with a higher affinity to Rac1 than the full length protein (Ahmed *et al.*, 1998). Research has also shown that arachidonate causes a conformational change of p47^{phox} (Swain *et al.*, 1997), and arachidonate or SDS required for activation of a cell free NADPH oxidase system (Abo *et al.*, 1992). It is possible that arachidonate also causes a conformational change in p67^{phox} favorable for Rac binding. An inactive conformation of the protein may be induced by post-translational modification of p67^{phox} by *sf9* insect cells during the purification procedure. To examine the possibility that recombinant p67^{phox} exists in an inactive conformation when expressed using a baculovirus expression system in this laboratory, experiments were repeated as above in the presence of excess arachidonate. To minimize oxidation of the un-saturated fatty acid, fresh arachidonate (Sigma) was re-suspended in high purity methanol that had been bubbled through with argon, then stored under argon in a sealed vial. After use the arachidonate was stored at -80°C. The addition of 3µM p67^{phox} had no effect on 0.5µM Rac1·mantGMPPNP fluorescence in the presence of 100µM arachidonate (figure 5.6.).

5.5. Interaction of p67^{phox} with Rac1·but-edaGMPPNP

The coumarin derivatised, non-hydrolysable GTP analogue, but-edaGMPPNP has recently been synthesized in this laboratory (M.R. Webb, unpublished results). It was hoped that due to the exposed nature of the fluorophore (3.4.), a Rac1·but-edaGMPPNP complex

Figure 5.6. Effect of arachidonate on the interaction of Rac1 with p67^{phox}

Rac1·mantGMPPNP (0.5μM) was incubated in 20mM Tris·HCl pH7.6, 1mM MgCl₂, 1mM DTT, 100μM arachidonate at 20.1°C and emission scans were recorded before (dotted line) and after the addition of p67^{phox} (3μM) (solid line). p67^{phox} had no significant effect on Rac1·mantGMPPNP fluorescence in the presence of 100μM arachidonate under these conditions. The addition of 50mM KCl (present in similar experiments undertaken by Nisimoto *et al.*, 1997 – see figure 5.5.) to the reaction mixture following the addition of p67^{phox} did not affect Rac1·mantGMPPNP fluorescence. The concentration of methanol in the reaction mix was <1%.



could be used to monitor the interaction with p67^{phox}. Multiple mixing of a solution containing 0.1 μ M of the fluorescent nucleotide analogue, but-edaGMPPNP in 20mM Tris-HCl pH7.6, 1mM MgCl₂, 1mM DTT, 10 μ M BSA resulted in a ~35% decrease in fluorescence. This decrease in fluorescence is probably due to adsorption of the fluorophore to pipette tips following mixing of the solution (data not shown). In an attempt to minimize this effect, multiple mixings of a solution with increasing concentrations of BSA were undertaken and the fluorescence measured. It was hoped that BSA would 'block' sites on pipette tips and reduce this effect. The greatest improvement was obtained when 20 μ M BSA was added to the buffer solution, although a ~15% decrease in fluorescence was still observed following 12 successive mixings. 20 μ M BSA was added to all buffer solutions for subsequent titrations using Rac1 complexed to but-edaGMPPNP. Titration of p67^{phox} into a solution containing 0.1 μ M Rac1-but-edaGMPPNP in 20mM Tris-HCl pH7.6, 1mM MgCl₂, 1mM DTT, 20 μ M BSA resulted in no significant change in but-edaGMPPNP fluorescence (following correction for the addition of small aliquots of p67^{phox} and the effect of mixing) (data not shown.). It is possible that p67^{phox} does not interact with Rac1-but-edaGMPPNP under these conditions, or that but-edaGMPPNP is not sensitive to p67^{phox} binding.

5.6. Using labelled p67¹⁻¹⁹⁹ to measure the interaction with Rac1

To try and devise a method to monitor the direct interaction of p67¹⁻¹⁹⁹ with Rac1, p67¹⁻¹⁹⁹ has been labelled with a number of thiol reactive probes. Although the fragment contains four cysteines, reaction of p67¹⁻¹⁹⁹ with 5,5'-dithiobis-(2-nitrobenzoic acid) (DTNB) has been used to estimate the number of reactive cysteines on the native **peptide**. Thiol ^{polypeptide} disulphide exchange provides the most convenient method of assaying thiol groups, as the liberated aromatic thiol (NTB) is brightly coloured, with an Abs_{max} of 412nm. This is the basis of the reaction with DTNB, also known as the Ellman assay. The addition of excess DTNB results in the formation of stoichiometric amounts of NTB. The concentration of

NTB was calculated using a molar extinction coefficient of $13600 \text{ M}^{-1} \text{ cm}^{-1}$ at 412nm, pH7-8 (Dawson *et al.*, 1984). $11 \mu\text{M}$ NTB was produced following incubation of excess DTNB with $5 \mu\text{M}$ p67¹⁻¹⁹⁹. These results indicate that p67¹⁻¹⁹⁹ contains two reactive thiols accessible to DTNB (figure 5.7.). The other two cysteines may participate in the formation of a disulphide bond, or be buried within the tertiary structure of the protein.

The p67¹⁻¹⁹⁹ protein has been labelled with a number of environmentally sensitive fluorophores including *N*-[2- (1-maleimidyl)ethyl] -7- (diethylamino) coumarin -3-carboxamide (MDCC), IDCC and MPLCC. These labelled proteins all show similar labelling stoichiometries (figure 5.8.) with ~10% increase in fluorescence upon incubation with Rac1·GTP (Q61L) (figure 5.9.). However, this fluorescence change was variable, possibly due to the instability of p67¹⁻¹⁹⁹. A small fluorescence change may be observed because there is little or no Rac1 binding under these conditions, or because the position of the fluorophore(s) may not be sensitive to Rac1 binding. It is also possible that a small amount of denatured or conformationally inactive protein with exposed thiol groups is modified with the fluorescent probe, with little or no labelling of the conformationally active protein.

5.7. Effect of p67¹⁻¹⁹⁹ on hydrolysis of GTP by Rac1

As another attempt to examine the interaction of Rac1 with p67¹⁻¹⁹⁹, the effect of p67¹⁻¹⁹⁹ on the rate of GTP hydrolysis under single turnover conditions has been examined. It was hoped that p67¹⁻¹⁹⁹ would have an effect on GTP hydrolysis and provide a direct measure of this interaction. By forming a complex of Rac1 with GTP (2.6.9.), the rate of GTP hydrolysis has been monitored using MDCC-PBP as described previously (3.3.). When $2 \mu\text{M}$ Rac1·GTP is incubated with $10 \mu\text{M}$ MDCC-PBP in 20mM Tris·HCl pH7.6, 1mM MgCl_2 at 20.1°C , GTP is hydrolysed by Rac1 with an observed first order rate constant of $1.3 \times 10^{-3} \text{ s}^{-1}$. The addition of p67¹⁻¹⁹⁹ had little effect on the on the rate of GTP hydrolysis

Figure 5.7. Reaction of p67¹⁻¹⁹⁹ with 5,5'-dithiobis-(2-nitrobenzoic acid) (DTNB)

p67¹⁻¹⁹⁹ (5 μ M) was added to DTNB (100 μ M) in 20mM Tris·HCl pH 8.0, 200mM NaCl, 15°C and the absorbance at 412nm measure over time. DTNB may be used to estimate the number of reactive thiols of a protein as it reacts with thiol groups to produce stoichiometric amounts of NTB. As 1 μ M of NTB has an absorbance at 412nm of 0.0136 (extinction co-efficient for NTB = 13600 M⁻¹cm⁻¹, 412nm), [NTB] = 0.152/0.0136 = 11 μ M. DTNB (100 μ M) showed no change in absorbance at 412nm in the absence of p67¹⁻¹⁹⁹ under the same conditions. The line shown represents a join of the data points. Consistent results were obtained with two independent reactions. Circles represent time points taken every 15 seconds using a Beckman DU640 spectrophotometer.

Figure 5.8. Absorbance spectra of MDCC-p67¹⁻¹⁹⁹

Absorbance spectra of 12 μ M MDCC-p67¹⁻¹⁹⁹. The relative A_{430}/A_{280} may be used to assess labelling of the protein (taking into account absorbance at 280nm by the fluorophore). $(0.299 / 46800\text{M}^{-1}\text{cm}^{-1}) = 6.3\mu\text{M} / ((0.365 / 30110\text{M}^{-1}\text{cm}^{-1}) - 0.165 \times 0.365)$ = 12.0 μ M. This indicates that labelling is likely to have a stoichiometry of less than one molecule of MDCC to one molecule of p67¹⁻¹⁹⁹. Similar labelling stoichiometries were obtained when p67¹⁻¹⁹⁹ was labelled with other thiol reactive fluorophores (data not shown). Without further characterisation of the labelled protein, the possibility cannot be ruled out that a proportion of the p67¹⁻¹⁹⁹ is labelled with two molecules of MDCC, with a proportion of protein modified with a single molecule of MDCC or unlabelled under these conditions. It is also possible that due to the instability of this fragment, a small percentage of protein is denatured with exposed thiol groups, with the majority of protein in a folded, ordered conformation. If this were the case, the possibility exists that none of the active protein is labelled with MDCC due to steric constraints imposed by secondary and tertiary structures of p67¹⁻¹⁹⁹.

Figure 5.7.

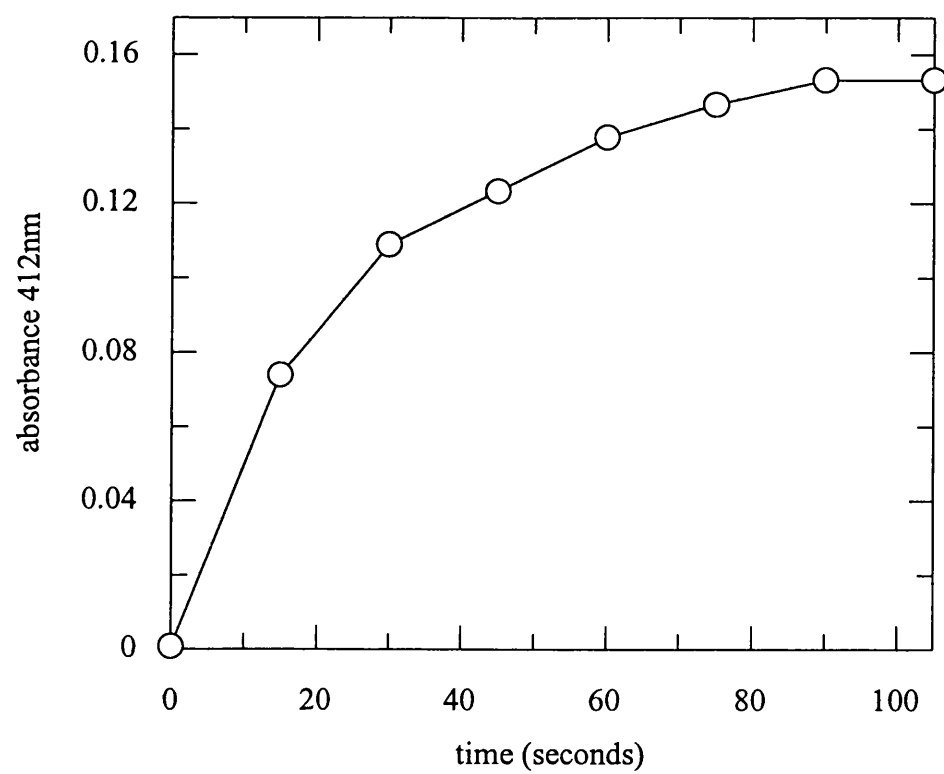


Figure 5.8.

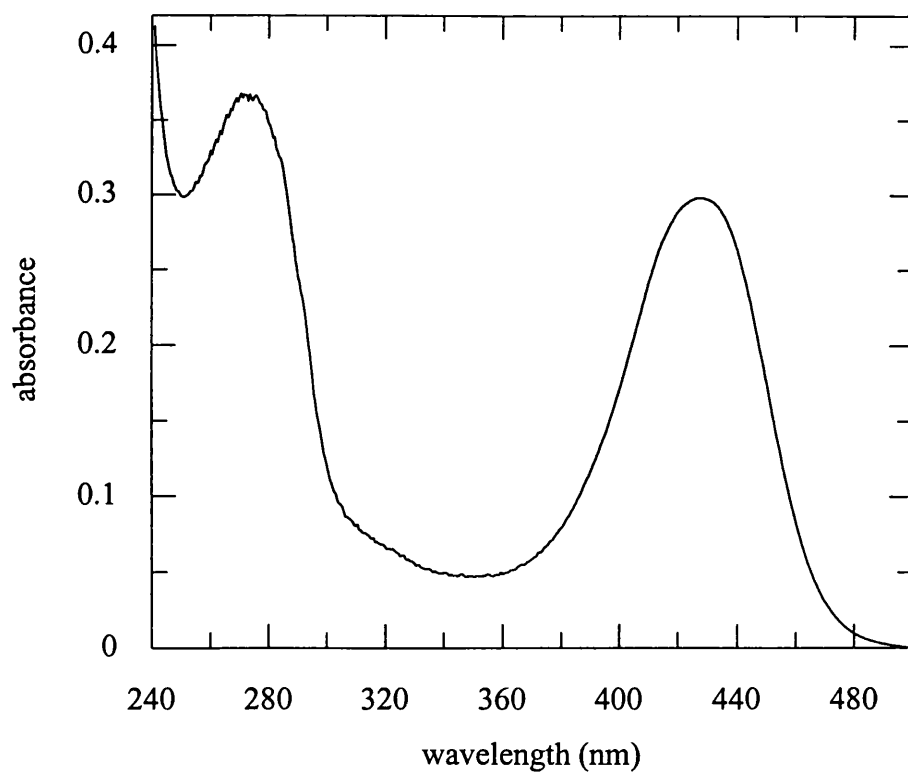
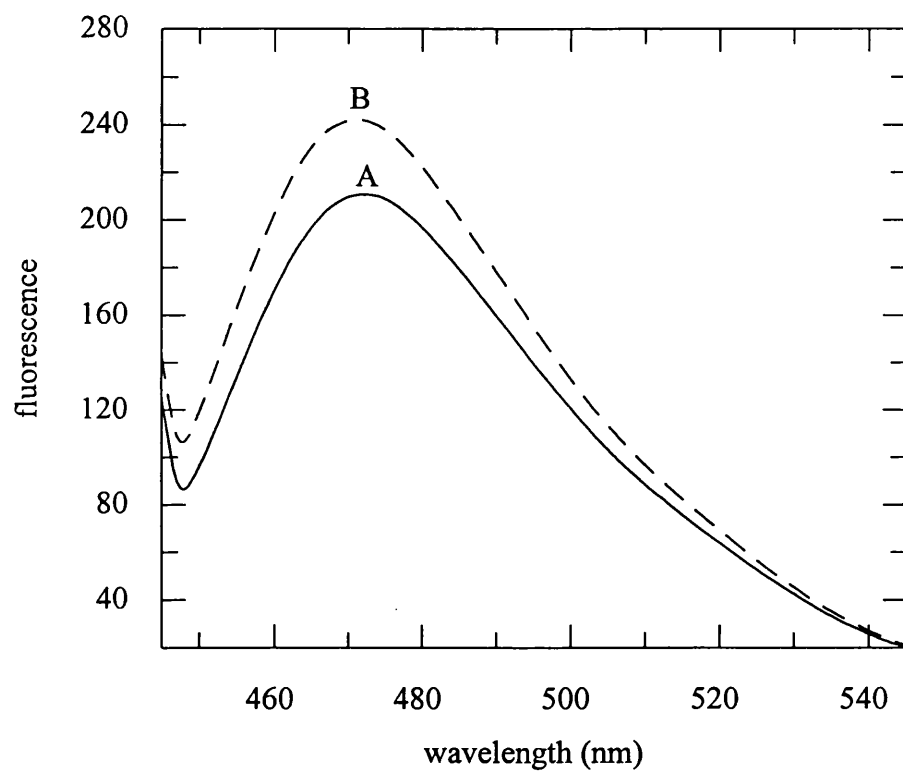


Figure 5.9. Interaction of Rac1·GTP (Q61L) with MDCC-p67¹⁻¹⁹⁹

Emission spectra of MDCC-p67¹⁻¹⁹⁹ (0.5 μ M) before (A) and after the addition of 5 μ M Q61L Rac1 (B) in 20mM Tris·HCl pH7.6, 1mM MgCl₂, 9mM NaCl, 1mM DTT, 20°C. A 10% increase (average of two independent scans) in MDCC-p67¹⁻¹⁹⁹ fluorescence was observed. Excitation 430nm.



by Rac1 under these conditions, with an observed first order rate constant of $0.8 \times 10^{-3} \text{ s}^{-1}$ (figure 5.10.).

5.8. Summary of results

p67^{phox}, the component of the NADPH oxidase that interacts with Rac1 has been successfully purified from baculovirus infected insect cells. Although a previous report indicates a fluorescence change when p67^{phox} binds to Rac1 complexed with mantGMPPNP, these results could not be repeated. Purification of p67^{phox} from insect cells indicates that this protein is susceptible to minor proteolytic degradation. Although fractions containing the larger of the two major species purified (2.3.4.) were used for subsequent biochemical studies, it is possible that this protein is truncated at the N terminus, causing disruption of TPR motifs. It is also possible that extended incubation of *Sf9* insect cells to express p67^{phox} in this laboratory causes this protein to adopt a conformationally in active state; this conformational change may be induced by post-translational modification of the protein by the insect cells.

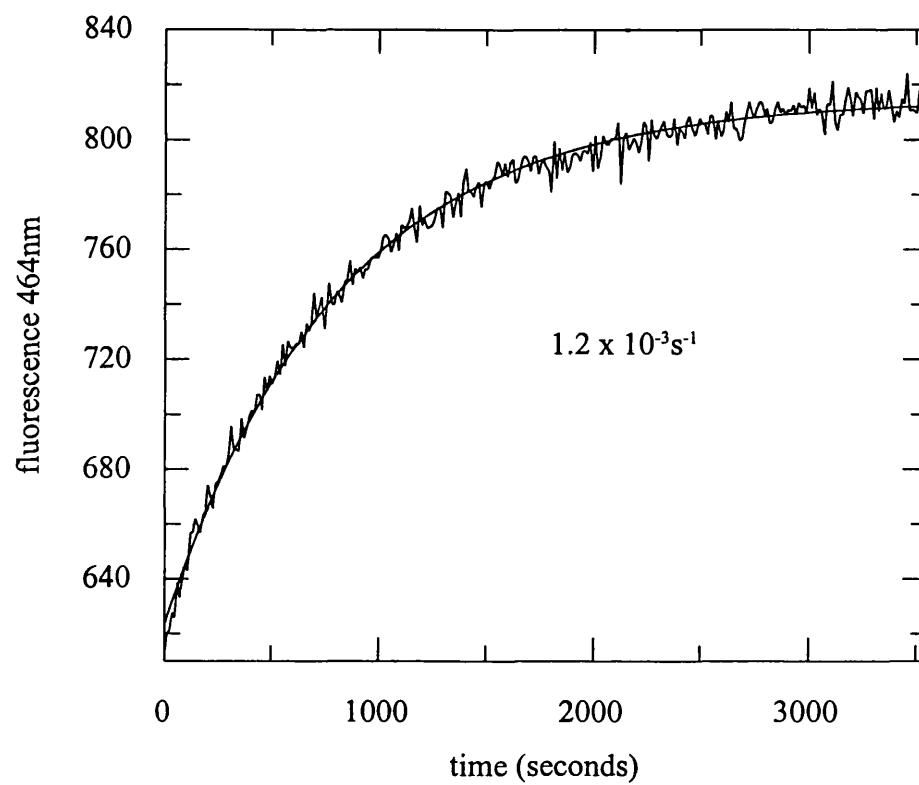
In addition, the interaction of p67^{phox} with Rac1 complexed to but-edaGMPPNP has also been examined. It was hoped that due to the exposed nature of the fluorophore and the high fluorescence quantum yield (3.4.1.) this fluorescent analogue would provide a sensitive method to monitor this interaction. This coumarin derivatised nucleotide analogue non-specifically adsorbs to pipette tips. To minimize this effect, 20 μM BSA was added to all solutions when using this nucleotide analogue. p67^{phox} or p67^{I-199} had little effect on the fluorescence of a Rac1·but-edaGMPPNP complex (data not shown).

Despite showing stability problems, p67^{I-199} has been successfully purified and labelled with a number of environmentally sensitive fluorophores. However, none of these labelled proteins show a significant fluorescence change when incubated with Rac1·GTP. It is possible that the position of the fluorophore is not sensitive to Rac1 binding, or that a

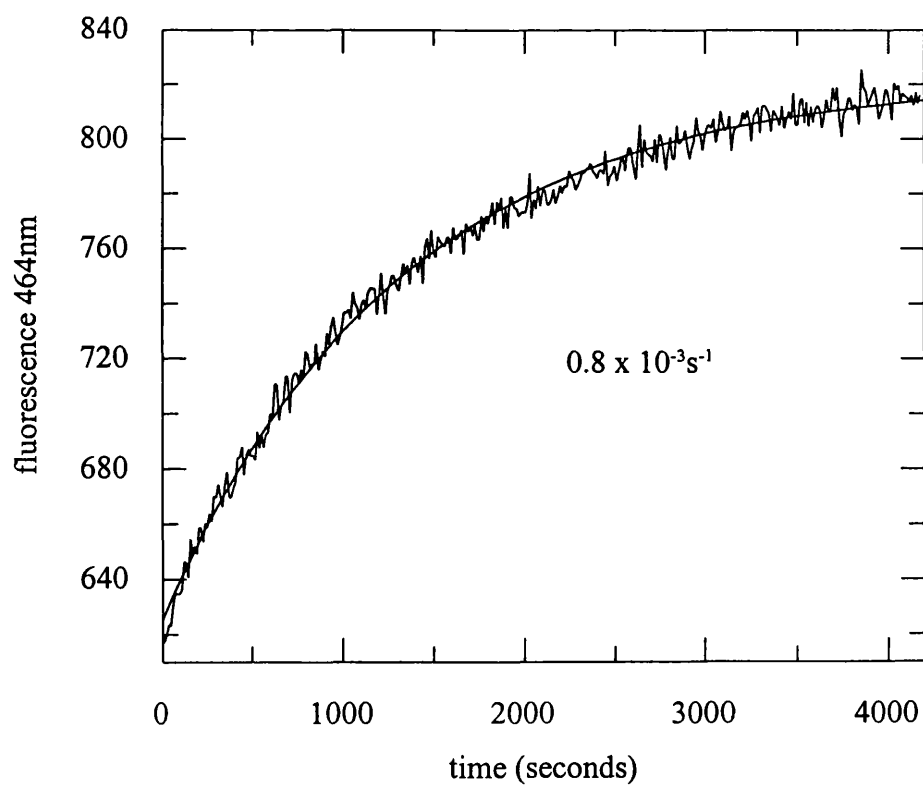
Figure 5.10. Effect of p67¹⁻¹⁹⁹ on the rate of GTP hydrolysis by Rac1

Time course for the hydrolysis of GTP by Rac1. MDCC-PBP (10 μ M) was incubated with 2 μ M Rac1·GTP in 20mM Tris·HCl pH7.6, 1mM MgCl₂, 20.1°C in the absence (A) or presence (B) of 2 μ M p67¹⁻¹⁹⁹. The fluorescence emission was measured over time and lines show best fits to single exponentials. Rate constants of 1.2x10⁻³s⁻¹ and 0.8x10⁻³s⁻¹ were obtained for Rac1 in the absence and presence of p67¹⁻¹⁹⁹ respectively. Similar hydrolysis rates were obtained when 2 μ M Rac·GTP was incubated with 5 μ M or 15 μ M p67¹⁻¹⁹⁹ (data not shown). Excitation 425nm.

A



B



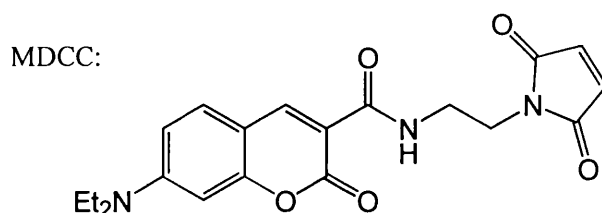
significant proportion of the active protein is not labelled under these conditions. Experiments have shown that a p67^{phox} construct lacking the first N terminal 58 residues destabilises the Rac1 binding region, perhaps by disrupting TPRs or similar tertiary structure motif. It is likely that a conformationally active N terminal domain is essential for the interaction of Rac1 with p67^{phox}, with the stability of the fragment dependent on the remainder of the protein. In addition, the effect of the additional N and C terminal residues of the p67¹⁻¹⁹⁹ expressed in this laboratory (figure 5.1.) on the tertiary structure of this domain has yet to be established. A recent report has indicated that the three tandemly arranged TPR motifs at the N terminus of p67^{phox} are essential for the interaction with Rac1; this may explain the lack of detectable binding between Rac1 and the p67¹⁷⁰⁻¹⁹⁹, reported to contain the Rac1 binding region (Koga *et al.*, 1999).

6. THE INTERACTION OF RAC1 WITH GDI

6.1. Introduction

RhoGDI (GDI) forms stable complexes with Rho family proteins, but does not interact with any other members of the Ras superfamily (1.14.). Post-translational isoprenylation of Rho proteins is essential for tight interaction with GDI, and GDI inhibits GDP dissociation from post-translationally modified Rac1, but has no effect on *E.coli* expressed Rac1 (Sasaki *et al.*, 1993). In the cell, this modification is geranylgeranylation.

In this laboratory, correctly post-translationally modified Rac1 is produced in insect cells using a baculovirus expression system. Rac1 expressed in *E.coli* is not modified. Unless otherwise stated, *E.coli* Rac1 refers to *E.coli* expressed Rac1 truncated at the C-terminus (aa's 1-184). R.W. Stockley has previously labelled GDI at Cysteine 79 with the fluorescent probe N- 2-[1-(maleimidyl) ethyl]-7-(diethylamino) coumarin-3-carboxamide (MDCC) in this laboratory (1.14.1.).



Equal proportions of diastereoisomers are thought to form when a thiol reacts randomly with either of the two olefinic carbons of the maleimide. Results from this laboratory (R.W. Stockley & M.R.Webb) indicate that the two diastereoisomers of MDCC-GDI have different fluorescent properties and binding affinities for Rac1. For most measurements using this system, the signal from the tighter binding diastereoisomer dominates, and the weaker binding isomer can be disregarded (for a full discussion see Newcombe *et al.*, 1999, Brune *et al.*, 1994). The labelled protein provides a direct signal

to monitor the Rac1·GDI interaction and shows ~70% decrease in fluorescence emission upon binding modified (geranylgeranylated) Rac1. The labelled protein has been well characterised, and shows an affinity for baculovirus Rac1 within a factor of 2 for unlabelled GDI.

Detailed mechanistic studies with modified (baculovirus expressed) Rac1 presents a number of experimental difficulties when the protein is purified from tissue or baculovirus-infected insect cells, due to the presence of the isoprenyl group. These include the need for detergents, and difficulties in physical processes such as concentrating. In addition, relatively low yields of unstable protein are often obtained, and the system is not easily manipulated, such as the nucleotide bound to Rac1. These problems also make it difficult and time consuming to produce and study Rac mutants.

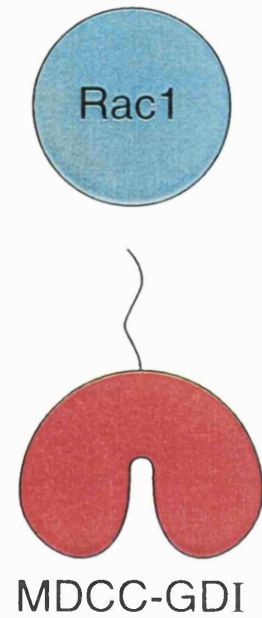
To try and overcome such problems, a novel approach has been developed in this laboratory using synthetic peptides corresponding to the C-terminal region of Rac1. These peptides have been chemically modified by attachment of a farnesyl group to the single cysteine corresponding to Cys 188 of Rac (1.13.1.). It was hoped that a combination of C-terminally truncated, *E.coli* expressed Rac1 and a farnesyl-modified peptide (corresponding to the missing C-terminus of Rac1) would mimic baculovirus Rac and interact with GDI (figure 6.1.). Although this residue of Rac1 is geranylgeranylated in vivo, a farnesyl group was chosen to chemically modify C-terminal peptides because of the availability of farnesyl bromide, and the likelihood that the hydrophobic interaction of GDI with the lipid would not be very specific. This method has been used to study the mechanism of interaction of Rac with GDI, including the use of Rac1 point mutants to investigate the role of different regions of Rac1 in GDI interaction. Because the binding of the modified peptide and the 'rest' of Rac are separated, this method is likely to be very sensitive to conformational changes induced by different nucleotides and mutants. GDI maintains Rac1 in an inactive (GDP bound) state. The mechanisms that trigger the

Figure 6.1. Proposed mechanism for the interaction of unmodified Rac1 and a farnesylated peptide with MDCC-GDI

GDI has previously been labelled with a fluorescent coumarin (MDCC) at position 79. This labelled protein shows a 70% decrease in fluorescence emission on binding geranylgeranylated (baculovirus expressed) Rac1 and has an affinity for Rac1 within a factor of 2 of unlabelled GDI (R.W. Stockley & M.R. Webb, see Newcombe *et al.*, 1999).

A combination of truncated Rac1 (shown in blue) and a farnesyl modified peptide (corresponding to the missing C-terminus of modified Rac1) 'mimics' geranylgeranylated Rac1 and interacts with GDI (shown in red). This system has been used to study the mechanism of interaction of Rac1 with MDCC-GDI and investigate the role of different regions of Rac1 in GDI interaction.

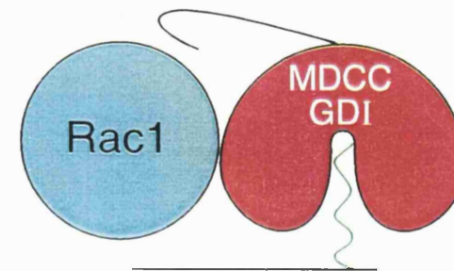
E. coli (un-modified) rac1



Farnesyl-modified peptide



Rac1 induced
quenching of
MDCC fluorescence



Complex formation

dissociation of Rac1 and GDI are poorly understood, despite the potential importance of this dissociation. This system provides a useful method to probe for factors that accelerate dissociation of Rac from GDI; the elucidation of this mechanism is a long term goal of this laboratory.

6.2. Farnesylated peptides

Quantitative farnesylation of 3 peptides has been achieved (figure 6.2.). A Rac1 C-terminal 7-mer, KRKCLLL (residues 186-192) which corresponds to the missing C-terminus of *E.coli* Rac that has been truncated at K184 (with one residue omitted to ensure no overlap with the protein), and a C-terminal 12-mer, PVKKRKRKCLLL (residues 181-192) which extends across the stretch of basic amino acids, but overlaps Rac by 4 residues. PVKKRKRKC, the C-terminus of native, modified Rac following proteolytic cleavage of the 3 terminal leucines (1.13.1.), failed to react with farnesyl bromide under a range of conditions. Quantitative farnesylation of this peptide has only recently been achieved following chemical methylation of the peptide (2.5.2.). Due to this, binding data with Rac1 and Rac1 mutants have typically been determined with the farnesyl 12-mer. Results with the modified 9-mer peptide will be described in later sections (6.15.).

6.3. Effect of Rac1 and farnesyl-12mer on MDCC-GDI fluorescence

An initial approach to study the interaction of Rac1 with GDI was to examine the effect of Rac1 on the labelled GDI. It was hoped that in the presence of farnesyl 12-mer, *E.coli* Rac1 would bind to GDI and similarly quench the MDCC-GDI fluorescence, providing a sensitive assay to monitor this interaction. Rac1 and farnesyl 12-mer were added to a solution containing MDCC-GDI, and the fluorescence emission measured. Figure 6.3. shows that there is ~30% quenching of MDCC-GDI fluorescence upon addition of farnesyl 12-mer and Rac1, suggesting that a complex forms. This is 50% of the signal change observed when baculovirus Rac1 interacts with MDCC-GDI (Newcombe *et al.*,

Figure 6.2. C-terminal regions of Rac1 proteins and Rac1 peptide sequences

C-terminal sequences of *E.coli* and baculovirus (baculo) expressed Rac1 proteins and Rac1 C-terminal peptides. Amino acids are designated by the single letter amino acid code. Colour scheme: residues coloured red are proteolytically removed in vivo during the post-translational modification process, residues coloured green are overlapping residues of Rac and peptide sequences, and residues coloured blue show the cysteine that is the site for in vivo isoprenylation.

C-terminus of full length *E. coli* rac1:

...PPPVKKRKRC

C-terminus of full length baculo rac1:

...PPPVKKRKRC

C-terminus of truncated rac1 :

...PPPVKK

“7-mer”:

KRC

“9-mer”:

PPVKKRKRC

“12-mer”:

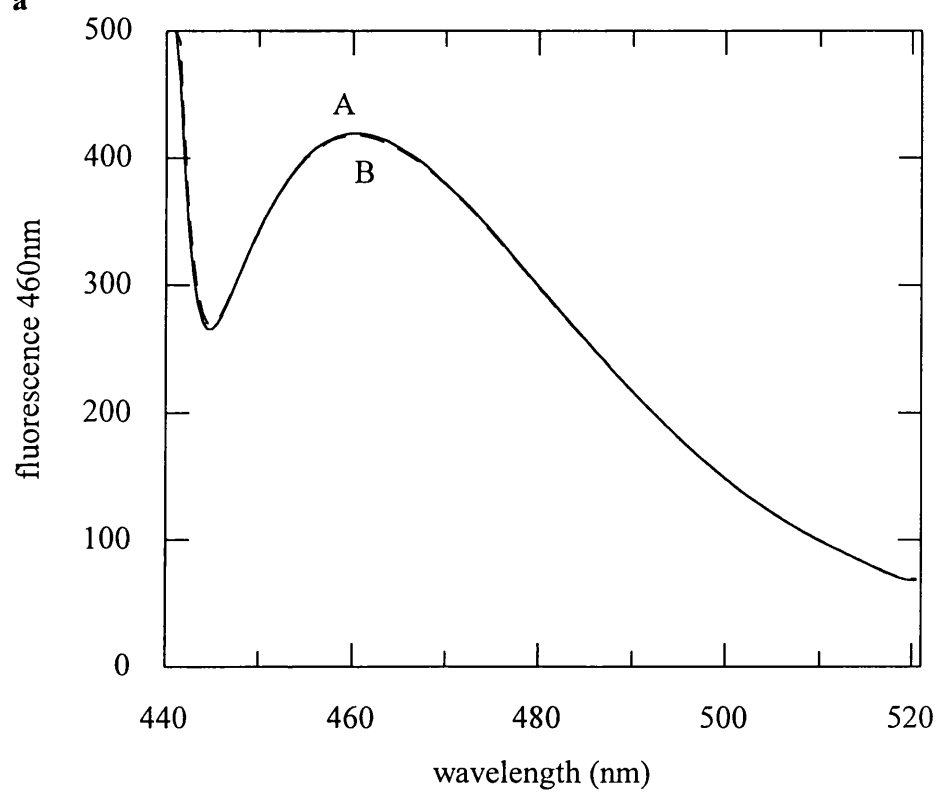
PPVKKRKRC

Figure 6.3. Emission spectra of MDCC-GDI

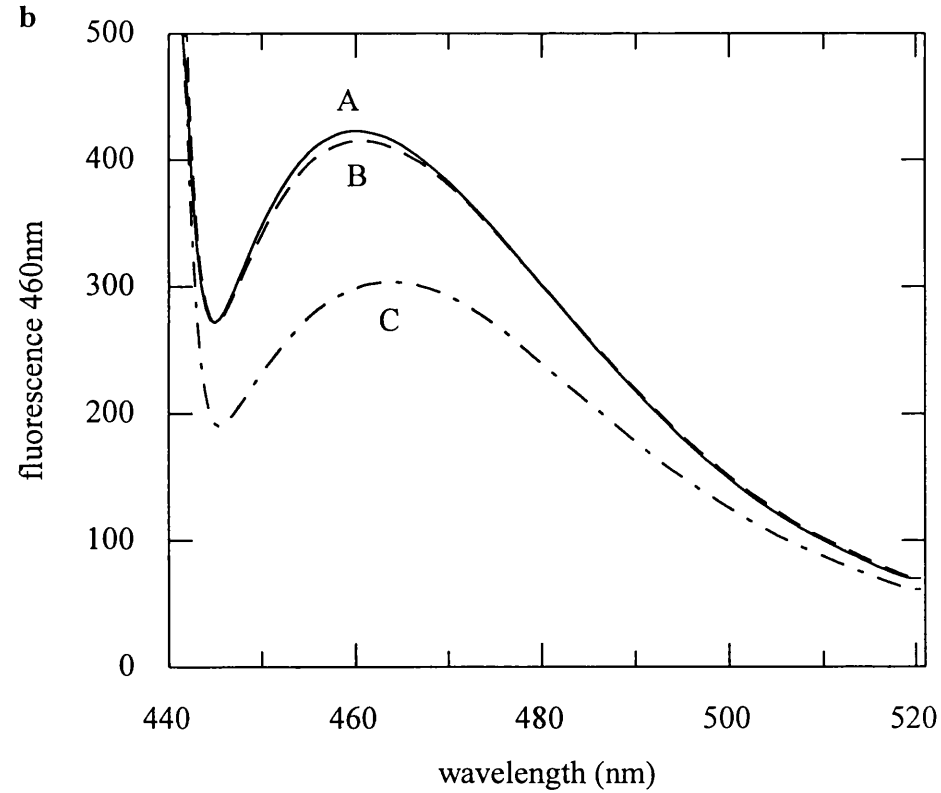
Figure 6.3a. MDCC-GDI (0.1 μ M) was incubated in 20mM Tris-HCl pH7.6, 1mM MgCl₂, 5 μ M BSA, 1mM DTT, 20°C. Emission spectra were measured before (A) and after the addition of 0.5 μ M Rac1. (B)

Figure 6.3b. MDCC-GDI (0.1 μ M) was incubated in buffer under conditions as described above. Emission spectra were measured before (A) and after the addition of 15 μ M farnesyl-12mer (B), or after addition of 15 μ M farnesyl-12mer together with 0.5 μ M Rac1 (C).

a



b



1999). A reduced signal change may be observed in this system because Rac1 binding is not saturating under these conditions, because the Rac1 and the peptide are not covalently attached or due to properties of the farnesyl group and the peptide. These factors will be discussed in later sections. Rac1 or farnesyl 12-mer alone had no effect on MDCC-GDI fluorescence (figure 6.3.) indicating that both components are required for a fluorescence change. It should also be noted that *E.coli* Rac1 might interact with MDCC-GDI in the absence of farnesyl-12mer, with the modified peptide required for an observed signal change.

6.4. Effect of BSA on MDCC-GDI fluorescence

Multiple additions of buffer into a solution containing MDCC-GDI caused a decrease in fluorescence greater than would be expected for the effect of dilution. This fluorescence decrease is probably due to adsorption of the labelled GDI at low concentrations to the cuvette walls or pipette tips. To try and minimise this 'background' effect, titrations of buffer were carried out into solutions containing increasing amounts of BSA. It was hoped that BSA would 'block' sites on the cuvette walls and pipette tips and minimise this effect. The greatest improvement was obtained with a concentration of 5 μ M BSA (figure 6.4.). For subsequent titrations, 5 μ M BSA was added to the cuvette prior to protein additions and mixing.

6.5. Displacement of MDCC-GDI from a Rac1-MDCC-GDI complex

If the Rac1 induced quenching of MDCC-GDI fluorescence reflects a direct interaction between GDI and Rac1, it would be expected that the addition of unlabelled GDI would displace the bound MDCC-GDI and reverse the Rac induced quenching. The dissociation of MDCC-GDI from Rac should be accompanied by a fluorescence change that can be measured. Figure 6.5. shows that the addition of unlabelled GDI to a solution containing MDCC-GDI, farnesyl 12-mer and Rac1 increased the fluorescence change to 100% of

Figure 6.4. Effect of BSA on MDCC-GDI fluorescence

MDCC-GDI (0.3 μ M) was incubated in 20mM Tris·HCl pH 7.6, 1mM MgCl₂, 1mM DTT with varying concentrations of BSA at 30°C (○ = No BSA, □ = 5 μ M BSA, ▲ = 10 μ M BSA, ■ = 20 μ M BSA). Aliquots of buffer were titrated in and the solution mixed. The fluorescence emission of MDCC-GDI was measured following each addition at 460nm (excitation 430nm).

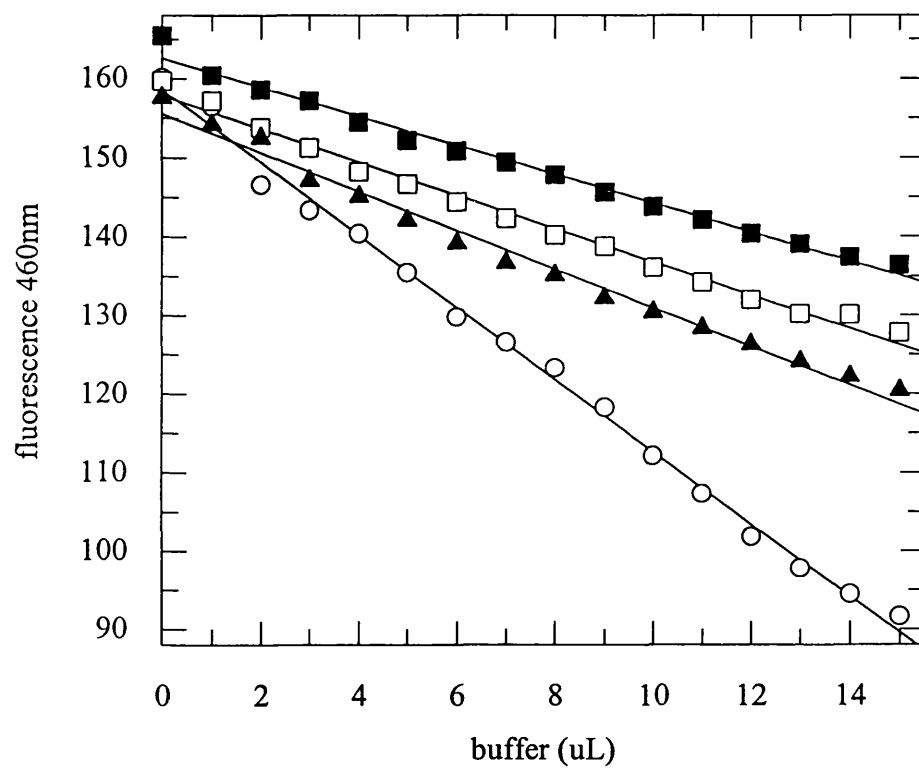
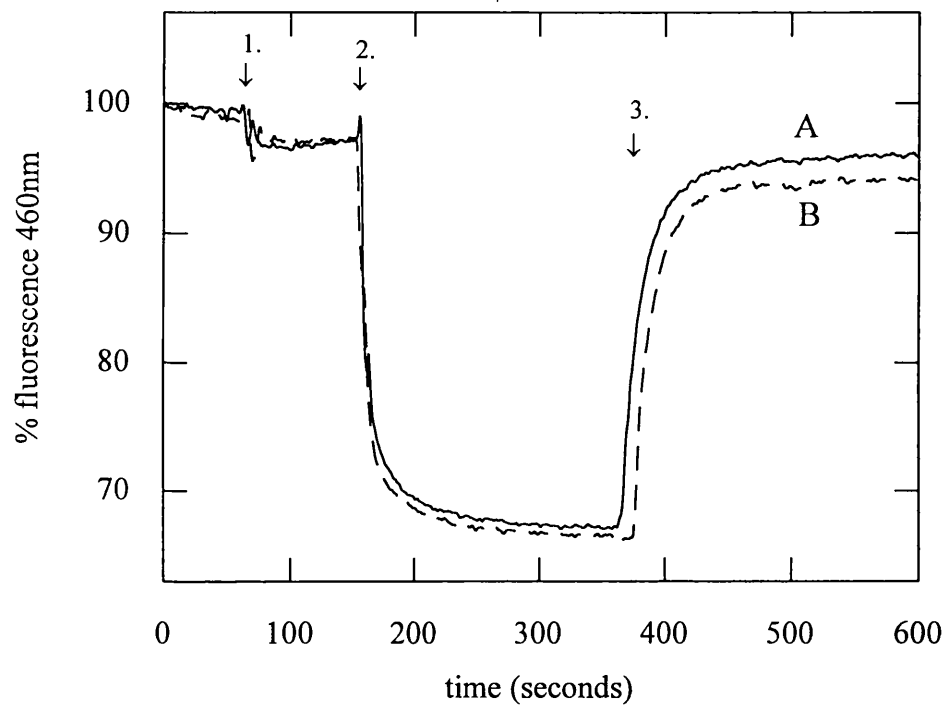


Figure 6.5. Displacement of MDCC-GDI from a Rac1·MDCC-GDI complex

MDCC-GDI (0.1 μ M) was incubated in 20mM Tris·HCl pH 7.6, 1mM MgCl₂, 5 μ M BSA, 1mM DTT, 20°C and the fluorescence measured over time. 15 μ M farnesyl 12-mer was added (1.) followed by 0.5 μ M Rac1 (2.) and quenching of fluorescence was observed. Addition of 2.5 μ M unlabelled GDI (3.) reversed the MDCC-GDI fluorescence to 100% of the free MDCC-GDI (Data shown not corrected for dilution effects). Excitation 430nm. A = experiment using Rac1, B = equivalent experiment using cdc42 (aa's 1-184).



that of free MDCC-GDI, suggesting that the labelled GDI is displaced from the complex by unlabelled GDI. The kinetics of this dissociation have been examined and will be discussed in later sections (see stopped flow results). A similar fluorescence change was observed when *E.coli* expressed cdc42 (aa's 1-184) was used (figure 6.5).

6.6. Effect of NaCl on the Rac1·MDCC-GDI interaction

The salt dependence of the Rac1·MDCC-GDI interaction was examined by adding increasing amounts of NaCl to a solution containing MDCC-GDI, Rac1 and farnesyl 12-mer (figure 6.6.). The increase in MDCC-GDI fluorescence with increasing NaCl concentrations up to 100mM suggests that increasing the ionic strength of the buffer reduces the affinity of the Rac1·MDCC-GDI interaction. This is likely to affect ionic interactions between the two proteins, or between the polybasic region of the peptide and the region close to the lipid binding pocket of GDI. NaCl had no effect on MDCC-GDI fluorescence in the absence of Rac1 or farnesyl 12-mer (data not shown).

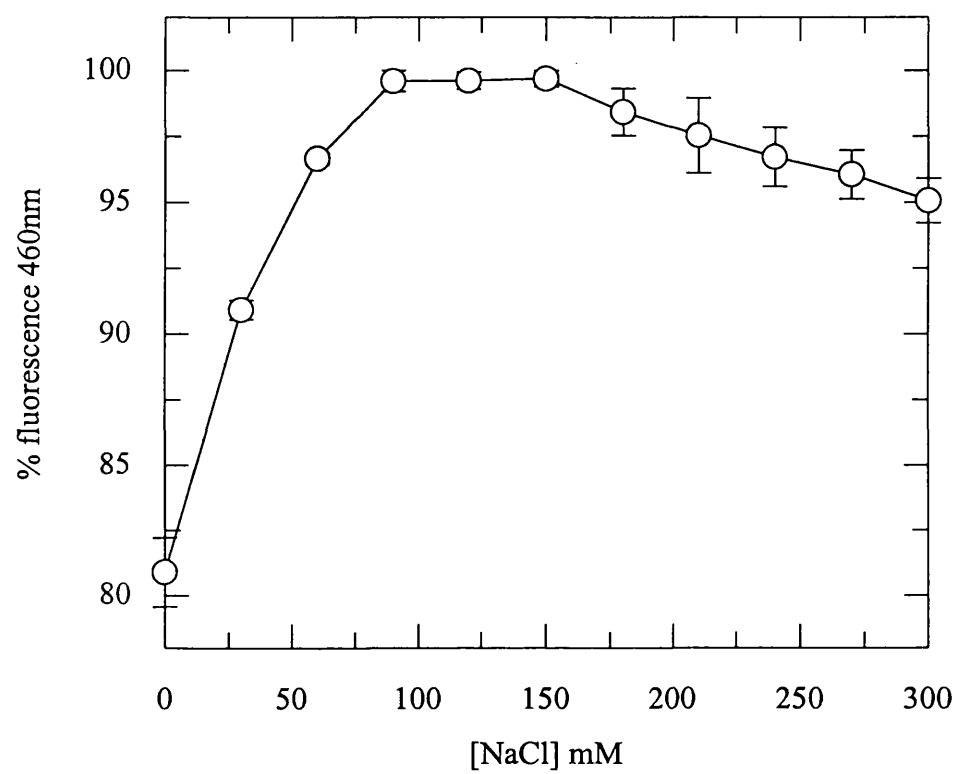
6.7. Affinity of the Rac1·MDCC-GDI interaction

The Rac1 induced quenching of MDCC fluorescence provided a direct method to measure the strength of interaction with GDI. The order of binding of the farnesyl 12-mer to MDCC-GDI has not been established. Kinetic data obtained by premixing two components (Rac1, farnesyl 12-mer or MDCCC-GDI) then rapidly mixing with the third do not distinguish between random and ordered additions, as no lag phase is observed (6.16.1.). Due to this, individual K_d values for Rac1 binding to MDCC-GDI (in the presence of saturating concentrations of farnesyl 12-mer) and farnesyl 12-mer binding to MDCC-GDI (in the presence of saturating concentrations of Rac1) will be considered.

Dissociation constants for the interaction of Rac1 with MDCC-GDI were obtained by titrating Rac into a solution containing MDCC-GDI and excess farnesyl 12-mer and the

Figure 6.6. The effect of NaCl concentration on the Rac1·MDCC-GDI interaction

MDCC-GDI (0.3 μ M) was mixed with Rac1 (2 μ M) and farnesyl 12-mer (10 μ M) in 20mM Tris·HCl pH7.6, 1mM MgCl₂, 5 μ M BSA, 1mM DTT, 20°C and the decrease in fluorescence monitored. Increasing concentrations of NaCl were added, and the fluorescence measured. Data points represent an average of 2 measurements, corrected for the diluting effect of NaCl additions. The solid line is a join of experimental points. Excitation 430nm.



quenching of MDCC-GDI fluorescence measured (figure 6.7a). Subtraction of the fluorescence decrease due to the addition of buffer alone corrected the data for the effects of dilution and mixing (figure 6.7b). The corrected data were fitted to an equilibrium binding equation to calculate the K_d . In the presence of saturating concentrations of farnesyl-12mer, Rac1 bound to MDCC-GDI with a K_d of <50nM, less than two orders of magnitude weaker than the interaction of baculovirus (modified) Rac1 (R.W. Stockley & M.R. Webb – see Newcombe *et al.*, 1999); the value of the latter calculated from association and dissociation rate constants. This suggests that Rac1 has significant interactions with GDI in addition to the C-terminal region and the isoprenyl group.

Titration were carried out at 100nM MDCC-GDI, so this K_d value represents an upper limit. This is because the K_d value is much less than the [MDCC-GDI], and a significant proportion of Rac1 in the early stages of titration will bind to MDCC-GDI. In order to obtain an accurate K_d , the [MDCC-GDI] should ideally be below the K_d , with Rac1 titrations spanning the K_d value for the interaction. Titrations using 30nM MDCC-GDI did not give reproducible data, probably because the [MDCC-GDI] is too low to give a measurable signal.

6.7.1. Affinity of the farnesyl 12-mer-MDCC-GDI interaction

To examine the affinities of farnesylated 7-mer and 12-mer peptides with MDCC-GDI and Rac1, the farnesylated peptide was titrated into a solution containing MDCC-GDI and Rac1 (figure 6.8.) under buffer conditions as described previously (figure 6.7.). Data was fitted to binding curves and gave a K_d of 4 μ M for farnesyl 12-mer and 31 μ M for farnesyl 7-mer. The farnesyl 12-mer showed much tighter binding than the farnesyl 7-mer, despite the 12-mer having 4 overlapping residues with the protein. This suggests that a complete polybasic C-terminal region is likely to be important in the interaction with GDI. The binding curve of farnesyl 12-mer was unaffected by the presence of 15 μ M un-

Figure 6.7. Interaction of Rac1 with farnesyl 12-mer and MDCC-GDI

Figure a. MDCC-GDI (0.1 μ M) was mixed with 15 μ M farnesyl 12-mer in 20mM Tris-HCl pH 7.6, 1mM MgCl₂, 1mM DTT 5 μ M BSA at 20°C. Rac1 (O) or buffer (●) was titrated into this solution and the fluorescence emission measured. Lines show a join of the data points. Figure b. Data (above) were fitted to a binding curve following correction for the diluting effects of buffer and mixing. As neither component (Rac1 or MDCC-GDI) was in large excess under these conditions, the line shows a best fit to a quadratic equation where [Rac1·MDCC-GDI] =

$$EL = \frac{Et + Lt + Kd \pm \sqrt{(Et + Lt + Kd)^2 - 4Et Lt}}{2}$$

and the fluorescence =

$$F = \frac{Et 100 + EL (F_{EL} - 100)}{Et}$$

Where: Et = [total MDCC-GDI]

Lt = [total Rac1]

F_{EL} = fluorescence of EL

Kd = dissociation constant

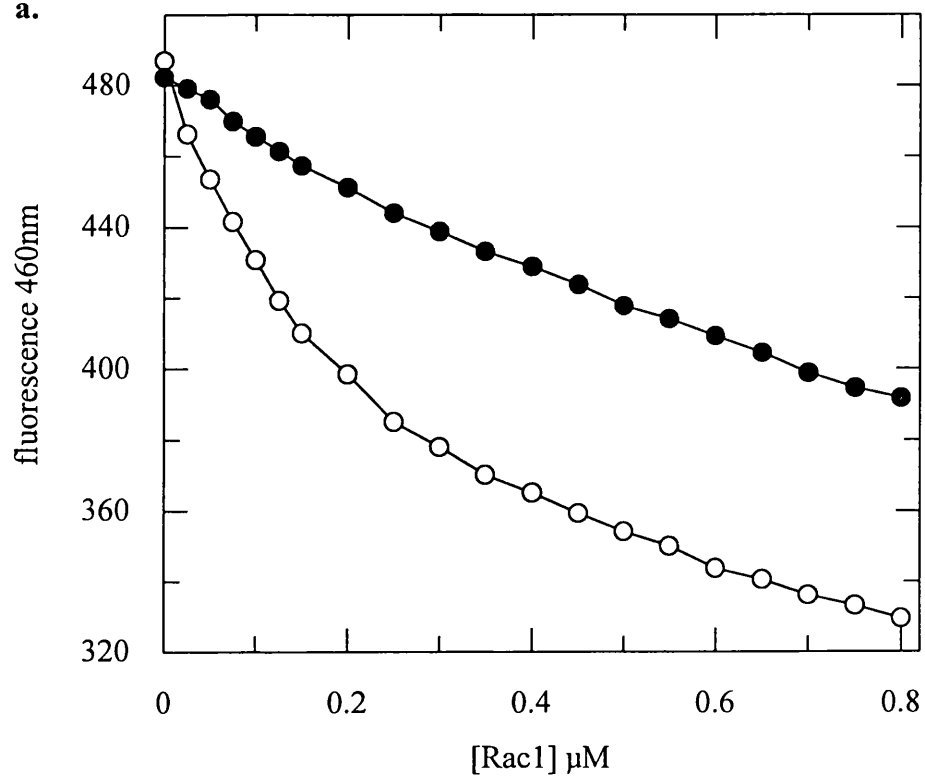
Fluorescence intensities are defined as:

F = 100 when E = Et

F = F_{EL} when E = 0

and gives a Kd of <0.05 μ M (average of 6 titrations). Unless otherwise stated, all titration curves were fitted to the binding equation above.

a.



b.

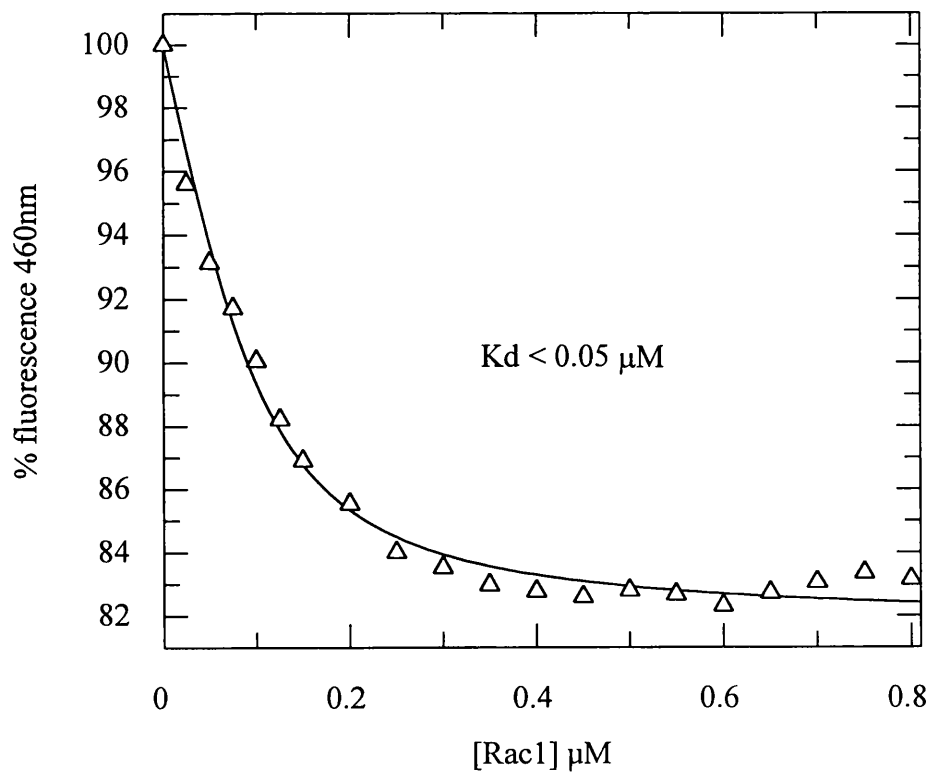
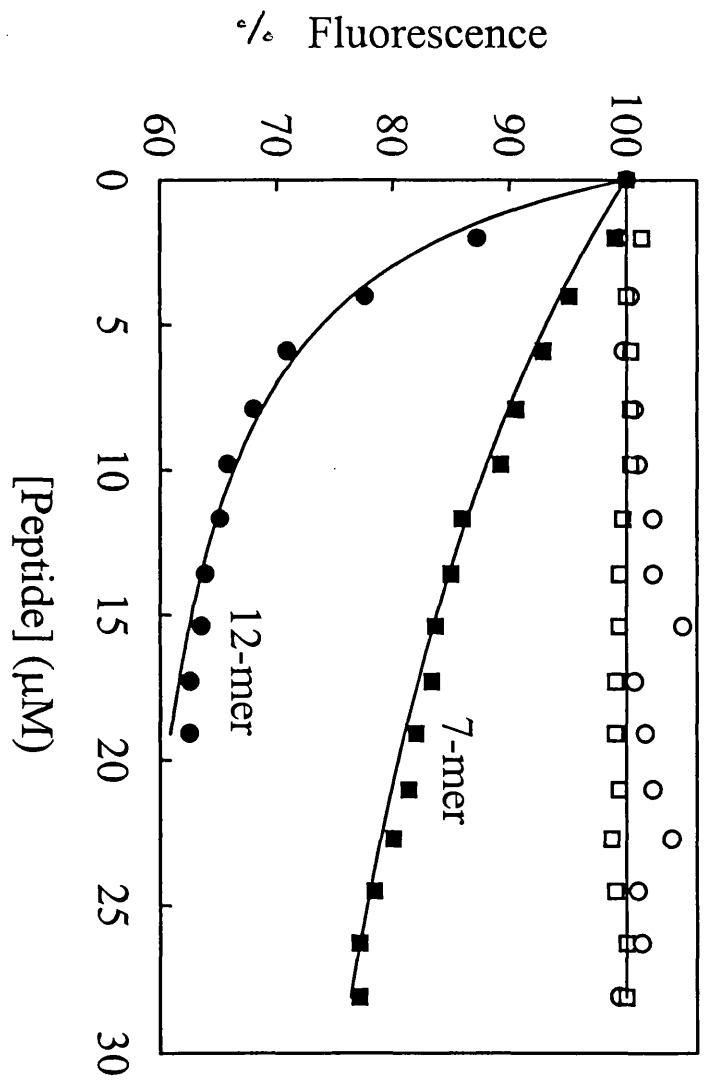


Figure 6.8. Interaction of farnesylated peptides with Rac1 and MDCC–GDI

MDCC–GDI (0.3 μ M) was mixed with 2 μ M Rac1. Peptides were titrated into this solution and the fluorescence emission measured. Data are corrected for the decrease in fluorescence on addition of similar aliquots of buffer. The peptides were farnesyl 12-mer (filled circles), farnesyl 7-mer (filled squares), 12-mer (open circles) and 7-mer (open squares). The lines are the best fit to binding curves and give a K_d of 4 μ M for the farnesyl 12-mer (fluorescence change 47%) and 31 μ M for the farnesyl 7-mer (49%). Excitation 430nm, emission 460nm (from Newcombe *et al.*, 1999).



modified 12-mer in the cuvette (data not shown), suggesting that the unmodified peptide binds weakly in this system.

6.8. Interaction of Rac1·GTP with MDCC-GDI

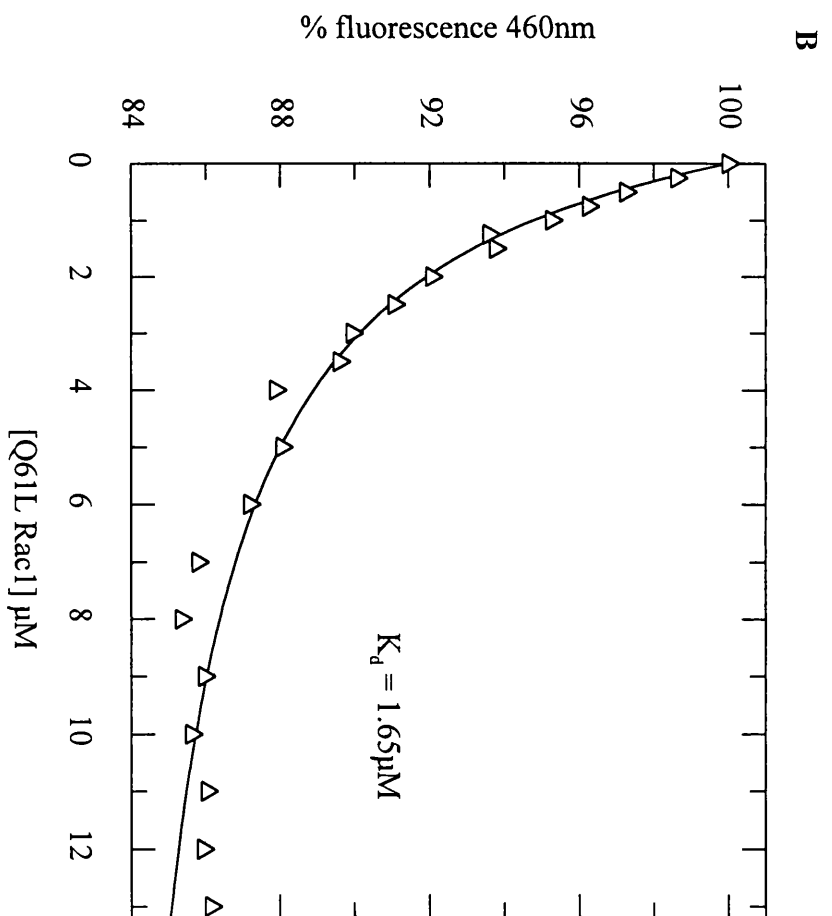
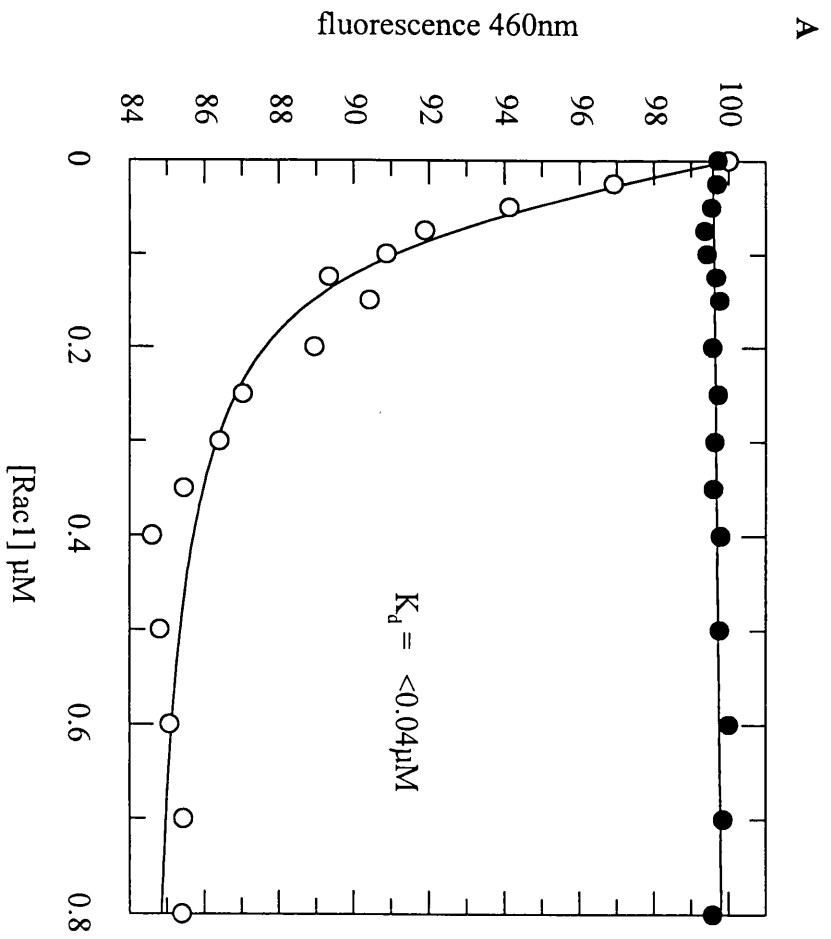
Although the majority of recent reports indicate that the GTP bound form of Rac interacts weakly with GDI (Longenecker *et al.*, 1999), several groups have addressed whether Rho family proteins in the GTP bound forms interact with GDI. These results have led to differing conclusions: the GTP and GDP bound forms interact with a similar affinity (Nomanbhoy & Cerione, 1996), or the GTP conformation binds weakly to GDI (Sasaki *et al.*, 1993). To examine the interaction of the GTP bound form of Rac1 with GDI, Q61L Rac1 was used. This has a greatly reduced rate of intrinsic nucleotide hydrolysis and is predominantly GTP bound. Analysis of the GTP bound to the Rac mutant has been shown to be >94% (4.4.). Complexes of wild type Rac1 with the non-hydrolysable GTP analogue, GMPPNP have also been used. Rac1·GMPPNP complexes have been obtained with >92% purity (2.6.10.). Both of these have been used to assess the ability of Rac1 in the triphosphate bound conformation to bind to MDCC-GDI.

Titration of Rac1·GTP (Q61L) and Rac1·GMPPNP into a solution containing MDCC-GDI and farnesyl-12mer indicated that the K_d in both cases was greatly increased (figure 6.9). To confirm that Rac1 remained active following nucleotide exchange for GMPPNP, the nucleotide bound to the protein was exchanged back to GDP. This fully restored binding of Rac1 to MDCC-GDI in the peptide assay (figure 6.9a). The decrease in fluorescence observed with the Q61L mutant may be explained by the small percentage of Rac1·GDP in the solution (<5%). These results indicate that regions of Rac1 involved in the conformational change between the two nucleotide states are important for the interaction with GDI. Attempts to hydrolyse GTP bound to the Q61L Rac1 at various temperatures were unsuccessful; the slow rate of intrinsic hydrolysis of the protein (4.8.), and the high affinity of the mutant for GTP prevented nucleotide exchange for GDP. Due

Figure 6.9. Interaction of Rac1·GMPPNP and Q61L Rac1·GTP with MDCC-GDI and farnesyl 12-mer

A.) MDCC-GDI (0.1 μ M) was mixed with 15 μ M farnesyl 12-mer in 20mM Tris·HCl, pH7.6, 1mM MgCl₂, 1mM DTT, 5 μ M BSA at 20°C. Rac1·GMPPNP (●) was titrated into this solution and the fluorescence emission measured (excitation 430nm). Data corrected for the small decrease in fluorescence on addition of similar amounts of buffer. No fluorescence change was observed when Rac1·GMPPNP was titrated into this solution. When Rac1·GMPPNP had its nucleotide exchanged back to GDP, binding to MDCC-GDI was fully restored (O), indicating that the Rac1 remained active.

B) Q61L Rac1 was titrated into a solution containing MDCC-GDI and farnesyl 12-mer as described above. The line is the best fit to a binding curve and gives a K_d of 1.65 μ M. The apparent weak affinity may be explained by a small amount of Q61L Rac1·GDP in the solution.



to this, the possibility cannot be ruled out that mutation at position 61 reduces the affinity of Rac1 for GDI.

6.9. Interaction of full length Rac1 with MDCC-GDI

To examine the role of the C terminal region in interaction with GDI, titration experiments were undertaken using full length *E.coli* expressed Rac1. This protein has a complete C terminus, but is not post-translationally modified (figure 6.2.). As with truncated Rac1, titrations of full length Rac1 into a solution containing MDCC-GDI in the absence of farnesyl 12-mer showed little or no fluorescence change (data not shown). A number of reports have shown that isoprenylation of Rho proteins is essential for tight interaction with GDI (Leonard *et al.*, 1992), and these results obtained with full length Rac probably reflect the absence of a complex between the Rac1 and MDCC-GDI in the absence of modified peptide.

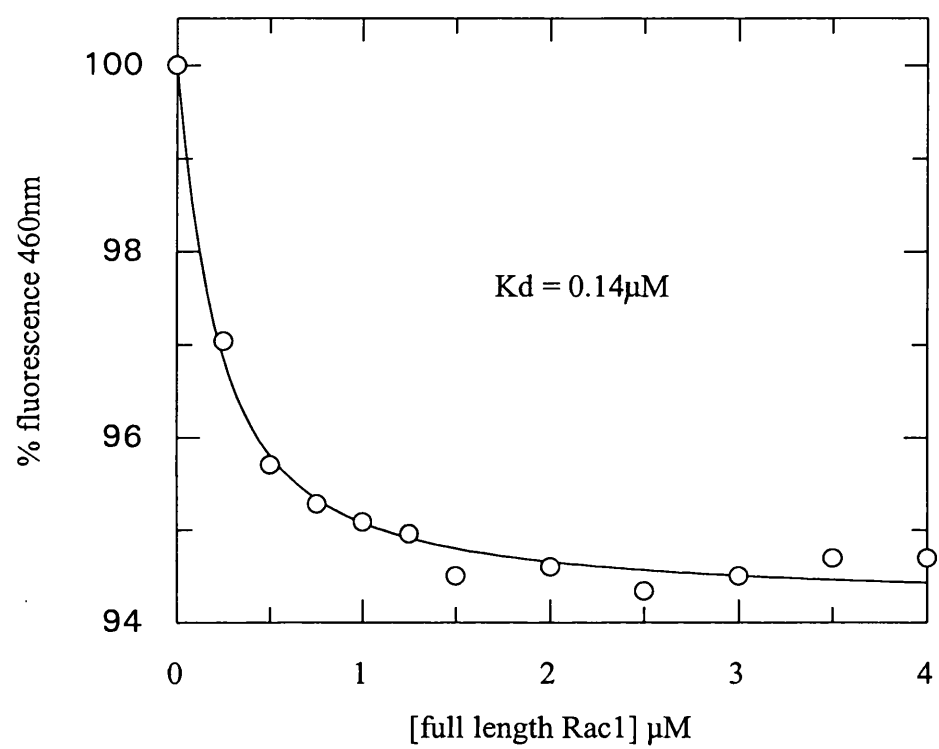
A fluorescence change was observed when full length Rac was titrated in the presence of farnesyl 12-mer with a K_d of $0.14\mu\text{M}$, but consistently gave an end point with a fluorescence change reduced by ~60% relative to truncated Rac1-GDP (figure 6.10.). These results suggest that the farnesyl group is required for a full fluorescence change in the peptide assay. It is possible that the C terminal region of full length Rac1 and the modified peptide sterically hinder the formation of a complex, resulting in a weaker affinity of full length Rac1 for GDI associated with a smaller fluorescence change.

6.10. Inhibition of nucleotide dissociation by GDI

As GDI inhibits guanine nucleotide dissociation from post-translationally modified Rac1 (Hiraoka *et al.*, 1992), another test of the complex of Rac-GDI-farnesyl-12mer was to examine the effect of GDI on Rac nucleotide exchange. To determine whether GDI inhibited GDP dissociation from Rac1 when incubated with the farnesyl 12-mer, the dissociation of mantGDP was determined using fluorescence energy transfer under

Figure 6.10. Interaction of full length Rac1 with MDCC-GDI and farnesyl 12-mer

MDCC-GDI (0.1 μ M) was mixed with farnesyl 12-mer in 20mM Tris·HCl pH 7.6, 1mM MgCl₂, 1mM DTT, 5 μ M BSA at 20°C. Full length Rac1 was titrated into this solution and the fluorescence emission measured (excitation 430nm). Data corrected for the small decrease in fluorescence on addition of small amounts of buffer. The line is a best fit to a binding curve and gives a K_d of 0.14 μ M (average of two titrations). The observed fluorescence change was significantly reduced compared to truncated (aa's 1-184) Rac1.



pseudo-first order conditions as described previously (3.2.1.), and the data fitted to single exponentials (figure 6.11.). To produce conditions of accelerated nucleotide exchange, excess ethylenediaminetetraacetic acid (EDTA) was added to chelate Mg^{2+} ions required for tight binding of the nucleotide to the protein. The use of EDTA has been well documented in similar studies with Ras (Lenzen *et al.*, 1998). An alternative method to create conditions of accelerated nucleotide exchange is to use $(NH_4)_2SO_4$ (3.2.1.). However, $(NH_4)_2SO_4$ was not used in these experiments to accelerate nucleotide exchange as it results in a large increase in ionic strength, which is likely to weaken the Rac·GDI interaction.

The first-order rate constant for mantGDP dissociation under these conditions was $2.5 \times 10^{-2} s^{-1}$. As expected, 2-fold excess of GDI in the absence of farnesyl-12mer had no effect on the nucleotide exchange of *E.coli* Rac1 (table 6.1.). When GDI was incubated with Rac1 in the presence of 10 μM farnesyl 12-mer, the rate of nucleotide exchange was reduced by 65% (figure 6.11.). For the ternary complex, if it is assumed that Rac1 in complex with GDI cannot undergo nucleotide exchange, and that the rate of dissociation of Rac1 is more rapid compared to nucleotide exchange of free Rac1, it can be calculated that ~75% of the Rac1 is likely to be complexed to GDI at any one time. These results indicate that GDI inhibits nucleotide exchange from Rac1 in the predicted manner. Neither excess farnesyl-12mer or un-labelled peptide alone affected nucleotide exchange of Rac1 (table 6.1.). GDI also inhibited nucleotide exchange from truncated cdc42 (aa's 1-184) in the presence of farnesyl 12-mer by a similar factor (data not shown).

6.11. The interaction of cdc42·GDP and cdc42·GMPPNP with MDCC-GDI

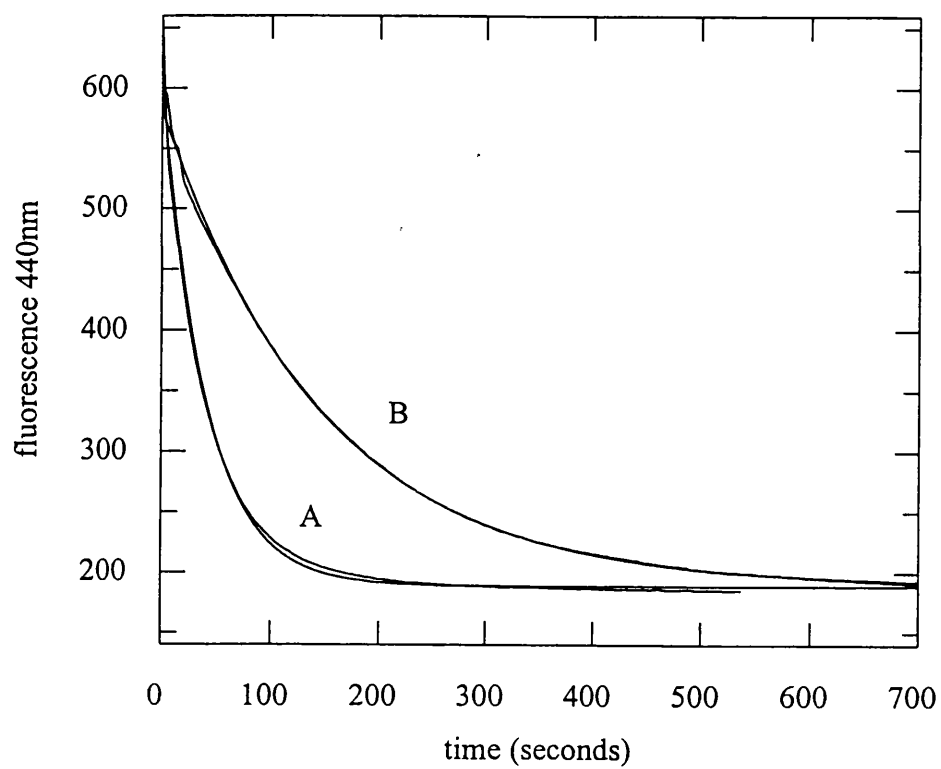
To further examine the interaction of Rac1 with GDI in the presence of farnesylated peptide, a number of control titrations were undertaken. At least one report has shown that cdc42·GMPPNP binds to GDI with a similar affinity as cdc42·GDP (Nomanbhoy & Cerione, 1996). To examine the interaction of cdc42 in both GDP and GMPPNP

Figure 6.11. Inhibition of nucleotide exchange by GDI and farnesyl-12mer

Rac1-mantGDP (1 μ M) was incubated in 20mM Tris.HCl pH7.6, 1mM DTT, 0.5mM EDTA, 30°C with 20 μ M GDP in the absence (A) and presence (B) of 2 μ M GDI and 10 μ M farnesyl 12-mer. The dissociation of mantGDP from Rac1 was monitored by fluorescence resonance energy transfer by excitation of Rac1 tryptophan(s) at 290nm under accelerated exchange conditions. The data were fitted to single exponentials. Values of $2.5 \times 10^{-2} \text{s}^{-1}$ were obtained for Rac1 alone (A), and $0.7 \times 10^{-2} \text{s}^{-1}$ in the presence of 2 μ M GDI and 10 μ M modified peptide (B).

Table 6.1. The effect of GDI and 12-mer peptides on the rate of Rac1 nucleotide exchange

^a The effect of GDI and farnesyl 12-mer on the dissociation of mantGDP from Rac1 was examined as described (figure 6.11.). + and – represent components present or absent in the reaction mixture. A combination of GDI and farnesyl 12-mer reduced the rate by ~4 fold.



The effect of GDI and farnesyl 12-mer on the dissociation rate of GDP from Rac1 ^a

Rac1-mantGDP (1 μ M)	farnesyl 12-mer (10 μ M)	unmodified 12-mer (10 μ M)	GDI (2 μ M)	$k \times 10^{-2} \text{s}^{-1}$
+	-	-	-	2.5
+	+	-	+	0.7
+	-	-	+	2.3
+	+	-	-	2.2
+	-	+	-	2.5
+	-	+	+	2.3

conformations, similar equilibrium titration experiments were undertaken using *E.coli* expressed cdc42, truncated at the C-terminus (aa's 1-184) (figure 6.12.). These results indicate that truncated cdc42·GDP binds tightly to GDI in the peptide assay with a K_d of 0.1 μ M. In the GMPPNP conformation, cdc42 showed little or no affinity for GDI. These results act as a positive control for the peptide assay and provides further indication that conformational changes between the two nucleotide states of Rho family proteins are important for interaction with GDI. The binding affinity determined for the cdc42·GDP interaction may not be directly comparable with Rac1·GDP titrations, as farnesylated Rac C-terminal peptides were used for all titration experiments.

6.12. The interaction of N-Ras with MDCC-GDI

As a negative control, N-Ras (with a complete C-terminus) was titrated into a solution containing MDCC-GDI and farnesyl 12-mer as described previously for Rac1 (figure 6.13.). The addition of 0.25 μ M Rac following 20 μ M N-Ras induced a ~20% quenching of MDCC-GDI fluorescence (data not shown). These results suggest that N-Ras binds weakly, if at all to GDI in the peptide assay. Despite a similar overall fold of Ras and Rac (figure 1.6.), a number of differing regions have been identified from structural comparisons. These include the insertion loop (aa's 123-135), present in Rac and other Rho family proteins, the effector loop (aa's 30-40) and the C-terminus (figure 1.2.). An additional region of divergence between Rac and Ras and between the 2 nucleotide bound forms of Rac has recently been identified as the switch II region (figure 1.7.) (Hirshberg *et al.*, unpublished results). The regions of structural divergence between Rac and Ras are likely to be important for interaction with GDI and these regions have been examined by site-directed mutagenesis. The interaction of Rac1 mutants with GDI will be described in later sections (6.14.).

Figure 6.12. Interaction of cdc42 with farnesyl 12-mer and MDCC-GDI

MDCC-GDI (0.1 μ M) was mixed with 15 μ M farnesyl 12-mer in 20mM Tris·HCl pH 7.6, 1mM MgCl₂, 1mM DTT 5 μ M BSA at 20°C. cdc42·GDP (figure a) or cdc42·GMPPNP (figure b) were titrated into this solution and the fluorescence emission measured. Excitation 430nm.

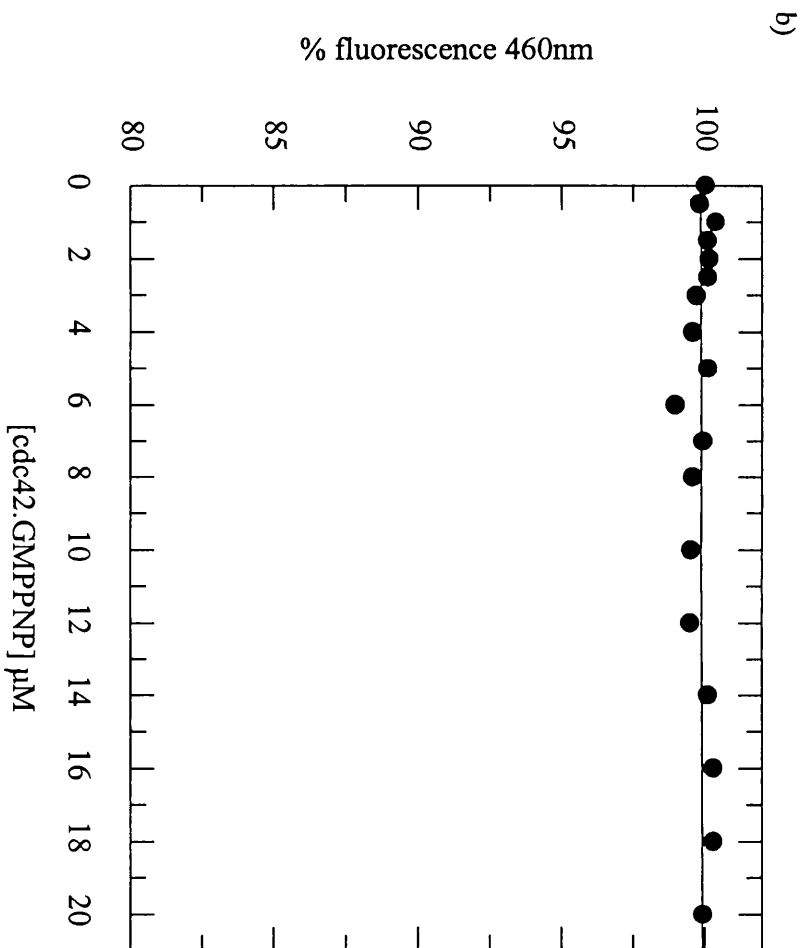
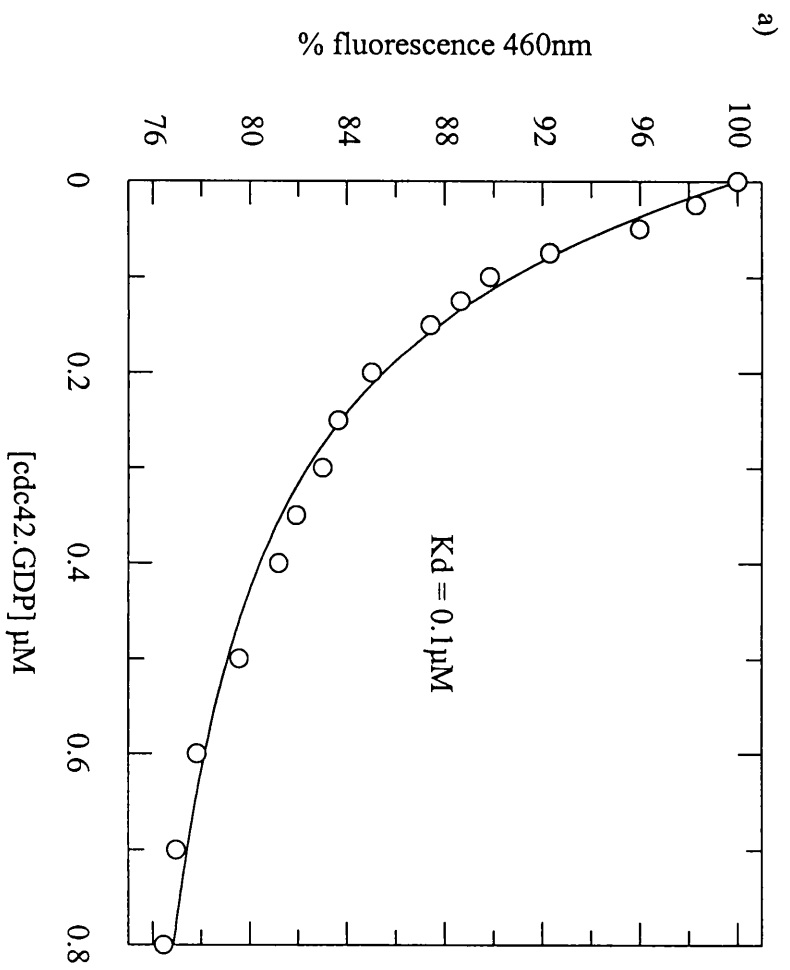
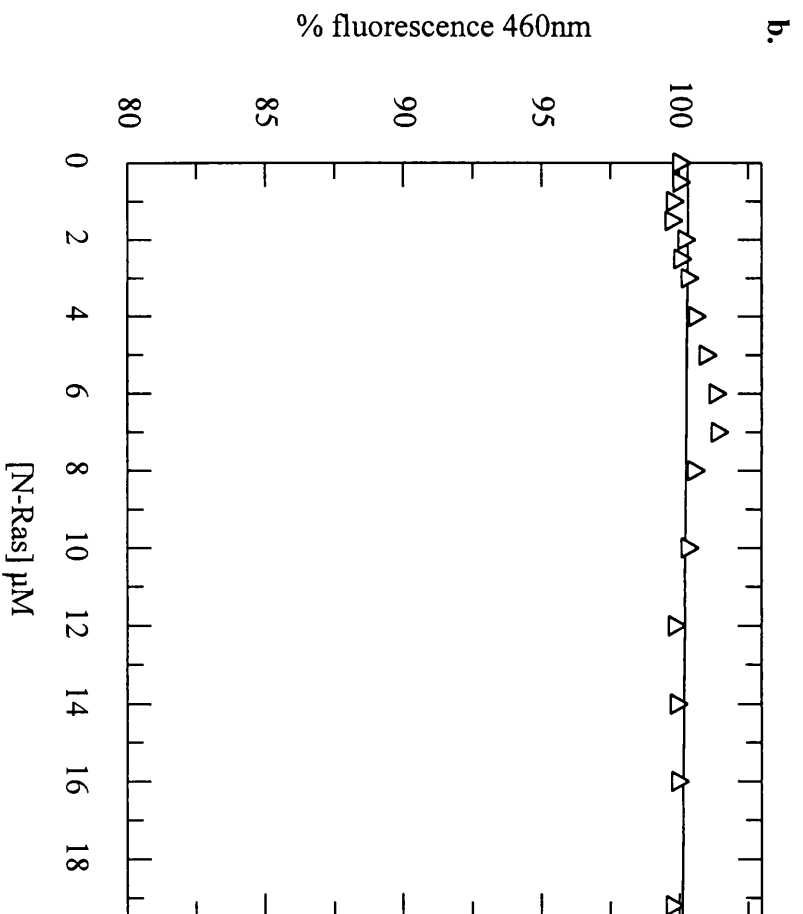
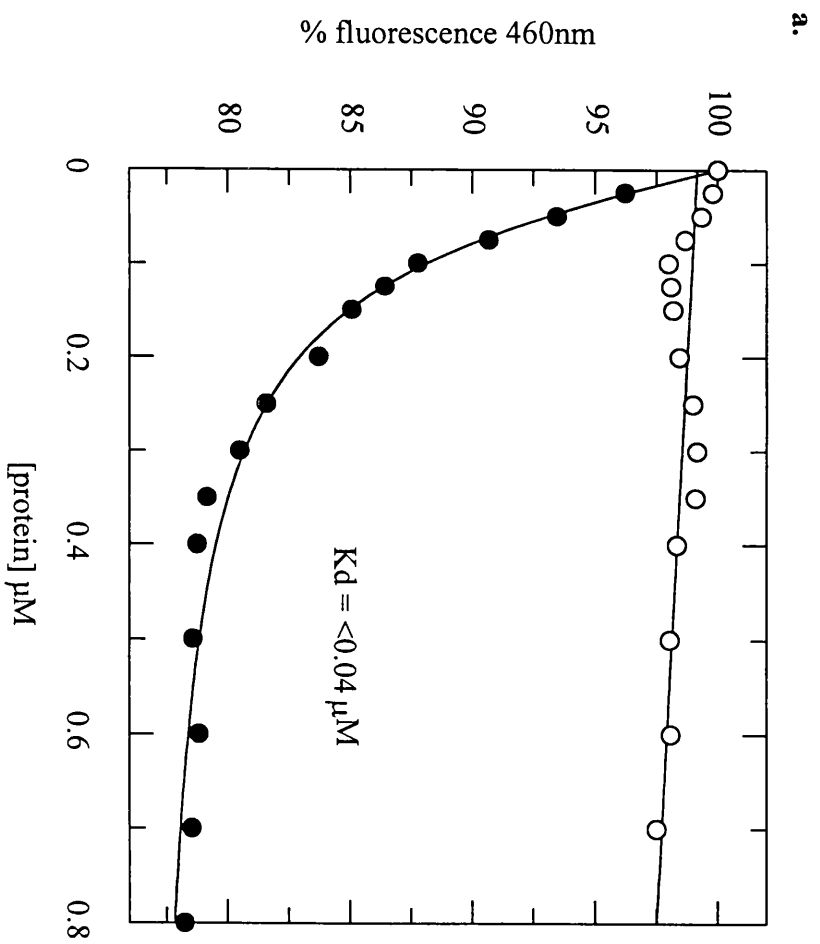


Figure 6.13. The interaction of N-Ras with MDCC-GDI and farnesyl-12mer

Figure a. MDCC-GDI (0.1 μ M) was mixed with farnesyl-12mer (15 μ M) in 20mM Tris·HCl, pH7.6 1mM MgCl₂, 1mM DTT, 5 μ M BSA at 20°C. Rac1 (●) or N-Ras (○) were titrated into this solution and the fluorescence emission measured. Data were corrected for the decrease in fluorescence due to the addition of similar amounts of buffer. *Figure b.* High concentrations of N -Ras (Δ) were titrated into a solution containing MDCC-GDI and farnesyl 12-mer under the same conditions as described above.



6.13. Effect of GDI on Rac1 · mantGDP fluorescence

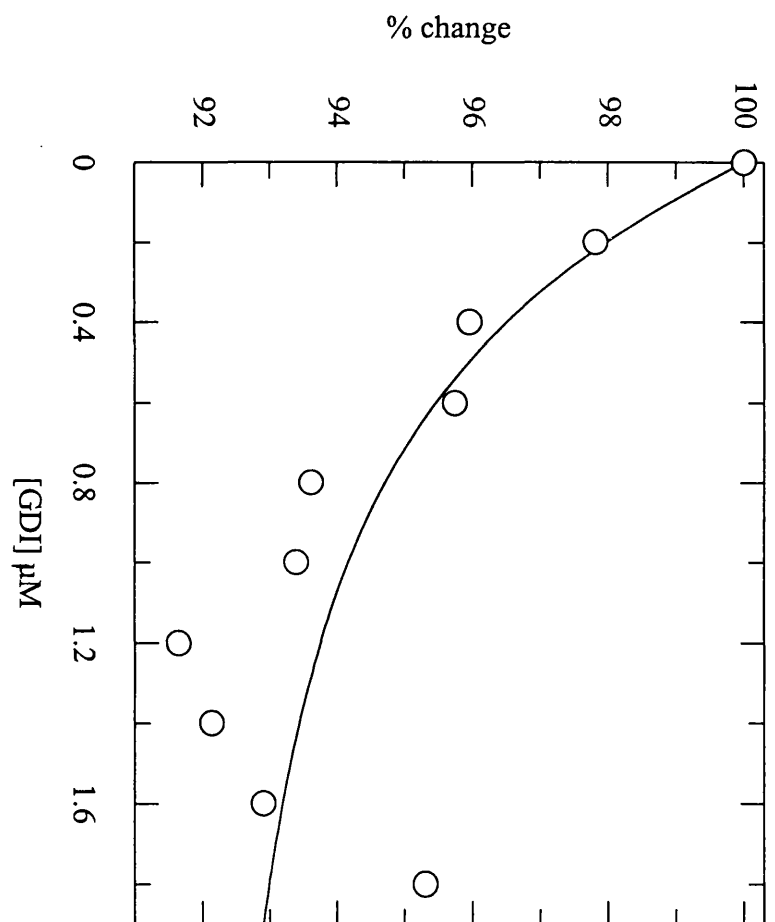
A recent report by Cerione's laboratory has shown that when 200nM GDI is incubated with 80nM isoprenylated cdc42 containing bound mantGDP (in 20mM Tris·HCl pH 8.0, 2mM MgCl₂, 50mM NaCl) a 20% quenching of mant fluorescence is observed (Nomanbhoy & Cerione, 1996). To examine the effect of GDI on a Rac1·mantGDP complex in the presence of modified peptide, GDI was titrated into a solution containing Rac1·mantGDP and excess farnesyl 12-mer, and the fluorescence change measured (figure 6.14:). The addition of GDI caused a quenching of mantGDP fluorescence, but the overall change after correction for the addition of similar amounts of buffer was <10%. It is possible that a reduced fluorescence change is observed in the peptide assay because the Rac and the peptide are not covalently attached to each other, or because the peptides have been farnesylated rather than geranylgeranylated (1.13.1.). The variation in fluorescence signal may also be due to structural differences between variable regions of Rac1 and cdc42 in the GDP bound states. Due to the relatively small signal change and errors associated with additions and mixing, the GDI induced quenching of mantGDP fluorescence was not used to determine binding constants for the Rac1·GDI interaction.

6.14. Interaction of Rac1 mutants with GDI

Although the regions of GDI involved in the interaction with Rac1 have been identified with the use of GDI mutants (Gosser *et al.*, 1997), there are few reports examining the regions of Rac1 involved in this interaction. This is probably due to difficulties in expressing and purifying Rac proteins using a eukaryotic expression system. One advantage of the peptide assay is that *E.coli* expressed Rac1 proteins may be used to examine this association. As one approach to identify the regions of Rac1 involved in the interaction with GDI, a number of Rac1 point mutants have been successfully made in regions of major divergence between Rho and Ras family proteins (chapter 4.). The insertion loop (aa's 120-137) is the major gross structural difference between Rac and Ras, and point mutations in this region have been designed from the Rac1·GMPPNP

Figure 6.14. Effect of GDI on Rac1·mantGDP fluorescence

Equilibrium binding measurement of the interaction of Rac1·mantGDP with GDI. Rac1·mantGDP (0.5 μ M) was incubated in 20mM Tris·HCl pH7.6, 1mM MgCl₂, 5 μ M BSA, 10 μ M farnesyl 12-mer at 30°C. Aliquots of GDI were titrated sequentially and the fluorescence emission measured at 440nm (excitation 360nm). Data corrected for the small decrease in fluorescence on addition of buffer alone.



structure as they are likely to have exposed functional groups that may be involved in the interaction with other molecules. Mutations have also been made in the region of the effector loop (aa's 30-40) - an area that may be of particular importance due to its closeness to the nucleotide binding pocket and differences between Rac·GDP and Ras·GDP structures (1.13.). In addition, a Rac1/H-Ras 'insertion loop' chimaera has also been made to examine the importance of this region in the interaction with GDI (see 2.6.4. for design and construction).

The binding of mutant Rac1 proteins has been quantified by titrations using MDCC-GDI and farnesyl 12-mer as described previously for wild type Rac1 (6.7.) and averages of K_d values obtained for at least two independent experiments are summarised in table 6.2. These results show that the majority of point mutations have little effect on the interaction with GDI. I33D and F37E mutations in the effector loop have a significant effect on this interaction, with K_d values for these mutants increased by several orders of magnitude (figure 6.15.). Structural considerations for the effects of the Rac1 mutations on GDI binding will be covered in the discussion.

6.14.1. Effect of GDI on the rate of nucleotide exchange from I33D Rac1

A further test of the interaction of GDI with the I33D Rac1 mutant was to examine the effect of GDI on Rac nucleotide exchange. To determine whether GDI had an effect on nucleotide exchange from the I33D Rac1, the mutant protein was incubated with farnesyl 12-mer and GDI. Nucleotide exchange was examined using fluorescence resonance energy transfer under conditions of accelerated exchange essentially as described (3.2.1.), and the data was fitted to a single exponential. GDI had no effect on the rate of nucleotide exchange from the I33D Rac1 mutant (figure 6.16.). These results suggest that point mutation of Rac1 at this position to corresponding residues of Ras significantly reduces the affinity of the Rac1·GDI interaction. As the F37E protein has only recently been

Table 6.2. Dissociation constants for Rac1 and Rac1 mutants from MDCC-GDI

^a Titrations of Rac1 into a solution containing MDCC-GDI were undertaken as described in section 6.7. unless otherwise stated. 15µM farnesyl 12-mer was present, and Rac1 proteins were truncated (aa's 1-184). K_d values are the average of at least two determinations. ^b Titrations were undertaken using 100nM MDCC-GDI. Therefore these values represent an upper limit. ^c Little or no fluorescence change was observed, and this value represents the limit imposed by the errors in the measurement. ^d Rac1·GMPPNP had its nucleotide exchanged back to GDP (figure 6.9.). This fully restored binding to MDCC-GDI, indicating that the Rac remained active. ^e These titrations gave an end point with a fluorescence change reduced by ~60% relative to Rac1·GDP. ^f Addition of 0.25µM Rac1 in the presence of 20µM N-Ras and farnesyl 12-mer showed a full fluorescence change, suggesting that high concentrations of Ras do not inhibit Rac1 binding. ^g E127A Rac1 has recently been purified and titration experiments have yet to be undertaken. ^h Titrations with E131K Rac1 were not undertaken as this protein was not fully truncated at the C-terminus. ⁱ It is possible that additional mutations are present in the K133E Rac1 protein (see table 4.1.).

*Dissociation constants for unmodified Rac1 and Rac1 mutants
from MDCC-GDI^a*

Protein and peptide	Kd (μM)
Rac1 · GDP	<0.04 ^b
Rac1 · GMPPNP	>10 ^{c,d}
cdc42 · GDP	0.1
cdc42 · GMPPNP	>10 ^c
Full length N-Ras · GDP	>10 ^{c,f}
Full length Rac1	0.14 ^e
Rac1 + unmodified 12-mer	0.53 ^e
Rac1 + no peptide	>10 ^c
<i>Rac1 mutants</i>	
A27K	<0.03
I33D	>10 ^c
T35A	<0.04
F37E	>10 ^c
D63E	<0.05
Q61L	1.65
D124S	<0.04
E127A ^g	-
K130A	<0.03
E131K ^h	-
K133E ⁱ	0.17
Rac1/H-Ras chimaera	<0.04

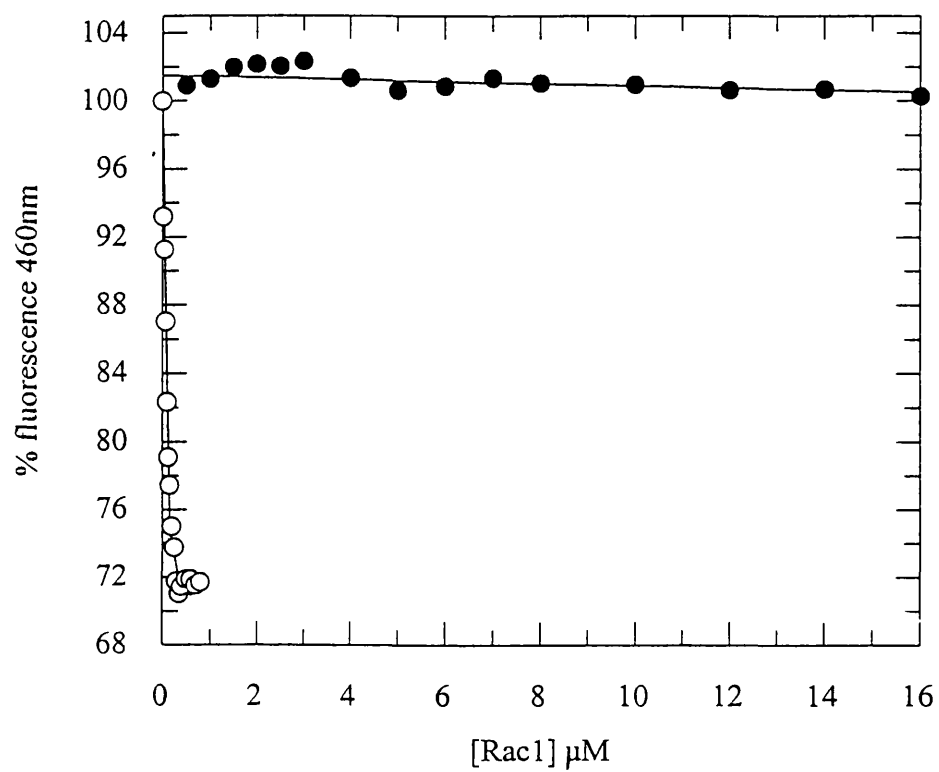
Figure 6.15. Interaction of I33D and F37E Rac1 mutants with MDCC-GDI

a) MDCC-GDI (0.1 μ M) was incubated with 15 μ M farnesyl 12-mer in 20mM Tris·HCl pH7.6, 1mM MgCl₂, 1mM DTT, 5 μ M BSA at 20°C. I33D Rac1 (●) was titrated and the fluorescence emission measured (excitation 430nm). Line shows a best fit to a straight line.

b) MDCC-GDI (0.1 μ M) was incubated with 15 μ M farnesyl 12-mer in 20mM Tris·HCl pH7.6, 1mM MgCl₂, 1mM DTT, 5 μ M BSA at 20°C. F37E Rac1 was titrated and the fluorescence emission recorded (excitation 430nm). Line shows a best fit to a straight line.

Data were corrected for the small decrease in fluorescence on addition of similar amounts of buffer. Even after the addition of high concentrations of Rac1 (16 μ M) little change in MDCC-GDI fluorescence was observed with either Rac1 mutant. To confirm that the lack of fluorescence change was not due to inactive GDI or farnesyl 12-mer, a titration with wild type Rac1 into the same reaction mixture (15 μ M farnesyl 12-mer in 20mM Tris·HCl pH7.6, 1mM MgCl₂, 1mM DTT, 5 μ M BSA at 20°C) was associated with a ~30% quenching of MDCC-GDI fluorescence (figure 6.15a, (O)).

a)



b)

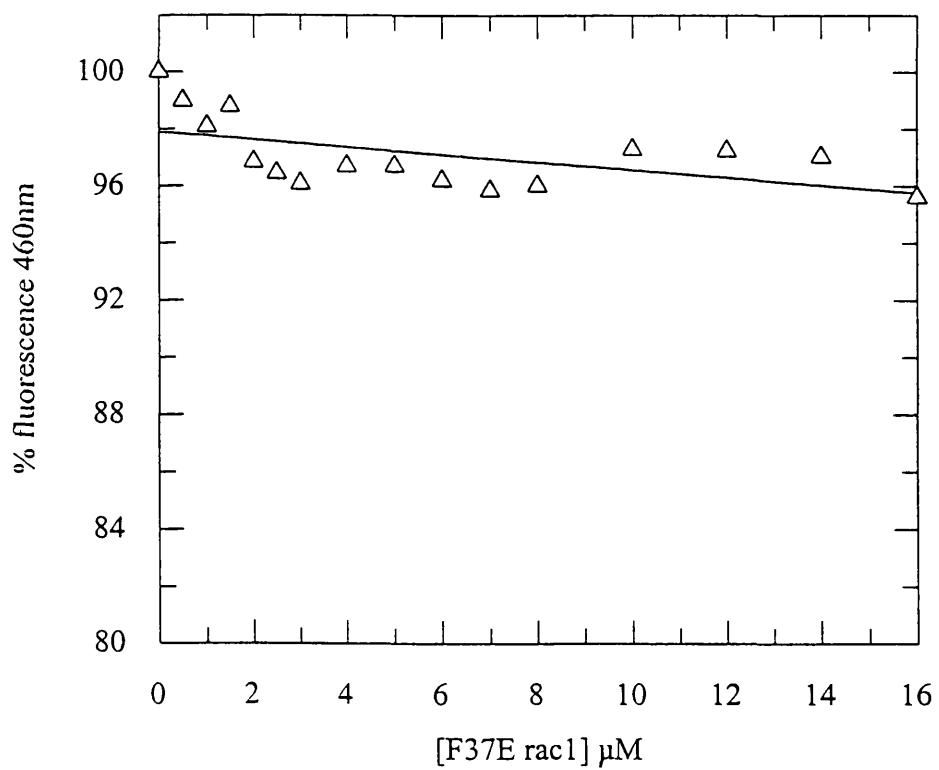
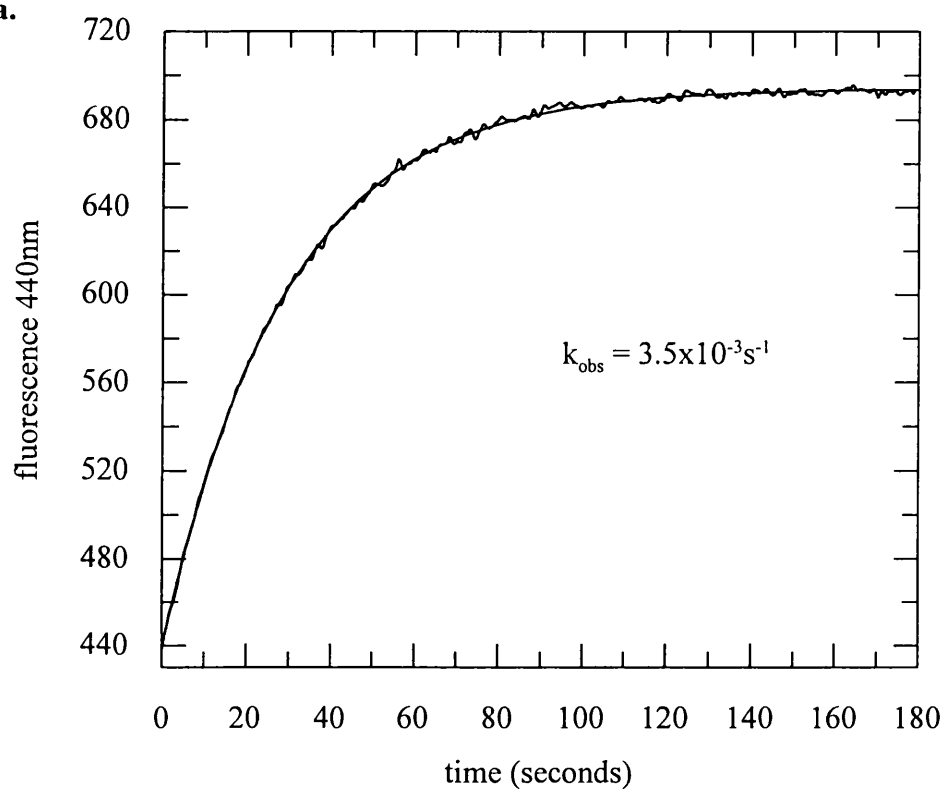


Figure 6.16. Effect of GDI and farnesyl 12-mer on the rate of GDP dissociation from I33D Rac1

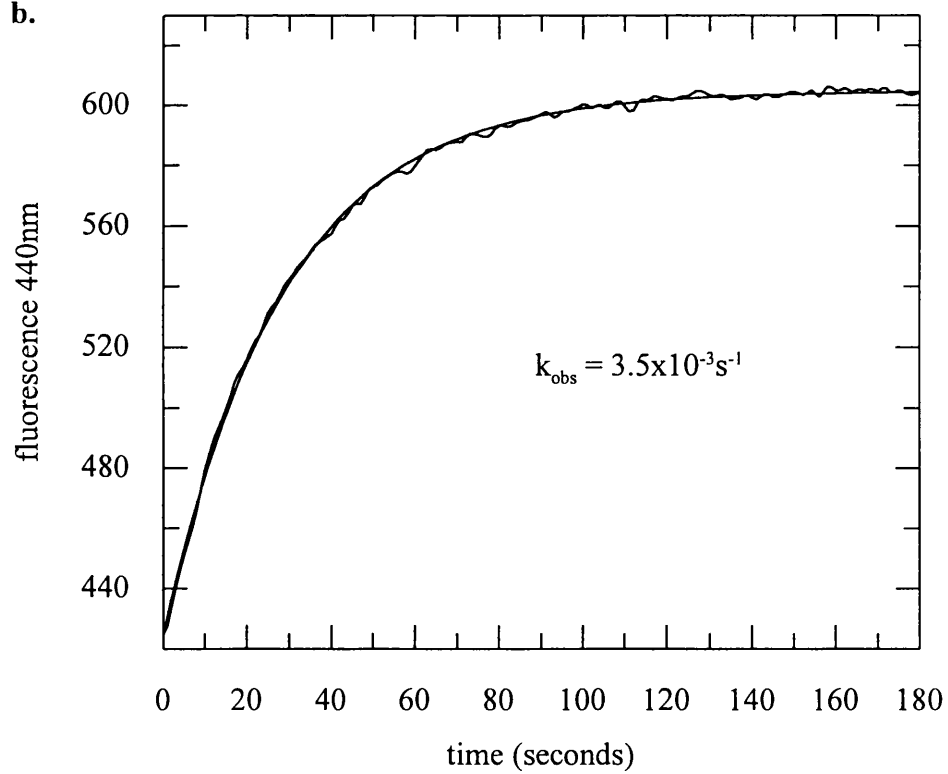
Association of mantGDP with I33D Rac1 was examined under pseudo-first order conditions essentially as described (3.2.2.). I33D Rac1 (1 μ M) was incubated with mantGDP (20 μ M) in 20mM Tris·HCl pH7.6, 1mM EDTA, 1mM DTT in the absence (a.) or presence of farnesyl 12-mer (15 μ M) and GDI (2 μ M) (b.). Mant fluorescence was monitored over time using fluorescence resonance energy transfer (3.2.1.) with excitation at 290nm. Data was fitted to a first order rate equation and rate constants are the average of at least two determinations. Protein from two preparations of I33D Rac1 gave the same results.

To confirm that the GDI and farnesyl 12-mer were active, the effect of the GDI and farnesyl 12-mer (from the same solutions) on wild type Rac1 was examined. Under the conditions described above, the rate of nucleotide exchange from wild type Rac1 was reduced ~4 fold (data not shown).

a.



b.



obtained and has yet to be fully characterised in this laboratory (4.5.1.), the effect of GDI on the rate of nucleotide exchange of this mutant has yet to be established.

6.15. Binding studies with a farnesylated C-terminal 9-mer

Attempts to farnesylate quantitative yields of a Rac1 C-terminal 9-mer (sequence PVKKRKRRKC) were unsuccessful under a wide range of conditions. The 3 C-terminal leucines are absent from this peptide, making it more hydrophilic. It is likely that the increased hydrophilicity of the 9-mer reduces the solubility of the peptide in organic solvent and prevents efficient modification with the hydrophobic farnesyl group. It was hoped that C-terminal methylation of this peptide would improve farnesylation. This C-terminal 9-mer has recently been methylated, then subsequently farnesylated as described (2.5.2.). The advantage of using this peptide for binding studies is that the sequence corresponds to the native sequence of Rac1 following post-translational modification (1.13.1.).

6.15.1. Affinity of the farnesyl 9-mer · MDCC-GDI interaction

To examine the affinity of the methylated, farnesylated 9-mer, the modified peptide was titrated into a solution containing MDCC-GDI and Rac1, essentially as described (6.7.1.). The modified 9-mer showed significantly tighter binding than the farnesyl 12-mer, with a dissociation constant of 1.5 μ M (figure 6.17.). These results are consistent with previous data which has shown that geranylgeranylated, non-proteolysed Rac1 (with a complete -LLL motif) binds to GDI, but with a weaker affinity than the fully processed protein with the 3 terminal leucines removed (Hancock & Hall, 1993). These results indicate that removal of the 3 terminal leucines increases the affinity of the farnesylated peptide.

Figure 6.17. Binding studies using a farnesylated Rac1 C terminal 9-mer

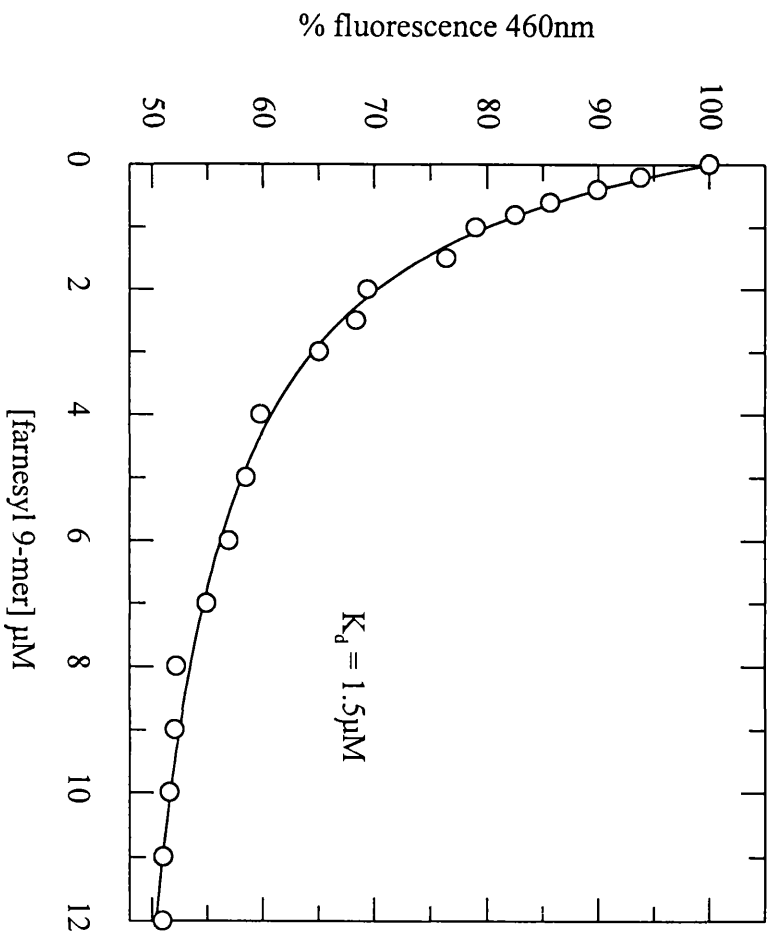
a). The affinity of the farnesyl 9-mer-MDCC-GDI interaction (in the presence of excess Rac1) was examined by titrating farnesyl-9mer into a solution containing MDCC-GDI (0.1 μ M) and Rac1 (0.5 μ M) in 20mM Tris·HCl pH7.6, 1mM MgCl₂, 1mM DTT, 5 μ M BSA at 20°C and the fluorescence emission measured. Excitation 430nm. Data corrected for the small decrease in fluorescence on addition of similar amounts of buffer. The line is a best fit to a binding curve and gives a K_d (average of 3 determinations) of 1.5 μ M. Consistent results were obtained with 2 preparations of farnesyl 9-mer. Unmodified 9mer (12 μ M) or methylated (but not farnesylated) 12-mer had no effect on MDCC-GDI fluorescence under the same conditions (data not shown).

b). The affinity of the Rac1·GDI interaction (in the presence of saturating concentrations of farnesyl 9-mer) was measured by titrating Rac1 into a solution containing MDCC-GDI (0.1 μ M) and farnesyl 9-mer (15 μ M) in 20mM Tris·HCl pH7.6, 1mM MgCl₂, 1mM DTT, 5 μ M BSA at 20°C and the fluorescence emission measured. Excitation 430nm. Data corrected for the small decrease in fluorescence on addition of similar amounts of buffer. The line is a best fit to a binding curve and gives a K_d (average of 3 determinations) of

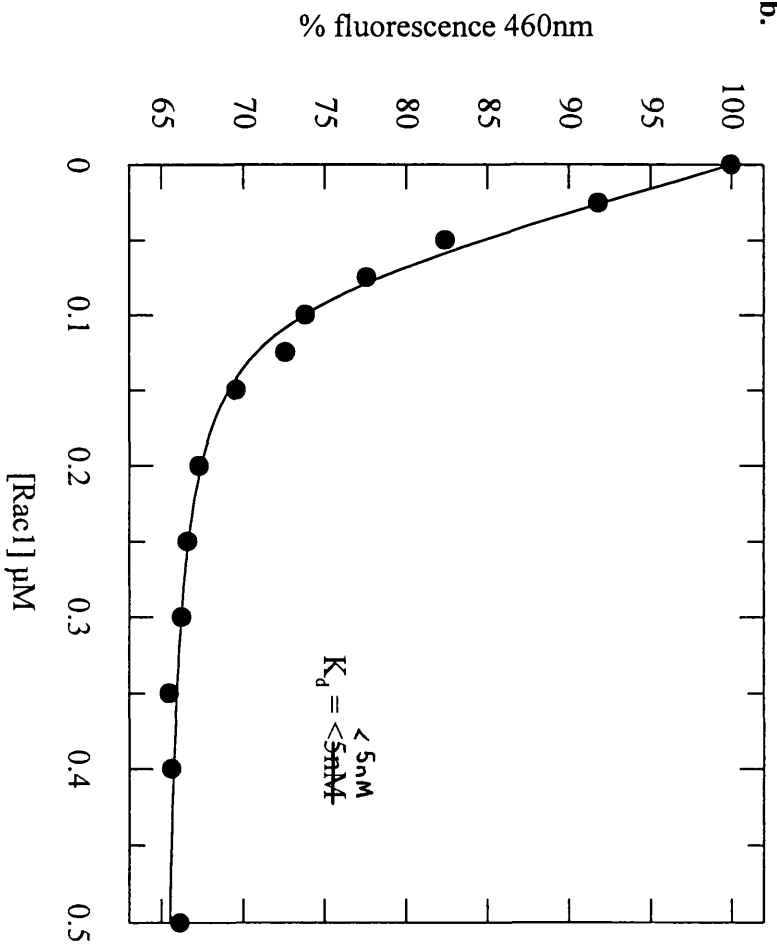
~~<5nM.~~

<5nM.

a.



b.



6.15.2. Affinity of the Rac1 · MDCC-GDI interaction in the presence of modified 9-mer

To examine the affinity of the Rac1 · MDCC-GDI interaction in the presence of modified peptide, dissociation constants were obtained by titrating Rac1 into a solution containing MDCC-GDI and excess modified 9-mer, and the quenching of MDCC-GDI fluorescence measured. Unmodified 9-mer or methylated 9-mer had no effect on MDCC-GDI fluorescence under the same conditions (data not shown). In the presence of excess modified 9-mer, Rac1 binds tighter to GDI than in the presence of excess farnesyl 12-mer with a K_d of $< 5 \text{ nM}$, around ~~one~~^{one} order of magnitude weaker than fully processed (baculovirus expressed) Rac1.

As both peptides are modified with a farnesyl group, it is possible that the modified 9-mer peptide induces further conformational changes in the C-terminal domain of GDI, resulting in an increased affinity for Rac1. It is possible that in addition to contacts with the disordered N-terminal region of GDI (1.14.1.), Rac1 forms contacts (perhaps via the switch II region) with the structured C-terminal domain of GDI. Because the binding of Rac1 to MDCC-GDI in the presence of modified 9-mer under these conditions is tight, an accurate value of the K_d is not easily determined from such equilibrium binding data, as titrations are not practical at low concentrations ($< K_d$) needed. To further examine the affinity of the Rac1 · GDI interaction, the kinetics of the Rac1 association and dissociation have been measured in real time using rapid reaction techniques.

6.16. Analysis of the Rac1 · GDI interaction by stopped-flow spectrofluorimetry

One of the limitations of using a conventional fluorimeter is that it is difficult to follow fluorescent changes that occur within the first few seconds of mixing, as it takes this duration to add the sample and close the lid. Because ligand binding is typically a rapid process, the interaction of Rac1 with GDI has been examined using stopped-flow fluorimetry. In this technique, samples are rapidly mixed, and fluorescent changes can be

followed over a millisecond time scale. A typical set-up is shown in figure 6.18. Solutions of each reactant are placed in syringes (B). Movement of a drive plate (A) initiates flow of samples, and shortly after the reactants emerge from a mixing chamber they flow into an observation cell where measurements can be made. (D) At this point, the recorder is triggered and a continuous recording of the fluorescence change made. The back syringe acts as a stopping device by hitting a metal block (reviewed by Eccleston, 1987). This rapid mixing method has been used to measure the interaction of Rac1 and GDI in real time.

6.16.1. Kinetic mechanism of Rac1 binding to MDCC-GDI

The use of stopped flow allowed the transient kinetics of the Rac1·GDI interaction to be measured. To simplify the analysis of this reaction, experiments were carried out under pseudo-first order conditions with Rac1 in large excess over GDI. Under these conditions, the concentration of Rac1 will remain essentially constant during the time course of the reaction, so that the rate of formation of Rac1·GDI will follow first order kinetics.

Rapid mixing of excess *E.coli* Rac1 with 50nM MDCC-GDI and excess farnesyl 9-mer resulted in a decrease in fluorescence; as no lag was observed the data could be well fitted to a single exponential (figure 6.19a.). When two of the three components (Rac1, GDI or farnesyl 9-mer) are premixed before rapid mixing of the final component, no lag phase was seen when any combination was used and the kinetic data obtained does not distinguish between random and ordered additions (data not shown). Therefore the interaction of truncated Rac1 with MDCC-GDI in the presence of saturating concentrations of farnesyl 9-mer has been considered.

The data obtained suggests a saturating rate at high [Rac] (figure 6.19b.). These results also indicate that the binding of Rac1 to MDCC-GDI is not responsible for the observed fluorescence change, or the observed rate would show a linear dependence to the Rac

Figure 6.18. Diagram of the stopped flow apparatus

A, drive; B, reactant syringes with solutions shown in green; C, mixer; D, observation cell; E, back syringe; F, stopping bar.

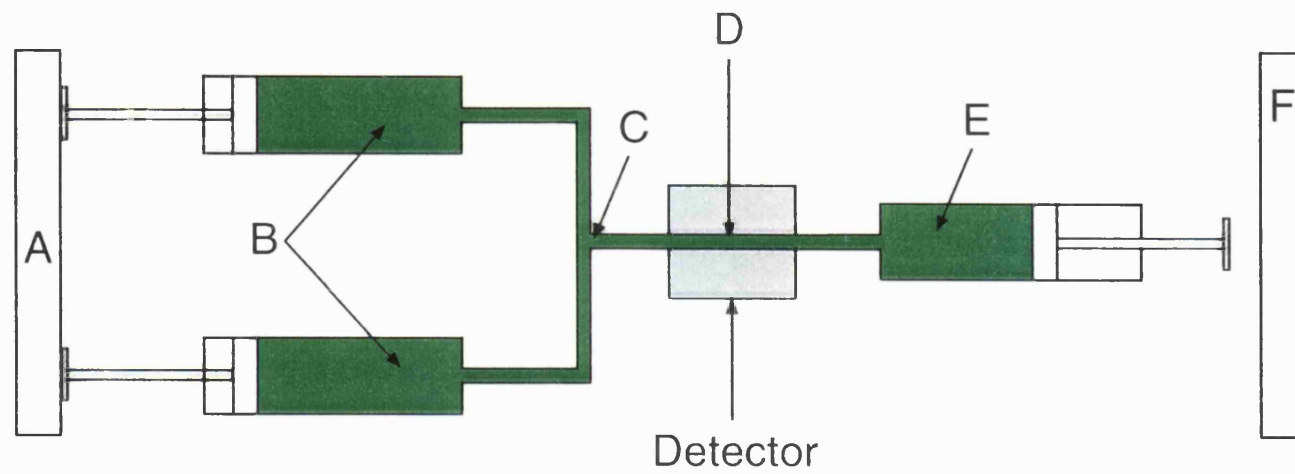
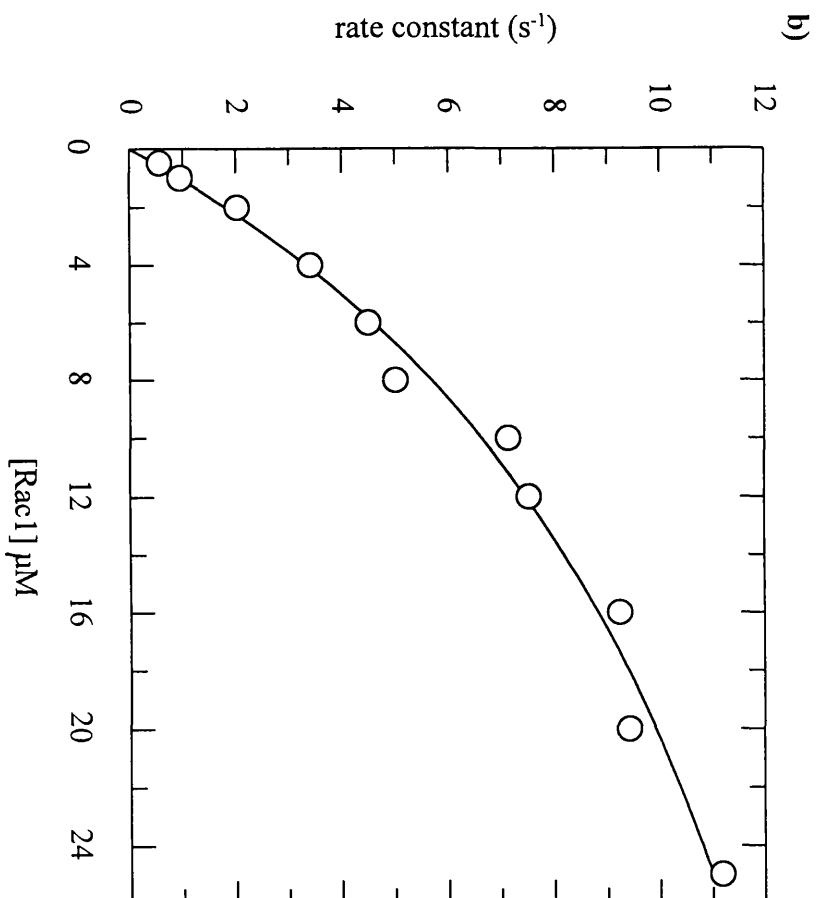
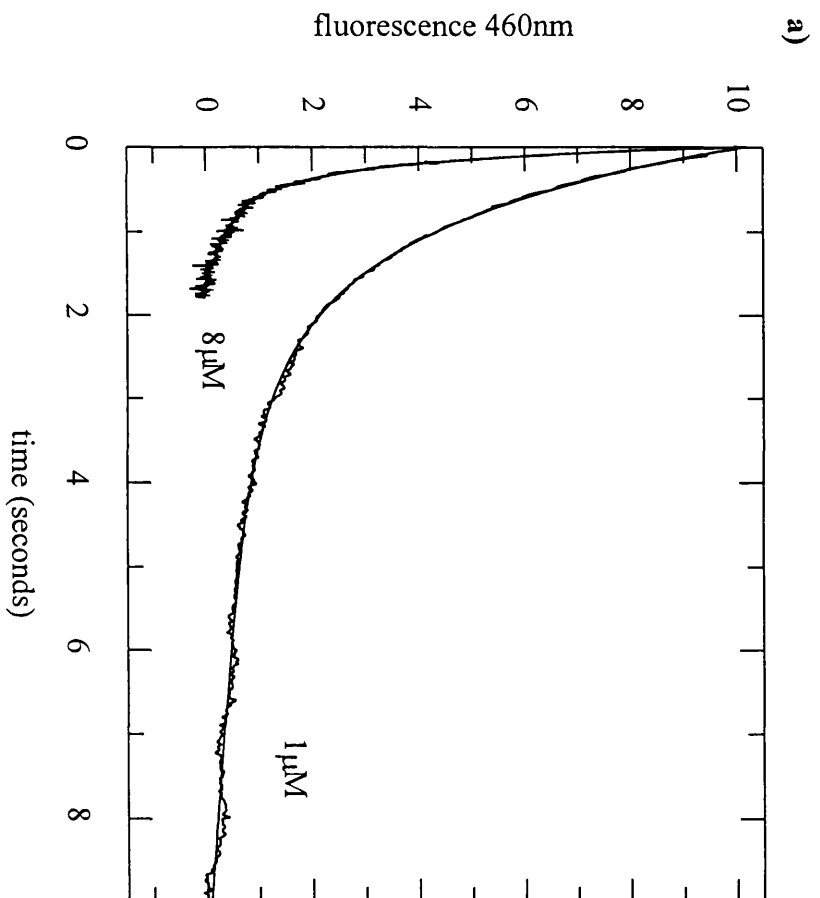


Figure 6.19. Kinetics of the Rac1·MDCC-GDI interaction

a. Association of *E.coli* Rac1 with MDCC-GDI. MDCC-GDI (50nM) was mixed with a large excess of Rac1 in the presence of farnesyl 9-mer (4μM) (mixing chamber concentrations) in 20mM Tris·HCl pH7.6, 1mM MgCl₂, 1mM DTT, 5μM BSA at 20°C and the quenching of MDCC fluorescence monitored over time. Time courses at Rac1 concentrations shown. Data were fitted to single exponentials (+ a slope) and give observed first order rate constants of 1.0 s⁻¹ (1μM Rac1) and 4.6 s⁻¹ (8μM Rac1). Controls run in the absence of Rac1 and farnesyl peptide showed a drift in fluorescence (R.W. Stockley & M.R. Webb, see Newcombe *et al.*, 1999). Although this may be due to photobleaching of the fluorophore, it is more likely to be due to protein adsorption on surfaces.

b. Dependence of observed first order rate constants on Rac1 concentration (mixing chamber concentrations of Rac1 shown). Conditions as described in figure 6.19a. Data were fitted to single exponentials as described above and at least 2 runs averaged at each concentration. The line represents the best hyperbolic fit to the data with a maximum rate constant of 19.6 s⁻¹ and half maximum rate at 19.6μM Rac1.



concentration, where $k_{\text{obs}} = k_{+1}[\text{Rac1}] + k_{-1}$. A plot of k_{obs} against time would give a straight line of slope k_{+1} with the intercept of the y-axis, k_{-1} .

The simplest interpretation consistent with the data is to assume that this interaction is a 2 step process, with a rapid equilibrium binding step followed by a slow conformational change, with the second step giving rise to an observed fluorescence change. Scheme 6.1. describes the simplest reaction scheme for the interaction of Rac1 with MDCC-GDI. The result of a rapid equilibrium of the initial binding step is that the rate of formation of the Rac1·MDCC-GDI* is controlled at any one time by the fraction of Rac1·MDCC-GDI complex at equilibrium. The data were fitted well to single exponentials and the line is a best fit to a hyperbolic curve (figure 6.19b), where step 1 is assumed to be rapid, so the observed rate constant (k_{obs}) equals:

$$k_{\text{obs}} = \frac{k_{+2}}{1 + (K_1 [\text{Rac}])} + k_{-2} \quad \text{equation 6.1.}$$

Where K_1 = equilibrium dissociation constant of the first step (k_{-1}/k_{+1}), so that a plot of k_{obs} against $[\text{Rac}]$ gives a hyperbolic relationship. A value for $k_{+2} + k_{-2}$ is given by the maximum value of the hyperbolic curve of 19.6s^{-1} , and the fitting the full set of data to equation 6.1. allowed determination of the dissociation constant of the initial rapid binding process, k_{-1}/k_{+1} of $19.6\mu\text{M}$. The intercept of the y-axis = k_{-2} . However, this value is close to zero and cannot be determined accurately from the fitted curve (see figure 6.19b.). A value for k_{-2} has been determined independently by a displacement reaction (6.16.2.).

Concentrations of Rac1 $>25\mu\text{M}$ were not used to try and obtain a saturating rate under these conditions (figure 6.19b.). This is because the effect of [modified peptide] at high

Scheme 6.1. Kinetic mechanism of Rac1 binding to MDCC-GDI

A two step binding model has been used to interpret kinetic data. Step 2 (k_{+2}) represents a conformational change that includes a fluorescence change (*) of MDCC-GDI. The equilibrium constant and forward and reverse rate constants for step a are defined as K_a , k_{+a} and k_{-a} respectively.



[Rac1] under these conditions is currently unknown. As the order of binding of the farnesyl 9-mer and Rac1 to MDCC-GDI has not been established, it is possible that the modified peptide binds to GDI under these conditions in the absence of Rac1, with the binding of Rac1 required for an observed fluorescence change. However, it is also possible that the three components bind simultaneously under these conditions, and it may be important to have the modified peptide and the Rac1 at similar concentrations. As the farnesyl 9-mer used for these experiments was limited due to practical problems (2.5.1.), experiments at high [Rac1] and [farnesyl 9-mer] have yet to be investigated.

6.16.2. Dissociation of the Rac1·MDCC-GDI complex

Dissociation kinetics have been measured by displacing MDCC-GDI from its complex with unmodified Rac1 by mixing with a large excess of unlabelled GDI (figure 6.20.). Premixing of a solution containing 0.1 μM MDCC-GDI plus equimolar Rac1 and excess farnesyl 9-mer, then rapidly mixing with excess unlabelled GDI produced an exponential decay in fluorescence; this is assumed to be controlled by the dissociation rate constant (k_{-2}) of Rac1 from MDCC-GDI.

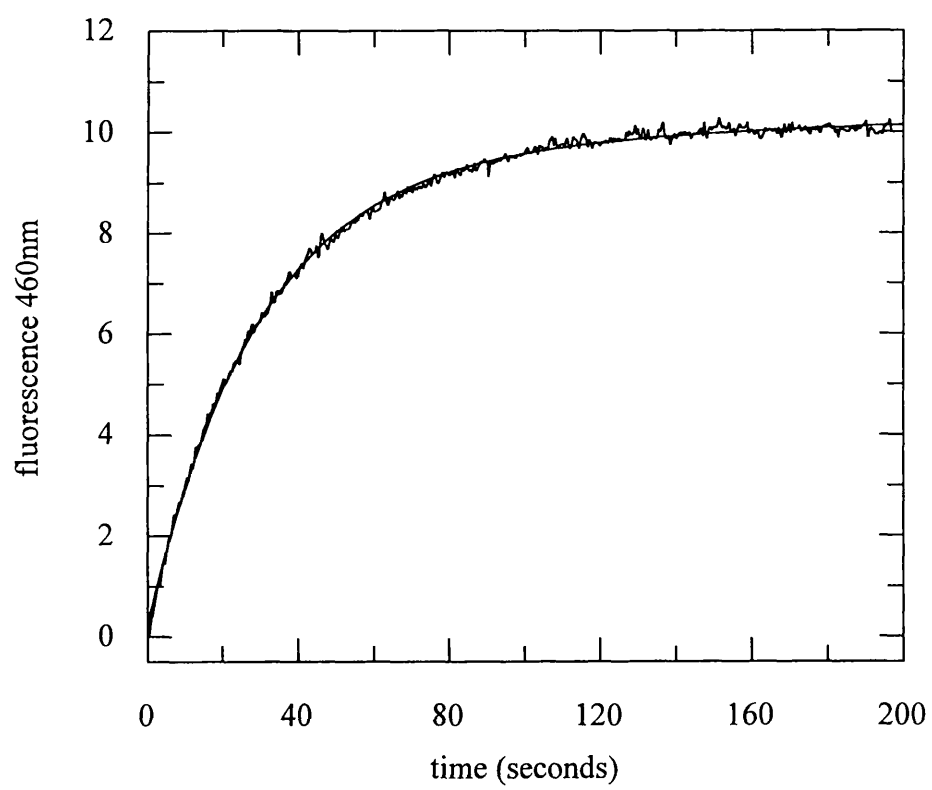
The data were fitted well to a single exponential and gave a first order rate constant of $3.3 \times 10^{-2} \text{s}^{-1}$. As inactive Rac1 exists mainly as cytosolic complex with GDI in vivo, this slow rate of dissociation is likely to be too slow to explain the biological activities of Rac1 in the cell. This system should be useful to examine the factors that dissociate the Rac1·GDI complex.

6.16.3. Affinity of the Rac1·MDCC-GDI interaction

Using these figures, an overall dissociation constant (K_d) for the interaction of Rac1 with MDCC-GDI may be calculated. As the value for k_{-2} is small ($3.3 \times 10^{-2} \text{s}^{-1}$), k_{+2} may be assigned a first order rate constant of 19.6s^{-1} . The overall K_d for the reaction may be defined as $K_1 \times K_2$ (where K_1 and K_2 represent the dissociation constant and equilibrium

Figure 6.20. Displacement kinetics (k_2) of MDCC-GDI from a complex with Rac1

MDCC-GDI (0.1 μ M) was incubated in a syringe with equimolar *E.coli* Rac1 and modified farnesyl-9mer. MDCC-GDI was then displaced from its complex with Rac1 by pushing this solution against unlabelled GDI (4 μ M) (mixing chamber concentrations) in buffer A at 20°C. The line shows a best fit to a single exponential and the fitted curve corresponds to a rate constant of 3.3x10⁻²s⁻¹ (average of 4 runs).

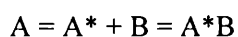


constant (k_{-a}/k_{+a}) for steps 1. and 2. Respectively). Using best fit values of 19.6×10^{-6} M, $k_{+2} = 19.6\text{s}^{-1}$ and $k_{-2} = 3.3 \times 10^{-2}\text{s}^{-1}$, the $K_d =$

$$19.6 \times 10^{-6} \text{ M} \times (3.3 \times 10^{-2} \text{ s}^{-1} / 19.6 \text{ s}^{-1}) = 33 \text{ nM}$$

The calculated K_d value for this interaction determined from association and dissociation rate constants is within an order of magnitude of the K_d value determined from equilibrium titration experiments of ~~<5nM.~~ Minor discrepancies between overall K_d values obtained may be due to the concentration ranges used for titration experiments. Due to the tight binding of the Rac1 under these conditions, concentrations do not span the K_d value and therefore determination of an accurate K_d using this method is technically difficult (6.7.).

These results indicate that Rac1 has an affinity for MDCC-GDI (in the presence of excess farnesyl 9-mer) less than two orders of magnitude weaker than modified Rac1. Although this two step binding model has been used to interpret these results, the analysis of two step processes may become complex, as other possible binding mechanisms may produce hyperbolic behaviour between the observed rate constant and [Rac1]. These include isomerisation of one of the proteins prior to complex formation:



The analysis of the Rac1·MDCC-GDI interaction described here also assumes that only a signal from MDCC-GDI·Rac1 is observed, whereas MDCC-GDI·Rac1 (prior to an isomerisation step) may also contribute to the signal. Other possibilities that would produce hyperbolic behaviour are discussed further in Gutfreund (1997).

CHAPTER 7. CONCLUSION

7.1. Interaction of Rac1 with p67^{phox}

Spectroscopic studies have been used in an attempt to investigate the interaction of Rac1 with p67^{phox}, a component of the phagocyte NADPH oxidase (1.3.). p67^{phox} has been successfully purified from baculovirus infected insect cells. Although a previous report indicates a fluorescence change when p67^{phox} binds to Rac1 complexed with the fluorescent nucleotide analogue, mantGMPPNP (Nisimoto *et al.*, 1997), these results could not be repeated. Purification of p67^{phox} from insect cells indicates that this protein is susceptible to minor proteolytic degradation. Although fractions containing the larger of the two major species purified (2.3.4.) were used for subsequent biochemical studies, it is possible that this protein is truncated at the N terminus, causing disruption of TPRs (tetracoipeptide repeats). Due to the relatively large size of p67^{phox}, determination of the molecular weight of this purified protein could not be accurately determined by mass spectrometry. It is also possible that extended incubation of *Sf9* insect cells to express p67^{phox} in this laboratory causes this protein to adopt a conformationally inactive state. This conformational change may be induced by post-translational modification of the protein by the insect cells. It has also been reported that p67^{phox} is unstable, with significantly reduced Rac1 binding affinity following >48 hours at -80°C (Leto *et al.*, 1991). This suggests that p67^{phox} may adopt an inactive conformation during expression, or shortly after purification of the protein from insect cells.

The interaction of p67^{phox} with Rac1 complexed to the non-hydrolysable fluorescent analogue, but-edaGMPPNP has also been examined. It was hoped that due to the exposed nature of the fluorophore and the high fluorescence quantum yield (3.4.1.), this fluorescent analogue would provide an alternative and sensitive method to monitor this interaction. However, p67^{phox} and p67¹⁻¹⁹⁹ had little effect on the fluorescence of a

Rac1·but-edaGMPPNP complex. It is possible that this nucleotide analogue is not sensitive to the Rac1·p67^{phox} interaction or no binding occurs under these conditions.

7.2. Interaction of Rac1 with p67¹⁻¹⁹⁹

Despite showing stability problems (5.2.), p67¹⁻¹⁹⁹ has also been successfully purified from *E.coli* and labelled with a number of environmentally sensitive fluorophores. However, none of these labelled proteins show a significant fluorescence change when incubated with Q61L Rac1·GTP. It is possible that the positions of the fluorophores are not sensitive to Rac1 binding, or that a significant proportion of the active protein is not labelled under these conditions.

Secondary structure prediction of p67¹⁻¹⁹⁹ indicates an almost completely α helical domain, and sequence alignment with known protein structures suggests that p67^{phox} shares greatest homology with the tetracoipeptide region (TPR) (Koga *et al.*, 1999). It is possible that N terminal truncation of the full length protein disrupts TPRs or similar tertiary structure motif. It is likely that a conformationally active N terminal domain is essential for the interaction of Rac1 with p67^{phox}, with the stability of this fragment dependent on the remainder of the protein. The effect of the additional N and C terminal residues of the p67¹⁻¹⁹⁹ expressed in this laboratory (figure 5.1.) on the tertiary structure of this domain has yet to be established. A recent report has indicated that the three tandemly arranged TPR motifs at the N terminus of p67^{phox} are essential for the interaction with Rac1 (Koga *et al.*, 1999); this may explain the lack of detectable binding between Rac1 and the p67¹⁷⁰⁻¹⁹⁹ peptide, reported to contain the Rac1 binding region.

7.3. Interaction of Rac1 with GDI

Fluorescent approaches have also been developed to monitor the interaction of Rac1 with its guanine nucleotide dissociation inhibitor, RhoGDI (GDI). In an attempt to overcome problems inherent in using baculovirus expressed Rac1 (6.1.), a novel approach has been

developed using synthetic peptides corresponding to the C terminal region of Rac1. These peptides have been successfully modified on the single cysteine (corresponding to residue Cys188 of fully processed Rac1). A combination of *E.coli* expressed, truncated Rac1 and farnesylated peptide mimics isoprenylated Rac1 and interacts with MDCC-GDI (6.3.), resulting in a >30% quenching of MDCC-GDI fluorescence at saturating concentrations of Rac1. This system has been used to examine the interaction of Rac1 and a number of Rac1 mutants, to investigate the role of different regions of Rac1 in GDI interaction. Because the modified peptide and the 'rest' of Rac1 are separated, this system is likely to be sensitive to conformational changes in the Rac1 structure induced by different nucleotides and Rac1 mutations.

As no fluorescence change is observed when truncated Rac1 or the farnesyl peptide is added alone, it is assumed that a ternary complex between the three components (MDCC-GDI, Rac1 and farnesyl peptide) is required for an observed fluorescence change. The structure of the C terminal domain of GDI indicates that Cys 79 (the site of MDCC labelling) is close to the base of the lipid binding pocket suggested for the lipid (Keep *et al.*, 1997, Gosser *et al.*, 1997). It is possible that truncated Rac1 (in the absence of farnesylated peptide) binds to GDI, despite the lack of fluorescence change. However, the results presented here are consistent with nucleotide dissociation experiments (Sasaki *et al.*, 1993) indicating that truncated Rac1 binds weakly to GDI. Although modified peptides in the absence of truncated Rac1 cause little or no change in MDCC-GDI fluorescence, structural studies suggest that a farnesylated peptide binds to the C terminal domain of GDI in the absence of Rac1 and induces a conformational change in the GDI structure. It is therefore possible that the farnesylated peptide induces a conformational change in the GDI structure favourable for Rac1 binding, with an additional conformational change (and an associated quenching of MDCC fluorescence) occurring upon interaction with Rac1.

Truncated Rac1 (in the presence of saturating concentrations of farnesyl 9-mer) binds tightly to GDI, less than two orders of magnitude weaker than Rac1; the value in the latter case being derived from kinetic measurements (Newcombe *et al.*, 1999). This suggests that the main bulk of the Rac1 has significant interactions with GDI remote from the lipid binding region. Structural data has indicated that GDI may be divided into two regions: a flexible N terminal domain of ~60 aa's that is disordered in the absence of small G protein and a well ordered C terminal domain containing the lipid binding pocket. This suggests that the interaction between Rac1 and GDI is more complex than the interaction of two more or less globular proteins, with almost any region of the Rac1 structure being involved.

In contrast, a farnesyl 12-mer peptide (in the presence of saturating concentrations of truncated Rac1) binds several orders of magnitude weaker than modified Rac1. A number of factors may contribute to this weaker affinity. Although Rac1 is geranylgeranylated *in vivo*, chemical farnesylation of C terminal peptides was chosen due to the availability of the farnesyl bromide. Presumably the smaller farnesyl group sits in the hydrophobic pocket in the C-terminal domain of GDI, but interactions with the complete surface of the pocket may not be involved. The effect of this alternative lipid moiety on Rac1 binding has yet to be established. *In vivo*, Rac1 is geranylgeranylated on the cysteine of the C terminal -CLLL motif, followed by proteolytic cleavage of the three terminal residues (-LLL) and methylation of the resulting cysteine (1.13.1.). Geranylgeranylated Rac1 (with the complete -CLLL motif) has been shown to bind to GDI, but with a weaker affinity than fully processed Rac1 (Hancock & Hall, 1993). As the farnesyl 12-mer contains a complete C terminal sequence, it is possible that this is one reason for the reduced affinity of the Rac1-GDI interaction. Rac1 and the C terminal 12-mer also have four overlapping residues (Rac1 = residues 1-184, farnesyl 12-mer = 180-192). These overlapping residues may sterically hinder the interaction of Rac1 and GDI, reducing the binding affinity under these conditions.

A farnesyl 7-mer, in which the polybasic region is incomplete, binds an order of magnitude weaker than farnesyl 12-mer, and the C terminal 12-mer in the absence of bound lipid seems to bind to GDI, as seen from titration experiments (table 6.2.). These results suggest that an extended C terminal region (containing the polybasic region in the case of Rac1) is important for the interaction with GDI. Despite both Rac isoforms binding to GDI, Rac1, but not Rac2 (figure 1.2.) contains a polybasic stretch at the C terminus. This indicates that the polybasic sequence of Rac1 may not be essential for the interaction with GDI. This region is currently under investigation using mutant C terminal peptides in this laboratory.

7.3.1. Interaction of Rac1·GTP with GDI

These results also indicate that guanosine triphosphate complexes of truncated Rac1 are unable to bind tightly to GDI (at least two orders of magnitude weaker than the GDP bound form – see table 6.2.). The weak interaction between the Q61L Rac1·GTP and GDI may be explained by the small amount of Q61L Rac1 with diphosphate bound (~6%). The majority of recent reports have shown that the GTP bound forms of Rho family proteins bind weakly to GDI. However, a number of earlier reports indicate that both the GDP and GTP bound forms of bind with a similar affinity, or the GTP bound form binds weakly (6.8.). The major technique used in these earlier reports is also equilibrium titration experiments, and discrepancies may in part be due to concentrations used. As described previously (6.7.), it is technically very difficult to obtain an accurate K_d value unless concentration ranges used span the K_d value. A major aim of this report was to use farnesylated peptides to determine the relative importance of different parts of Rac1 in GDI binding. The C terminal region, represented by the farnesylated peptide, contributes to binding, and the modified peptide may bind independently of whether GTP or GDP is bound to Rac1. The conformation of the C terminal region is not defined in the available structures (Hirshberg *et al.*, 1997, Hirshberg, Newcombe & Webb, unpublished results). However, once the contribution of the remainder of the Rac1 is added, this could result in

tight binding of the GDP form and weak binding of Rac1 in the GTP conformation. These results suggest that the regions involved in the conformational change between the GDP and GTP bound forms of Rac1 are important for the interaction with GDI.

7.3.2. Interaction of Rac1 mutants with GDI

The mechanistic aspects of the interaction of Rac1 with GDI are poorly understood. The structure of GDI has been solved by both NMR and crystallography (Gosser *et al.*, 1997, Keep *et al.*, 1997), and recently X-ray diffraction studies have been undertaken on the RhoA-GDI complex, following co-expression and purification of the complex from *Saccharomyces cerevisiae* (Longenecker *et al.*, 1999). Although detailed characterisation of the contacts between individual amino acids is not possible from this low resolution structure, the structure suggests that residues Arg 68, Leu 69, Pro 71, Pro 75, His 105, Phe 106 and Pro 108 of RhoA (residues of switch II and helix $\alpha 3$) are close enough to form contacts with the flexible C-terminus of GDI.

One of the most important questions with respect to the structure of GDI is the conformation of the N-terminal region in complex with RhoA. Residues 23-59 of the N terminal region of GDI are essential for the inhibition of nucleotide dissociation and extraction of Rho proteins from membranes, but these residues are disordered in the absence of small G protein (Gosser *et al.*, 1997, Keep *et al.*, 1997). It is possible that the N terminal domain of GDI interacts with Rac1, causing structural alterations and allowing the geranylgeranyl group of Rac1 to become available to GDI. This model would be consistent with proposed 2 step kinetics of membrane extraction reported by Nomanbhoy *et al.* (1999) and consistent with results presented in this report.

To examine the regions of Rac1 involved in the interaction with GDI, a number of Rac1 mutants have been made (Chapter 4.). As expected, point mutations in the insertion loop to corresponding residues of cdc42 (figure 1.2.) (D124S, K130A, E131K) showed little

change in the basic biochemical properties of Rac1, or dissociation constants for the interaction with GDI. Point mutations in this region to reverse a charge of exposed residues in this loop (eg. E127A) also had little effect on affinity for GDI, suggesting that this region is not essential for the Rac1-GDI interaction. However, two mutations in the effector loop of Rac1 (aa's 30-40), I33D and F37E (residues changed to the corresponding amino acids in Ras) (figure 4.2.), significantly reduce the interaction of Rac1 with GDI. This has been determined by Rac1 dependent quenching of MDCC-GDI fluorescence in the presence of farnesyl modified peptides, and the effect of GDI on nucleotide exchange of I33D Rac1, both in the presence of excess farnesyl 12-mer. Crystal structures of Rho family proteins reveal that the effector loop (residues 30-40) shows significant conformational change between the two nucleotide bound states. This loop is therefore a potential region involved in the Rac1-GDI interaction. Both I33D and F37E Rac1 mutants are purified with bound GDP and it is therefore unlikely that these point mutations cause a major alteration to the Rac1 structure. However, nucleotide exchange experiments using mantGDP reveal no detectable interaction between F37E Rac1 and the fluorescent nucleotide under accelerated exchange conditions (figure 4.4.). It is possible that this mutant does not bind this fluorescent analogue, or that a fluorescence change is not observed when this mutant binds mantGDP. As this mutant has only recently been purified, the nucleotide binding properties of this protein are currently under investigation using alternative techniques in this laboratory.

7.3.3. Interaction of the Rac1/H-Ras chimaera with GDI

Complete removal of the insertion loop and replacement with the corresponding 8 residues of Ras (2.6.4.) also has little effect on the interaction of Rac1 with GDI in the peptide assay. These results are consistent with the results described by Wu *et al.*, (1997) using a prenylated (baculovirus expressed) cdc42/Ras 'insertion loop' chimaera and provide further evidence that the insertion loop of Rac1 does not play a major role in the interaction with GDI. Wu *et al.*, (1997) have also reported that although the insertion loop

is not essential for the interaction with GDI, this loop is required for GDI to inhibit nucleotide exchange from cdc42. Early experiments with the Rac1/H-Ras chimaera and farnesyl 12-mer under conditions as described (figure 6.11.) indicate that the insertion loop does not play a major role in the inhibitory action of GDI under these conditions (data not shown). The effect of GDI on nucleotide dissociation from the Rac1/Ras chimaera in the presence of excess farnesyl 9-mer is currently under investigation.

Reported experiments using a Ras chimaeric protein (with the insertion loop and C-terminal 8 residues of cdc42) (Wu *et al.*, 1997) did not render GDI sensitivity to Ras, indicating that other conserved regions of Rho family proteins are essential for GDI interaction. As point mutations at positions 33 or 37 of Rac1 significantly reduce the interaction with GDI, it is possible that residues 32-38 of the effector loop confer Rho family specificity for the GDI interaction. This would be in agreement with a low resolution structure of the RhoA·GDI complex indicating that the N-terminal region of GDI forms a loop, making possible contacts with the effector loop and the switch II region. To further investigate this possibility, the construction of an *E.coli* expressed, truncated H-Ras vector containing D33I and E37F mutations has been designed and is currently under development in this laboratory.

7.4. The role of the effector loop in GDI interaction

Recent reports also indicate a role the effector loop in the interaction of Rho proteins with GDI. Treatment of cells with the cytotoxins *Clostridium difficile* A and B cause disaggregation of actin structures. These toxins monoglucosylate Rho proteins at the effector domain residue, threonine 37 (residue 35 of Rac proteins). Glucosylation at this residue of RhoA does not significantly alter binding of guanine nucleotides, and has only a small affect on intrinsic GTPase activity (reduced by a factor of ~ 5) (Genth *et al.*, 1999). However, glucosylated Rho showed no binding to GDI, as examined by coprecipitation experiments (Genth *et al.*, 1999). In addition, GDI completely extracted

unmodified (non-glucosylated) RhoA from membranes, but was incapable of releasing glucosylated RhoA. RhoA in complex with GDI is not a substrate for these toxins, and these results suggest that this may be due to the inaccessibility of the toxin recognition site, or inaccessibility of threonine 37 of RhoA. The fact that glucosylated RhoA does not form a complex with GDI provides further evidence that GDI interacts with the effector loop of Rho family proteins. Results in this laboratory using the peptide binding assay have shown that a T35A Rac1 mutant binds to GDI with a similar affinity to wild type Rac1, whereas I33D and F37E Rac1 mutants significantly reduce this interaction. These results suggest that T35 of Rac1 is not an essential residue for GDI binding, and supports results from Genth *et al.*, (1999) that glucosylation at threonine 37 (corresponding residue 35 of Rac1 – figure 1.2.) is likely to sterically hinder the interaction of the N terminal domain of GDI with the effector loop of Rho family proteins. Primary sequence alignment reveals that I33 and F37 are conserved residues in Rho family proteins and form an extended basic region (figure 4.2.) that is absent in Ras proteins. Residues 33-37 of the effector loop of Rac1 may form an essential binding motif, providing GDI specificity for Rho family proteins.

A recent report by Fauré *et al.* (1999) has shown that phosphoinositides partially open, but do not fully dissociate a RhoA·GDI complex. These results show that phosphoinositides enhance both ADP ribosylation and GDP/GTP exchange in the prenylated RhoA·GDI complex, and further investigation revealed that this was due to limited opening of the RhoA·GDI complex, without the release of RhoA (Fauré *et al.*, 1999). In addition, the [$\gamma^{35}\text{S}$]GTP incorporation was markedly increased in the presence of phosphoinositides. A complex between unprenylated RhoA (expressed in *E.coli*) and GDI was also purified, but this complex was not sensitive to phosphoinositides. The extent of ADP ribosylation of RhoA in the unprenylated RhoA·GDI complex (in the absence of phosphoinositides) was as high as that found for prenylated RhoA·GDI

complex treated with PtdIns₄P, and similar to that found for GST-RhoA immobilised on glutathione sepharose beads.

These results indicate that the phosphoinositide effect on the RhoA·GDI complex is mediated by the isoprene moiety of RhoA. A complex between unprenylated RhoA and GDI is accessible to the ADP-ribosyl transferase of *Clostridium botulinum*, and suggests that the two recombinant RhoA·GDI complexes (with prenylated and unprenylated RhoA) differ by their interacting sites. Unprenylated RhoA is likely to interact with GDI via protein·protein contacts, but prenylated RhoA has additional interactions involving its prenyl tail and the hydrophobic pocket of GDI. This suggests the formation of a partially opened RhoA·GDI complex in which the two proteins may partially dissociate, releasing the isoprenyl group at the C terminus of RhoA. This partially opened complex may bind to membranes via the isoprenyl group of RhoA allowing membrane association, with full dissociation of GDI mediated by additional stimuli.

The results presented here and recent published reports suggest that the association of Rho family proteins with GDI involves at least two distinct regions of the Rac1 structure. It is possible that dissociation of the Rac1·GDI complex occurs via two distinct steps. In the first step, phosphoinositides or other stimuli may partially open the complex, allowing nucleotide exchange and interaction with membranes. The second step would then be full dissociation of the complex, with release of GDI into the cytosol. Three specific membrane proteins have also been identified that associate with a RhoA·GDI complex that do not correspond to GDS, GAP or ERM proteins (Fauré *et al.*, 1999). A membrane associated protein has been reported to release prenylated Rab from a Rab·GDI complex (Dirac-Svejstrup *et al.*, 1997), and it is possible that a similar membrane factor is involved in fully dissociating the Rho·GDI complex. The interaction of Rac1 with saturating concentrations of farnesyl modified peptide as described in this report, may represent the protein·protein interactions that occur between Rac1 and GDI in a partially

dissociated state. This system is likely to be useful to examine additional regions of Rac1 involved in the interaction with GDI and to investigate factors that fully dissociate the Rac1·GDI complex.

ACKNOWLEDGMENTS

I would like to express my thanks to Dr. Martin Webb for his guidance and advice and over the past 3 years, in particular for his help and patience with the analysis of kinetic data. My gratitude also for his assistance with fluorescence techniques and for supplies of fluorescent nucleotide analogues. I would also like to thank Jackie Hunter for sharing her knowledge and experience of protein purification procedures, baculovirus methods, for stocks of farnesyl labelled peptides and GDI. Thanks to Dr. Martin Brune for his advice on molecular biology techniques and fluorescence labelling and Dr. Molly Strom for her help in the early stages of DNA sequencing. I am also grateful to Dr. Steve Howell for performing mass spectrometry of protein samples, and Dr. Miri Hirshberg for her comments on the Rac structures, and for the on going crystallographic collaboration between our laboratories. Many thanks also to the Photographics department for colour figures and media labs for endless amounts of L-broth. In conclusion I would like to thank my wife Claire for her support over the years we have been together; without her help I would not have got to where I am today. Thanks also for putting up with my grumpiness over the last few months and for much needed help proof-reading and preparation of the final draft (now that I've finished I promise I will finish decorating the living room!). Thanks also to my parents for their continuing support and interest not only in the past 3 years, but also over the last 6 years as a student.

REFERENCES

- Abo A, Boyhan A, West I, Thrasher AJ, Segal AW. Reconstitution of Neutrophil NADPH Oxidase Activity in the Cell-free System by Four Components: p67^{phox}, p47^{phox}, p21rac1, and Cytochrome b245. *J.Biol.Chem.* 1992;267:16767-70.
- Abo A, Qu J, Cammarano MS, Dan C, Fritsch A, Baud V, *et al.* PAK4, a novel effector for Cdc42Hs, is implicated in the reorganisation of the actin cytoskeleton and in the formation of filopodia. *EMBO J.* 1998;17(22):6527-40.
- Adams AE, Johnson DI, Longnecker RM, Sloat BF, Pringle JR. CDC42 and CDC43, two additional genes involved in budding and the establishment of cell polarity in the yeast *Saccharomyces cerevisiae*. *J Cell Biol.* 1990;111:131-42.
- Adamson P, Marshall CJ, Hall A, Tilbrook PA. Post-translational modifications of p21rho proteins. *J.Biol.Chem.* 1992;267:20033-8.
- Adamson P, Patterson HF, Hall A. Intracellular localization of the p21rho proteins. *J Cell Biol.* 1992b ;119:617-27.
- Adra CN, Manor D, Ko JL, Zhu S, Horiuchi T, Van Aelst L, *et al.* RhoGDIγ: A GDP-dissociation inhibitor for Rho proteins with preferential expression in brain and pancreas. *Proc. Natl. Acad. Sci* 1997;94:4279-84.
- Ahmed S, Prigmore E, Govind S, Varyard C, Kozma R, Wientjes FB, *et al.* Cryptic Rac-binding and p21 Cdc42HS/Rac-activated sites of NADPH Oxidase Component p67^{phox}. *J.Biol.Chem.* 1998;273 (25):15693-707.
- Altschul SF, Madden TL, Schaffer AA, Zhang J, Zhang Z, Miller W, Lipman DJ. Gapped BLAST and PSI-BLAST: a new generation of protein database search programs. *Nucleic Acids Res.* 1997;25:3389-3402
- Armstrong SA, Hannah VC, Goldstein JL, Brown MS. CAAX Geranylgeranyl Transferase Transfers Farnesyl as Efficiently as Geranylgeranyl to RhoB. *J.Biol.Chem.* 1995;270(14):7864-8.
- Aspenström P. The Rho GTPases Have Multiple Effects on the Actin Cytoskeleton. *Exp Cell Res.* 1999;246:20-5.
- Backlund PS. Carboxyl methylation of the low molecular weight GTP-binding protein G25K: regulation of carboxyl methylation by RhoGDI. *Biochem.. Biophys. Res. Comm.* 1993;192(2):534-42.
- Backlund PS. Post-translational Processing of RhoA. *J.Biol.Chem.* 1997;272 (52):33175-80.
- Bagrodia S, Taylor SJ, Creasy CL, Chernoff J, Cerione RA. Identification of a Mouse p21 cdc42/Rac Activated kinase. *J.Biol.Chem.* 1995;270(39):22731-7.
- Bagrodia S, Dérjard B, Davis RJ, Cerione RA. Cdc42 and Pak-mediated Signalling Leads to Jun Kinase and p38 Mitogen-Activated Protein Kinase Activation. *J.Biol.Chem.* 1995b ;270(47):27995-8.
- Barbacid M. ras genes. *Annu. Rev. Biochem.* 1987;56:779-827.
- Barrett T, Xiao B, Dodson EJ, Dodson G, Ludbrook SB, Nurahomed K, *et al.* The structure of the GTPase-activating domain from p50 RhoGAP. *Nature* 1997;385:458-61.
- Bar-Sagi D, Feramisco JR. Induction of membrane ruffling and fluid-phase pinocytosis in quiescent fibroblasts by ras proteins. *Science* 1986;233:1061-8.
- Bashour A, Fullerton AT, Hand MJ, Bloom GS. IQGAP1, a Rac- and Cdc42-binding Protein, Directly Binds and Cross-links Microfilaments. *J.Cell. Biol.* 1997;137(7):1555-66.
- Bender A, Pringle JR. Multicopy suppression of the cdc24 budding defect in yeast by CDC42 and three newly identified genes including the Ras-related gene RSR1. *Proc. Natl. Acad. Sci* 1989;86:9976-80.
- Best A, Ahmed S, Kozma R, Lim L. The Ras-related GTPase Rac1 Binds Tubulin. *J.Biol.Chem.* 1996;271:3756-62.
- Bokoch GM, Quilliam LA, Bohl BP, Jesaitis AJ, Quinn MT. Inhibition of Rap1A binding to cytochrome b558 of NADPH oxidase by phosphorylation of Rap1A. *Science* 1991;254:1794-6.
- Bourmeyster N, Vignais PV. Phosphorylation of Rho GDI Stabilizes the RhoA-RhoGDI Complex in Neutrophil Cytosol. *Biochem. Biophys. Res. Comm.* 1996;218:54-60.
- Brill S, Li S, Lyman CW, Church DM, Wasmuth JJ, Weissbach L, *et al.* The Ras GTPase-activating-protein-

related human IQGAP2 harbors a potential actin binding domain and interacts with calmodulin and Rho family GTPases. *Mol Cell Biol.* 1996;16:4869-78.

Brownbridge GG, Lowe PN, Moore KJM, Skinner RH, Webb MR. Interaction of GTPase Activating Proteins (GAPs) with p21ras Measured by a Novel Fluorescence Anisotropy Method. *J.Biol.Chem.* 1993;268,(15):10914-9.

Brune M, Hunter JL, Corrie JET, Webb M. Direct, Real-Time Measurement of Rapid Inorganic Phosphate Release Using a Novel Fluorescent Probe and Its Application to Actomyosin Subfragment I ATPase. *Biochemistry* 1994;33,(27):8262-71.

Burgering BMT, Bos JL. Regulation of Ras-mediated signalling: more than one way to skin a cat. *Trends Biochem Sci.* 1995;20, January:18-22.

Chang EH, Furth ME, Scolnick EM, Lowy DR. Tumorigenic transformation of mammalian cells induced by a normal gene homologous to the oncogene of Harvey murine sarcoma virus. *Nature* 1984;297:479-83.

Chardin P, Boquet P, Maduale P, Popoff MR, Rubin EJ, Gill DM. The mammalian G protein rhoC is ADP-ribosylated by *Clostridium botulinum* exoenzyme C3 and affects actin microfilaments in Vero cells. *EMBO J.* 1988;8:1087-92.

Chen MX, Cohen PT. Activation of protein phosphatase 5 by limited proteolysis or the binding of polyunsaturated fatty acids to the TPR domain. *FEBS lett.* 1997;400(1):136-40.

Chuang T, Xu X, Knaus UG, Hart MJ, Bokock GM. GDP Dissociation Inhibitor Prevents Intrinsic and GTPase Activating Protein-stimulated GTP Hydrolysis by the Rac GTP-binding Protein. *J.Biol.Chem.* 1993;268:775-8.

Chuang T, Bohl BP, Bokock G. Biologically Active Lipids Are Regulators of Rac.GDI Complexation. *J.Biol.Chem.* 1993b ;268,(35):26206-11.

Chuang T, Xu X, Quilliam LA, Bokock GM. SmgGDS stabilizes nucleotide-bound and -free forms of Rac1 GTP-binding protein and stimulates GTP/GDP exchange through a substituted enzyme mechanism. *Biochem J.* 1994;303:761-7.

Clarke S, Vogel JP, Deschenes RJ, Stock J. Posttranslational modification of the Ha-Ras oncogene protein: evidence for a third class of carboxyl methyltransferases. *Proc. Natl. Acad. Sci* 1988;85(13):4643-7.

Colombo MI, Inglese J, D'Souza-Schorey C, Beron W, Stahl PD. Heterotrimeric G proteins Interact with the Small GTPase ARF. *J.Biol.Chem.* 1995;270(41):24564-71.

Crichton TE. 1993. In *Proteins*. pp26-28. W.H. Freeman and Company.

Crossen R, Gruenwald S. 1997. In *Baculovirus expression system manual*. 4th ed.: Pharmingen.

Cuff JA, Clamp ME, Siddiqui AS, Finlay M, Barton GJ. Jpred: a consensus secondary structure prediction server. *Bioinformatics.* 1998;14:892-893

Daniels RH, Bokoch GM. p21-Activated protein kinase: a crucial component of morphological signaling? *Trends Biochem Sci.* 1999;24(9):350-5.

Das AK, Cohen PT, Barford D. The structure of tetratricopeptide repeats of protein phosphatase 5: implications for TPR-mediated protein-protein interactions. *EMBO J.* 1998;17(5):1192-1199

Dawson RM, Elliott DC, Elliott WH, Jones KM. 1984. In *Data for Biochemical Research*. 3rd ed. Oxford: Oxford Scientific Publications, Clarendon Press, Oxford.

DeMendez I, Garrett MC, Adams AG, Leto TL. Role of p67^{phox} SH3 Domains in Assembly of the NADPH Oxidase System. *J.Biol.Chem.* 1994;269(23):16326-32.

Derry JM, Ochs HD, Francke U. Isolation of a novel gene mutated in Wiscott-Aldrich syndrome. *Cell* 1994;78:635-44.

Desrosiers R, Tanguay RM. Methylation of Drosophila histones at proline, lysine, and arginine residues during heat shock. *J.Biol.Chem.* 1988;263(10):4686-92.

Didsbury JR, Uhling RJ, Snyderman R. Isoprenylation of the low molecular mass GTP-binding proteins Rac1 and Rac2: Possible role in membrane localization. *Biochem. Biophys. Res Comm.* 1990;171:804-12.

Didsbury JR, Weber RF, Bokock GM, Evans T, Snyderman R. rac, a Novel ras-related Family of Proteins That Are Botulinum Toxin Substrates. *J.Biol.Chem.* 1989;264:16378-82.

Diekmann D, Abo A, Johnston C, Segal AW, Hall A. Interaction of Rac with p67^{phox} and Regulation of

Phagocytic NADPH Oxidase Activity. *Science* 1994;265:531-3.

DiNubile MJ, Huang S. High concentrations of phosphatidylinositol-4,5-bisphosphate may promote actin filament growth by three potential mechanisms: inhibiting capping by neutrophil lysates, severing actin filaments and removing capping protein- β 2 from barbed ends. *Biochim. Biophys. Acta.* 1997;1358(3):261-78.

Dirac-Svejstrup AB, Sumizawa T, Pfeffer SR. Identification of a GDI displacement factor that releases endosomal Rab GTPases from RabGDI. *EMBO J.* 1997;16:366-472.

Dorseuil O, Reibel L, Bokock GM, Camonis J, Gacon G. The Rac Target NADPH Oxidase p67^{phox} Interacts Preferentially with Rac2 Rather Than Rac1. *J.Biol.Chem.* 1996;271,(1):83-8.

Dudler T, Gelb MH. Palmitoylation of Ha-Ras Facilitates Membrane Binding, Activation of Downstream Effectors, and Meiotic Maturation in Xenopus Oocytes. *J.Biol.Chem.* 1996;271 (19):11541-7.

Eccleston JF, Moore KJ, Morgan L, Skinner RH, Lowe PN. Kinetics of Interaction between Normal and Proline 12 Ras and the GTPase-activating Proteins p120-GAP and Neurofibromin. *J. Biol. Chem.* 1993;268, (36):27012-27019

Eccleston JF. In *Spectrophotometry & spectrofluorimetry*. 1987. (Harris DA, Bashford CL., Ed.) pp 137-164.

El Benna J, Dang PM, Gaudry M, Fay M, Morel F, Hakim J, *et al.* Phosphorylation of the Respiratory Burst Oxidase Subunit p67^{phox} during Human Neutrophil Activation. *J.Biol.Chem.* 1997;272(27):17204-8.

Eyk JEV, Arrell DK, Foster DB, Strauss JD, Heinonen TYK, Furmaniak-Kazmierczak E, *et al.* Different Molecular Mechanisms for Rho Family GTPase-dependent, Ca²⁺-independent Contraction of Smooth Muscle. *J.Biol.Chem.* 1998;273 (36):23433-9.

Faris SL, Rinckel LA, Huang J, Hong Y, Kleinberg ME. Phagocyte NADPH Oxidase p67^{phox} Possesses a Novel Carboxylterminal Binding Site for the GTPases Rac2 and Cdc42. *Biochem. Biophys. Res. Comm.* 1998;247:271-6.

Fauré J, Vignais PV, Dagher MC. Phosphoinositide-dependent activation of rhoA involves partial opening of the RhoA/Rho-GDI complex. *Eur J Biochem.* 1999;262:879-89.

Feuerstein J, Goody RS, Webb MR. The Mechanism of Guanosine Nucleotide Hydrolysis by p21 c-Ha-ras. *J.Biol.Chem.* 1989;264 (11):6188-90.

Fiorentini C, Donelli G, Matarrese P, Fabbri A, Paradisi S, Boquet P. *Escherichia coli* Cytotoxic Necrotizing Factor 1: Evidence for Induction of Actin Assembly by Constitutive Activation of the p21 Rho GTPase. *Infect Immun.* 1995;63(10):3936-44.

Flatau G, Lemichez E, Gauthier M, Chardin P, Paris S, Fiorentini C, *et al.* Toxin-induced activation of the G protein p21 Rho by deamination of glutamine. *Nature* 1997;387:729-33.

Foster R, Hu K, Nolan KM, Thissen J, Settleman J. Identification of a Novel Human Rho Protein with Unusual Properties: GTPase Deficiency and In Vivo Farnesylation. *Mol. Cell. Biol.* 1996;16(6):2689-99.

Freeman JL, Abo A, Lambeth DJ. Rac "Insert Region" Is a Novel Effector Region That Is Implicated in the Activation of NADPH Oxidase, but Not PAK65. *J.Biol.Chem.* 1996;271,(33):19794-801.

Fuchs A, Bouin A, Rabilloud T, Vignais PV. The 40-kDa component of the phagocyte NADPH oxidase (p40^{phox}) is phosphorylated during activation in differentiated HL60 cells. *Eur J Biochem.* 1997;249:531-9.

Fujii H, Ichimori K, Hoshiai K, Nakazawa H. Nitric Oxide Inactivates NADPH Oxidase in Pig Neutrophils by Inhibiting Its Assembly Process. *J.Biol.Chem.* 1997;272 (2):32773-8.

Fukimoto Y, Kaibuchi K, Hori Y, Fujioka H, Araki S, Ueda T, *et al.* Molecular cloning and characterization of a novel type of regulatory protein (GDI) for the rho proteins, ras p21-like small GTP-binding proteins. *Oncogene* 1990;5:1321-8.

Gabig TG, Crean CD, Mantel PL, Rosli R. Function of Wild-Type or Mutant Rac2 and Rap1A GTPases in Differentiated HL60 Cell NADPH Oxidase Activation. *Blood* 1995;85 (3):804-11.

Galisteo ML, Chernoff J, Su Y, Skolnik EY, Schlessinger J. The Adaptor protein Nck Links Receptor Tyrosine Kinases with the Serine-Threonine Kinase Pak1. *J.Biol.Chem.* 1996;271(35):20997-1000.

Garrett MD, Major GN, Totty N, Hall A. Purification and N-terminal sequence of the p21rho GTPase-activating protein, rhoGAP. *Biochem J.* 1991;276:833-6.

Gatti A, Huang Z, Tuazon PT, Traugh JA. Multisite Autophosphorylation of p21-activated Protein Kinase γ -PAK as a Function of Activation. *J.Biol.Chem.* 1999;274(12):8022-8.

- Genth H, Aktories K, Just I. Monoglucosylation of RhoA at Threonine 37 Blocks Cytosol-Membrane Cycling. *J. Biol. Chem.* 1999;274(41):29050-29056
- Gibson TJ, Hyvonen M, Musacchio A, Saraste M. PH domain: the first anniversary. *Trends Biochem Sci.* 1994;19, September:349-53.
- Gill SC, von Hippel PH. Calculation of Protein Extinction Coefficients from Amino Acid Sequence Data. *Anal Biochem.* 1989;182:319-26.
- Glaven JA, Whitehead IP, Nomanbhoy T, Kay R, Crione RA. Lfc and Lsc Oncoproteins Represent Two New Guanine Nucleotide Exchange Factors for the Rho GTP-binding Protein. *J. Biol. Chem.* 1996;271,(44):27374-81.
- Gorvel JP, Chang TC, Boretto J, Azuma T, Chavrier P. Differential properties of D4/LyGDI versus RhoGDI: phosphorylation and rho GTPase selectivity. *FEBS lett.* 1998;422(2):269-73.
- Gosser YQ, Nomanbhoy TK, Aghazadeh B, Manor D, Combs C, *et al.* C-terminal binding domain of Rho GDP-dissociation inhibitor directs N-terminal inhibitory peptide to GTPases. *Nature* 1997;387:814-9.
- Graham DL, Eccleston JF, Lowe PN. The Conserved Arginine in Rho-GTPase-Activating Protein Is Essential for Efficient Catalysis but Not for Complex Formation with Rho.GDP and Aluminium Fluoride. *Biochemistry* 1999;38:985-91.
- Grogan A, Reeves E, Keep N, Wientjes F, Totty NF, Burlingame AL, *et al.* Cytosolic phox proteins interact with and regulate the assembly of coronin in neutrophils. *J Cell Sci.* 1997;110:3071-81.
- Guasch RM, Scambler P, Jones GE, Ridley AJ. RhoE Regulates Actin Cytoskeleton Organisation and Cell Migration. *Mol. Cell. Biol.* 1998;18(8):4761-71.
- Gutfreund F. In *Kinetics for the life sciences*. 1995. Cambridge University Press.
- Haataja L, Groffen J, Heisterkamp N. Characterization of RAC3, a Novel Member of the Rho Family. *J. Biol. Chem.* 1997;272,(33):20384-8.
- Hall A. Ras-Related GTPases and the Cytoskeleton. *Mol Biol Cell.* 1992;3:475-9.
- Hall A. Rho GTPases and the Actin Cytoskeleton. *Science* 1998;279:509-14.
- Hancock JF, Hall A. A novel role for RhoGDI as an inhibitor of GAP proteins. *EMBO J.* 1993;12,(5):1915-21.
- Harden N, Lee J, Loh Y, Tan I, Leung T, Manser E, *et al.* A Drosophila Homolog of the Rac- and Cdc42-Activated Serine/Threonine Kinase PAK Is a Potential Focal Adhesion and Focal Complex Protein That Co-localizes with Dynamic Actin Structures. *Mol. Cell. Biol.* 1996;16(5):1896-908.
- Harhammer R, Gohla A, Schultz G. Interaction of G protein G $\beta\gamma$ dimers with small GTP-binding proteins of the Rho family. *FEBS lett.* 1996;399:211-4.
- Hart MJ, Callow MG, Souza B, Polakis P. IQGAP1, a calmodulin-binding protein with a RasGAP-related domain, is a potential effector for cdc42Hs. *EMBO J.* 1996;15:2997-3005.
- Hart MJ, Eva A, Evans T, Aaronson SA, Cerione RA. Catalysis of guanine nucleotide exchange on the CDC42Hs protein by the dbl oncogene product. *Nature* 1991;354:311-4.
- Hart MJ, Maru Y, Leonard D, Witte ON, Evans T, Cerione RA. A GDP dissociation inhibitor that serves as a GTPase inhibitor for the Ras-like protein CDC42Hs. *Science* 1992;258:812-5.
- Hartwig JH, Bokock GM, Carpenter CL, Jamney PA, Taylor LA, *et al.* Thrombin Receptor Ligation and Activated Rac Uncap Actin Filament Barbed Ends through Phosphoinositide Synthesis in Permeabilized Human Platelets. *Cell* 1995;82:643-53.
- Hirata K, Kikuchi A, Sasaki T, Kuroda S, Kaibuchi K, Matsuura Y, *et al.* Involvement of rho p21 in the GTP-enhanced Calcium Ion Sensitivity of Smooth Muscle Contraction. *J. Biol. Chem.* 1992;267(13):8719-22.
- Hiratsuka T. New ribose-modified fluorescent analogs of adenine and guanine nucleotides available as substrates for various enzymes. *Biochim. Biophys. Acta.* 1983;742:496-508.
- Hirshberg M, Stockley RW, Dodson G, Webb MR. The crystal structure of human Rac1, a member of the rho-family complexed with a GTP analogue. *Nat Struct Biol.* 1997;4 (2):147-52.
- Imajoh-Ohmi S, Tokita K, Nakamura M, Kanegasaki S. Topology of Cytochrome b558 in Neutrophil Membrane Analyzed by Anti-peptide Antibodies and Proteolysis. *J. Biol. Chem.* 1992;267 (1):180-4.
- Ischiropoulos H, al-Mehdi AB. Peroxynitrite-mediated oxidative protein modifications. *FEBS lett.* 1995;364(3):

279-82.

Isomura M, Kikuchi A, Ohga N, Takai Y. Regulation of binding of RhoB p20 to membranes by its specific regulatory protein, GDP dissociation inhibitor. *Oncogene* 1991;6:119-24.

Jakobi R, Chen C, Tuazon PT, Traugh JA. Molecular Cloning and Sequencing of the Cytostatic G Protein-activated Protein Kinase PAK1. *J.Biol.Chem.* 1996;271(11):6206-11.

Jeanteur P. 1999. in *Cytoskeleton and Small G Proteins* (Jeanteur P.,Ed) Springer.

John J, Rensland H, Schlichting I, Vetter I, Borasio GD, Goody RS, *et al.* Kinetic and structural analysis of the Mg²⁺-binding site of the guanine nucleotide-binding protein p21 H-ras. *J.Biol.Chem.* 1993;268:923-9.

Johnson JL, Park J, Benna JE, Faust LP, Inanami O. Activation of p47^{phox}, a cytosolic Subunit of the Leukocyte NADPH Oxidase. *J.Biol.Chem.* 1998;272(52):35147-52.

Joneson T, Bar-Sagi D. A Rac1 Effector Site Controlling Mitogenesis through Superoxide Production. *J.Biol.Chem.* 1998;273 (29):17991-4.

Joneson T, McDonough M, Bar-Sagi D, Van Aelst L. RAC Regulation of Actin Polymerization and Proliferation by a Pathway Distinct from Jun Kinase. *Science* 1996;274:1374-6.

Joseph G, Pick E. "Peptide Walking" Is a Novel Method for Mapping Functional Domains in Proteins (Its application to the Rac1-dependent activation of the NADPH oxidase). *J.Biol.Chem.* 1995;270 (49):29079-82.

Joyal JL, Annan RS, Ho Y, Huddleston ME, Carr SA, Hart MJ, *et al.* Calmodulin Modulates the Interaction between IQGAP1 and Cdc42. *J.Biol.Chem.* 1997;272(24):1549-15425.

Keep NH, Barnes M, Barsukov I, Badii R, Lian L, Segal AW, *et al.* A modulator of the rho family G proteins, rhoGDI, binds these G-proteins via an immunoglobulin-like domain and a flexible N-terminal arm. *Structure* 1997;5:623-33.

King AJ, Diaz SH, Barnard D, Miao W, Bagrodia S, Marshall MS. The protein kinase Pak3 positively regulates Raf-1 activity through phosphorylation of serine 338. *Nature* 1998;396:180-3.

Kinsella BT, Erdman RA, Maltese WA. Posttranslational modification of H-ras p21 by farnesyl versus geranylgeranyl isoprenoids is determined by the COOH-terminal amino acid. *Proc. Natl. Acad. Sci* 1991;88:8934-8.

Kishi K, Sasaki T, Kuroda S, Itoh T, Takai Y. Regulation of Cytoplasmic Division of *Xenopus* Embryo by rho p21 and Its Inhibitory GDP/GTP Exchange Protein (rho GDI). *J.Cell. Biol.* 1993;120(5):1187-95.

Kjeldgaard M, Nyborg J, Clark BFC. The GTP binding motif: variations on a theme. *FASEB J.* 1996;10:1347-68.

Kloc M, Reddy B, Crawford S, Etkin LD. A Novel 110-kDa Maternal CAAX Box-containing Protein from *Xenopus* Is Palmitoylated and Isoprenylated When Expressed in Baculovirus. *J.Biol.Chem.* 1991;266(13):8206-12.

Knaus UG, Morris S, Dong HJ, Chernoff J, Bokoch GM. Regulation of human leukocyte p21-activated kinases through G protein-coupled receptors. *Science* 1995;269:221-3.

Koga H, Terasawa H, Nunoi H, Takeshige K, Inagaki F, Sumimoto H. Tetratricopeptide Repeat (TPR) Motifs of p67^{phox} Participate in Interaction with the Small GTPase Rac and Activation of the Phagocyte NADPH Oxidase. *J.Biol.Chem.* 1999;274(35):25051-60.

Krengel U, Shlichting L, Scherer A, Schumann R, Frech M, John J, Kabsch W, Pai EF, Wittinghofer A. Three-dimensional structures of H-Ras p21 mutants: molecular basis for their ability to function as switch molecules. *Cell.* 1990;62(3):539-548

Kuroda S, Fukata M, Kobayashi K, Nakafuku M, Nomura N, *et al.* Identification of IQGAP as a Putative Target for the Small GTPases, Cdc42 and Rac1. *J.Biol.Chem.* 1996;271,(38):23363-7.

Lamarche N, Tapon N, Stowers L, Burbelo PD, Aspenstrom P, *et al.* Rac and Cdc42 Induce Actin Polymerization and G1 Cell Cycle Progression Independently of p65PAK and the JNK/SAPK MAP Kinase Cascade. *Cell* 1996;87:519-29.

Lancaster CA, Taylor-Harris PM, Self AJ, Brill S, van Erp HE, *et al.* Characterization of rhoGAP. *J.Biol.Chem.* 1994;269,(2):1137-42.

Leeuw T, Fourest-Lieuvain A, Wu C, Chenevert J, Clark K, Whiteway M, *et al.* Pheromone response in yeast: association of Bem1p with proteins of the MAP kinase cascade and actin. *Science* 1995;270(5239):1210-3.

Lelias J, Adra CN, Wulf GM, Guillemot J, Khagad M, Caput D, *et al.* cDNA cloning of a human mRNA preferentially expressed in haematopoietic cells and with homology to a GDP-dissociation inhibitor for the rho GTP-binding proteins. *Proc. Natl. Acad. Sci* 1993;90:1479-83.

Lemmon MA, Ferguson KM, Schlessinger J. PH domains: diverse sequences with a common fold recruit signaling molecules to the cell surface. *Cell* 1996;85:621-4.

Lenzen C, Cool RH, Prinz H, Kuhlmann J, Wittinghofer A. Kinetic Analysis by Fluorescence of the Interaction between Ras and the Catalytic Domain of the Guanine Nucleotide Exchange Factor Cdc25. *Biochemistry* 1998;37:7420-7430

Leonard D, Hart MJ, Platko JV, Eva A, Henzel W, Evans T, *et al.* The Identification and Characterization of a GDP-dissociation Inhibitor (GDI) for the CDC42Hs Protein. *J.Biol.Chem.* 1992;267(32):22860-8.

Leonard DA, Satoskar RS, Wu WJ, Bagrodia S, Cerione RA. Use of a spectroscopic readout to characterize the interactions of Cdc42Hs with its target/effector, mPAK-3. *Biochemistry* 1997;36(5):1173-1180

Leto TL, Garrett MC, Fujii H, Nunoi H. Characterization of Neutrophil NADPH Oxidase Factors p47^{phox} and p67^{phox} from Recombinant Baculoviruses. *J.Biol.Chem.* 1991;266(29):19812-8.

Leusen JH, de Boer M, Bolscher BG, Hilarius PM, Weening RS, Ochs HD, *et al.* A point mutation on gp91^{phox} of cytochrome b558 of the human NADPH oxidase leading to defective translocation of the cytosolic proteins p47^{phox} and p67^{phox}. *The J Clin Invest.* 1994;93(5):2120-6.

Leusen JHW, Fluiter K, Hilarius PM, Roos D, Verhoeven AJ, Bolscher BGJM. Interactions between the Cytosolic Components p47^{phox} and p67^{phox} of the Human Neutrophil NADPH Oxidase That Are Not Required for Activation in the Cell-free System. *J.Biol.Chem.* 1995;270 (19):11216-21.

Leusen JHW, Verhoeven AJ, Roos D. Interactions between the components of the human NADPH oxidase: Intrigues in the phox family. *J Lab Clin Med.* 1996;128:461-76.

Longenecker KL, Read P, Derewenda U, Dauter Z, Garrard S, Walker L, *et al.* How RhoGDI binds Rho. *Acta Crystallogr D Biol Crystallogr.* 1999 Sep;55 (Pt 9):1503-15

Mach H, Middaugh R, Lewis RV. Statistical Determination of the Average Values of the Extinction Coefficients of Tryptophan and Tyrosine in Native Proteins. *Anal Biochem.* 1992;200:74-80.

Machesky LM, Atkinson SJ, Ampe C, Vanderckhove J, Pollard TD. Purification of a cortical complex containing two unconventional actins from *Acanthamoeba* by affinity chromatography on profilin-agarose. *J.Cell. Biol.* 1994;127:107-15.

Mackay DJG, Hall A. Rho GTPases. *J.Biol.Chem.* 1998;273 (33):20685-8.

Manser E, Chong C, Zhao Z, Leung T, Michael G, Hall C, *et al.* Molecular Cloning of a New Member of the p21-Cdc42/Rac-activated Kinase (PAK) family. *J.Biol.Chem.* 1995;270(42):25070-8.

Manser E, Huang H, Loo T, Chen X, Dong J, Leung T, *et al.* Expression of Constitutively Active α -PAK reveals Effects of the Kinase on Actin and Focal Complexes. *Mol. Cell. Biol.* 1997;17(3):1129-43.

Manser E, Leung T, Salihuddin H, Zhao Z, Lim L. A brain serine/threonine protein kinase activated by Cdc42 and Rac1. *Nature* 1994;367:40-6.

Marcus S, Polverino A, Chang E, Robbins D, Cobb MH, Wigler MH. Shk1, a homolog of the *Saccharomyces cerevisiae* Ste20 and mammalian p65PAK protein kinases, is a component of a Ras/Cdc42 signaling module in the fission yeast *Schizosaccharomyces pombe*. *Proc. Natl. Acad. Sci* 1995;92(13):6180-4.

Martinez O, Goud B. Rab proteins. *Biochim. Biophys. Acta.* 1998;1404(1-2):101-12.

McCallum SJ, Wu WJ, Cerione RA. Identification of a Putative Effector for Cdc42Hs with High Sequence Similarity to the RasGAP-related Protein IQGAP1 and a Cdc42Hs Binding Partner with Similarity to IQGAP2. *J.Biol.Chem.* 1996;271 (36):21732-7.

McPhail L. SH3-dependent Assembly of the Phagocyte NADPH Oxidase. *J. Exp. Med.* 1994;180:2011-5.

Menard L, Tomhave E, Casey PJ, Uhling RJ, Snyderman R, *et al.* Rac1, a low-molecular-mass-GTP-binding – protein with high intrinsic GTPase activity and distinct biochemical properties. *Eur J Biochem.* 1992;206:537-546

Miki H, Suetsugu S, Takenawa T. WAVE, a novel WASP-family protein involved in actin reorganisation induced by Rac. *EMBO J.* 1998;17(23):6932-41.

Miura Y, Kikuchi A, Musha T, Kuroda S, Yaku H, Sasaki T, *et al.* Regulation of Morphology by rho p21 and Its

- Inhibitory GDP/GTP Exchange Protein (rhoGDI) in Swiss 3T3 Cells. *J.Biol.Chem.* 1993;268(1):510-5.
- Mizuno T, Kaibuchi K, Ando S, Musha T, Hiraoka K, *et al.* Regulation of the Superoxide-generating NADPH Oxidase by a Small GTP-binding Protein and Its Stimulatory and Inhibitory GDP/GTP Exchange Proteins. *J.Biol.Chem.* 1992;267 (15):10215-8.
- Moore KJ, Webb MR, Eccleston JF. Mechanism of GTP Hydrolysis by p21N-Ras Catalyzed by GAP: Studies with a Fluorescent GTP Analogue. *Biochemistry* 1993;32;7451-7459
- Moore MS. Ran and nuclear transport. *J.Biol.Chem.* 1998;273:22857-60.
- Moss J, Vaughan M. Structure and function of ARF proteins: Activators of Cholera Toxin and Critical Components of Intracellular Vesicular Transport Processes. *J.Biol.Chem.* 1995;270(21):12327-30.
- Mullins RD, Heuser JA, Pollard TD. The interaction of Arp2/3 complex with actin: Nucleation, high affinity pointed end capping, and formation of branching networks of filaments. *Proc. Natl. Acad. Sci* 1998;95:6181-6.
- Musacchio A, Gibson T, Rice P, Thompson J, Saraste M. The PH domain: a common piece in the structural patchwork of signalling proteins. *Trends Biochem Sci.* 1993;18, September:343-53.
- Na S, Chuang T, Cunningham A, Turi TG, Hanke JH, Bokoch GM, *et al.* D4-GDI, a Substrate of CPP32, Is Proteolyzed during Fas-induced Apoptosis. *J.Biol.Chem.* 1996;271(19):11209-13.
- Nagata K, Puls A, Futter C, Aspenstrom P, Schaefer E, Najata K, *et al.* The MAP kinase kinase MLK2 co-localizes with activated JNK along microtubules and associates with kinesin superfamily motor KIF3. *EMBO J.* 1998;17 (1):149-58.
- Nakanishi A, Imajoh-Ohmi S, Fujinawa T, Kikuchi H, Kanegashaki S. Direct Evidence for Interaction Between COOH-terminal Regions of Cytochrome b558 Subunits and Cytosolic 47-kDa Protein during Activation of an O₂⁻ generating System in Neutrophils. *J.Biol.Chem.* 1992;267 (27):19072-4.
- Narumiya S. The Small GTPase Rho: Cellular Functions and Signal Transduction. *J Biochem (Tokyo).* 1996;120:215-28.
- Nelson M, McClelland M. Use of DNA Methyltransferase/Endonuclease Enzyme Combinations for Megabase Mapping of Chromosomes. *Methods Enzymol.* 1992;216:279-302.
- Newcombe AR, Stockley RW, Hunter JL, Webb MR. The Interaction between Rac1 and Its Guanine Nucleotide Dissociation Inhibitor (GDI) Monitored by a Single Fluorescent Coumarin Attached to GDI. *Biochemistry* 1999;38:6879-86.
- Nisimoto Y, Freeman JLR, Motalebi SA, Hirshberg M, Lambeth D. Rac binding to p67^(phox). Structural basis for the interactions of the Rac1 effector region and insert region with components of the respiratory burst oxidase. *J.Biol.Chem.* 1997;272 (30):18834-41.
- Nobes CD, Lauritzen I, Mattei M, Paris S, Hall A, Chardin P. A New Member of the Rho Family Rnd1, Promotes Disassembly of Actin Filament Structures and Loss of Cell Adhesion. *J.Cell. Biol.* 1998;141 (1):187-97.
- Noda M, Yasuda-Fukazawa C, Moriishi K, Kato T, Okuda T, Kurokawa K, *et al.* Involvement of rho in GTPγS-induced enhancement of phosphorylation of 20kDa myosin light chain in vascular smooth muscle cells: inhibition of phosphatase activity. *FEBS lett.* 1995;367:246-50.
- Nomanbhoy TK, Cerione RA. Characterization of the Interaction between RhoGDI and Cdc42Hs Using Fluorescence Spectroscopy. *J.Biol.Chem.* 1996;271 (17):10004-9.
- Nomanbhoy TK, Erickson JW, Cerione RA. Kinetics of Cdc42 membrane extraction by Rho-GDI monitored by real-time fluorescence resonance energy transfer. *Biochemistry* 1999;38(6):1744-1750
- Oswald E, Sugai M, Labigne A, Wu HC, Fiorentini C, Boquet P, *et al.* Cytotoxic necrotizing factor type 2 produced by virulent *Escherichia coli* modifies the small GTP-binding proteins Rho involved in assembly of actin stress fibers. *Proc. Natl. Acad. Sci* 1994;91:3814-8.
- Ottillie S, Miller PJ, Johnson DI, Creasy CL, Sells MA, Bagrodia S, *et al.* Fission yeast pak1+ encodes a protein kinase that interacts with Cdc42p and is involved in the control of cell polarity and mating. *EMBO J.* 1995;14(23):5908-19.
- Pai EF, Krengel U, Petsko GA, Goody RS, Kabsch W, Wittinghoffer A. Redefined crystal structure of the triphosphate conformation of H-ras p21at 1.3Å resolution: implications for the mechanism of GTP hydrolysis. *EMBO J.* 1990;9(8):2351-9.
- Park H, Kim IS, Park J. Phosphorylation Induces Conformation Changes in the Leukocyte NADPH Oxidase Subunit p47^{phox}. *Biochem. Biophys. Res. Comm.* 1999;259:38-42.

- Park J, Baboir BM. Activation of the Leukocyte NADPH Oxidase Subunit p47^{phox} by Protein Kinase C. A Phosphorylation-Dependent Change in the Conformation of the C-Terminal End of p47^{phox}. *Biochemistry* 1997;36:7474-80.
- Park M, Imajoh-Ohmi S, Nunoi H, Kanegasaki S. Synthetic Peptides Corresponding to Various Hydrophilic Regions of the Large Subunit of Cytochrome b558 Inhibit Superoxide Generation in a Cell-Free System from Neutrophils. *Biochem Biophys. Res. Comm.* 1997b ;234:531-6.
- Philips MR, Pillinger MH, Staud R, Volker C, Rosenfeld MG, Weissman G, *et al.* Carboxyl Methylation of Ras-Related Proteins During Signal Transduction in Neutrophils. *Science* 1993;259:977-80.
- Polverino A, Frost J, Yang P, Hutchison M, Neiman AM, Cobb MH, *et al.* Activation of Mitogen-activated Protein Kinase Cascades by p21-activated Protein Kinases in Cell-free Extracts of Xenopus Oocytes. *J.Biol.Chem.* 1995;270(44):26067-70.
- Privé GG, Milburn MV, Tong L, DeVos AM, Yamaizumi Z, Nishimura S, *et al.* X-ray crystal structures of transforming p21 ras mutants suggest a transition-state stabilization mechanism for GTP hydrolysis. *Proc. Natl. Acad. Sci* 1992;89:3649-53.
- Qui R, Chen J, Kim D, McCormick F, Symons M. An essential role for Rac in Ras transformation. *Nature* 1995;374:457-9.
- Quinn M, Mullen ML, Jesaitis AJ. Human Neutrophil Cytochrome b Contains Multiple Hemes. *J.Biol.Chem.* 1992;267 (11):7303-9.
- Ramesh N, Antón IM, Martinez-Quiles N, Geha RS. Waltzing with WASP. *Trends Cell Biol.* 1999;9:15-9.
- Ridley AJ, Paterson HF, Johnson CL, Diekmann D, Hall A. The Small GTP-binding Protein rac Regulates Growth Factor-Induced Membrane Ruffling. *Cell* 1992;70:401-10.
- Ridley AJ, Self AJ, Kasmi F, Paterson HF, Hall A, *et al.* rho family GTPase activating proteins p190, bcr and rhoGAP show distinct specificities in vitro and in vivo. *EMBO J.* 1993;12 (13):5151-60.
- Rittinger K, Walker PA, Eccleston JF, Smerdon SJ, Gamblin SJ. Structure at 1.65Å of RhoA and its GTPase-activating protein in complex with a transition-state analogue. *Nature* 1997;389:758-62.
- Rittinger K, Walker PA, Eccleston JF, Nurmahomed K, Owen D, Laue E, *et al.* Crystal structure of a small G protein in complex with the GTPase-activating protein rhoGAP. *Nature* 1997b ;388:693-7.
- Rohatgi R, Ma L, Miki H, Lopez M, Kirchhausen T, Takenawa T, *et al.* The Interaction between N-WASP and the Arp2/3 Complex Links Cdc42-Dependent Signals to Actin Assembly. *Cell* 1999;97:221-31.
- Rohn TT, Nelson LK, Davis AR, Quinn MT. Inhibition of GTP binding to Rac2 by peroxynitrite: potential role for tyrosine modification. *Free Radic. Biol. Med.* 1999;26(9-10):1321-31.
- Ron D, Zannini M, Lewis M, Wickner RB, Hunt LT, Graziani G, *et al.* A region of proto-dbl essential for its transforming activity shows sequence similarity to a yeast cell cycle gene, CDC24, and the human break point cluster gene, bcr. *New Biol.* 1991;3:372-9.
- Rubin EJ, Gill DM, Boquet P, Popoff MR. Functional Modification of a 21-Kilodalton G Protein when ADP-Ribosylated by Exoenzyme C3 of *Clostridium botulinum*. *Mol. Cell. Biol.* 1988;8:418-26.
- Rudolph MG, Wittinghofer A, Vetter IR. Nucleotide binding to the G12V-mutant of Cdc42 investigated by X-ray Diffraction and fluorescence spectroscopy: two different nucleotide states in one crystal. *Protein Sci.* 1999;8(4):778-87.
- Sanders LC, Matsumura F, Bokock GM, Lanerolle P. Inhibition of Myosin Light Chain Kinase by p21-Activated Kinase. *Science* 1999;283:2083-5.
- Sanger F, Nicklen S, Coulston AR. DNA sequencing with chain-terminating inhibitors. *Proc. Natl. Acad. Sci* 1977;74:5463.
- Sasaki T, Kato M, Takai Y. Consequences of Weak Interaction of rho GDI with the GTP-bound Forms of rho p21 and rac p21. *J.Biol.Chem.* 1993;268,(32):23959-63.
- Satoh T, Nakamura S, Nakafuku M, Kaziro Y. Studies on ras proteins. Catalytic properties of normal and activated ras proteins purified in the absence of protein denaturants. *Biochim. Biophys. Acta* 1988;949(1):97-109.
- Sawai T, Asada M, Nunoi H, Matsuda I, Ando S. Combination of arachidonic acid and guanosine 5'-O-(3-thiotriphosphate) induce translocation of rac p21s to membrane and activation of NADPH oxidase in a cell-free system. *Biochem. Biophys. Res Comm.* 1993;195 (1):264-9.

- Schafer DA, Jennings PB, Cooper JA. Dynamics of capping protein and actin assembly in vitro: uncapping barbed ends by phosphoinositides. *J. Cell. Biol.* 1996;135(1):169-79.
- Schalk I, Zeng K, Wu SK, Stura EA, Matteson J, Huang M, *et al.* Structure and mutational analysis of Rab GDP-dissociation inhibitor. *Nature* 1996;381(6577):42-8.
- Scherle P, Behrens T, Staudt LM. Ly-GDI, a GDP-dissociation inhibitor of the RhoA GTP binding protein, is expressed preferentially in lymphocytes. *Proc. Natl. Acad. Sci* 1993;90:7568-72.
- Schmidt G, Sehr P, Wilm M, Selzer J, Mann M, *et al.* Gln 63 of Rho is deaminated by *Escherichia coli* cytotoxic necrotizing factor-1. *Nature* 1997;387:725-9.
- Scopes RK. Making an Extract. Protein Purification - Principles and Practice. 2nd ed. Virginia,USA: Springer-Verlag, 1982:21-40.
- Segal AW. The NADPH oxidase and chronic granulomatous disease. *Mol Med Today* 1996; March '96:129-35.
- Segal AW, Shatwell KP. The NADPH Oxidase of Phagocytic Leukocytes. *Ann.NY. Acad.Sci.* 1997;832:215-22.
- Sells MA, Knaus UG, Bagrodia S, Ambrose DM, Bokoch GM, Chernoff J. Human p21-activated kinase (Pak1) regulates actin organisation in mammalian cells. *Curr Biol.* 1997;7(3):202-10.
- Shaw G. The pleckstrin homology domain: an intriguing multifunctional protein module. *Bioessays.* 1996;18:35-46.
- Shih TY, Weeks MO, Young HA, Scolnick EM. Identification of a sarcoma virus-coded phosphoprotein in non-producer cells transformed by Kirsten or Harvey murine sarcoma virus. *Virology* 1979;96:64-79.
- Shimizu K, Kaibuchi K, Nonaka H, Yamamoto J, Takai Y. Tissue and subcellular distributions of an inhibitory GDP/GTP exchange protein (GDI) for the Rho proteins by use of its specific antibody. *Biochem. Biophys. Res. Comm.* 1991;175(1):199-206.
- Shinjo K, Koland JG, Hart MJ, Narasimhan V, Johnson DI, Evans T, *et al.* Molecular cloning of the gene for the human placental GTP- binding protein Gp (G25K): identification of this GTP binding protein as the human homolog of the yeast-cell division-cycle protein cdc42. *Proc. Natl. Acad. Sci* 1990;87:9853-7.
- Silvius JR, l'Heureux F. Fluorimetric Evaluation of the Affinities of Isoprenylated Peptides for Lipid Bilayers. *Biochemistry* 1994;33:3014-22.
- Skinner J, Sinclair C, Romeo C, Armstrong D, Charbonneau H, Rossie S. Purification of a Fatty Acid-stimulated Protein-serine/threonine Phosphatase from Bovine Brain and Its Identification as a Homolog of Protein Phosphatase 5. *J.Biol.Chem.* 1997;272(36):22464-71.
- Somlyo AP, Somlyo AV. Signal transduction and regulation in smooth muscle. *Nature* 1994;372:231-6.
- Steele-Mortimer O, Gruenberg J, Clague MJ. Phosphorylation of GDI and membrane cycling of rab proteins. *FEBS lett.* 1993;329(3):313-8.
- Sulciner DJ, Irani K, Yu Z, Ferrans VJ, Goldschmidt-Clermont P, *et al.* rac1 Regulates a Cytokine-Stimulated, Redox-Dependent Pathway Necessary for NF-kB Activation. *Mol. Cell. Biol.* 1996;16(12):7115-21.
- Sumimoto H, Hata K, Mizuki K, Ito T, Kage Y, *et al.* Assembly and Activation of the Phagocyte NADPH Oxidase. *J.Biol.Chem.* 1996;271,(36):22152-8.
- Swain SD, Helgerson SL, Davis AR, Nelson LK, Quinn MT. Analysis of Activation-induced Conformational Changes in p47^{phox} using Tryptophan Fluorescence Spectroscopy. *J.Biol.Chem.* 1997;272:29502-10.
- Symons M. Rho family GTPases: the cytoskeleton and beyond. *Trends Biochem Sci.* 1996;21:178-81.
- Takahashi K, Sasaki T, Mammoto A, Takaishi K, Kameyama T, *et al.* Direct Interaction of the Rho GDP Dissociation Inhibitor with Ezrin/Radixin/Moesin Initiates the Activation of the Rho Small G Protein. *J.Biol.Chem.* 1997;272 (37):23371-5.
- Takaishi K, Kikuchi A, Kuroda S, Kotani K, Sasaki T, Takai Y. Involvement of rho p21 and Its Inhibitory GDP/GTP Exchange protein (rho GDI) in Cell Motility. *Mol. Cell. Biol.* 1993;13:72-9.
- Tapon N, Hall A. Rho, Rac and cdc42 GTPases regulate the organisation of the actin cytoskeleton. *Curr Opin Cell Biol.* 1997;9:86-92.
- Tapon N, Nagata K, Lamarche N, Hall A. A new Rac target POSH is an SH3-containing scaffold protein involved in the JNK and NF-kB signalling pathways. *EMBO J.* 1998;17 (5):1395-404.

- Teo M, Manser E, Lim L. Identification and Molecular Cloning of a p21 cdc42/rac1-activated Serine/threonine Kinase That Is Rapidly Activated by Thrombin in Platelets. *J.Biol.Chem.* 1995;270(44):26690-7.
- Teramoto H, Coso OA, Miyata H, Igishi T, Miki T, *et al.* Signaling from the Small GTP-binding Proteins Rac1 and Cdc42 to the c-Jun N-terminal Kinase/Stress-activated Protein Kinase Pathway. *J.Biol.Chem.* 1996;271(44):27225-8.
- Tolias KF, Cantley LC, Carpenter CL. Rho family GTPases bind to phosphoinositide kinases. *J.Biol.Chem.* 1995;270(30):17656-9.
- Trincle-Mulcahy L, Ichikawa K, Hartshorne DJ, Siegman MJ, Butler TM. Thiophosphorylation of 130kDa Subunit Is Associated with a Decreased Activity of Myosin Light Chain Phosphatase in α -Toxin-permeabilized Smooth Muscle. *J.Biol.Chem.* 1995;270(31):18191-4.
- Tsukita S, Oishi K, Sato N, Sangara J, Kawai A, Tsukita S. ERM Family Members as Molecular Linkers between the Cell Surface Glycoprotein CD44 and Actin-based Cytoskeletons. *J.Cell Biol.* 1994;126(2):391-401.
- Tu H, Wigler M. Genetic evidence for Pak1 autoinhibition and its release by Cdc42. *Mol Cell Biol.* 1999;19(1):602-11.
- Ueda T, Kikuchi A, Ohga N, Yamamoto J, Takai Y. Purification and Characterisation from Bovine Brain Cytosol of a Novel Regulatory Protein Inhibiting the Dissociation of GDP from the Subsequent Binding of GTP to rhoB p20, a ras p21-like GTP binding protein. *J.Biol.Chem.* 1990;265(16):9373-80.
- Valencia A, Chardin P, Wittinghofer A, Sander C. The ras Protein Family: Evolutionary Tree and Role of Conserved Amino Acids. *Biochemistry* 1991;30(19):4637-48.
- Venkatasubramanian K, Hirata F, Gagnon C, Corcoran BA, O'Dea RF, Axelrod J, *et al.* Protein methyltransferase and leukocyte chemotaxis. *Mol Immunol.* 1980;17(2):201-7.
- Wei Y, Zhang Y, Derewenda U, Liu X, *et al.* Crystal structure of RhoA-GDP and its functional implications. *Nat Struct Biol.* 1997;4 (9):699-703.
- Wientjes FB, Hsuan JJ, Totty NF, Segal AW. p40^{phox}, a third cytosolic component of the activation complex of the NADPH oxidase to contain src homology 3 domains. *Biochem J.* 1993;296:557-61.
- Woodman RC, Ruedi JM, Jesaitis AJ, Okamura N, Quinn MT, Smith RM, *et al.* Respiratory burst oxidase and three of the four oxidase-related polypeptides are associated with the cytoskeleton of human neutrophils. *J Clin Invest.* 1991;87(4):1345-51.
- Wu W, Leonard DA, Cerione RA, Manor D. Interaction between Cdc42Hs and RhoGDI Is Mediated through the Rho Insert Region. *J.Biol.Chem.* 1997;272 (42):26153-8.
- Wu W, Lin R, Cerione RA, Manor D. Transformation Activity of Cdc42 Requires a Region Unique to Rho-related Proteins. *J.Biol.Chem.* 1998;273 (27):16655-8.
- Yu L, Quinn MT, Cross AR, Dinauer MC. Gp91^{phox} is the heme binding subunit of the superoxide-generating NADPH oxidase. *Proc. Natl. Acad. Sci* 1998;95:7993-8.
- Zhang B, Zhang Y, Collins CC, Johnson DI, Zheng Y. A Built-in Arginine Finger Triggers the Self-stimulatory GTPase-activating Activity of Rho Family GTPases. *J.Biol.Chem.* 1999;274(5):2609-12.
- Zhang B, Zheng Y. Negative Regulation of Rho Family GTPases Cdc42 and Rac2 by Homodimer Formation. *J.Biol.Chem.* 1998;273 (40):25728-33.
- Zhang S, Han J, Sells M, Chernoff J, Knaus UG, Ulevitch RJ, *et al.* Rho Family GTPases Regulate p38 Mitogen-activated Protein Kinase through the Downstream Mediator Pak1. *J.Biol.Chem.* 1995;270(41):23934-6.
- Zheng Y, Cerione R, Bender A. Control of the yeast bud-site assembly GTPase Cdc42. Catalysis of guanine nucleotide exchange by Cdc24 and stimulation of GTPase activity by Bem3. *J.Biol.Chem.* 1994;269:2369-72.
- Zong H, Raman N, Mickelson-Young LA, Atkinson SJ, Quilliam LA. Loop 6 of RhoA confers specificity for effector binding, stress fiber formation, and cellular transformation. *J. Biol. Chem.* 1999;274(8):4551-4560.

The Interaction between Rac1 and Its Guanine Nucleotide Dissociation Inhibitor (GDI), Monitored by a Single Fluorescent Coumarin Attached to GDI

**Anthony R. Newcombe, Richard W. Stockley,
Jackie L. Hunter, and Martin R. Webb**

National Institute for Medical Research, The Ridgeway, Mill Hill,
London, NW7 1AA, U.K.

Biochemistry[®]

Reprinted from
Volume 38, Number 21, Pages 6879–6886

The Interaction between Rac1 and Its Guanine Nucleotide Dissociation Inhibitor (GDI), Monitored by a Single Fluorescent Coumarin Attached to GDI

Anthony R. Newcombe, Richard W. Stockley, Jackie L. Hunter, and Martin R. Webb*

National Institute for Medical Research, The Ridgeway, Mill Hill, London, NW7 1AA, U.K.

Received December 18, 1998; Revised Manuscript Received March 31, 1999

ABSTRACT: The interaction of rac with guanine nucleotide dissociation inhibitor protein (rhoGDI) is described, using GDI fluorescently labeled on its single cysteine with *N*-[2-(1-maleimidyl)ethyl]-7-diethylaminocoumarin-3-carboxamide (MDCC). The labeled GDI shows a 70% decrease in fluorescence emission on binding geranylgeranylated rac1•GDP and has an affinity for rac1 within a factor of 2 of the unlabeled GDI. The labeled GDI was used to determine the kinetic mechanism of the interaction by measuring the association and dissociation in real time. The kinetics are interpreted in terms of a two-step mechanism: binding of rac to GDI and then a conformational change of the complex with an overall dissociation constant of 0.4 nM. The conformational change has a rate constant of 7.3 s⁻¹ (pH 7.5, 30 °C), and the reverse has a rate constant of 1.4 × 10⁻³ s⁻¹. To overcome difficulties inherent in using and manipulating lipid-modified rac, we also used a combination of unmodified rac1, expressed in *Escherichia coli* and produced with C-terminal truncation (thus lacking the cysteine that is the site of lipid attachment), and farnesylated C-terminal peptide. This combination can mimic geranylgeranylated rac1, producing a complex with the coumarin-labeled GDI, and was used to examine the relative importance of different regions of rac1 in interaction with GDI.

Rac is a small G protein with a range of signal-transducing roles within different cell types. Along with other members of the rho family, rho and cdc42, it is involved in control of the cytoskeleton (reviewed by ref 1). It has an apparently quite separate role, particularly in macrophages, in assembly and control of the NADPH oxidase complex, which forms superoxide in response to bacterial infection (reviewed by ref 2).

Small G proteins in the rho family interact strongly with a protein, guanine nucleotide dissociation inhibitor, rhoGDI (GDI) (3). Although this protein is named because it has the property of strongly inhibiting nucleotide dissociation, its cellular function probably lies elsewhere. For example in quiescent neutrophils (and some other cell types), rac is almost entirely present in the cytosol as a tight complex with GDI. Activation causes dissociation of the rac•GDI complex and movement to the membrane (4). The molecular basis for this transfer is not clear, and GDI may function as a control point to keep rac deactivated in the cytosol. Thus nucleotide exchange to a triphosphate may control this translocation (5). Understanding how this activation occurs is a long-term goal of the work described here.

Such understanding requires investigation of the molecular interaction between GDI and small G proteins of the rho

family, including the mechanism by which the proteins interact and what features of the two proteins are important for binding. Structural studies suggest that this interaction may be complex, as GDI is partly disordered in the absence of bound small G protein (6, 7) and becomes ordered in the rac•GDI complex. To facilitate studies of rac-GDI interaction, we have developed a fluorescence probe on GDI that provides a direct signal for rac binding and so allows us to follow the formation and dissociation of the complex in real time. The probe is a coumarin bound to the single cysteine at position 79 of GDI and was used to investigate GDI interaction with rac1, one of two very similar human rac proteins.

In doing so, we address two problems that have hampered such studies. First, the main signal for interaction has previously been the inhibition of nucleotide exchange and of GAP activation (3, 8, 9). Both types of inhibition are likely to be due to steric constraints in the complex with GDI and/or the slow dissociation of the complex (see below). However, this property does not produce a direct signal for interaction. Methylanthraniloyl nucleotides complexed to rac (10) and GDI with Cys-79 labeled with fluorescein (7) have also been used to study the interaction. To provide a direct signal, we have labeled the single cysteine of GDI with a coumarin that shows a large fluorescence change on rac binding to the GDI. This then provides a sensitive measurement of the interaction directly, and we have used this to determine the kinetics of association by rapid reaction techniques to follow the interaction in real time.

For the exploitation of such labeled protein, it is important to have sufficient characterization to show that it is an homogeneous preparation and the extent to which the

* To whom correspondence should be addressed. Tel: (44) 181 959 3666. Fax: (44) 181 906 4477. E-mail: m-webb@nimr.mrc.ac.uk.

¹ Abbreviations: GDI, rho-family guanine nucleotide dissociation inhibitor (rhoGDI); MDCC, *N*-[2-(1-maleimidyl)ethyl]-7-diethylaminocoumarin-3-carboxamide; MDCC-GDI, GDI labeled with MDCC; MDCC-PBP, A197C mutant of the *E. coli* phosphate-binding protein labeled with MDCC; 7-mer, peptide KRKCLLL; 12-mer, PVKKRKRCCLLL; mantGDP, 2'(3')-*O*-methylanthraniloyl-GDP; GMPPNP, guanylylimidodiphosphate.

labeling modifies its biochemical properties. Inherent in the preparation is the presence of two diastereoisomers as produced by the reaction of the cysteine with the coumarin-maleimide; this reaction is described in detail in the Results. We have experience of this type of labeling particularly with MDCC-PBP, which is the phosphate-binding protein of *Escherichia coli* labeled with the same coumarin-maleimide used here to obtain a fluorescence signal that is sensitive to inorganic phosphate binding (11, 12). We draw on parallels with that system both for the strategy to produce a successful labeled GDI and in its subsequent characterization. In both cases, it seems that the two diastereoisomers have different fluorescence and binding affinities for rac1, and this must be accommodated in the analysis of the results. In practice, for most measurements the signal from the tighter binding diastereoisomer dominates and the weaker binding can be discounted: for the tighter-binding isomer the affinity for rac1 is affected very little by the presence of the coumarin.

The second problem encountered in investigating the interaction with GDI is that rac and its family require lipid modification at the C-terminus in order to interact fully (8, 9). In the cell this modification is geranylgeranylation, and here we use rac1 produced in insect cells using a baculovirus expression system. The full processing of rac1 in eukaryotic cells is the cleavage of the three C-terminal leucines from the protein, following which the newly C-terminal cysteine is carboxymethylated and S-geranylgeranylated. Rac1 expressed in *E. coli* is not modified. Throughout this paper, *E. coli* rac1 is referred to as unmodified and baculovirus rac1 as modified. Unless otherwise stated, the unmodified rac1 is truncated, amino acids 1–184.

Studies with lipid-modified proteins present experimental difficulties in vitro, for example by the need for detergents and difficulties in physical processes such as concentrating. Furthermore, the system is not easily manipulated, for example, precise control of the nucleotide bound to rac. We show that the combination of truncated, unmodified rac1 and farnesylated C-terminal peptide can mimic the geranylgeranylated rac and thereby allow us to test and quantify various features of the rac-GDI interaction. Farnesylation was achieved by reacting the Cys residue of such peptides with farnesyl bromide. The farnesyl group was chosen to modify the peptide because of the ready availability of farnesyl bromide to achieve this chemically and the likelihood that the hydrophobic interaction of GDI with the lipid would not be very specific for the geranylgeranyl group. Hydrophobic interactions have little or no directionality. Here, attempts to farnesylate peptides which terminate at the cysteine were not successful, probably because such peptides are very hydrophilic, containing a group of six basic amino acids. Peptides that include the three leucines were successfully farnesylated, and data are presented using these.

EXPERIMENTAL PROCEDURES

Human rac1 was obtained from *Spodoptera frugiperda* 9 cells infected with a recombinant baculovirus prepared by Dr. Martin Page (Glaxo-Wellcome). The gene was expressed, and cell membranes containing post-translationally modified rac1 were isolated using standard techniques. The insoluble membrane fraction was resuspended in 50 mL of 20 mM

Tris-HCl, pH 7.6, 1 mM MgCl₂, and 1 mM phenylmethylsulfonylfluoride, sonicated, and then centrifuged to remove all soluble protein. The membrane pellet was resuspended in this buffer (50 mL) containing 1 mM DTT and 60 mM *n*-octyl glucoside (Sigma), which solubilizes weakly associated membrane bound proteins, and incubated for 1 h at 4 °C. The suspension was centrifuged and the supernatant containing rac1 retained. The supernatant was applied to a Mono-S cation exchange column (1 mL, Pharmacia) equilibrated in 50 mM sodium phosphate, pH 6.5, 1 mM MgCl₂, 1 mM DTT, and 30 mM *n*-octyl glucoside. A salt gradient was applied in this buffer from 0 to 1 M NaCl, and the eluted rac1 was stored on ice until required with a typical yield of 1 mg from 2 L of insect cells. Purity of this rac was >95% as determined by SDS-PAGE: this purity was achieved in part during the membrane preparation and extraction resulting in ~50% purity.

Rac1 was also prepared from *E. coli*. L-broth (100 mL) containing 50 µg mL⁻¹ ampicillin was inoculated with *E. coli* strain JM109 containing the pGEX2T-rac1 plasmid and incubated at 37 °C overnight. An aliquot (10 mL) of this was added to each of eight 500 mL portions of L-Broth (total volume 4 L) containing 50 µg mL⁻¹ ampicillin. The cells were grown with vigorous shaking at 37 °C until an absorbance of 0.8 cm⁻¹ at 600 nm was obtained. Expression was induced by the addition of 1 mM IPTG, and the cells grown at 37 °C for a further 4 h. Cells were harvested by centrifugation, and the cell pellet was resuspended in 20 mM Tris-HCl, pH 7.6, and 1 mM MgCl₂ (buffer A) containing 1 mM PMSF. The pellet was freeze-thawed and sonicated. The soluble protein fraction was separated from the cell debris by ultracentrifugation and loaded onto a glutathione-Sepharose column (7 mL, Pharmacia) equilibrated in buffer A. The column was then equilibrated with buffer A containing 2.5 mM CaCl₂. GST-rac1 fusion protein was cleaved with thrombin while bound to the column. An Antithrombin III agarose column (5 mL, Sigma), equilibrated in buffer A containing 2.5 mM CaCl₂, was connected in series to the glutathione-Sepharose column in order to remove the thrombin after cleavage. Buffer A (50 mL) containing 2.5 mM CaCl₂ and 500 units of human thrombin (Sigma) was passed at 50 µL min⁻¹. Rac1 was pooled, dialyzed against buffer A, concentrated, and stored at -80 °C. Typical yield is 24 mg of the wild-type protein with purity >95% as determined by SDS-PAGE.

The concentration of rac1 was determined using a calculated extinction coefficient (13) of 29 828 M⁻¹ cm⁻¹. Rac1 from *E. coli* has no post-translational modification and a GSP N-terminus replacing the wild-type methionine: this mutation gives higher solubility. The accidental mutation, F78S (14), was removed by standard procedures. When *E. coli* strain JM109 was used, the rac1 was truncated by proteolysis so amino acids 1–184 were obtained (14). When BL21 strain was used the protein was full-length. Single-point mutants were prepared using a Stratagene site-directed mutagenesis kit, and sequences were confirmed using dideoxy sequencing (USB Sequenase V2 kit). The molecular mass of the *E. coli* proteins was determined by electrospray mass spectrometry (15). The identity of nucleotide bound was determined by HPLC using a Partisil SAX-10 column (Whatman) eluting at 2 mL min⁻¹ with 0.5 M (NH₄)₂HPO₄, adjusted to pH 4.0 with HCl.

The cDNA of human GDI and the expression vector pRSET A (Invitrogen) were used in order to express full-length GDI in *E. coli*. pRSET A produces a protein that contains an N-terminal polyhistidine fusion tag. Since this tag was not required, it was removed during the subcloning procedure. The GDI cDNA fragment was isolated from the pGEX2T-GDI (8), ligated with pRSET A using T4 DNA ligase (Boehringer Mannheim), and then transformed into competent *E. coli* DH5 α cells. Recombinant pRSETA-GDI without the polyhistidine tag was prepared using standard techniques and transformed into competent *E. coli* (BL21 strain) for expression. General cloning techniques were performed as described in ref 16.

L-broth (100 mL) containing 200 $\mu\text{g mL}^{-1}$ ampicillin was inoculated with BL21 (pRSETA-GDI) cells and grown at 37 °C overnight. This starter culture (10 mL) was added to each of eight 500 mL aliquots of L-broth (total volume 4 L) containing 200 $\mu\text{g mL}^{-1}$ ampicillin. This was grown to an absorbance at 600 nm of 0.8, and 0.5 mM IPTG was added. The induced cells were grown for a further 3 h, harvested by centrifugation, and resuspended in buffer A plus 1 mM PMSF. The cells were broken by sonication, and the soluble fraction was separated by ultracentrifugation. GDI was purified on a Q-Sepharose column (100 mL, Pharmacia) and equilibrated with buffer A, eluting with a linear salt gradient (1.8 L) in buffer A from 0 to 0.3 M NaCl. Samples of the fractions were analyzed by SDS-PAGE, and those containing GDI were pooled and concentrated. Typical yield was 40–50 mg.

GDI (5 mg) was applied to a 1 mL Mono-Q column, equilibrated in 20 mM Tris·HCl, pH 8.0, and 125 mM NaCl, and eluted with a linear salt gradient in 20 mM Tris·HCl, pH 8.0, and 125–250 mM NaCl. The protein solution was adjusted to pH 7.5, concentrated, and stored at –80 °C. GDI was analyzed by SDS-PAGE, N-terminal amino acid sequencing, and electrospray mass spectrometry. The concentration was measured using the calculated molar extinction coefficient 27 370 $\text{M}^{-1} \text{cm}^{-1}$ at 280 nm.

GDI (210 μM) was labeled by stirring with 420 μM MDCC (11) in 20 mM Tris·HCl, pH 8.0, for 45 min at 22 °C. The protein was passed through a 0.2 μm membrane filter, isolated using a PD10 column (Pharmacia) equilibrated in 20 mM Tris·HCl, pH 7.6, and then stored at –80 °C.

Trans, trans-farnesyl bromide (Sigma) was redistilled at low pressure and stored at –80 °C. Peptides, synthesized at NIMR, were labeled in a multiphase reaction mixture containing the following: 10 mM Tris·HCl, 4 mM EDTA, 0.85% (v/v) farnesyl bromide, 8 mg mL^{-1} peptide, and 20% (v/v) dimethyl formamide. The reaction under nitrogen, typically for 7 h, was continually stirred, and the pH was maintained at 8.0 by occasional addition of 1 M Tris base. The extent of reaction was determined by HPLC on a reverse-phase silica column (Whatman Partisil-10 ODS C18, 25 \times 0.46 cm). The 40 min gradient was 10% (v/v) acetonitrile, 0.1% trifluoroacetic acid in water, to 60% acetonitrile, 0.1% trifluoroacetic acid, at 1 mL min^{-1} . The products were purified on this column, and following concentration, they were stored at –20 °C in 50% (v/v) acetonitrile/water. Mass spectrometry (15) confirmed that the peptide had a single farnesyl attached.

Complexes of unmodified rac1 with GTP, GDP, or mantGDP were obtained by exchange of at least a 10-fold

excess of the nucleotide with rac1 under conditions which facilitate rapid exchange, excess EDTA over Mg^{2+} , typically 40 mM EDTA and 20 mM $(\text{NH}_4)_2\text{SO}_4$ in 20 mM Tris·HCl, pH 7.6, for 5 min at 30 °C. The protein was isolated on a PD-10 column and the bound nucleotide analyzed by HPLC as described above. For complexes with the nonhydrolyzable analogue GMPPNP, 150 nmol of rac1 was incubated with 600 nmol of GMPPNP and 12 unit alkaline phosphatase linked to agarose beads (Sigma) in 200 mM $(\text{NH}_4)_2\text{SO}_4$ and 20 mM Tris·HCl, pH 7.6, at 20 °C for 2 h with end-over-end stirring. Samples were analyzed by HPLC as described above. When all of the GDP had been hydrolyzed, the mixture was centrifuged briefly to remove the phosphatase beads and the supernatant was desalted on a PD-10 column.

Experiments using [^3H]GDP were quantified using a filter-binding assay, similar to that used previously (17, 18), following incubation of 1 μM rac1 together with varying concentrations of GDI with a 10-fold excess of [^3H]GDP in 40 mM EDTA, 20 mM $(\text{NH}_4)_2\text{SO}_4$, and 20 mM Tris·HCl, pH 7.6, at 30 °C. Note that EDTA accelerates nucleotide exchange. Octylglucoside was present to the extent introduced with modified rac1, typically resulting in 1–2 mM. Exchange of mantGDP was followed using fluorescence energy transfer from rac1 tryptophan(s) to mant with excitation at 290 nm, emission at 440 nm, using the same buffer and equivalent nucleotide and protein concentrations as above.

Measurements. Absorbance spectra were obtained on a Beckman DU640 spectrophotometer. Fluorescence measurements were obtained on a Perkin-Elmer LS50B fluorimeter with a xenon lamp. For time-resolved measurements, slit widths were 2.5 nm on the excitation and 5 nm on the emission. Stopped-flow experiments were carried out in a HiTech SF61MX apparatus with a mercury/xenon lamp. There was a monochromator and 5 nm slits on the excitation light at 436 nm and a 455 nm cutoff filter on the emission. Mass spectrometry and tryptic analysis of MDCC-GDI were as previously described (15, 19).

RESULTS

Coumarin-Labeled GDI: Characterization. The single cysteine on GDI was labeled with a range of fluorophores, particularly coumarins that are environmentally sensitive. The resulting molecules were tested to determine if there was a fluorescence change on adding lipid-modified rac1. GDI labeled with the coumarin-maleimide, MDCC (11) gave the largest change of those combinations tested, ~3-fold decrease as shown in Figure 1. Thus, this labeled protein (MDCC-GDI) was characterized further and used in subsequent studies. Absorbance spectroscopy and mass spectral analysis showed that a single molecule of MDCC was covalently bound to GDI. The electrospray mass spectrum of MDCC-GDI gave a mass of 23 490 (± 2) Da, 398 greater than that predicted for GDI alone. Previous work (19) showed that, under conditions of processing for mass spectrometry, base-catalyzed hydrolysis of the succinimide ring can occur leading to ring opening and producing a mass for the label of 401 Da. However, this unwanted reaction is unlikely to occur to a significant extent under normal labeling conditions (19) and use of MDCC-GDI, when the pH remains at ~8.0 or below. A tryptic digest of MDCC-GDI was analyzed by

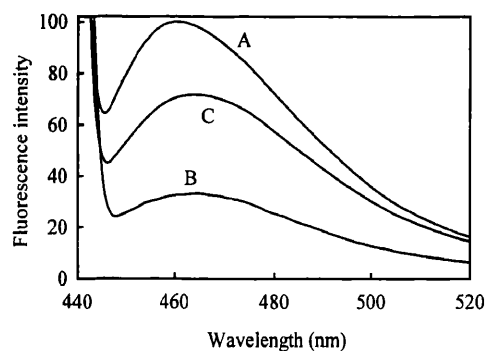


FIGURE 1: Emission spectra of MDCC-GDI. MDCC-GDI ($0.1 \mu\text{M}$) was incubated in 20 mM Tris-HCl, pH 7.6, 1 mM MgCl_2 , 5 μM BSA, and 1 mM DTT at 21 °C. Emission spectra were measured (A) before and (B) after addition of $0.3 \mu\text{M}$ modified rac1, or (C) 5 μM unmodified rac1 together with 15 μM farnesyl-12-mer (excitation at 431 nm). Unmodified rac1 or farnesyl-12-mer added on their own gave no fluorescence change.

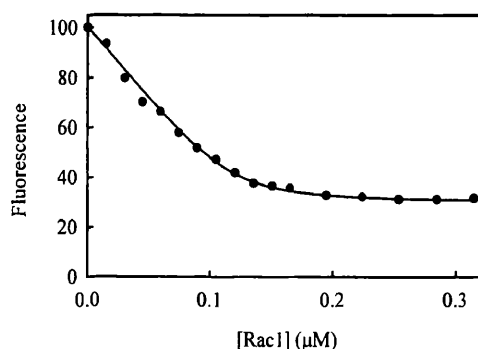
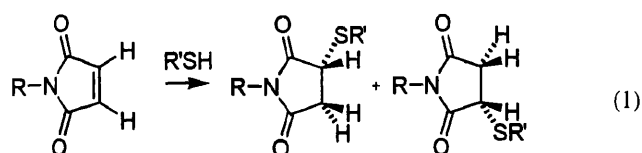


FIGURE 2: Equilibrium binding measurement of rac1-MDCC-GDI interaction. MDCC-GDI ($0.2 \mu\text{M}$) was incubated in 20 mM Tris-HCl, pH 7.6, and 1 mM MgCl_2 at 30 °C. Aliquots of modified rac1 were added sequentially and the fluorescence emission measured at 457 nm (excitation 431 nm).

HPLC to separate peptides that were then subjected to mass spectrometry (19). The only fluorescent species detected have masses of 4536 and 4553 Da, equivalent to that for amino acids 59–79, with either MDCC or the hydrolyzed species present. Again, the basic conditions during the digest are responsible for this partial hydrolysis. These data suggest that the single labeling is on Cys79.

The MDCC-GDI used in subsequent studies is therefore a single molecular species apart from the presence of diastereoisomers, as described below. It was important to show that the labeling has only limited effect on the rac-binding properties of GDI, and this was shown in several ways. A number of measurements described below address this point, and they will be reviewed in the Discussion.

Diastereoisomers. A titration of lipid-modified rac1 with MDCC-GDI (Figure 2) produced a linear decrease in fluorescence until $\sim 0.1 \mu\text{M}$ rac1, 50% of the total MDCC-GDI concentration. We think that this reflects equal proportions of diastereoisomers of MDCC-GDI, formed when a thiol reacts randomly with either of the two olefinic carbons of the maleimide to produce a chiral center:



where R = *N*-[2-(7-diethylaminocoumarin-3-carboxamido)-

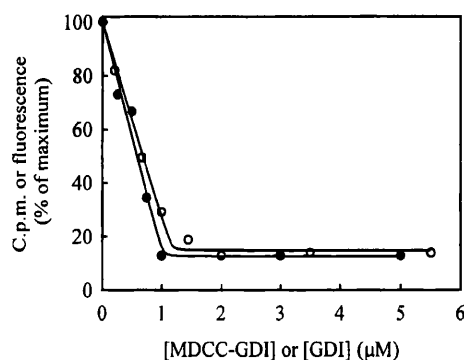


FIGURE 3: Effect of increasing concentration of unlabeled GDI or MDCC-GDI on the ability of modified rac1 to undergo nucleotide exchange. Rac1 ($1 \mu\text{M}$) in the presence of GDI was incubated with [^3H]GDP (MDCC-GDI, open symbols) or mantGDP (unlabeled GDI, closed symbols) for 10 min, and the extent of exchange was measured as described in Experimental Procedures. The lines are for tight equilibrium binding, allowing the concentration of rac1 to vary to give the best fit: essentially two straight lines that intercept at the concentration of GDI that saturates the rac1. For unlabeled GDI the best fit is at $1.02 \mu\text{M}$, for MDCC-GDI $1.16 \mu\text{M}$.

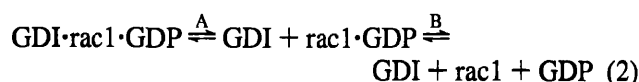
ethyl] and $\text{R'SH} = \text{GDI}$, attached via Cys-79. There is evidence that maleimides react with protein cysteines in this way, based on analysis of MDCC-labeled phosphate protein (19, 20).

The titration curve in Figure 2 is consistent with both diastereoisomers binding rac1 but only one dominating the fluorescent change. Further evidence for all of the labeled GDI binding rac1 comes from the titration in Figure 3, described below. This dominant putative diastereoisomer binds the rac1 tightly and is responsible for the linear fluorescence response to $\sim 0.1 \mu\text{M}$. The remaining small fluorescence change ($< 20\%$ of the total change) occurring from 0.1 to $0.2 \mu\text{M}$ is mainly due to the other diastereoisomer, binding rac1 somewhat more weakly. This titration is qualitatively similar to the situation with MDCC-labeled phosphate-binding protein titrated with its ligand P_i , for which the implications of diastereoisomers were further discussed (19). As a control $3 \mu\text{M}$ *E. Coli* rac1, lacking geranylgeranylation, gave no fluorescence change with MDCC-GDI in this concentration range (data not shown). An important conclusion from this titration is that measurements dependent on the coumarin fluorescence to determine rac binding are dominated by the tight binding diastereoisomer, and subsequent analysis will largely assume this by considering a single fluorescence change on rac binding.

Interaction of MDCC-GDI with Modified rac1. The relative affinities of MDCC-GDI and unlabeled GDI for modified rac1 were determined by titrating GDI into $0.3 \mu\text{M}$ MDCC-GDI-rac1 complex, although a precise treatment of these data was not possible because of the presence of the two diastereoisomers. As measured by fluorescence, 50% of the MDCC-GDI had been displaced from its complex with rac1, and hence there were equal amounts of MDCC-GDI-rac1 and GDI-rac1, when $0.47 \mu\text{M}$ GDI had been added. This suggests that the labeling of GDI has very little effect on its affinity for rac1.

The effect of GDI on modified rac1 was measured by the inhibition of nucleotide exchange due to GDI binding, using either mantGDP or [^3H]GDP: the presence of coumarin fluorescence interfered with mant fluorescence measurement

and so required the use of radioactivity. A time course of nucleotide exchange in the absence of GDI (data not shown) gave a rate constant for GDP release from the modified rac1 ($1.5 \times 10^{-3} \text{ s}^{-1}$, 30 °C at 1 mM Mg^{2+}) similar to that of unmodified rac1 ($1.1 \times 10^{-3} \text{ s}^{-1}$). The rate constant for modified rac1 in the presence of excess GDI was $<6 \times 10^{-6} \text{ s}^{-1}$. This reflects the fact that almost all of this rac1 is bound to GDI and only the small proportion unbound at any time can undergo exchange:



where GDP* represents radioactively or mant-labeled GDP. This scheme is consistent with the rate constant that we obtain later. The exchange rate of GDP to GDP* in the presence of GDI is controlled by the dissociation of GDI and then GDP (eq 2), as both GDP and GDI binding (eq 3) are fast. If $k_{-\text{GDI}}$ and $k_{+\text{GDI}}$ are the forward and reverse rate constants for step A and $k_{-\text{GDP}}$ is the forward rate constant for step B, the exchange rate constant should be $k_{-\text{GDI}}k_{-\text{GDP}}/(k_{+\text{GDI}} + k_{-\text{GDP}})$. $k_{-\text{GDP}}$ is $1.5 \times 10^{-3} \text{ s}^{-1}$, and $k_{-\text{GDI}}$ is $1.4 \times 10^{-3} \text{ s}^{-1}$. At $5.5 \mu\text{M}$ GDI, we can approximately use the saturating first-order rate constant, 7.3 s^{-1} , for $k_{+\text{GDI}}$ (see Figure 5 and text). Thus the exchange rate constant would be $0.29 \times 10^{-6} \text{ s}^{-1}$.

In practice, a small but variable proportion of baculovirus rac1 (typically 20%, but depending on preparation) does not have its nucleotide exchange inhibited by GDI and thus presumably interacts weakly or not at all with GDI due to damage or lack of proper lipid modification. The effect of different concentrations of unlabeled GDI or MDCC-GDI on rac-nucleotide exchange is shown in Figure 3. In both cases the maximum extent of inhibition is seen at ~1:1 ratio of rac1:GDI. The fact that there is ~15% exchange even at high GDI is due to the portion of "damaged" rac1. This is added evidence that all molecules of MDCC-GDI can bind rac1, but therefore only one diastereoisomer gives a large fluorescence change.

Kinetic Mechanism of rac1 Binding to GDI. The fluorescent MDCC-GDI was used to measure the association and dissociation of GDI·rac1 in real time for modified rac1. We use a two-step binding model for interpreting these data, although other models are also possible (see Discussion):



Step 2 represents a conformational change that includes the fluorescence change. The equilibrium constant and forward and reverse rate constants for step i are defined as K_i , k_i , and k_{-i} , respectively. Rapid mixing of rac1 with MDCC-GDI in a stopped-flow apparatus allowed the association kinetics to be measured (Figure 4). It was not possible to use high (saturating) rac1 concentrations, because rac1 as prepared was in a high ionic strength solution and it proved impossible to remove salt by dialysis or gel filtration and maintain active protein. Furthermore detergent present in the rac solution became more of a problem at high concentrations, as this affects the fluorescence signal. However, rates

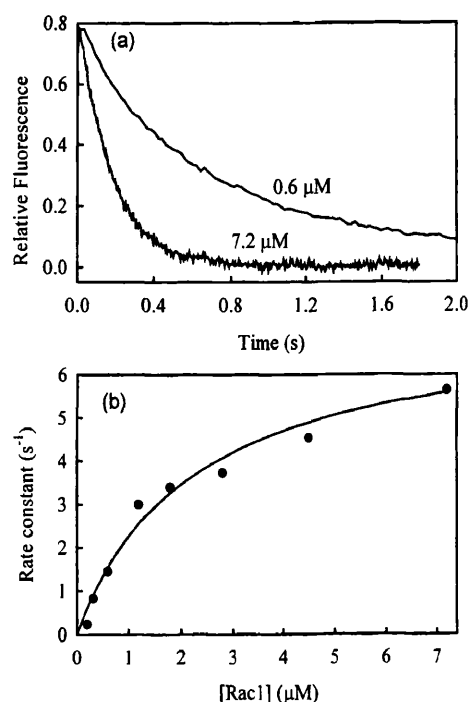


FIGURE 4: Association kinetics of modified rac1 with MDCC-GDI. MDCC-GDI (50 nM) was mixed with a large excess of rac1 and the fluorescence followed with time at 30 °C. (a) Time courses at rac1 concentrations shown. Controls run without rac1 showed a drift in fluorescence, probably due to protein adsorption on surfaces. These were subtracted to give the curves shown, but this correction had little effect on the rate constants: this effect caused a fluorescence amplitude change of 3% of the signal due to rac1 binding in the first 2 s. (b) Dependence of first-order rate constants on rac1 concentration. The data were fit to single exponentials and at least 4 runs averaged at each concentration. The line is the best fit for a two-step binding mechanism (eq 3) where step 1 is assumed rapid, so that the observed rate constant equals $k_2/(1 + [\text{rac1}]K_1) + k_{-2}$. $1/K_1$ is $2.2 \mu\text{M}$ and k_2 is 7.3 s^{-1} . From data in Figure 5, k_{-2} is $1.4 \times 10^{-3} \text{ s}^{-1}$.

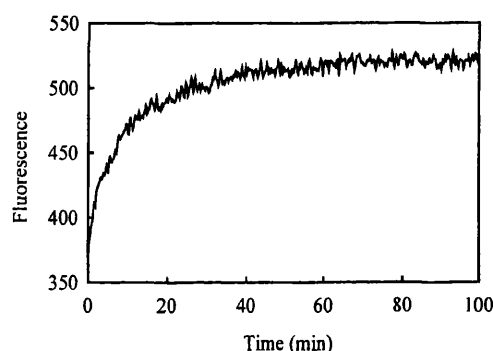


FIGURE 5: Displacement kinetics of MDCC-GDI from its complex with modified rac1 by unlabeled GDI. MDCC-GDI ($0.3 \mu\text{M}$) with a small excess of rac1 was incubated with unlabeled GDI ($30 \mu\text{M}$). Solution and fluorescence conditions were as in Figure 2. The data shown is after correction for the drift in fluorescence observed when MDCC-GDI alone was incubated for this time period.

were measured at sufficiently high concentrations of rac1 to demonstrate the onset of saturation of the kinetics and to obtain an estimate of k_2 (Figure 4b).

Dissociation kinetics were measured by displacing MDCC-GDI from its complex with modified rac1 by mixing with a large excess of unlabeled GDI (Figure 5), and the curve was fit to a single exponential with a rate constant of $1.4 \times 10^{-3} \text{ s}^{-1}$. The converse measurement, mixing unlabeled GDI·rac1 with excess MDCC-GDI, gave a similar rate constant for unlabeled GDI dissociation ($2.2 \times 10^{-3} \text{ s}^{-1}$, data not shown).

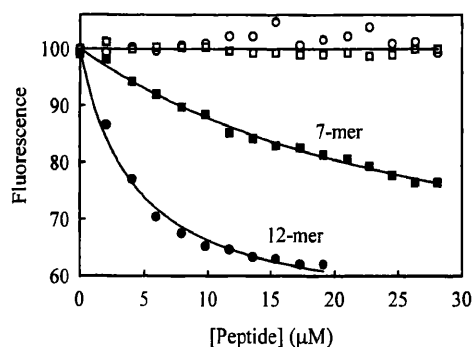


FIGURE 6: Interaction of farnesylated C-terminal peptides with unmodified rac1 and MDCC-GDI. MDCC-GDI (0.3 μ M) was mixed with 2 μ M truncated rac1 (1–184) in 20 mM Tris·HCl, pH 7.6, 1 mM MgCl₂, and 1 mM DTT containing 5 μ M BSA at 20 °C. Peptides were titrated into this solution, and the fluorescence emission was measured. Data are corrected for the decrease in fluorescence on addition of similar aliquots of buffer. The peptides were farnesyl-12-mer (filled circles), farnesyl-7-mer (filled squares), 12-mer (open circles), and 7-mer (open squares). The lines are the best fit to binding curves and give a K_d of 4 μ M for the farnesyl 12-mer (fluorescence change 47%) and 31 μ M for the farnesyl 7-mer (49%).

C-Terminal Peptides of rac1. To circumvent the problems of working with lipid-modified rac1 to study interaction with GDI, we investigated the possibility of using unmodified rac1 produced in *E. coli*, together with a farnesylated peptide corresponding to the C-terminus of lipid-modified rac1. Three peptides have so far been tested. VKKRKRKC, the C-terminus of the native modified rac (without the C-terminal methylation), failed to react with farnesyl bromide to a significant extent under a range of conditions. This is probably because this peptide is very hydrophilic. In contrast conditions were found to obtain almost quantitative farnesylation of the two other peptides. The 7-mer KRKCLLL is equivalent to amino acids 186–192, the part of *E. coli* rac1 lost on truncation at K184 (14), except R185 was omitted to ensure no overlap. The 12-mer PVKKRKRKCLLL extends this sequence across the group of basic amino acids.

Figure 1 shows that there is a fluorescence change on mixing farnesyl-12-mer, truncated unmodified rac1, and MDCC-GDI, suggesting that a complex forms. A series of measurements was done to characterize the interactions: titrations of peptides with MDCC-GDI and rac1 are shown in Figure 6. The 12-mer showed much tighter binding than the 7-mer. The unlabeled peptides produced little or no fluorescence change, as did the farnesyl peptides in the absence of rac. It is worth pointing out here that the fluorescence change may be more a measure of the lipid being present in its pocket on GDI, rather than binding of rac and/or peptide per se. This point is considered in the Discussion. As these controls confirm, the fluorescence change seems to be a measure of the formation of a complex analogous to that between native lipid-modified rac and GDI. To confirm that the unlabeled 12-mer binds only weakly, we showed the binding curve of farnesyl 12-mer to be unaffected by the presence of 15 μ M unlabeled 12-mer. Finally the complex formation was shown to be reversible by addition of excess unlabeled GDI to it. Following mixing 15 μ M farnesyl 12-mer, 0.1 μ M MDCC-GDI, and 0.5 μ M rac1, the addition of 2.5 μ M GDI caused an increase of fluorescence to 99% of that of free MDCC-GDI, suggesting that the labeled GDI was displaced from the complex by the excess unlabeled GDI.

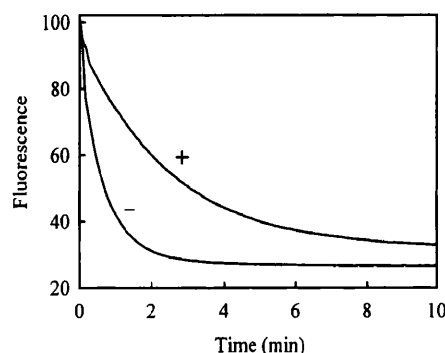


FIGURE 7: Inhibition of rac1-nucleotide exchange by GDI and farnesyl-12-mer. rac1·mantGDP (1 μ M) was incubated at 30 °C with 20 μ M GDP in the presence (+) or absence (–) of 2 μ M GDI and 10 μ M farnesyl-12-mer in 20 mM Tris·HCl, pH 7.6, 1 mM DTT, and 0.5 mM EDTA. The data were fit to single exponentials: $2.5 \times 10^{-2} \text{ s}^{-1}$ for rac alone and $0.7 \times 10^{-2} \text{ s}^{-1}$ in the presence of GDI and the peptide.

Table 1: Dissociation Constants for Unmodified rac1 from MDCC-GDI^a

rac and peptide	K_d (μ M)
rac1·GDP	<0.04 ^b
rac1·GMPPNP	>10 ^{c,d}
rac1·GTP (Q61L)	1.65
full-length rac1·GDP	0.14 ^e
rac1·GDP + unmodified 12-mer	0.53 ^e
rac1·GDP with no peptide	>10 ^e
full-length N-ras·GDP	>20 ^{e,f}
Cdc42.GDP (a.a. 1–184)	0.1
Cdc42.GMPPNP (a.a. 1–184)	>10 ^e

^a Titrations of rac1 into a solution of 0.1 μ M MDCC-GDI were done equivalent to those in Figure 6. Unless otherwise stated, 15 μ M farnesyl-12-mer was present and the rac1 was truncated (aa 1–184). Fluorescence was corrected by subtracting values using a control of buffer alone with no rac1. The K_d values are an average of at least two determinations. ^b Measurements were at 100 nM MDCC-GDI, so that this value represents an upper limit. Attempts to do the measurements at 30 nM MDCC-GDI did not give reproducible data. ^c No fluorescence change was observed, and this value represents the limit imposed by the errors in the measurement. ^d Rac1·GMPPNP had its nucleotide exchanged back to GDP, and this fully restored binding to MDCC-GDI, showing that the rac1 remained active. ^e These titrations gave an end point with a fluorescence change reduced ~50% relative to rac1·GDP with farnesyl-12-mer (Figure 6). ^f Addition of 0.25 μ M rac1 in the presence of 20 μ M N-ras and the farnesyl peptide showed a full fluorescence change, suggesting that the ras does not inhibit rac1 binding.

Another test of the ternary complex was to return to the effect of bound GDI on rac nucleotide exchange (eqs 2 and 3 and Figure 7). Under conditions where it is predicted that ~75% of the unmodified rac is complexed with GDI, the nucleotide exchange rate was reduced by ~65%. For the ternary complex, we assume that nucleotide exchange cannot occur when unmodified rac is bound to GDI and that dissociation of rac1 is much more rapid than nucleotide exchange of free rac1. All rac1 can undergo exchange, but at a rate reduced by the proportion of rac1 complexed to GDI at any time. Control measurements showed that GDI alone, farnesyl-12-mer alone, or GDI plus unlabeled 12-mer had no effect on the rac1-nucleotide exchange rate.

The farnesyl 12-mer was then used to assess some of the factors that may determine rac1 interaction with GDI. This was done by titrations of rac1 with MDCC-GDI plus farnesyl-12-mer (Table 1). The dissociation constant obtained for truncated unmodified rac1·GDP was <40 nM.

Because this method uses unmodified rac1, it allows precise control of the nucleotide bound in the complex. The above measurements with the peptides used rac1•GDP (aa 1–184). The Leu61 mutant of rac1 has a greatly reduced rate of intrinsic hydrolysis, so that the nucleotide bound in the protein as prepared is >95% GTP. Rac1 bound with the nonhydrolyzable GTP analogue, GMPPNP, was prepared with ~98% nucleotide purity. Thus rac1•GTP (Leu61) and rac1•GMPPNP (wild type) were used to assess the ability of triphosphate-bound rac1 to complex with GDI. In each case the K_d of the rac is greatly increased (Table 1). This suggests that the rac1 in the GTP state does not bind significantly to GDI: the binding that was observed could be explained by the small amount of rac1 with diphosphate bound. Measurements with cdc42 gave similar results.

When full-length unmodified rac1 was titrated in the presence of farnesyl-12-mer, the apparent binding was reduced several-fold relative to truncated rac1 (Table 1) and the total signal change during the titration was reduced. As a control, full-length N-ras showed no binding. Truncated rac on its own showed little or no binding, but weak binding of rac1 with unlabeled 12-mer was observed, again with reduced signal change. This may indicate that the hydrophobic lipid is needed for the full fluorescence change as mentioned above. These results suggest that the identities of amino acids in the C-terminal region of rac1 are important for the specific binding to GDI.

DISCUSSION

We have investigated the kinetic mechanism of the interaction between rac1 and GDI using two novel techniques. The coumarin-labeled GDI provides a direct fluorescence signal to study the interaction of rac with GDI. We have developed a novel assay using unmodified rac1 together with lipid-modified peptide corresponding to the C-terminus of rac1 that will allow us to probe factors important for the rac-GDI interaction.

It was important to characterize MDCC-GDI fully in order to use it with confidence. MDCC-GDI is a single species, apart from the probable presence of diastereoisomers. So far, fluorescence labels that do not lead to diastereoisomers (e.g., iodoacetamides) have only produced labeled GDI with little or no fluorescence change on binding modified rac. A similar situation was found with PBP labeled with MDCC and related molecules (19, 20). In that case a detailed study including crystal structure allowed us to understand to some extent how the fluorescence change arises and showed a significant difference in environment of the two diastereoisomers. In the case of GDI, equivalent data are not available, but the structure of the C-terminal domain of GDI suggests that the cysteine (and hence the coumarin) is close to the base of the binding pocket suggested for the lipid (6, 7). This may explain the apparent need for a lipid to obtain a full fluorescence change, even after taking into account much weaker binding in the absence of a lipid.

To make use of the signal that responds to the binding of modified rac, it was important for us to show to what extent the presence of the coumarin label affects the rac-binding properties of GDI. The coumarin fluorescence change is dominated by that due to one diastereoisomer, and this is assumed in subsequent analyses. Figure 3 together with the competition binding between unlabeled and labeled GDI

suggests that the binding affinity is affected very little. The dissociation kinetics of GDI and MDCC-GDI are also not much different (Figure 5). Thus, we may assume that the kinetic and thermodynamic data obtained using the fluorescent label are similar to that for unmodified GDI.

The kinetics of rac1 association and dissociation were measured in real time and interpreted in terms of the two-step mechanism in eq 3. The conformational change (k_2) has a rate constant of 7.3 s^{-1} (pH 7.5, 30 °C), while $1/K_1$ is $2.2 \mu\text{M}$. Modeling the association data, particularly the fact that no lag is observed at any rac concentration, suggests that $k_1 > 3 \times 10^6 \text{ M}^{-1} \text{ s}^{-1}$ and $k_{-1} > k_2$. This suggests that the measured dissociation rate constant ($1.4 \times 10^{-3} \text{ s}^{-1}$) is approximately k_{-2} . These values give an overall dissociation constant (K_d) of 0.4 nM. Because the binding is very tight, K_d is not easily determined from the equilibrium binding data, as such titrations are not practical at the very low concentrations ($\leq K_d$) needed. The preliminary report of a deepening of the lipid-binding pocket on binding of farnesyl peptide (7) is a potential structural correlation with the conformation change identified here kinetically.

The combination of a lipid-modified peptide and C-terminally truncated, unmodified rac mimics geranylgeranylated rac in interaction with GDI. An important question is what this approach tells us of the interactions between rac and GDI. The order of binding of peptide and unmodified rac1 to GDI is not established; kinetic data obtained so far do not distinguish between random and ordered addition (A. R. Newcombe and M. R. Webb, unpublished results). There is no evidence of binding of one component in the absence of the other. We will therefore compare the single K_d for modified rac1 binding to GDI with the two individual K_d values for farnesylated peptide binding to GDI in the presence of saturating unmodified rac1 and unmodified rac1 binding to GDI in the presence of saturating farnesylated peptide. In doing so, we will consider the binding in terms of the lipid, the C-terminus of rac1, and "the rest" of rac1.

A striking feature is that the unmodified rac1 in the presence of saturating farnesyl-12-mer binds tightly to GDI, less than 2 orders of magnitude weaker than the modified rac1, the value in the latter case being derived from the kinetic measurements. This suggests that the main bulk of the rac1 molecule has significant interactions with GDI remote from the lipid-binding region. GDI structural data indicate that GDI can be divided essentially into two regions, a well-ordered C-terminal domain containing a lipid-binding pocket and an N-terminal region that is disordered in the absence of bound small G protein (6, 7). This suggests that the interaction is more complex than that of two more-or-less rigid globular proteins, and there may be large areas of well-ordered interactions in the complex with essentially any region of the rac1 structure being involved.

In contrast, the farnesyl peptides in the presence of saturating unmodified rac1 bind much weaker than the modified rac1. Two components that may be factors in this weaker binding are the difference in lipid and the presence of LLL when compared with native, modified rac1. Presumably the smaller farnesyl group sits in the hydrophobic pocket; hydrophobic interactions are generally nonspecific, although the complete surface of the pocket may not be involved. As described above, it seems likely that the full fluorescence change requires the lipid in this pocket.

Several pieces of evidence suggest that the basic amino acids near the C-terminus of rac are important for interaction with GDI. They are conserved between different members of the rho family. The C-terminus seems to bind to GDI in the absence of the lipid, as seen from the titration of unmodified peptide in the presence of rac1 (Table 1). The farnesyl-7-mer, in which the basic amino acid region is incomplete, binds an order of magnitude weaker than the farnesyl-12-mer.

Our data show that guanosine triphosphate complexes of truncated rac are unable to bind tightly to GDI (at least 2 orders of magnitude weaker). Several reports have addressed whether the GTP form of modified rac binds, but with conflicting conclusions: GTP and GDP complexes having similar binding (8, 10) or the GTP complex bind weakly (9, 21). The major technique used in these reports was also titrations, and discrepancies may in part be due to the concentration ranges used. It is technically very difficult to determine K_d values unless the concentration ranges used span that K_d value. An advantage of the technique here is that the concentration ranges can span the observed K_d . In the current work, a major aim of using the peptides is to determine the relative importance of the different parts of rac1 in binding. The C-terminal region, represented here by the peptide, contributes to binding, and this contribution may be independent of whether GTP or GDP is bound. This region is not defined in the available structures (ref 14; M. Hirshberg, A. R. Newcombe, and M. R. Webb, unpublished results). However, once the contribution of the remainder of the rac protein is added, this could result in tight binding of the GDP form and weak binding for the GTP form. Because here the two contributions are separated, the technique is very sensitive to the conformational changes induced by the different nucleotides.

This suggests that regions involved in conformational changes on conversion from GDP to GTP states will be important in determining the binding to GDI. It also seems likely that regions that distinguish the rho family from other small G proteins that do not bind to GDIs will be important. Our results show that unmodified N-ras binds very weakly, if at all, in the peptide assay. The basic C-terminal patch is one such region that differs from ras, but others have been identified from a comparison of rac1 and ras structures, although the overall folds are similar (14). The insertion loop present in rac and other rho family members (aa 123–135) is the main gross structural difference from ras. Another difference is at the effector loop, and this may be significant here because of its closeness to the nucleotide-binding site and differences in this loop between the rac•GDP and GMPPNP structures (M. Hirshberg, A. R. Newcombe, and M. R. Webb, unpublished results).

MDCC-GDI should be useful in examining these aspects further. In addition it provides a way to probe for factors that accelerate the dissociation of rac from GDI. The observed dissociation with a half time of several minutes is

too slow to explain the action of rac in the cell, in which it begins as a complex with GDI prior to activation. An example is the activation of the NADPH oxidase complex (22).

ACKNOWLEDGMENT

We thank Dr. A. Hall (University College, London) for giving the original *E. coli* expression systems for rac1 and GDI, Dr. M. Page (Glaxo-Wellcome) for the baculovirus expression system for rac1 and assistance in setting up this system, and C. Pickford (NIMR) for N-ras. We thank Dr. M. Hirshberg (Cambridge) for many helpful discussions.

REFERENCES

1. Symons, M. (1996) *Trends Biochem. Sci.* 21, 178–181.
2. Segal, A. W., and Abo, A. (1993) *Trends Biochem. Sci.* 18, 43–47.
3. Ueda, T., Kikuchi, A., Ohga, N., Yamamoto, J., and Takai, Y. (1990) *J. Biol. Chem.* 265, 9373–9380.
4. Quinn, M. T., Evans, T., Loetterle, L. R., Jesaitis, A. J., and Bokoch, G. M. (1993) *J. Biol. Chem.* 268, 20983–20987.
5. Bokoch, G. M., Bohl, B. P., and Chuang, T. (1994) *J. Biol. Chem.* 269, 31674–31679.
6. Keep, N. H., Barnes, M., Barsukov, I., Badii, R., Lian, L., Segal, A. W., Moody, P. C. E., and Roberts, G. C. K. (1997) *Structure* 5, 623–633.
7. Gosser, Y. Q., Nomanbhoy, T. K., Aghazadeh, B., Manor, D., Combs, C., Cerione, R. A., and Rosen, M. K. (1997) *Nature* 387, 814–819.
8. Hancock, J. F., and Hall, A. (1993) *EMBO J.* 12, 1915–1921.
9. Chuang, T. H., Xu, X., Knaus, U. G., Hart, M. J., and Bokoch, G. M. (1993) *J. Biol. Chem.* 268, 775–778.
10. Nomanbhoy, T. K., and Cerione, R. A. (1996) *J. Biol. Chem.* 271, 10004–10009.
11. Corrie, J. E. T. (1994) *J. Chem. Soc., Perkin Trans. 1*, 2975–2982.
12. Brune, M., Hunter, J., Corrie, J. E. T., and Webb, M. R. (1994) *Biochemistry* 33, 8262–8271.
13. Gill, S. C., and von Hippel, P. H. (1989) *Anal. Biochem.* 182, 319–326.
14. Hirshberg, M., Stockley, R. W., Dodson, G., and Webb, M. R. (1997) *Nat. Struct. Biol.* 4, 147–152.
15. Aitken, A., Howell, S., Jones, D., Madrazo, J., and Patel, Y. (1995) *J. Biol. Chem.* 270, 5706–5709.
16. Sambrook, J., Fritsch, E. F., and Maniatis, T. (1989) *Molecular cloning. A laboratory manual*, 2nd ed., Cold Spring Harbor Laboratory Press, Cold Spring Harbor, NY.
17. Hall, A., and Self, A. J. (1986) *J. Biol. Chem.* 261, 10963–10965.
18. Neal, S. E., Eccleston, J. F., Hall, A., and Webb, M. R. (1988) *J. Biol. Chem.* 263, 19718–19722.
19. Brune, M., Hunter, J. L., Howell, S. A., Martin, S. R., Hazlett, T. L., Corrie, J. E. T., and Webb, M. R. (1998) *Biochemistry* 37, 10370–10380.
20. Hirshberg, M., Henrick, K., Haire, L. L., Vasisht, N., Brune, M., Corrie, J. E. T., and Webb, M. R. (1998) *Biochemistry* 37, 10381–10385.
21. Sasaki, T., Kato, M., and Takai, Y. (1993) *J. Biol. Chem.* 268, 23959–23963.
22. Abo, A., Webb, M. R., Grogan, A., and Segal, A. W. (1994) *Biochem. J.* 298, 585–591.

BI9829837